The Cellular Mechanism Underlying Neuronal Changes in Alzheimer's Disease

by

Tracey Dickson BSc. (Hons)

Submitted in fulfilment of the requirements

for the Degree of

Doctor of Philosophy

University of Tasmania

May, 2000

This thesis contains no material which has been accepted for a degree or diploma by the University or any other institution, except by way of background information and duly acknowledged as such.

To the best of my knowledge and belief, no material previously published or written by another person has been utilised except where due reference is made in the text of this thesis.

Tracey Dickson

COPYRIGHT STATEMENT

Tracey Dickson

Double labelling of a bulb-like neurofilament (green) immunopositive dystrophic neurite with a tau (red) core in an Alzheimer's disease case (74 yrs)

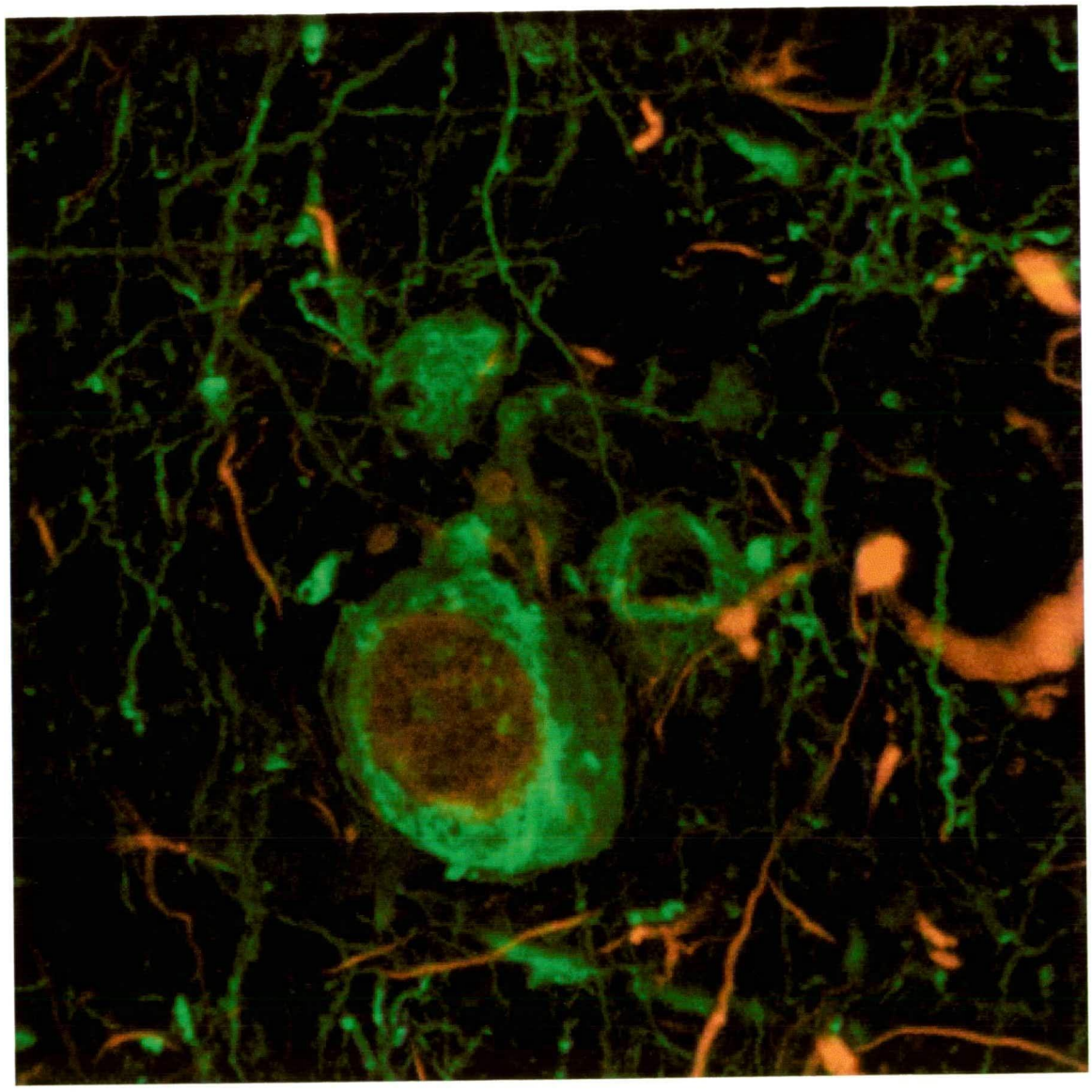

Part of the work contained in this thesis has been published or submitted for publication as follows:

1. **Dickson, T.C.**, King, C.E., McCormack, G. and Vickers, J.C. (1999) Neurochemical diversity of the dystrophic neurites in the early and late stages of Alzheimer's disease. *Experimental Neurology* 156, 100-110.

2. **Dickson, T.C.**, Saunders, H.L. and Vickers, J.C. (1997) Relationship between apolipoprotein E and the amyloid deposits and dystrophic neurites of Alzheimer's disease. *Neuropathology and Applied Neurobiology* 23, 483-491.

3. **Dickson, T.C.,** Adlard, P.A. and Vickers, J.C. (2000) The sequence of cellular changes following localised axotomy to cortical neurons in glia-free culture. *Journal of Neurotrauma* – Submitted

4. King, C.E., **Dickson, T.C.,** Jacobs, I., McCormack, G., Riederer, B.M. and Vickers, J.C. (2000) Acute CNS axonal injury models a subtype of dystrophic neurite in Alzheimer's disease. *Alzheimer's Report* 3, 31-40.

5. Saunders, H.L., **Dickson, T.C.** and Vickers, J.C. (1998) Immunolocalisation of ß-amyloid precursor protein to plaques associated synaptic alterations in the early and late stages of Alzheimer's disease. *Alzheimer's Report* 1, 111-119.

6. Vickers, J.C., **Dickson, T.C.,** Adlard, P.A., Saunders, H.L., King, C.E. and McCormack, G. (2000) The cause of neuronal degeneration in Alzheimer's disease. *Progress in Neurobiology* 60, 139-165.

7. King, C.E., Jacobs, I., **Dickson, T.C.** and Vickers, J.C. (1997) Physical damage to rat cortical axons mimics early Alzheimer's neuronal pathology. *Neuroreport* 8, 1663-1665.

8. King, C.E, Adlard, P.A., **Dickson, T.C.** and Vickers, J.C. (1999) The neuronal response to physical injury and its relationship to the pathology of Alzheimer's disease. *Clinical and Experimental Pharmacology and Physiology* – In Press.

ABSTRACT

The cause of the degeneration of nerve cells, and the loss of specific synaptic connections, that underlies the emergence and progressive development of dementia in sufferers of Alzheimer's disease remains elusive. Furthermore, although individually the ß-amyloid plaque, neurofibrillary tangle and dystrophic neurite, pathological hallmarks of the disease, have been extensively investigated, the mechanism that links these structures also remains to be defined. This thesis, therefore, sought to address three aims that were principally associated with the relationship between the pathological structures and the mechanism underlying Alzheimer's disease. Firstly, to determine the neurochemical and morphological diversity of abnormal neurites associated with ß-amyloid plaque formation in the early and late stages of Alzheimer's disease. Secondly, to examine the relationship between apolipoprotein E immunolabelling and ß-amyloid deposition, neuritic plaques and neurofibrillary tangles using immunofluorescent double labeling techniques. Finally, to develop an *in vitro* experimental model that mimics the effects of ß-amyloid plaques on surrounding neuronal processes.

The major conclusions from these investigations were that the dystrophic neurites associated with subsets of ß-amyloid plaques develop through a distinct morphological and neurochemical sequence. This sequence of change is intimately linked to various components of the neuronal cytoskeleton, including neurofilaments. The similarity between these changes and those present within axons undergoing a response to physical damage lead to the development of a new hypothesis that ß-amyloid plaque deposition causes

physical damage to surrounding neurites which results in the formation of dystrophic neurites. This hypothesis was further supported by results obtained from an *in vitro* model of physical damage. In summary, this study further clarified the relationship between ß-amyloid plaques and dystrophic neurites, particularly with regard to determining the role of specific cytoskeletal changes. Identification of the earliest pathological changes that occur in Alzheimer's disease is necessary for the development of effective therapeutic strategies aimed at preventing or slowing the ongoing neuronal changes that ultimately lead to cell death and dementia.

ACKNOWLEDGEMENTS

I wish to thank my supervisor Dr James Vickers for his never-ending patience, guidance and enthusiasm. I would also like to thank Professor H. Konrad Muller for providing the opportunity to undertake these Ph. D. studies in the Department of Pathology.

Thank-you to the many staff and students of the department, particularly Carolyn King and Paul Adlard. Our friendship has contributed greatly to the enjoyment of my studies. The contributions made by technical staff, particularly Graeme McCormack and Irene Jacobs are also gratefully acknowledged.

Particular mention and acknowledgement is due to the Tasmanian Masonic Medical Research Foundation for providing funds for my scholarship.

Finally, to my family and friends, especially my parents and Ro, thank-you for your continued love and support.

ABBREVIATIONS

AD	Alzheimer's Disease
ApoE	Apolipoprotein E
APP	Amyloid Precursor Protein
CERAD	Consortium to Establish a Registry for Alzheimer's Disease
CgA	Chromagranin A
CNS	Central Nervous System
DAB	3,3' Diaminobenzidine
DN	Dystrophic Neurite
DNA	Deoxyribonucleic Acid
FAD	Familial Alzheimer's disease
FITC	Fluorescein Isothiocyanate
GAP43	Growth Associated Protein 43
GFAP	Glial fibrillary acidic protein
HRP	Horseradish Peroxidase
IF	Intermediate Filament
MAP	Microtubule Associated Protein
MF	Microfilament
MT	Microtubule
NF	Neurofilament
NF-H	High molecular weight Neurofilament subunit
NF-L	Low molecular weight Neurofilament subunit

NF-M	Medium molecular weight Neurofilament subunit
NFT	Neurofibrillary tangle
PAGE	Polyacrylamide Gel Electrophoresis
PBS	Phosphate Buffered Saline
PHF	Paired Helical Filament
PI	Post injury
PMI	Post-mortem Interval
PS	Presenilin
R-NFH	Rabbit antibody to NFH
R-NFM	Rabbit antibody to NFM
SDS	Sodium Dodecyl Sulfate
SFG	Superior Frontal Gyrus
TBS	Tris Buffered Saline
TRITC	Tetramethyl Rhodamine Isothiocyanate
TTBS	Tris Buffered Saline with Tween

TABLE OF CONTENTS

INTRODUCTION

Alzheimer's disease (AD) is the major cause of dementia in late middle-aged and elderly individuals, affecting approximately 11% of the population over 65 years and up to 50% of individuals over 85 years (Hof & Morrison, 1994). The main locus of effect for this disease is the cerebral cortex, whereby dementia results from the degeneration of select subgroups of neurons. The disease process selectively damages brain regions and neural circuits critical for cognition and memory, including neurons in the neocortex, hippocampus, amygdala, basal forebrain cholinergic system and brainstem monoaminergic nuclei (Ulrich, 1985; Braak & Braak, 1991; Price et al., 1991; Vickers et al., 1992a; Hof et al., 1995). Ultimately, this degeneration results in a loss of connectivity of crucial cortical circuits, thereby resulting in widespread cognitive impairment.

Sufferers of AD experience gradually increasing forgetfulness, decreasing attention span and alterations in mood, often with frustration and agitation. The interval between initial diagnosis and death can vary considerably, usually between three and fifteen years and with this decline comes an increasing dependence on primary carers and health-care system assistance. Consequently, AD imposes both a considerable social and financial burden on the population. It is estimated that there are three to four million patients in the USA alone who currently have AD and that number is expected to double in the next twenty years (Roses, 1995). Currently there are no treatments available which have proven to be effective in slowing or interrupting the progression of AD.

There are specific abnormal structures that occur in the brains of individuals with AD including extracellular accumulations of ß-amyloid into plaque like deposits and intracellular neurofibrillary changes in both the cell bodies (neurofibrillary tangles (NFTs)) and also

associated nerve cells processes (dystrophic neurites (DNs)). A major obstacle hindering research and treatment development is the lack of understanding of the cellular mechanisms underlying the neuronal pathology of this neurodegenerative disorder. This thesis will, therefore, seek to investigate the relationship between these pathological hallmarks of AD with a particular emphasis on the association between ß-amyloid plaques and clusters of abnormal or dystrophic neurites. The implications of this relationship will be discussed with regards to defining the role of neurofilaments (NFs) in not only the development of DNs but also in the mechanism underlying AD as a whole.

BACKGROUND

A number of different neuronal cytoskeletal proteins are altered in the development of neurofibrillary pathology in AD. There is evidence that a modified form of the microtubule associated protein, tau, is an integral component of paired helical filaments (PHFs), the major component of the NFT (Wischik et al., 1988). Furthermore, an increasing body of literature now implicates the NF triplet protein as the first cytoskeletal element to undergo change in AD, preceding the development of more classical tau pathology (Vickers et al., 1996). In addition, a correlation between a neuron's content of the NF triplet protein and its subsequent vulnerability to pathology development (Vickers et al., 1992a, 1994a) and degeneration (Morrison et al., 1987; Hof et al., 1990; Hof & Morrison, 1990) has been reported. Cumulatively, these results suggest that alterations in the neuronal cytoskeleton, particularly the NF triplet proteins, contribute to the pathogenesis of AD. Therefore, the structure and function of the normal cytoskeleton as well as the profound cytoskeletal changes that occur in neurons and their processes in AD are the major themes discussed in the following review of the literature .

1.1 Neuronal Cytoskeleton

Many of the changes that occur in AD and ultimately result in nerve cell death, connection loss and dementia involve components of the neuronal cytoskeleton. The cytoskeleton is an intracellular structure which occurs in most vertebrate cells. Specialised cytoskeletons contribute to many cellular functions, including maintenance of mechanical integrity and wound healing in epidermal cells, cell polarity in simple epithelia, contraction in muscle cells, hearing and balance in the inner-ear cells, neuromuscular junction formation between muscle cells and motor neurons and axonal transport in neurons. This skeleton is composed of three main fibrillar components namely microtubules (MTs) (25 nm diameter), microfilaments

(MFs) (5 nm diameter) and intermediate filaments (IFs) (10 nm diameter). It has been established that the first two classes are involved in a variety of cellular events including cell division, locomotion, protoplasmic streaming, cellular polarity and anchorage. However, a well defined function of IFs cannot be given at present.

One of the unique properties of neurons that enables them to form complex nervous systems is their ability to extend long cytoplasmic processes, axons and dendrites, which allow cells to communicate with other cells in a highly specific manner. The growth and maintenance of these processes is critically dependent on the neuronal cytoskeleton. In addition to the development and maintenance of neuronal morphology the neuronal cytoskeleton also has more dynamic roles in the transport of materials in both directions along axons and dendrites, in cell division in developing neurons and in mediating plastic changes in neuronal morphology and function in the adult brain. These changes may underlie the long term modifications required for learning and memory.

1.1.1 Microtubules

Neuronal MTs have many functional roles. They are likely to be involved in cell division and motility during development, the growth of axons and dendrites, the maintenance of neuronal morphology, transport of components along axons and dendrites and neuronal plasticity. MTs are structurally and functionally polar with a fast growing (plus) and a slow growing (minus) end. In axons they are uniformly oriented with their plus-ends pointing toward the distal end, whereas in dendrites, their orientations are mixed (Baas et al., 1988).

MTs isolated from brain contain a number of polypeptide components including dimers of α- and ß- tubulin, which assemble to form a linear polymer, a heterogeneous collection of proteins, known as microtubule associated proteins (MAP), and a third class of proteins known as 'motor proteins'. Molecular variation in MT composition occurs at both the level of the forms of α- and ß- tubulins present and the nature of the associated MAPs.

α- and ß- tubulin are each encoded by up to six different genes. The protein tubulin can also be modified in several ways; phosphorylation, acetylation, detyrosination and glutamylation. These factors combine to result in considerable tubulin diversity. In the elongation of axons of the neuron, tubulin molecules are transported toward the end of pre-exisiting MTs via a mechanism called slow axonal flow/transport. Two different hypotheses have been presented to explain this mechanism; the transport of soluble monomers and /or oligomers versus the transport of polymerised MTs (Kobayashi et al., 1998).

Cytoskeletal organisation and dynamics depend on protein self-associations and interactions with regulatory elements such as MAPs. The MAP family includes large proteins - MAP1A, MAP1B (also known as MAP5), MAP1C, MAP2 and MAP4, which have a comparatively high molecular weight range, between 180 and 350 kDa and smaller components like tau and MAP2C, which have lower molecular weights within the range of 30-60 kDa (Fulton, 1984; Lewis et al., 1988). Both groups possess a similar carboxy-terminal amino acid sequence, which acts as the MT binding site (Lewis et al., 1988).

Expression of the various isoforms is dependent on the stage of development and differentiation of the neuron (Matus, 1988). Further to this, the cellular localisation of individual MAPs is quite specific. MAP3 (270 kDa) is specific to astroglial cells and NF rich axons (Parysek et al., 1984). MAP5 (320 kDa) is localised to neuronal axons, dendrites and cell bodies but not terminals (Riederer et al., 1986). MAP4 (270 kDa), in contrast to the other neuronal MAPs, has a ubiquitous distribution (Mandelkow & Mandelkow, 1995). The most widely studied of the MAPs are MAP2, which consist of two isoforms (a and b), of approximate molecular weight of 280 kDa, and is found only in nerve cell bodies and dendrites (Bernhardt & Matus, 1984), and tau, which is 55-62 kDa and is generally believed to be only associated with axonal MTs (Binder, 1985). MAP2 and tau share homologous repetitive motifs in the carboxy-terminal region that contribute to MT binding, however,

MAP2 has a much larger extension towards the amino-terminus. MAP4 also resembles MAP2 and tau in having a homologous repeat domain that interacts with MTs (Mandelkow & Mandelkow, 1995).

Initially, tau was described by Weingarten and colleagues (Weingarten et al., 1975) as a heat stable protein that co-purified with tubulin through repeated cycles of polymerisation and facilitated the formation of MTs. Studies of cloned mouse (Lee et al., 1988), human (Goedert et al., 1989) and bovine (Himmler et al., 1989) tau revealed a family of proteins derived from alternatively spliced transcripts of a single gene, located on the long arm of chromosome 17 (Neve, 1986) with predicted molecular masses between 35 and 40 kDa. In the human brain this alternative splicing gives rise to the expression of six different isoforms (Goedert et al., 1989). Isoforms contain either three or four imperfect sequence repeats of 31 or 32 amino acids in the carboxy-terminal region of the molecule that mediate, due to the presence or absence of exon 10 in the mRNA (Goedert et al., 1989), the binding of tau to MTs (Butner & Kirchner, 1991).

Investigations have demonstrated that MAPs are capable of contributing to the assembly and stability of MTs *in vivo*, that is, cells transfected with MAP2 (Ferralli et al., 1994) and tau (Lee & Rook, 1992; Bramblett et al., 1993) all had increased MT stability. Experiments showing that cells failed to form neuritic processes containing stable MTs when treated with anti-sense strategies designed to decrease the cellular synthesis of these MAPs provides further evidence that tau and MAP2 are MT - stabilising proteins *in vivo* (Caceres & Kosik, 1990; Dinsmore & Soloman, 1991). Other *in vivo* studies suggest that the claim that tau and MAP2 act to stabilise MTs may be too simplistic. Hirokawa's laboratory showed that homozygous tau-knockout mice contained no immunologically recognisable tau, yet the mice were phenotypically normal, with very subtle differences in MT polymer, neurons, axons or MT-dependent functions (Harada et al, 1994). This result suggests that in circumstances where there is no tau, the stabilisation of MTs may be achieved by other MAPs.

It has also recently become clear that the phosphorylation of specific sites rather than the overall extent of phosphorylation, may be an important factor in modulating the ability of tau to bind MTs and promote MT stabilisation. For example, phosphorylation of tau by cAMP-PK decreases tubulin binding, while phosphorylation by CaMKII does not alter this parameter (Johnson, 1992). Similarly phosphorylation of specific tau residues differentially affects the activity of tau on MT assembly (Brandt et al., 1994).

The MAPs have also been implicated in the interaction of MTs with other cytoskeletal elements and cellular organelles (Hirokawa, 1982; Hirokawa et al., 1988). Studies using quick-freeze, deep etch electron microscopy have confirmed that MAPs form structural side-arms which interconnect MTs with MTs and other cytoplasmic elements (Hirokawa, 1982; Hirokawa et al., 1988). Investigations into the mechanism of membranous organelle movement along MTs in anterograde fast axonal transport (Brady et al., 1982) led to the discovery of unidirectional cytoplasmic MT-based motor proteins (Paschal et al., 1987), so called because they generate movement along MTs using the chemical energy of adenosine tri-phosphate hydrolysis. Examples include kinesin which acts as a motor for anterograde fast axonal transport (Bloom et al. 1988) and dynein which is thought to be the motor for the retrograde transport of membranous organelles in fast axonal transport (Schroer et al., 1989). Recent evidence also suggests that the motor proteins may affect the organisation of dendritic MTs (Sharp et al., 1995, 1996).

1.1.2 Microfilaments

Actin MFs play a direct role in a variety of cell processes. They are by far the major cytoskeletal component on the leading edge of the growth cone and with MTs are a major constituent of the cytoskeleton of presynaptic nerve terminals (Hirokawa et al., 1989). The protein actin has also been demonstrated to be in great abundance in dendritic spines (Matus et al., 1982). Actin was first characterised as a self-assembling 43 kDa protein with a single

nucleotide binding site. Actin-associated proteins have been implicated in the regulation of filament assembly (eg profilin (Blikstad et al., 1980), stabilisation (eg tropomyosin (Gunning et al., 1998), crosslinking and bundling (eg brain spectrins fodrin and spectrin (Riederer et al.,1986) and filament-membrane linking or anchoring (eg ankyrin (Nelson & Lazarides 1984).

The force generation for projection and retraction of processes from growth cones during neuronal development is likely to be provided by the actin network. The growth cone lamellipodia and filopodia, which perform the initial scanning movement, are rich in MFs. In contrast, MTs form the core of the growth cone base (Brandt, 1998). Actin filaments are intrinsically polar, highly dynamic structures which are able to quickly assemble and disassemble. They are capable of exerting net movement through a process known as "treadmilling", which involves the assembly of filaments at one site (plus-end) and disassembly at the other (the minus-end). This assembly process produces the force for growth cone mobility (Forscher et al., 1992).

The growth associated protein 43, (GAP43) is tightly associated with the growth cone membrane skeleton, which via regulation of actin polymerisation is responsible for causing directional changes in axon growth. GAP43 co-sediments with actin filaments and its phosphorylation, on serine 41 by protein kinase C, is spatially regulated so that phosphorylated GAP43 is found in areas where growth cones make productive stable contacts with other cells. In contrast unphosphorylated GAP43 which binds calmodulin, is always found in parts of the growth cone which are retracting (He et al., 1997).

1.1.3 Intermediate filaments

Of the three major constituents of the cytoskeleton, IFs remain the least understood with respect to structure and function. IFs generally constitute approximately one percent of total protein, although in some cells, such as neurons and epidermal keratinocytes, IFs are

especially abundant accounting for up to 85 percent of the total protein of fully differentiated cells (Fuchs & Cleveland, 1998).

Despite their diversity, members of the IF superfamily share a common structure in which three distinct domains can be identified, a central rod of conserved length and sequence (about 310 amino acid residues) (Steinert & Roop, 1988) occurring in a helical conformation, flanked by a non-helical amino-terminal headpiece of variable length and a non-helical carboxy-terminal tail showing considerable length differences between different IF proteins. The highly conserved rod domain has been proposed to be the organising centre for filament assembly, as well as for other shared structural and morphological characteristics of the IF proteins. Variability in the molecular weights and functions of IFs found in different cell types has been attributed to the hypervarible carboxy-terminal and amino-terminal domains of these proteins. IF assembly, unlike MT or MF assembly, does not appear to require co-factors or associated proteins (Schliwa & Potter, 1986). It remains uncertain as to whether all IF polypeptides are incorporated into the IF network as they are synthesised, or whether they exist in a post-translational soluble form in the cytoplasm from which filaments are formed (Schliwa & Potter, 1986).

NFs correspond to the IF component of the neuronal cytoskeleton and can be further subdivided into subclasses based on their molecular and genetic structure, as well as their specific expression in different cells and in development. They are usually found in bundles, are long and unbranched and appear to be of constant diameter. Under electron microscopy thin, wispy protrusions can be seen forming bridge-like structures between adjacent filaments. Such side-arms are absent from the 10 nm filaments of other cell types.

At least four IF types have been identified so far in central or peripheral neurons, including the NF triplet (class IV of the five major IF classes defined by sequence analysis), vimentin (class III), peripherin (class III), α-internexin (class IV) and nestin (a novel "sixth" class). These

subtypes are variably and differentially expressed in accordance with the neurons changing demands for plasticity and stability of cell shape as they migrate, elaborate neurites, and establish a permanent fibre trajectory. The postnatal replacement of the transitional forms, such as vimentin, peripherin and α-internexin by the NF triplet proteins and the subsequent modification of the NF composition and structure during development coincide with a shift in demand for plastic, intermediate networks to a need for more stable filaments to support the highly polar morphologies characteristic of mature neurons.

The protein vimentin (52-58 kDa) is abundant in most central nervous systems (CNSs) before they differentiate. During this period vimentin filaments mediate cell division and changes in cell shape and may also assist in initial neurite outgrowth (Nixon & Shea, 1992). Peripherin (56-61 kDa) appears in some neurons, particularly those of the peripheral nervous system, after their final division and after migrating cells have reached their destination (Escurat et al., 1990). Like vimentin, the expression of peripherin is increased after axotomy (Oblinger et al., 1989) suggesting a principal role for this IF protein in maintaining plasticity during outgrowth and regeneration. α-internexin (66 kDa), another of the neuronal filaments, helps maintain plasticity during outgrowth and regeneration (Patcher & Liem, 1985). It persists as the dominant IF system in small calibre axons. The most recently described of the neuronal IF family is 'nestin' or neuroepithelial stem cell protein (Lendahl et al., 1990). It functions in neuroblast migration and is expressed only in the early developing nervous system in radial glial cells, the progenitors of both neurons and glia. The final class associated with the nervous system are the NF triplet proteins. Due to the association between this class of IF protein and AD (Dahl et al., 1982; Perry et al., 1985; Cork et al., 1986; Haugh et al., 1986; Miller et al., 1986, Dickson et al., 1988; Masliah et al.,1993b; Vickers et al.,1994b; Su et al., 1996) more detailed discussions of their structure, assembly, phosphorylation patterns and dynamics will be given below.

1.2 Neurofilament triplet

The most widely studied NF proteins in the CNS are collectively referred to as the NF triplet proteins, which form heteropolymers thought to be composed of varying combinations of NF-M (160 kDa) and NF-H (200 kDa) subunits with NF-L (68 kDa) mw subunits (Lee et al., 1993). These subunits are both genetically and structurally interrelated. As the triplet proteins are, collectively, the most predominant neuronal IF, the combined heteropolymer of all three subunits is often referred to as a 'NF' although strictly it is just one type of NFs. This system of nomenclature will be adopted for the purpose of this review.

NFs arise at a time in late embryonic development when neurites are growing but have not yet reached their targets (Tapscott et al., 1981). Normally NFs extend throughout the axon, dendrites and soma of a cell but are absent from the nerve terminals due to the action of proteases (Schlaepfer, 1987). Those subunits localised to the soma and dendrites are dephosphorylated on their carboxy-terminal domains whereas NFs within the axon are predominantly phosphorylated (Torack et al., 1996; Vickers, 1997). In the past it has been thought that NFs primary role in neurons was structural ie maintaining axonal calibre (Hoffman et al., 1987). Other studies have suggested that NFs may be involved in other cellular functions including the control of ionic balance, regulation of chemical processes and the distribution of information amongst the major cellular domains (Schlaepfer, 1987). However, more recently, gene targeting studies studies suggest that NFs are not required for axogenesis and that individual NF proteins play distinct roles in filament assembly and in the radial growth of axons (Hirokawa & Takeda, 1998; Julien, 1999).

1.2.1 Structure

Each of the three triplet proteins conforms to the standard structure of the IFs in that they have three structural domains consisting of an amino-terminal region, an α-helical central rod or core domain and a carboxy-terminal region ie a head-rod-tail organisation (Figure 1.1). The amino-terminal of each of the NF triplet subunits is similar to that of the other neuronal IFs.

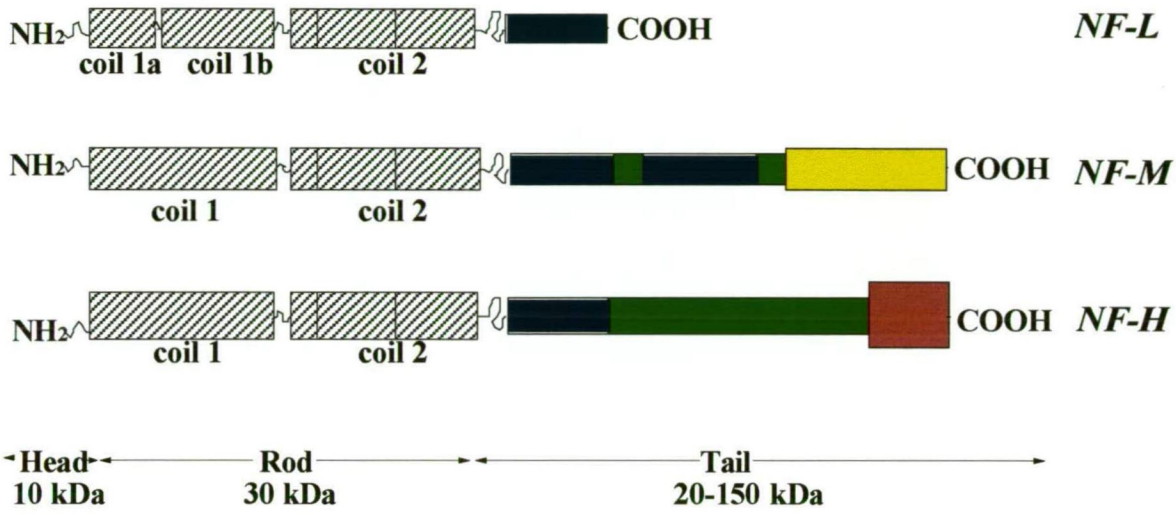

Figure 1.1

Diagramatic representation of the amino acid sequences of the three NF triplet subunits. The vertical lines within coil 2 indicate areas where the heptad pattern is broken due to the insertion of an extra amino acid. The blue areas correspond to areas in which the sequences are particularly rich in glutamic acid whilst the green segments represent areas in which the sequence contain variable numbers of lysine-serine-proline repeats, KSP regions. At the end of NF-M is a domain with a high concentration of lysine and glutamic acid, KE region, this area is represented by the yellow bar. The carboxyterminus of NF-H (red box) is rich in lysine, glutamic acid, as in NF-M, and also proline. Modified from Shaw, 1991.

This domain is comprised predominantly of ß-sheet and ß-turn structures, consists of 60-100 amino acids and is particularly rich in serine, glycine, alanine and arginine and contains several proline residues. Arginine is notably abundant in this region, predicting that the domain as a whole would have a basic pH. There is only minor homology between amino-head sequences of the NFs. The central core domain is relatively highly conserved (45-60% sequence homology) between the three NF triplet polypeptides and with other IF proteins. It is approximately 37 kDa in size, consists of 310-330 amino acids, and has an α-helical coiled-coil secondary structure. The central domain consists of long amino acid sequences exhibiting a heptad repeat of hydrophobic amino acids. In NF-L there are major breaks at two regions within the core. The two breaks or linkers, which contain proline residues, split the core into three regions, coil 1a, 1b and 2. NF-M and NF-H are unusual in that the break in the heptad repeat at coil 1a doesn't occur, so that these proteins have a single unbroken coil 1 (Lee et al., 1988a).

In contrast to the other IF subunits known, which consist of subunits with molecular weights around 50 kDa, the NF triplets are relatively large. The greater mass of NF-H and NF-M, in particular, is due to long extensions of sequence on the carboxy-terminal side of the conserved core domain (Lasek et al., 1985). The length of this carboxy-terminal tail domain is also responsible for much of the biochemical variability that exists between the NF triplet subunits. On the basis of distinct types of amino acid sequence, the carboxy-terminal appears to be made up of four distinct subregions. The initial segment, which contains proline and is neutral or slightly basic, is consistent between the three subunits and is proposed to have a role in acting as a hinge for the carboxy-terminal domain so that it can extend away from the plane of the central domain (Shaw, 1991). The second region is variable in length and contains many charged residues such as glycine, alanine, lysine and, in particular, glutamic acid which may act to electrostatically repulse the structure away from the central domain. NF-L only contains these first two regions. The third region of the carboxy-terminal domain of NF-M and NF-H is characterised by variable numbers of the lysine-serine-proline repeat motif and is, therefore,

often termed the KSP region or segment. In mammalian NF-M, there are two distinct sets of KSP sequences which are separated by a further glutamic acid rich sequence. In NF-H, in rats for example, the number of KSP containing sequences may be more than 50 (Dautigny et al., 1988). The size of this region is greater in NF-H than NF-M. The final region, at the extreme carboxy-terminus of NF-H is a region rich in lysine, glutamic acid and proline which is approximately 20 kDa in size (Lee et al., 1988a). Lack of sequence homology in this region between species suggests that the function of this region is not vitally important. In NF-M this final region is also rich in glutamic acid and lysine (KE), however, there is no proline present. In contrast to NF-H this region is highly conserved in sequence between species, however, similar motifs are not found in other proteins, therefore suggesting a NF specific function.

1.2.2 Axonal transport and Assembly dynamics

NFs are obligate heteropolymers requiring NF-L with either NF-M or NF-H for polymer formation (Lee et al., 1993). *In vitro* reassembly studies showed that purified NF-M and NF-H proteins do not form IF structures alone (Geisler & Weber, 1981; Liem & Hutchinson, 1982; Hisanaga & Hirokawa, 1990b; Hirokawa, 1991). NF-L subunits were capable of forming filaments *in vitro*. Negative staining revealed that these filaments had a relatively smooth structure. Reassembly in the presence of all three subunits produced filaments with rough walls and sidearm projections (Liem & Hutchinson, 1982; Hisanaga & Hirokawa, 1988,1989). More recent studies have shown that NF-L can associate with stoichiometric amounts of NF-M and NF-H, again supporting the idea that all three subunits are integral components of the NF structure (Cohlberg et al., 1995).

Although NF-L forms the backbone of the complete NF polymer, NF-M and NF-H integrate in the peripheral dimer arrays, which leaves their tails/sidearms protruding up to 30 nm away from the filament backbone and enables them to associate with other NFs and MTs in the axoplasm. The 10 nm filament is constructed by two coiled - coil dimers of protein subunits

lining up in a staggered fashion to form an antiparallel tetramer. Eight tetramers pack together in a helical array to make a rope-like 10 nm filament.

The co-ordinated expression of genes for NF-L and NF-M precedes that of NF-H (Carden et al., 1987). In developing immature axons, NFs contain only NF-L and NF-M subunits, but in mature axons they contain all three subunits. Whether NF-H can be incorporated into pre-existing immature filaments as the axon matures, and whether NF-H subunits in the filaments of mature axons can undergo dynamic exchange with an unassembled pool of NF-H in certain neuronal compartments (such as the perikaryon) are yet to be determined definitively.

Following their synthesis in the perikaryon, NFs are moved into and through axons via slow axonal transport at a rate which varies (depending on the group of neurons, the age of the animal, and the location along the nerve) between 0.25 and 3 mm/day (Hoffman et al., 1983; Nixon & Logvinenko, 1986). Initial investigation of transport of NFs, measuring only the peak of the transported component, concluded that all three NF subunits were transported together in a single wave, which led to the proposal that NFs moved as polymers containing all three subunits (Hoffman & Lasek, 1975; Black & Lasek 1980). More recent examination has revealed the presence of a second pool of essentially stationary NFs within axons. This lead to the conclusion by some that the system is more dynamic than first proposed and that subunit exchange can occur (Nixon & Logvinenko, 1986; Nixon et al., 1987, 1994a). Investigations utilising fluorescently tagged NF-L subunits demonstrating rapid exchange of subunits between filaments and biotin tagged NF-L showing incorporation along the full length of existing NFs have supported this proposal (Angelides et al., 1989; Okabe et al., 1993). Similar results were found with NF-H although exchange of this subunit occurred faster than with NF-L (Takeda et al., 1994). However, there is disagreement regarding the fraction of filaments in the slower unassembled pool, estimated by one group to be as much as one third of the total newly synthesised pool (Nixon & Logvivnenko, 1986) and by another to be a negligible amount (Lasek et al., 1992). A more recent analysis of NF movement reports that the slow rate

of axonal transport of NFs may the result of rapid movements interrupted by prolonged pauses (Wang et al., 2000). These results help to reconcile many previous apparently conflicting results (Brady, 2000).

1.2.3 Phosphorylation

The NF triplet subunits are among the most highly phosphorylated neuronal proteins known (Wible, et al., 1989). They are continually modified in a complex pattern after synthesis by kinases, phosphatases and proteases which are modulated differently at various levels along the axon (Sternberger & Sternberger, 1983; Nixon & Lewis, 1986; Lee et al., 1987; Nixon et al., 1987). NF phosphorylation typically occurs relatively late in postnatal brain development (Carden et al., 1987) and is likely to coincide with the final establishment of specific axonal pathways. Site specific phosphorylation or dephosphorylation within different polypeptide domains of each NF subunit is believed to play a key role in modifying NF size, morphology and dynamics, subunit polymerisation and exchange, axonal transport and interactions with other cytoskeletal proteins, especially in damage and disease states (Hisanaga & Hirokawa, 1990a; Sihag & Nixon, 1991).

For the NF subunits, major *in vivo* phosphorylation sites in the amino-terminal head domain have been identified within [Ser55 on NF-L and within a phosphopeptide starting at Ser44 on NF-M (Sihag & Nixon 1990, 1991)] or adjacent to [a phosphopeptide starting at Ser25 on NF-M (Sihag & Nixon, 1990)] the sequences essential for *in vivo* assembly. The phosphate on Ser55 of NF-L displays rapid turnover immediately following NF-L synthesis in neurons (Sihag & Nixon, 1991), suggesting that head domain phosphorylation may block premature assembly prior to transport in neurites. These sites are acted upon by kinases distinct from those associated with carboxy-terminal phosphorylation. The amino-terminal sites *in vitro* have been found to be targeted by second messenger dependent protein kinases including A kinase (Hisanaga et al., 1994) and the cyclic AMP dependent phospho-kinase, PK A (Dosemeci & Pant, 1992).

Addition of most phosphate groups to the tail region of the NF triplet subunits takes place after they enter the axon and it continues throughout their journey. Multiple isoforms of NF-H and NF-M result from their differential phosphorylation at carboxy-terminal sites (Lee et al., 1987). Carden and colleagues (1987) predicted that phosphorylation induced extension of the carboxy-terminal domains of NF-H and NF-M away from the NF backbone would increase the distance between NFs thereby making effective space occupying structural supports in large calibre axons. However, Hisanga and Hirokawa (1989) found that removal of 90% of carboxy-terminal phosphates on NF-H subunit had no effect on the extended configuration of the side arm. The carboxy-terminal phosphorylated sites are preferred substrates for the second messenger independent kinase(s) associated with NFs eg cyclin dependent kinase (Hisanaga et al., 1991).

Both the level and phosphorylation state of NF-H have also been proposed to regulate the rate of NF transport. Phosphorylation of the NF-H tail domain occurs following the entry of the NFs into the axon and increases during transport (Nixon et al., 1987). The extent of phosphorylation of the KSP repeat domain also correlates with the slowing of the transport rate (Nixon et al., 1994b). A proposed mechanism to account for this slowing phenomena associated with phosphorylation of NF-H is that the phosphorylated tail domain of NF-H acts as a cross bridge between NFs (Hirokawa et al, 1984; Hisanaga & Hirokawa, 1988).

The amino-terminal head region of both NF-L and NF-M isolated from rat spinal cord are also modified by glycosylation (Dong et al., 1993). Three of four identified sites lie in the amino-terminal head region, and all three are located within (Ser27 on NF-L and Thr48 on NF-M) or near (Thr21 on NF-L) the domain essential for *in vivo* NF assembly. Similar modifications are present in the NF-H head and tail although precise sites have not yet been identified (Dong et al., 1993). These results indicate that other post-translational

modifications, independent of phosphorylation, may also play important roles in NF assembly and function.

1.3 Cytoskeletal responses to injury

Components of the cytoskeleton, particularly MTs and NFs, have been shown to undergo a series of alterations in response to neuronal damage. Many of these changes are thought to be preparative for an attempt at adaptive sprouting or regeneration. The changes that occur are dependent on the cellular compartment in which the cytoskeletal component is situated and also the type and severity of the injury.

In the axon, mild injury resulted in focal NF misalignment, followed by organelle and NF accumulation with concomitant swelling, representing impaired axoplasmic transport (Pettus & Povlishock, 1996). In more severe trauma, however, NFs initially became compacted and lamination was maintained before misalignment and swelling occurred. From these studies it was concluded that NFs undergo a significant increase in packing density following injury which is likely to be due to the loss of carboxy-terminal domains from the NF-M and NF-H subunits (Pettus & Povlishock, 1996). It has been proposed that retrograde transport of these cleavage products (Schlaepfer, 1987) may act as feedback signals to the cell body where they may alter NF gene expression (Traub et al.,1985). Other more recent studies suggest that the NF compaction may be a result of dephosphorylation of the side-arms, not cleavage (Okonkwo et al., 1998).

Various other phosphorylation associated changes have been noted in the NF response to injury. Interestingly the reactive axonal swellings, bulbs, that occur post-injury can be labelled with antibodies to dephosphorylated NFs. These epitopes are normally expressed only in the soma and dendrites (Meller et al., 1993a, 1993b, 1994; King et al., 1997). In contrast phosphorylation-dependent NF epitopes, normally localised to the axonal domain (Sternberger & Sternberger, 1983), appear in the cell bodies of acutely damaged CNS and

PNS neurons (Moss & Lewkowicz, 1983; Dräger & Hofbauer, 1984; Goldstein et al., 1987; Rosenfeld et al., 1987; Shaw et al., 1988; Tetzlaff et al., 1988; Koliastos et al., 1989; Mansour et al., 1989; Klosen et al., 1990; Martin et al., 1990; Yamada & Hazama, 1993). In addition, accompanying injury, there is a generalised hypertrophy or accumulation of NFs within the cell bodies (Torvik, 1976; Schlaepfer, 1987; Silveira et al., 1994).

The terminals of physically injured neurons also exhibit NF associated changes. This cellular compartment, through the action of proteases such as calpains, is normally devoid of NFs (Schlaepfer, 1987). However, following injury there is a tendency for NFs to accumulate within the terminals of injured axons (Gray & Hamlyn 1962; Guillery, 1965). Inhibition of protease activity has also been shown to lead to an accumulation of NFs within synaptic terminals (Roots, 1983). These results suggest that post-injury calpains localised to this distal region are ineffective (Meller et al., 1993b).

The changes that occur post-injury to the other major component of the cytoskeleton, MTs, are quite different to those exhibited by the NFs. Trauma sufficient to compromise axolemmal permeability is linked with a dissolution (Maxwell et al., 1997) or reduction in number (Meller et al., 1987) of MTs within damaged axons. Phosphorylated tau has also been localised to damaged central neurons (Kanayama et al., 1997). Due to the role of this protein in mediating interactions between elements of the growth cone cytoskeleton (Ditella et al., 1994) this accumulation is thought to be linked to preparation for a regenerative attempt by the injured cell.

1.4 Pathological Hallmarks of AD

The cytoskeletal alterations that occur within neurons post-injury exhibit a striking similarity to many of the changes that occur in AD, particularly in the early stages of the disease process. Furthermore, there is distinct link between aspects of the cytoskeleton, such as NFs and MTs, and the development of a number of hallmarks of AD. AD is characterised by the presence of extracellular deposits of insoluble ß-amyloid protein as plaques, as well as intracellular cytoskeletal pathology, such as NFTs and DNs. The pathological mechanism linking these hallmark structures is yet to be defined, however, abnormal processing of both NFs and MTs have been implicated in playing a role in the development of both DNs and NFTs.

1.4.1 Plaques

The deposition of dense plaques of ß-amyloid in the brain is an accepted pathological hallmark of AD, however, there is considerable diversity of opinion regarding the significance of plaque formation to the aetiology of the disease. Plaques are extracellular structures with complex molecular and cellular components. Their major constituent is ß-amyloid, a peptide of 39-43 amino acids, 4 kDa, that is produced by proteolytic cleavage of the larger amyloid precursor protein (APP) by proteases referred to as ß- and γ- secretase (Glenner & Wong, 1984; Masters et al., 1985). Cleavage of APP at the amino-terminus is thought to be by ß-secretase and at the carboxy-terminus by γ -secretase (Haass et al., 1993a, 1993b). APP is a large membrane spanning glycoprotein expressed in a variety of cells (Selkoe et al., 1988). The physiological role of APP is unclear. It has been proposed to have roles in cell-cell or cell-matrix adhesion, trans-membrane signal transduction, growth factor-like activity for neural cells after secretion, neuronal development and protection against excitotoxicity (Breen et al., 1991; Masliah et al., 1992; Narindrasorasak et al., 1992; Arai et al., 1994).

APP occurs in numerous different isoforms, which arise from alternative splicing of a single gene. The shortest of the major isoforms (695 amino acids) is expressed almost exclusively in

neurons, whereas the other two common forms (751 and 770 amino acids, respectively) are expressed in both neural and non-neural cells. Additional heterogeneity of the APP polypeptides arises from their post-translational modifications, including sulphation, phosphorylation and both N- and O-linked glycosylation (Pahlsson et al., 1992, Tomita et al., 1998). These modifications occur during the trafficking of the protein through the secretory pathway. APP is co-translationally translocated into the endoplasmic reticulum via its signal peptide and then matured during passage through the Golgi by acquiring sulphate, phosphate and sugar groups, following which a minor percentage of mature molecules is transported to the plasma membrane via secretory vesicles. At the cell surface the APP molecules have a diverse metabolic fate.

Some APP molecules undergo proteolysis by an unidentified protease designated α-secretase, which cleaves between lysine 687 and leucine 688, releasing the large soluble ectodomain (α-APP). The remaining 10 kDa fragment can also undergo cleavage by γ-secretase to release a peptide known as p3 (Figure 1.2). Alternatively, initial cleavage of the APP molecule may occur after methionine 671, by ß-secretase, resulting in the secretion of a truncated APP molecule, ß-APP (Seubert et al., 1992). Finally, the remaining 12 kDa fragment may then undergo cleavage via γ-secretase within the hydrophobic domain at either valine 711 or isoleucine 713 that release the 40- or 42- residue ß-amyloid peptides respectively (Figure 1.2). Approximately 90% of secreted ß-amyloid peptides are Aß1-40, a soluble form of the peptide whereas approx 10% of secreted ß-amyloid peptides are Aß1-42 and Aß1-43. The latter two species are highly fibrillogenic, readily aggregated, and deposited early and selectively in amyloid plaques (Mann et al., 1995, 1997). Currently, the precise cellular origin of the ß-amyloid that forms plaques and the reason for its misprocessing and conversion to an insoluble state remains largely unknown.

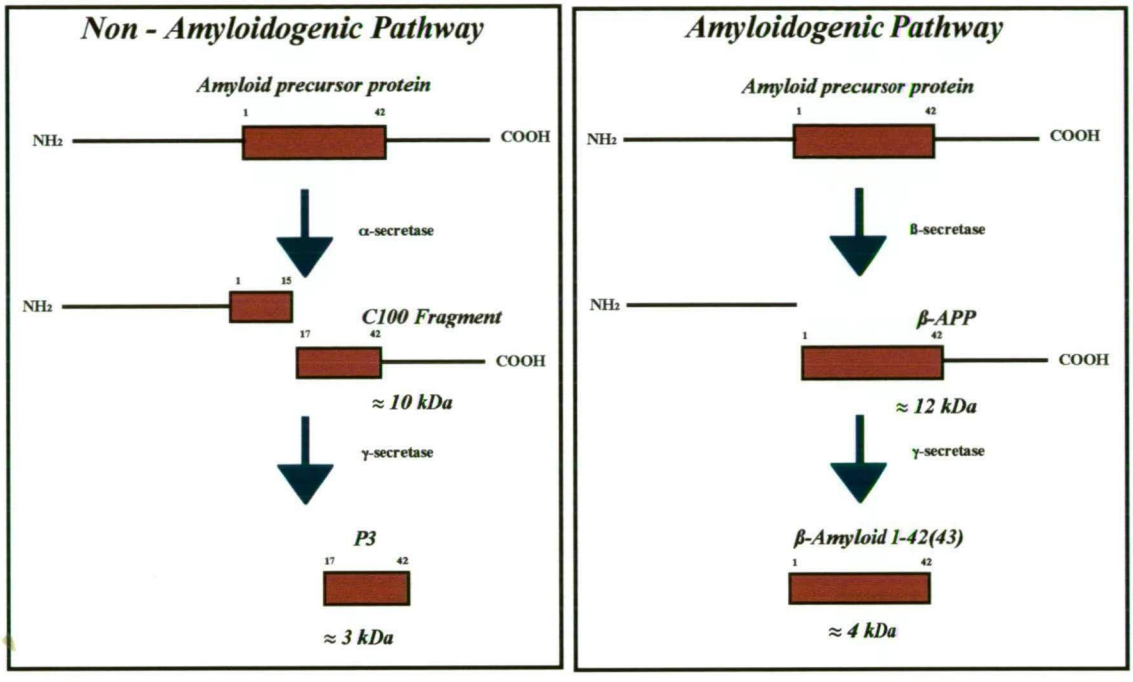

Figure 1.2

APP metabolism is illustrated in the above diagrams. The Non-Amyloidogenic Pathway illustrates the generation of p3 via the secretory pathway and the action of α- and γ- secretase. The Amyloidogenic Pathway shows the steps by which full-length Aß1-42 is produced in the endosomal-lysomal pathway through the action of β- and γ- secretase. Modified from Dickson, 1997.

The substance ß-amyloid has a number of characteristic biophysical properties, including high content of cross ß-pleated sheet and twisted fibrils 7.5 to 10 nm in diameter, at the ultrastructural level (Terry et al., 1964). Two major carboxy-terminal variants of ß-amyloid, Aß1-40 and Aß1-42(43), ending at Val40 and Ala42 respectively, have been identified in amyloid deposits in AD brain (Kang et al., 1987; Roher et al., 1993b). The major form of ß-amyloid produced during normal physiological metabolism of most cells is Aß1-40 (Haass et al.,1992). This is the most soluble of the peptides and is present in nanomolar concentrations in biological fluids (Seubert et al., 1992) including cerebrospinal fluid, plasma and urine. A shift to relatively greater production of Aß1-42 is apparently associated with significant pathology. This shift has been detected in cells of subjects with early onset AD (Scheuner et al., 1996) and in genetically engineered cells containing genes not associated with direct mutations of APP (Citron et al., 1997), which suggests that changes in the ratio of Aß1-42/Aß1-40 may be of fundamental importance to AD pathogenesis (Citron et al., 1997). It was also shown that Aß1-42 self aggregates into amyloid fibrils *in vitro* much faster than Aß1-40, suggesting that the carboxy-terminal properties of ß-amyloid determine its aggregation potential and are thus important factors underlying ß-amyloidogenesis (Jarret et al., 1993).

Immunocytochemical studies utilising antibodies directed to the various carboxy-terminal regions of ß-amyloid, demonstrate that more diffuse plaques are positive with antibody Aß1-42 than to Aß1-40, while dense-core plaques were equally labelled with both antibodies (Iwatsubo et al., 1994; Fukomoto et al., 1996). Based on these results, it has been proposed that either diffuse plaques represent an earlier stage of amyloid deposition and additional proteolytic events occur in dense-core plaques, or initial deposits of Aß1-42 serve as a nidus for the co-precipitation of the more soluble Aß1-40. Further to this, when investigating the chronological relationship regarding deposition of ß-amyloid protein species Aß1-40 and Aß1-42(43), in Downs syndrome brains using end-specific monoclonals that recognize both species, it was found that the ß-amyloid species initially deposited in the brain as plaques is Aß1-42(43) and Aß1-40 only appears a decade later (Iwatsubo et al., 1995). These

morphological observations were supported by protein analysis which revealed the most abundant peptide to be Aß1-42 (Roher et al.,1993a), while similar analyses from brains with mostly diffuse amyloid revealed abundant Aß17-42 (Gowing et al., 1994).

Whether APP, from which the ß-amyloid protein of neuritic plaques derives, is synthesised by neurons (Probst et al., 1991; Papolla et al., 1992), by other brain cells (Siman et al., 1989) or is derived from a systemic source (Selkoe, 1989) remains controversial. Recent studies, using rat hippocampal neurons and human NT2N neuronal cell lines show that ß-amyloid appears to be produced in endosomes or late Golgi: the endoplasmic reticulum is a site for production of Aß1-42 (Cook et al., 1997; Hartmann et al., 1997). Considerable evidence supports a model in which APP, internalised from the plasma membrane, is subject to ß-secretase cleavage within the late Golgi or endocytic compartments. Subsequently, γ-secretase cleavage of the residual approx 100 amino acid, membrane-bound fragment within the transmembrane domain leads to the formation and release of ß-amyloid into the extracellular space (Koo et al., 1996).

A large array of other molecules have been found to interact with ß-amyloid both *in vitro* and *in vivo*. These include α-1-antichymotrypsin, albumin, apoE, apoJ, apoA-I, serum amyloid P, complement components, laminin, transglutaminase, heat-shock proteins, acetylcholinesterase, gangliosides and proteoglycans (Terry et al., 1994; Dickson, 1997). In addition ß-amyloid fibrillar aggregates can also act as a nidus for the recruitment of astrocytes and microglia.

The majority of plaques in AD can be classified into four morphological types: diffuse, primitive, classic and compact or dense-cored. These plaques differ not only in their morphology but also in their association with other cell types and pathological inclusions such as PHFs, and the region of the brain in which they are predominantly located. Two hypotheses have been proposed to explain the formation of these plaque types. Firstly, that one type of plaque is converted into another, ie that the four plaque types represent stages in

the life history of a single type of plaque (Ikeda et al., 1990). Secondly, that each plaque type evolves independently of the others and, therefore, unique factors are involved in their formation (Armstrong, 1998). The subset of ß-amyloid plaques that are associated with reactive microglia and astrocytes and dystrophic neuritic processes (Terry et al., 1994; Dickson, 1997) are referred to as neuritic plaques. Neuritic plaques may occupy as much as 10% of the volume of the cortex in patients with AD (Verano et al., 1990). Within these neuritic plaques there is pronounced loss of synapses and severe distortion of those that remain (Masliah et al.,1990, 1991a,1991b).

The presence of plaques in the neocortex of apparently non-demented elderly persons is often accepted as part of normal aging (Arrigada et al., 1992b), therefore, making the determination of the pathological significance of such structures difficult. Other investigators suggest that because cerebral deposition of ß-amyloid may be a key mechanism in the development of AD, the presence of ß-amyloid containing plaques may represent presymptomatic or unrecognised early symptomatic AD (Morris et al., 1996, 1991; Price & Morris, 1999). Cases exhibiting this early pathology have been rated 0.5 on the Washington University Clinical Dementia Rating (CDR) scale (Berg, 1988), by which a CDR score of 0 indicates no cognitive impairment and a CDR score of 0.5, 1, 2 or 3 indicates questionable, mild, moderate, or severe dementia, respectively. The length of such a preclinical phase is likely to vary between individuals, and may be influenced by genetic susceptibility factors as well as environmental influences.

1.4.2 Neurofibrillary tangles

Profound cytoskeletal changes occur in neurons and their processes in AD. Accumulations of straight and paired helical filaments, in the cell bodies of neurons, predominantly perinuclear region, closely encircling the nucleus, results in the formation of another of the pathological hallmarks, the NFT. Similar filaments in neuronal cell processes are referred to as neuropil threads (Braak et al., 1986; Braak & Braak, 1988). The filamentous NFT structure is highly

insoluble, therefore, another pathological correlate of AD is the presence of intracellular PHF accumulations and ghost or tombstone tangles in the extracellular space after nerve cell death has occurred.

PHF are composed of filaments approximately 15 nm in diameter, and, when paired they have an average period of 160 nm and a maximum width of 24 nm (Kidd, 1964; Wisniewski et al., 1976). Using initially immunocytochemical based investigations (Grundke-Iqbal et al., 1986a; Kosik et al., 1984) and later conclusively by protein chemical techniques (Wischik et al., 1988; Lee et al., 1991) these abnormal fibrous structures have been shown to contain the microtubule associated protein, tau. In a normal neuron, tau promotes MT assembly and stabilisation. PHF-tau differs from normal adult tau by containing a higher proportion of isoforms encoded by transcripts with exon 3, having fewer isoforms and displaying a more acidic isoelectric charge (Ksiezak-Reding et al., 1990). In solution, normal tau lacks secondary structure or defined shape, however, it tends to associate into antiparallel dimers, and in this form may be prone to assembly into PHF (Wille et al., 1992).

Tau isolated from soluble PHFs is extensively and abnormally phosphorylated compared to normal tau at both Ser/Thr-Pro and non-Ser/Thr-Pro sites (Grundke-Iqbal et al., 1986b; Morishima-Kawashima et al., 1995). Interestingly, many of the same sites are also phosphorylated in foetal tau (Goedert et al., 1993; Morishima-Kawashima et al., 1995). In 1980, Jameson and collegues presented data suggesting that increasing the phosphorylation state of MAPs decreases their ability to promote MT assembly. Since this, subsequent studies have indicated that the phosphorylation of specific sites, rather than the overall extent of phosphorylation, is the important factor in modulating the ability of tau to bind MTs and promote microtubule assembly (Johnson et al., 1992; Drewes et al., 1995). Although the hyperphosphorylation of tau in both soluble and insoluble PHFs is well documented, the relationship between abnormal phosphorylation of soluble cytosolic tau and the formation of insoluble PHFs is unclear at present. Other investigators have suggested that the majority of

PHF-tau may not be abnormally phosphorylated (Wischik et al., 1995), particularly in the early stages of neurofibrillary pathology (Bondareff et al., 1995) and that phosphorylation may in fact protect tau from aggregation (Schneider et al., 1999).

The pathogenesis of AD has been shown to not only involve the abnormal hyperphosphorylation but also the glycosylation (the enzymatic covalent attachment of carbohydrates) of tau in PHFs. Unlike normal tau, the abnormally phosphorylated tau is glycosylated. The glycan(s) maintain the helically of PHFs, but does not have any apparent direct effect on the ability of tau to promote the assembly of MTs. Removal of glycans by enzymatic deglycosylation converts PHFs into bundles of straight filaments (Wang et al., 1996).

Immunological studies have shown localisation of variety of different proteins with the NFT structure. These include NF-M and NF-H subunits (Dahl et al., 1982; Perry et al., 1985; Cork et al., 1986; Haugh et al., 1986; Miller et al., 1986), tubulin (Schwab & McGeer, 1998) vimentin (Yen et al., 1983), MAP2 (Kosik et al., 1984), tau (Grundke-Iqbal et al., 1986a), ß-amyloid (Masters et al., 1985), lactotransferrin (Kawamata et al., 1993), amyloid-P component (Duong et al., 1989) and ubiquitin (Perry et al., 1987; Bancher et al., 1989, 1991). However, such studies suffer from the inherent inability to distinguish between molecules that form an integral part of the PHF and material that is associated with or adheres to the filamentous structures. This problem is compounded by the fact that some antibodies used to label NFs have been shown to cross-react with tau (Ksiezak-Reding et al., 1987; Nukina et al.,1987), thereby making it difficult to determine the extent to which this class of IFs is incorporated into the NFT structure.

Despite this controversy, abnormal phosphorylation of NF proteins has been proposed to be an important prerequisite for the formation of NFTs. Utilising antibodies that were developed against differentially phosphorylated NF proteins (Sternberger & Sternberger 1983; Cork et

al., 1986; Lichtenberg-Kraag et al.,1992) it has been shown that an abnormal accumulation of dephosphorylated NFs corresponds to a subcomponent of the early forms of NFTs. This labelling was shown to be distinct from parts of the structure labelled with either antibodies to tau or stained with thioflavine S (Vickers et al., 1992b, 1994b). Other groups have also shown that antibodies to NF proteins that do not cross-react with tau, label NFTs (Lee et al., 1988b; Zhang et al., 1989; Schmidt et al., 1990; Nakamura et al., 1997). Further to this, there is strong evidence that neurons containing the NF triplet protein, in association neocortices as well as medial temporal lobe structures, show a high degree of vulnerability to develop NFTs (Vickers et al., 1992b, 1994b) and degenerate (Morrison et al., 1987; Hof et al., 1990; Hof & Morrison, 1990). The cortical neurons that contain this cytoskeletal protein are principally a subset of pyramidal neurons in layers II, III and V (Morrison et al., 1987; Campbell & Morrison, 1989; Hof et al., 1990; Hof & Morrison, 1990; Vickers & Costa, 1992; Hiscock et al., 1998) and connectivity studies in non-human primates have shown that they provide specific corticocortical projections (Campbell et al., 1991; Hof et al., 1995). Cortical neurons that lack the NF triplet, such as inhibitory interneurons immunolabelled for specific calcium-binding proteins, do not develop NFTs and show relatively lower susceptibility to degeneration in AD (Ferrer et al., 1991; Hof & Morrison 1991; Hof et al., 1991a, 1993; Fonseca & Soriano, 1995; Sampson et al., 1997). Cumulatively, these results suggest a role for NFs in the formation of the NFT structure.

It has been suggested that the density of NFTs may be a better correlate of dementia severity than the density of plaques (Arriagada et al., 1992a; Bierer et al., 1995; Berg et al., 1998). Further to this, data accumulated by Thal and collegues (1998) show that neuronal cytoskeletal alterations progressively increase with advancing dementia until the end stage of AD in contrast to the frequencies of plaques and cortical microglial cells, and are, therefore, preferable for staging. Many of the cytoskeletal alterations occurring in NFTs have also been identified in the abnormal neuritic processes or DNs associated with plaques. Because NFT,

DNs and neuropil threads contain these similar filamentous constituents, it is likely that the genesis of these inclusions is the result of common mechanisms.

1.4.3 Dystrophic Neurites

A widely recognised pathological phenomenon in AD research is the association between degenerating cell processes, or DNs, and the ß-amyloid plaque (Hof & Morrison, 1994). The precise neuronal alterations that lead to DN formation are unknown, and it is not clear as to whether they represent abnormally sprouting dendrites or axons or some combination of both. Currently the balance of evidence suggest that they represent altered, probably abnormally sprouting axons (Masliah et al., 1993a; Praprotnik et al., 1996; Vickers et al., 1996).

Although DNs occur independently in the aged brain, in sites such as dorsal column nuclei in the lower medulla, the pars reticularis of the substantia nigra, the ventral pallidum, the cortex of the limbic lobe and the amygdala, they are concentrated in the vicinity of ß-amyloid plaques. Dystrophic type neurites are found not only in neuritic plaques in AD, but also in aged humans and other mammals (Tekirian et al., 1996) and in plaque-bearing APP transgenic mice (Masliah et al., 1996a), however, PHF-tau immunoreactive neurites are specific to humans and highly characteristic of AD (Dickson et al.,1988).

The heterogeneous nature of the epitopes expressed in DNs and the variable morphology of these abnormal structures has been noted by a number of investigators. The differential expression of these types of DNs throughout the course of AD is of particular interest as it provides clues as to the pathogenic mechanisms that may be involved in the development of this pathological structure. Reports have indicated that DNs may be distinguished by either tau- or NF- abundant forms (Dickson et al., 1988; Masliah et al.,1993b; Vickers et al.,1994b; Su et al., 1996). Similarly, some synaptic markers, and the APP are present in DNs that lack either NFs or tau (Yasuhara et al., 1994; Wang & Munoz, 1995; Saunders et al., 1998).

Recent investigations have shown that the occurrence of PHF-tau immunoreactive DNs as well as neuritic plaques are highly correlated with the severity of dementia in AD (Dickson et al., 1995; Cummings et al., 1996b). NF-triplet proteins have also been demonstrated in DNs (Dickson et al., 1988; Arai et al., 1990; Cras et al., 1991; Schmidt et al, 1991; Masliah et al., 1993b; Schmidt et al., 1994; Vickers et al., 1994b; Su et al., 1996, Nakamura et al., 1997; Su et al., 1998). Further to this, it has been shown in AD cases that NFs are present in a subset of plaque-associated abnormal neurites that are largely distinct from those that are labelled with tau antibodies and stained with thioflavine S (Dickson et al., 1988; Masliah et al., 1993b; Vickers et al., 1994b; Su et al., 1996, 1998; Nakamura et al., 1997). Studies have concluded that early DN forms are associated with profound neurofilamentous changes in the absence of tau abnormalities (Vickers et al., 1996). Others have indicated that significant tau pathology is a relatively late event in DN formation (Benzing et al., 1993; Su et al., 1996).

Accumulation of APP in DNs associated with ß-amyloid plaques has been noted by a number of investigators (Perry et al., 1988; ; Ghiso et al., 1989; Ishii et al., 1989; Cras et al., 1990; Shoji et al., 1990; Cole et al.,1991; Cras et al.,1991; Joachim et al., 1991; Martin et al., 1994; Yasuhara et al., 1994; Wang & Munoz, 1995; Zhan et al., 1995; Saunders et al., 1998). Findings suggest that APP accumulations in plaque associated neurites occurs prior to tau accumulation and is therefore more closely related to the appearance of neuritic dystrophy (Ishi et al., 1989; Cummings et al., 1992; McGeer et al., 1992).

The DNs in many neuritic plaques have also been observed to be labelled by anti-synaptophysin or anti-chromagranin A (CgA) antibodies (Masliah et al., 1989; Brion et al., 1991). It has been hypothesised by Brion and collegues that as synaptic vesicles, like other membranous organelles, move along MTs (fast neuroplasmic transport), their accumulation in abnormal plaque neurites might be indicative of axoplasmic flow disturbances in these neurites. Others have suggested, based on the localisation of such synaptic markers and growth associated proteins such as GAP43 to plaque associated DNs (Masliah et al., 1991b),

that abnormal neurites in plaques exhibit sprouting phenomena (Probst et al., 1983; Geddes et al., 1986). Antibodies to ubiquitin have also consistently been shown to detect DNs in AD cases (Perry et al., 1987). Current studies suggest that one of the major functions of ubiquitin is its involvement in protein degradation. Localisation of this protein to DNs has been suggested to indicate that the degradative pathway may be ineffective in removing these pathological structures in the AD brain (Perry et al., 1987).

Central to the understanding of DNs is determining how the deposition of ß-amyloid protein either leads to or is related to these lesions. While our knowledge of both ß-amyloid protein, tau and the other components of neurofibrillary pathology has vastly expanded, the relationship between the pathological lesions of AD remains elusive.

1.5 Mechanisms of AD pathogenesis

1.5.1 Amyloid cascade hypothesis

A common viewpoint is that the central pathological event in AD is the deposition of ß-amyloid as amyloid fibrils within plaques and cerebral blood vessels (Selkoe, 1994). The finding of accumulations of ß-amyloid in the cortex of non-demented individuals (Morris et al., 1991, 1996) in the absence of neurofibrillary changes has lead to the conclusion that depositions of amyloid precedes the development of other pathological changes. This assumption is the basis of the amyloid cascade hypothesis.

There are a number of lines of evidence on which this hypothesis is based. Cerebral ß-amyloid deposition is an invariant feature of AD, and the form of ß-amyloid deposit which is associated with the neuritic plaques is substantially more abundant in the brains of AD cases when compared to age matched control brains (Haass et al.,1992; Roher et al., 1993a; Gowing et al., 1994; Scheuner et al., 1996). In further support of the hypothesis is the finding that at least two genetically defined forms of AD appear to be caused by specific mutations in the APP gene, altered APP metabolism or expression and subsequent accelerated ß-amyloid

deposition (Selkoe, 1994). Finally, it is claimed that other than ß-amyloidosis, no compelling pathogenetic agent that can be said to be etiologic for AD has emerged.

Amongst those investigators that support the amyloid-cascade hypothesis, there is a lack of consensus regarding the mechanism by which ß-amyloid kills neurons. Some progress has been made in studying the toxic effects of ß-amyloid in cell cultures which induces the generation of DNs (Pike et al., 1992). Proposed mechanisms include toxicity mediated by; induction of reactive oxygen species (Behl et al., 1994), activation of microglia (Meda et al., 1995), its stimulation of tyrosine phosphorylation of focal adhesion kinase (Zhang et al., 1994), inhibition of surface phosphorylation by protein kinase C (Hogan et al., 1995), inhibition of ubiquitin-dependent protein degradation (Gregori et al., 1995), induction of inflammatory responses (London et al., 1996) or enhancement (Arias et al., 1995) or inhibition of neurotransmitter release (Kar et al., 1996). Further controversy exists as some investigators suggest the mechanism of neuronal death exerted by the toxic ß-amyloid is apoptotic whilst others propose a necrotic pathway (Suzuki, 1997; Gervais et al., 1999).

A number of criticisms have been directed towards the *in vitro* models of amyloid toxicity. A primary concern is that the concentration of amyloid used in almost all of the *in vitro* neurotoxic studies has been between 1 and 100 µg/ml, which is as much as 10 000 times the concentration of total ß-amyloid in the human CSF (Neve & Robakis, 1998). Further problems concern the specificity of the assays utilised. Most of the toxicity studies have utilised peptides that might behave differently from peptides generated *in vivo*. Interestingly, experiments in which neurons were grown on brain tissues from AD patients showed that neuronal survival was the same as that for controls (Carpenter et al., 1993). In addition, cortical and hippocampal neurons grew without inhibition on ß-amyloid depositions formed from synthetic ß-amyloid peptide. Finally, if ß-amyloid exerts a widespread toxic effect, then a falling gradient of damage from plaque out into neuropil might be expected, but such a gradient has not been seen (Terry et al., 1991). Evidence of amyloid toxicity has not been

satisfactorily revealed *in vivo* despite frequent *in vitro* demonstrations. Consequently the mechanism by which ß-amyloid exerts its effects in AD remains controversial.

1.5.2 Cytoskeletal hypothesis

In contrast to the amyloid hypothesis, others investigators believe ß-amyloid deposition is incidental and does not correlate with disease progression (Arriagada et al., 1992a; Terry, 1996). Furthermore, neuronal pathology such as NFTs, which are neuroanatomically localised to the areas of the brain affected by AD, are more likely to be the primary event of the disease leading to dementia (Arnold et al., 1991).

The theory that neuritic dystrophy precedes ß-amyloid deposition is, however, less popular. Evidence in favour of this hypothesis is that DNs can be seen in primates (Martin et al., 1994) and in young Downs Syndrome brains (Mattiace et al., 1991) before ß-amyloid is detected. It is also clear that neuronal changes similar to those in neuritic plaques can be detected in the aged brain in certain locations completely independent of amyloid. These sites include the dorsal column nuclei in the lower medulla, the pars reticularis of the substantia nigra, the ventral pallidum, the cortex of the limbic lobe and in the amygdala (Dickson et al., 1990).

As mutations of the APP gene are associated with fewer than one tenth of one percent of Alzheimer patients, and all four of the AD related genes that have been identified interact by various means with the cytoskeleton, Terry (1996) proposed a mechanism by which alterations in the cytoskeleton are the pathological initiating factor in AD. He suggests that dementia is the result of an initial deficiency in polymerised MTs, due the formation of PHF-tau. This destabilisation of the cytoskeleton, particularly the microtubular system in the perikaryon causes breakdown of the Golgi apparatus into small fragments which will have an effect on processing and targeting of proteins and, thus, on the processing of APP. This abnormal processing may well lead to abnormal amounts of ß-amyloid which is subsequently deposited in the extracellular space. The loss of MTs would have a major effect on axoplasmic

flow, resulting in diminished supply of substrate to the distant terminals in axons and dendrites and, therefore, the formation of dystrophic changes in the from of synaptic loss and degeneration, disconnection and finally dementia.

Although there is considerable evidence supporting both the amyloid cascade hypothesis and alternative cytoskeletal based systems as mechanisms for AD, enough definitive evidence is yet to be presented for either case. AD is likely to be a multi-factorial disease which should be approached from many perspectives, however, lack of consensus regarding the proposed mechanisms suggests that important aspects of the disease remain elusive.

1.6 Risk factors for AD

Although the pathological mechanisms linking the hallmarks of AD is yet to be clearly defined a number of risk factors have been outlined. The two best investigated are increased age and a positive family history.

1.6.1 Aging

Age is the single most important risk factor for dementias of all kinds including AD. Approximately 95% of cases of AD occur in individuals >60 years of age (Katzman & Kawas, 1994). All studies conducted to date consistently indicate a steep increase in both prevalence and incidence of AD with age. The age-specific prevalence of AD is generally higher for women than for men, which implies that specific gender-related hormones may also have an effect on AD development (Katzman & Kawas, 1994).

1.6.2 Genetic

A significant proportion of AD cases are termed familial AD (FAD) due to their genetic aetiology. 'Causative' gene defects have been identified in three early onset (<60 year) FAD genes located on chromosome 1, 14 and 21. Chromosome 21 contains the gene for APP. Six different mutations have been identified in the APP gene of FAD cases, however, overall these

mutations are responsible for only a small proportion (2%) of all FAD cases published. The majority of early-onset FAD cases have been associated with mutations in two novel genes which have been termed presenilin 1 (PS1) on chromosome 14 and presenilin 2 (PS2) on chromosome 1 (Table 1). Early-onset FAD accounts for about 5-10% of all cases and is notable clinically for its highly aggressive nature with early age at onset (typically <60 yrs), shorter duration of survival, and more prominent myoclonus, seizures, and aphasia (Jacobs et al., 1994). In 1993 Allen Roses and colleagues identified Apoε4, the allele encoding the protein ApoE4, as a 'susceptibility' gene for late-onset (>60 yrs) AD.

-APP

The APP gene encompasses approximately 400 kb of deoxyribonucleic acid (DNA), contains 19 exons, and encodes several alternatively spliced APP mRNA. The localisation of this gene to chromosome 21 appeared to explain the observation that patients with trisomy 21 (Down's syndrome) incur ß-amyloid deposits and develop classical AD neuropathology at a relatively early age (eg 4^{th}-5^{th} decade of life) (Mann et al., 1989; Iwatsubo et al., 1995). Close genetic examination of this gene in families with autosomal dominant AD resulted ultimately in the identification of six different missense mutations in APP, five associated with FAD (Chartier-Harlin et al., 1991; Goate et al., 1991; Murrel et al., 1991; Hendricks et al., 1992; Mullan et al., 1992) and one with the neuropathologically related syndrome of hereditary cerebral haemorrhage with amyloidosis of the Dutch type (Levy et al., 1990) (Figure 1.3). APP mutations in FAD families display a complete penetrance in that they cause dementia in every individual carrier. Mutations in the gene encoding APP have been shown to either cause an elevated production of total ß-amyloid (Citron et al., 1992; Cai et al., 1993; Citron et al., 1994) or an increase in the more fibrillogenic Aß1-42 (Suzuki et al., 1994; Tamaoka et al., 1994).

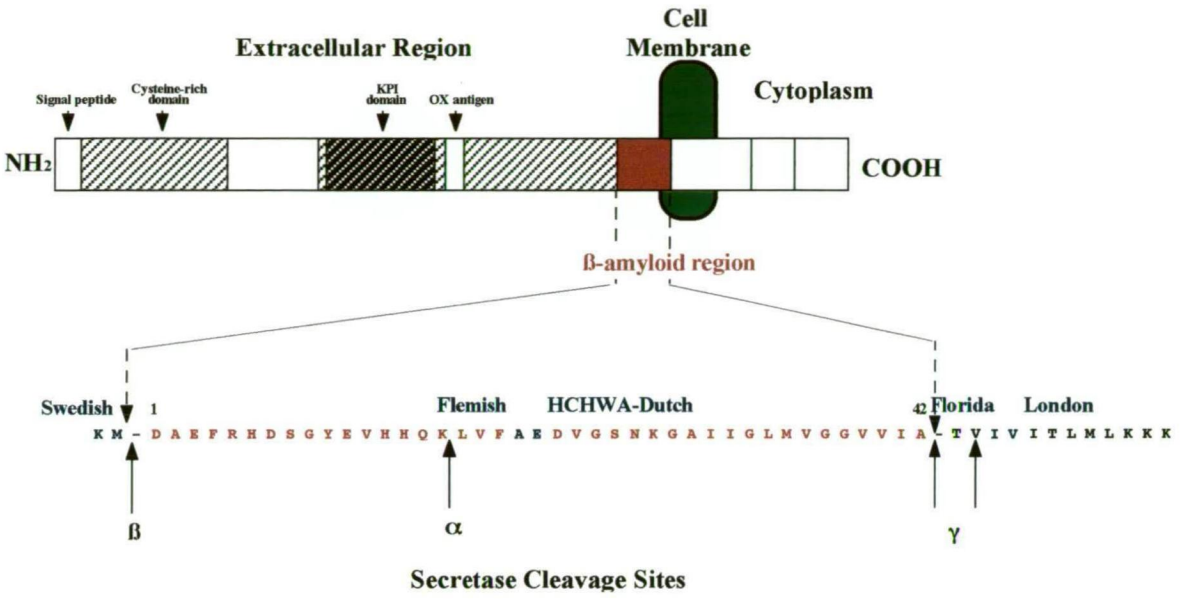

Figure 1.3

Schematic diagram of the membrane spanning, multi-domain glycoprotein APP (isoform 770 as indicated by the presence of both the Kunitz protease inhibitor domain (KPI) and the additional OX domain spliced into the extracellular region. The ß-amyloid peptide region (red box) contains part of the transmembrane domain and part of the extracellular domain of APP. The six missense mutations identified within the APP molecule, five associated with FAD and the sixth the related disease of hereditary cerebral haemorrhage with amyloidosis of the Dutch type, are indicated in blue. The proteolytic cleavage sites, and their associated enzymes, are represented by the vertical black arrows at the bottom of the diagram. Modified from Kwok, 1998.

Table 1.1

Familial AD mutations

Chrom.	Mutation	Biochemical Cause	Molecular effect	Age of onset
21	$APP_{670/671}$ (Swed)	Potentiation of ß-secretase	Increased Aß1-42(43) and Aß1-40 production	50s
	APP_{692} (Flemish)	Inhibition of α-secretase	Increased Aß1-42(43) production	
	APP_{716} (Florida)	Alteration of γ-secretase cleavage site	Increased Aß1-42(43) production	
	APP_{717} (London)	Alteration of γ-secretase cleavage site	Increased Aß1-42(43) production	
14	PS1 mutations	Alteration of APP processing	Increased Aß1-42(43) production	40s and 50s
1	PS2 mutations	Alteration of APP processing	Increased Aß1-42(43) production	50s
19	ApoE4 polymorphism		Increased ß-amyloid plaque density	60s and older

(Chartier-Harlin et al., 1991; Goate et al., 1991; Murrel et al., 1991; Mullan et al., 1992; Hendricks et al., 1992; Strittmatter et al., 1993a; Haas et al., 1994; Levy-Lahad et al., 1995; Rogaev et al., 1995; Sherrington et al., 1995)

The clinical and neuropathological characteristics of patients with FAD-related APP mutations share several features, including onset typically before 60 years of age (mean family onset between 43-55 years), autosomal-dominant inheritance fully penetrant by the early 60s, and clinical and pathological phenotypes indistinguishable from individuals with sporadic AD. Although APP mutations are virtually 100% penetrant, mutations in this gene are responsible for only a small proportion of all published cases of early onset FAD.

-Presenilins

The discoveries that the APP and ApoE genes were implicated in the early-onset and late-onset forms of familial AD, respectively, left open the question of which genes could explain the large majority of early-onset AD cases. Linkage analysis, followed by positional cloning lead to the identification in 1995 of two highly homologous FAD genes, PS1 and PS2 located on chromosomes 14 and 1, respectively (Levy-Lahad et al., 1995; Rogaev et al., 1995; Sherrington et al., 1995). The PS1 and PS2 genes encode predicted proteins of 463 and 448 amino acids, respectively. These proteins are 67% identical and are ubiquitously expressed, however, their normal function is not yet known. Recently, however, it has been hypothesised that PS proteins regulate APP processing. This theory is supported by studies showing that the normal cleavage of APP is dependent upon the expression of PS1 (De Strooper et al., 1998, 1999).

Both PSs are serpentine proteins with six to nine predicted transmembrane domains arranged as one large and several small hydrophilic loops (Figure 1.4). Although unknown, they could conceivably function as receptors, ion channels or pores, or intracellular membrane proteins with specific functions. *In situ* hybridisation experiments, have demonstrated that the expression patterns of PS1 and PS2 in the brain are extremely similar to each other and that messages for both are primarily detectable in neuronal populations. Immunochemical analyses indicate that PS1 and PS2 are similar in size and are localised to similar intracellular compartments (endoplasmic reticulum and golgi complex) (Kovacs et al., 1996). These

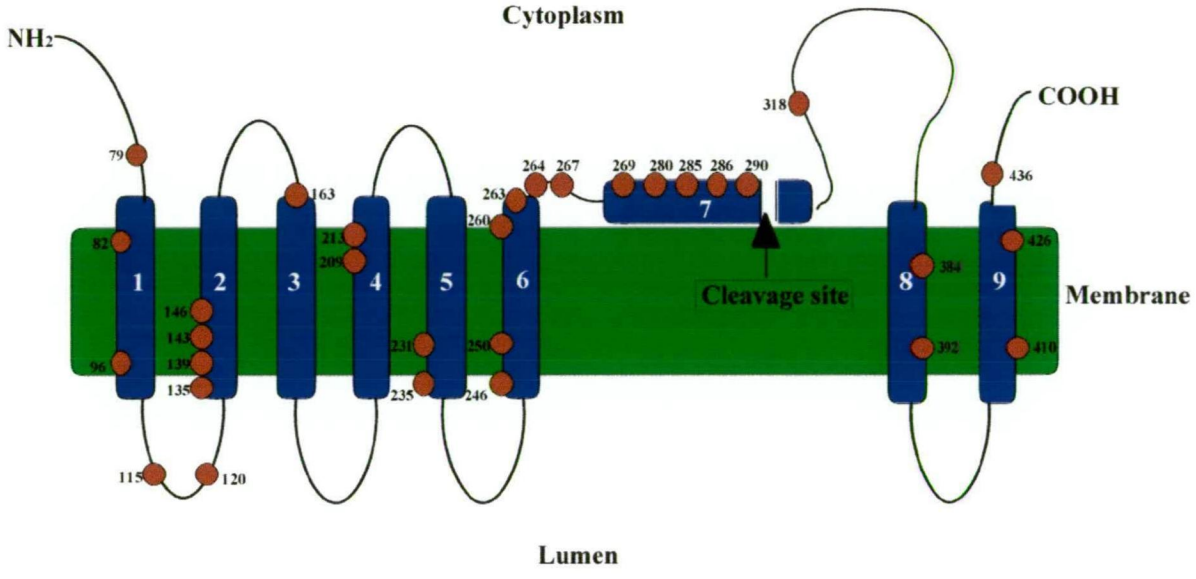

Figure 1.4

Schematic diagram of the predicted structure of PS1. Immunocytochemical analysis has indicated that both the amino- and carboxy-terminal ends of both the PS1 and PS2, as well as a portion of the large hydrophillic loop, projects into the cytosol of the cell. The pathogenic mutations in the PS1 gene are indicated by red circles. Regions of major clusters of missense mutations are located in transmembrane domain 2 and on the amino-terminal side of the normal proteolytic cleavage site. Modified from Kwok, 1998

findings are consistent with roles for both PS1 and PS2 in facilitating the processing and /or intracellular trafficking of proteins undergoing post-translational modification in the endoplasmic reticulum and Golgi complex. Recently it has been suggested that the PSs may traffic proteins such as APP and Notch to the appropriate cellular site where γ-secretase acts (Hardy & Israel, 1999).

At least 41 mutations in PS1 and two in PS2 have been identified in FAD kindred (Hardy, 1997; Kwok, 1998). With one exception, all of the PS1 and PS2 mutations are missense mutations that result in a single amino acid substitution. The age of onset of AD in families harbouring PS1 mutations is quite young, ranging from 29-56 years, whereas the age of onset in cases with PS2 mutations is somewhat older (40+ years). The vast majority of these mutations occur in or immediately adjacent to transmembrane domains.

Tanzi and coworkers (1997) have shown that, in the case of PS2, the carboxy-terminal fragment is found in detergent insoluble fractions, suggesting a cytoskeletal association. This finding raises the possibility that PS cytoplasmic domains may interact with the cytoskeleton, which could influence, for example, vesicle trafficking and endoplasmic reticulum calcium regulation. In addition Busciglio and collegues (1997) described an association between the carboxy-terminal fragment of PS1 and NFTs, also indicating an interaction between the PSs and the cytoskeletal elements (possibly tau protein) in AD.

There are, at present, three main hypotheses as to how mutations in the genes encoding the PSs contribute to AD pathology: 1) PS mutations result in altered APP processing and increased levels of ß-amyloid and/or the 1-42 form of ß-amyloid, 2) PS mutations promote apoptotic cell death pathways by enhancing levels of oxidative stress and 3) PS mutations cause aberrant subcellular calcium regulation which promotes excitotoxic and apoptotic cascades. These hypotheses are not mutually exclusive and may all prove to be more or less, correct.

Mutations in all three of the known pathogenic genes, the APP gene, PS1 gene and the PS2 gene have in common the fact that they alter APP processing such that an increased amount of Aß1-42(43) is produced (Citron et al., 1992; Cai et al., 1993; Citron et al., 1994; Suzuki et al., 1994; Tamaoka et al., 1994; Scheuner et al., 1996; Citron et al., 1998; Mehta et al., 1998; De Jonghe et al., 1999). These data provide the strongest possible evidence that the amyloid cascade hypothesis for the etiology and pathogenesis of AD is fundamentally correct. With regard to prevalence rates, mutations in the APP and PS genes clearly do not account for all cases of early onset FAD. A subset of early onset FAD is still genetically unaccounted for by known defects in these genes (Cruts et al., 1998). Recently two other candidate AD genes, alpha-1-antichymotrypsin (Kamboh et al., 1995) and bleomycin hydrolase (Montoya et al., 1998) have been reported to predispose to increased risk for AD perhaps by operating in conjunction with other mutations. The candidacy of both these genes as AD loci awaits further testing and confirmatory studies.

-ApoE

Apolipoproteins, in general, are lipid carrier molecules that serve a variety of functions throughout the body, including maintenance of the structure of lipoprotein particles and regulation of the metabolism of several different lipoproteins. Apolipoprotein E (ApoE), in particular, is unique among the apolipoproteins in that it has a special relevance to nervous tissue. The mature form of ApoE, present in human plasma and cerebrospinal fluid, is a single glycosylated 37 kDa polypeptide composed of 299 amino acids. ApoE mRNA is most abundant in the liver, followed by the adrenal glands and brain.

There are three allelic variants of the ApoE gene (ε2, ε3 and ε4) located at chromosome 19, each encoding a different isoform of ApoE inherited in a co-dominant fashion at a single genetic locus. The ApoE3 isoform has a cysteine at position 112 and an arginine at position 158; ApoE4 has arginine at both positions; and ApoE2 has cysteine at both positions. The ε3

allele is most common in the general population, found in approximately 78% of people, whereas the ε4 allele is found in approximately 15% and the ε2 allele in approximately 7% (Mahley et al., 1988). Epidemiological studies found that 1) carriers of the ε4 allele have an increased risk of developing AD in an allele dose-dependent manner (Corder et al., 1993), 2) the ApoE ε4 genotype decreases the age of onset of the disease, and finally 3) the inheritance of the ε4 allele correlates with increased deposition of ß-amyloid in blood vessels and plaques and a greater density of neuritic plaques in the cerebral cortex (Rebeck et al., 1993; Schmecel et al., 1993; Corder et al., 1994). Further to this, it has also been demonstrated that inheritance of the ε2 allele decreases the risk, and increases the age of onset, of AD (Corder et al., 1994). Although the ApoE genotype can indicate a degree of susceptibility, the ε4 allele is 'neither necessary nor sufficient to cause disease'. This is illustrated by the large percentage (approximately 50%) of individuals who develop AD without having inherited the ε4 allele and the observation that a number of very elderly individuals are cognitively and neuropathologically normal despite inheriting that gene (Rebeck et al.,1994; Blacker 1997). This susceptibility, however, can be further compounded by other AD risk factors including age and a history of head trauma (Mayeux et al., 1995).

Several lines of evidence, independent of genetic associations, have implicated the actual protein ApoE in the pathology of AD. Immunohistochemical studies have shown that ApoE is localised to the pathological hallmarks of AD such as ß-amyloid plaques (Wisniewski & Frangione, 1992; Kida et al., 1994; Gearing et al., 1995; Sheng et al., 1996) and NFTs (Benzing & Mufson, 1995; Han et al., 1994) and might promote ß-amyloid induced fibrillogenesis and microglial activation (Wisniewski et al., 1993; Barger & Harmon, 1997). Various mechanisms have been proposed to account for these interactions and suggest means by which inheritance of the ε4 allele increases the risk of AD development.

A number of mechanisms have been proposed by which the ApoE4 isoform may affect amyloid deposition. Both E3 and E4 isoforms were found to bind synthetic ß-amyloid, forming a complex that resisted dissociation by boiling in SDS (Sodium Dodecyl Sulphate). An oxygen mediated complex was implicated because binding was increased in oxygenated buffer, reduced in nitrogen-purged buffer, and prevented by reduction with dithiothreitol or 2-mercaptoethanol (Strittmatter et al., 1993a, 1993b). Similarly, although ß-amyloid can assemble into filaments spontaneously, addition of ApoE resulted in a ten to twenty fold increase in filament formation, as determined by light scattering and electron microscopy, with ApoE4 showing the highest catalytic activity (Ma et al., 1994). Based on these results, it has been hypothesised that ApoE4 acts as a 'pathological chaperone', that is, by binding to ß-amyloid, it increases amyloid deposition and thus increases the formation of plaques (Wisniewski & Frangione, 1992; Ma et al., 1994). This proposal is further supported by observations that inheritance of the ε4 allele is associated with increased levels of ß-amyloid plaque deposition along blood vessels and in the brain parenchyma (Rebeck et al., 1993; Schmechel et al., 1993; Corder et al., 1994; Olichney et al., 1996).

Another proposed mechanism linking ApoE with ß-amyloid, suggests that ε4 homozygotes have a reduced ability to suppress ß-amyloid formation, therefore, greater deposition occurs (Evans et al., 1995). Finally, a third group have suggested that the ApoE4 isoform 'clears' ß-amyloid less effectively and by doing so enables amyloid deposition and plaque formation (Rebeck et al., 1993). This was concluded after it was found that plaques and reactive astrocytes were strongly immunoreactive for both ApoE and the low density lipoprotein receptor related protein (LRP). LRP is one of the specific lipoprotein receptors for ApoE. It was suggested that ApoE/ß-amyloid complexes may be taken up by LRP expressed on activated astrocytes and on neurons, mediating clearance of ß-amyloid from the neuropil. Despite variations in conclusions made from the specific data obtained, collectively these investigations suggest that the ApoE4 isoform is kinetically different to ApoE3 and ApoE2 and, therefore, imply that ApoE with deficient functioning might play a role in plaque

formation and possibly neurodegeneration. Independent of this controversy regarding potential function of the molecule, it has been an important objective of many investigators to demonstrate or refute a link between ß-amyloid and ApoE.

In summary, four genes have been implicated to date in familial forms of AD: three that, when mutant, cause autosomal dominant forms of the disease (APP, PS1, and PS2) and one in which a naturally occurring polymorphism represents a major genetic risk factor for the development of the disease (ApoE). However, despite the genetic associations it should be remembered that the familial form of AD is relatively infrequent and the majority of AD cases (50-85%) are sporadic.

1.6.3 Head Trauma

Head injury, either a single episode leading to unconsciousness or hospitalisation, or repeated head injury, as in the case of boxers, is a risk factor for AD (Heyman et al., 1984; Mortimer et al., 1985; Graves et al., 1990; Mortimer et al., 1991; Katzman & Kawas, 1994). In addition, neuropathologic lesions, such as NFT, that occur following repetitive head injury, as experienced by boxers (Lampert & Hardman, 1984; Roberts et al., 1990; Tokuda et al., 1991; Geddes et al., 1996, 1999) or by individuals demonstrating self-abuse behaviour involving head injury (Hof et al., 1991b), are similar to those in AD, raising the possibility of a common pathogenesis. It is also notable that head injury and ApoE genotype may act synergistically to increase risk for AD (Mayeux et al., 1995) and that poor clinical outcome from head trauma is associated with inheritance of ε4 alleles (Jordan et al., 1997; Teasdale et al., 1997; Friedman et al., 1999).

1.7 Models of AD

The lack of an adequate animal model has been a serious impediment to the understanding of AD and the development of therapeutic drugs. Traditionally models of aged animals, as a means of studying pathological age dependent lesions, have been utilised, as have *in vitro*

systems investigating the effects of ß-amyloid on nerve cells. However, more recently, a number of transgenic animals have been developed to model aspects of AD pathology.

1.7.1 Aging animals

Perhaps the simplest of the animal models considered over past years are those which utilise aged animals to investigate the pathological lesions commonly associated with AD. Aged dogs (Wisniewski et al., 1970; Cummings et al., 1993, 1996a), cats (Cummings et al., 1996c), bears (Tekirian et al., 1996) and primates (Wisniewski et al., 1973; Heilbroner & Kemper, 1990; Martin et al., 1994; Nakamura et al., 1995) have all been shown to have ß-amyloid deposits. These deposits, in aged dogs and cats particularly, were found to exist purely of diffuse ß-amyloid and were not shown to develop into the neuritic pathology of AD as evidenced by silver staining or altered tau immunolabelling. Altered neurites were, however, found within plaques in aged dog brain ultrastructurally (Wisniewski et al., 1970). Considerable variation in susceptibility exists between different breeds of dogs, with the boxer breed being the most susceptible. In primates these species based differences are even more dramatic with Squirrel monkeys developing primarily vascular amyloid with age (Walker et al., 1990) as compared to Rhesus monkeys who develop not only diffuse amyloid deposits but also neuritic plaques with age, with little vascular amyloid (Walker et al., 1990). This cross-species variation within dogs and monkeys may reflect a similar heterogeneity within humans.

None of the early investigations of aging animals, including primates, revealed NFT of the PHF-type that predominates in AD (Wisniewski et al., 1970, 1973). More recently tau positive NFT have been detected in aged bears (Tekirian et al., 1996), sheep (Nelson & Saper, 1995), goats (Braak et al., 1994) and prosimian primates (Giannakopoulos et al., 1997) thereby increasing their usefulness as models of AD pathology.

1.7.2 Lesion models

Various groups have sought to create animal models for the behavioural impairments found in AD by selectively inducing lesions in areas known to degenerate in the AD brain, with significant impact on known functions (Wisniewski et al., 1982; Dahl et al., 1980). These models, although effective for modelling Huntingtons disease (Davies & Roberts, 1988; Sanberg et al., 1989) and aspects of Parkinson's disease (Mendez & Finn, 1975), may have a number of major drawbacks for modelling AD. Neurodegeneration in AD is widespread and many neurotransmitter systems are involved, therefore, although the toxin based lesions offer the opportunity to study the consequences of particular cell loss, they do not address the fundamental causes of neurodegeneration in AD. Further to this, the lesions produced by cholicine or aluminium do not adequately reproduce authentic AD-like pathological inclusions (Dahl et al., 1980; Wisniewski et al., 1982).

1.7.3 ß-amyloid toxicity models

In vitro culture models of AD, where large volumes of amyloid have been added directly to neurons resulting in cell death, have been claimed to model the proposed toxic effect of ß-amyloid in AD (Pike et al., 1993). The toxicity induced in this model is dependent on both the volume and fibrillar state of the amyloid added, as smaller volumes, more closely resembling those present in the brain, and non-fibrillar forms of the protein have been found to have no effect. Models utilising the injection of ß-amyloid into the aged Rhesus monkey cortex have also been developed (Geula et al., 1998). In these investigations it was found that both the age and species of the animal, and the fibrillar state of the ß-amyloid injected, affected the pathological outcome. This may account for differing results in earlier ß-amyloid microinjection studies (Podlisny et al., 1993, Kowall et al., 1992). It was shown that microinjection of plaque-equivalent concentrations of fibrillar, but not soluble, ß-amyloid in the aged Rhesus monkey cerebral cortex results in profound neuronal loss, tau phosphorylation and microglial proliferation (Geula, et al., 1998).

1.7.4 Transgenic models

The identification of various genetic risk factors and familial mutations associated with AD have made it possible, with varying degrees of success, to construct transgenic mice expressing genetic factors which either promote or cause aspects of the disease. Models based on gene knockout techniques provide important insights into the function of specific genes *in vivo* whereas transgenic mice harbouring and over expressing mutant forms of the genes associated with AD in humans are a valid tool to model and study the pathophysiological role of those genes. Although transgenics based on the PS1 and PS2 mutations and the ApoE ε4 allele risk factor have been developed, most transgenic studies have focussed on the APP gene.

One of the first reported transgenic mice lines was designed to express the human 751 amino acid isoform of APP (hAPP751) under regulation by the neuron-specific enolase promoter (Quon et al., 1991). These mice showed deposits labelled by antibodies to ß-amyloid and sometimes stained by thioflavine S but not stained by Congo red. Elderly animals from this line demonstrated larger ß-amyloid deposits and tau immunolabelled DNs (Higgins et al., 1994, 1995). Similarly other early models, expressing the 104 amino acids of hAPP695 under the regulation of the dystrophin neural promoter (Kammesheidt et al., 1992) and the first 104 carboxy-terminal amino acids of hAPP regulated by the NF-L promoter (Nalbantoglu et al., 1997), also showed age dependent neuronal alterations ie deposits of ß-amyloid, degenerating axons and dendrites and loss of neurons. However, while these constructs lead to age-related neurodegeneration, it is yet to be shown whether the abnormal neuronal changes match authentic AD specific nerve cell pathology.

At present there have been four groups which have developed transgenic mouse models that faithfully replicate the congophilic, amyloid fibril plaques of AD (Games et al., 1995; Hsiao et al., 1996; Sturchler-Pierrat et al., 1997; Moechars et al., 1999). Table 1.2 summarises the various pathological changes that were noted in these models in addition to ß-amyloid

deposits. It is clear from the combined studies that aging, in addition to the overexpression of APP bearing known FAD mutations, is essential for the emergence of a specific feature of AD-like pathology, the ß-amyloid plaque. The ß-amyloid plaques, of the transgenic models, have also been found to be associated with anbonormal neurites variably labelled for APP, synaptophysin, NFs and in two studies (Sturchler-Peirrat et al., 1997; Moechars et al., 1999), abnormal tau characteristics suggesting a pathological effect. However, there is no evidence of AD-specific PHFs within affected neurons, obvious neuron loss around plaques or NFTs. This pathological profile suggests that either APP misprocessing is not the central event in AD pathology (Terry, 1996) or that the pathology demonstrated by APP transgenic mice may model preclinical AD, which is characterised by the presence of ß-amyloid plaques associated with NF immunopositive DN but not extensive neurofibrillary pathology or neuronal degneration (Morris et al., 1996; Price & Morris 1999; Vickers et al., 2000). Further aging, for several more years, may therefore be required before these models exhibit the full spectrum of Alzheimer's associated pathology.

Recent reports indicate that immunisation of the young APP717 transgenics, developed by Games and collegues with ß-amyloid peptides essentially prevented plaque formation, neuritic dystrophy and astrogliosis and that treatment of older transgenic animals also markedly reduced the extent and progression of these AD like neuropathologies. This highlights the value of a model of the early stages of the disease and raises the possibility that immunisation with ß-amyloid may be effective in preventing and treating AD (Schenk et al., 1999). Before such a conclusion can be made, however, experiments determining whether depletion of the amyloid plaques is accompanied by an improvement in the behavioural/neurophysiological impairments, and a reduction in nerve cell death must be performed (St. George-Hyslop & Westaway, 1999).

Table 1.2

Transgenic lines demonstrating AD-like histopathology

FAD construct	Aß plaques	NFT	PHF	Dystrophic Neurites		
				NF	APP	Tau
hAPP717 (Games et al., 1995)	+	-	-	+	+	-
hAPP(Swed) (Hsiao et al., 1996)	+	-	-	+	+	-
hAPP(Swed)+ hAPP717 (Sturchler-Pierrat et al., 1999)	+	-	ND	+	+	+
hAPP(Swed)/ hAPP717 (Moechars et al., 1999)	+	-	ND	+	+	+

ND – not determined

Transgenic mice that overexpress FAD-linked mutations in human PS1 or PS2 have proven more valuable than those utilising 'knockout' technology with regards to providing further information associated with AD pathogenesis. These transgenic mice demonstrate increased levels of the Aß1-42/43 peptide in the brain relative to transgenic expressing the human wildtype PS and non-transgenic animals but do not result in amyloid plaque development (Borchelt et al., 1996; Duff et al., 1996; Citron et al., 1997; Oyama et al., 1998; Qian et al., 1998). However, crossing such animals with transgenic mice with the Swedish APP mutation leads to earlier ß-amyloid deposition in the brain (Borchelt et al., 1997; Holcomb et al., 1998).

AIMS

The reason for the degeneration of nerve cells, and the loss of specific synaptic connections, that underlies the emergence and progressive development of dementia in sufferers of AD remains elusive. Furthermore, although individually ß-amyloid plaques, NFTs and DNs have been extensively investigated, the mechanism that links these hallmark structures also remains to be defined. Due to their proposed role in the the development of the earliest pathological changes in nerve cells, and also the correlation between a neurons content of this protein class and its subsequent vulnerability to neurofibrillary pathology and degeneration, a comprehensive understanding of the role of NFs in the AD process is crucial. This thesis will, therefore, seek to address three aims that are principally associated with the role of NFs in the development of plaque associated pathology and the mechanism underlying AD.

Specific Aim 1

To determine the neurochemical and morphological diversity of abnormal neurites associated with ß-amyloid plaque formation in the early and late stages of AD.

Double labelling immunohistochemistry will be utilised to investigate neuritic plaques. A battery of mouse monoclonal and rabbit polyclonal antibodies directed to cytoskeletal and synaptic markers, will be used to establish the sequence of changes that occur within abnormal plaque associated neurites as AD progresses. Confocal microscopy will be used to perform detailed analysis of the morphology of ß-amyloid plaques in both preclinical and end-stage AD and to investigate the interaction between tau and NFs within individual DNs.

Specific Aim 2

To examine the relationship between ApoE immunolabelling and ß-amyloid deposition, neuritic plaques and NFTs using immunofluorescent double labelling techniques.

Although the inheritance of certain ApoE alleles has been recognised as a genetic risk factor for AD, the role of ApoE in the pathology underlying this disease is unclear. Several reports have emphasised the association of ApoE with either ß-amyloid plaque formation or the development of neurofibrillary pathology. Utilisation of multiple label immunohistochemical methods will enable the direct examination of the localisation of ApoE immunoreactivity relative to ß-amyloid plaques, DNs and NFTs. Determination of the role of the ApoE protein in AD may be crucial for elucidating the sequence of pathological events that ultimately result in dementia.

Specific Aim 3

To develop an in vitro model that mimics the effects of ß-amyloid plaques on surounding neuronal processes.

It has recently been proposed that the formation of ß-amyloid plaques in the brain causes physical damage to surrounding axons, and that it is the chronic stimulation of the stereotypical reaction of neurons to physical damage that leads to the cytoskeletal alterations that underlie neurofibrillary pathology and neurodegeneration (King et al., 1997; Vickers, 1997; King et al., 2000; Vickers et al., 2000). Therefore, newly developed cell culturing techniques will be utilised to investigate the stereotypy of neuronal cells to damage with a particular emphasis on the changes associated with NFs.

In summary, this study will seek to further clarify the relationship between ß-amyloid plaques and DNs, particularly with regard to determining the role of NFs within this relationship. Identification of the earliest pathological changes that occurs in AD is necessary for the development of effective therapeutic strategies aimed at preventing or slowing the ongoing neuronal changes that ultimately lead to cell death and dementia.

METHODS

2.1 Tissue source and processing

Human brain tissue was obtained from multiple sources as indicated in Table 2.1 and 2.2. Brains were either perfusion-fixed with 2% picric acid / 4% paraformaldehyde, or blocks of cerebral cortex were immersion-fixed in 4% paraformaldehyde. Throughout this thesis a total of fourteen confirmed AD cases were used (Table 2.2). This diagnosis was made according to the CERAD (Consortium to Establish a Register for Alzheimer's Disease) criteria (Mirra et al., 1991). In addition thirteen preclinical AD cases were also used (Table 2.1). The preclinical cases were defined by the presence of widespread ß-amyloid immunoreactive plaques in the neocortex, with the distinction that these plaques could not be defined as 'neuritic' based on thioflavine S staining or immunolabelling with PHF-tau or ubiquitin antibodies (Vickers et al., 1996; Saunders et al., 1998). Thus, these preclinical cases do not conform to CERAD criteria for diagnosis of clinical AD (Mirra et al., 1991). These preclinical cases also lacked neocortical NFTs. Cryopreserved blocks (30% sucrose solution) of the superior frontal gyrus (SFG) from each of the cases were sectioned on a freezing microtome (Leica CM1325) at 40-50 µm. No differences were observed in the immunolabelling profile for the various antibodies across varying post-mortem to fixation intervals (PMI) or different fixation protocols.

Table 2.1

Summary of preclinical AD cases

Age (y)	Sex	PMI (hrs)	Cause of death	Fixation details	Source
70	F	4.4	Cardiac failure	2	University of Tasmania, Hobart
61	M	19	Heart disease	2	University of Sydney, Sydney
62	M	24	Cardiac failure	2	University of Sydney, Sydney
71	M	32.5	Cardiac arrest	2	University of Sydney, Sydney
59	F	6	Cardiac failure	1	NH&MRC Brain Bank, Adelaide
80	M	20	COAD	1	NH&MRC Brain Bank, Adelaide
78	F	18	Cardiac failure	1	NH&MRC Brain Bank, Adelaide
86	F	25	Pneumonia	1	NH&MRC Brain Bank, Adelaide
90	M	2.16	Resp. failure	2	Sun Health Research Institute, USA
81	F	3	Cardiac arrest	2	Sun Health Research Institute, USA
84	M	3	Cardiac arrest	2	Sun Health Research Institute, USA
78	M	2.25	Pneumonia	2	Sun Health Research Institute, USA
91	M	3	Cardiac failure	2	Sun Health Research Institute, USA

1. Perfusion-fixed with 2% picric acid/ 4% paraformaldehyde
2. Blocks of cerebral cortex, immersion-fixed in 4% paraformaldehyde

Table 2.2

Summary of AD cases

Age (y)	Sex	PMI (hrs)	Cause of death	Fixation details	Source
65	M	3	AD	1	NH&MRC Brain Bank, Adelaide
71	F	13	AD	1	NH&MRC Brain Bank, Adelaide
73	M	6.5	AD	1	NH&MRC Brain Bank, Adelaide
72	F	4	AD	2	Sun Health Research Institute, USA
66	M	2.8	AD	2	Sun Health Research Institute, USA
84	F	3	AD	2	Sun Health Research Institute, USA
76	M	3.5	Heart Failure	2	Sun Health Research Institute, USA
83	M	3.5	Leukaemia	2	Sun Health Research Institute, USA
86	F	4	Cancer, AD	2	Sun Health Research Institute, USA
88	M	7	Failure to thrive	2	Sun Health Research Institute, USA
92	F	2.25	Pneumonia	2	Sun Health Research Institute, USA
74	F	2	Pneumonia	2	Sun Health Research Institute, USA
74	M	2.75	Resp. failure	2	Sun Health Research Institute, USA
83	M	2.83	Dementia, AD	2	Sun Health Research Institute, USA

1. Perfusion-fixed with 2% picric acid/ 4% paraformaldehyde
2. Blocks of cerebral cortex, immersion-fixed in 4% paraformaldehyde

2.2 Immunohistochemistry

Immunohistochemistry, particularly the indirect fluorescent method, is utilised throughout this thesis for the visualisation and localisation of a variety of proteins associated with AD and the neuronal response to injury. The indirect immunohistochemical method principally has two steps. The initial stage involves the incubation of a tissue preparation or cell monolayer with a 'primary' antibody, typically an immunoglobulin of the gamma type (IgG), that binds specifically to an antigenic site. Tables 2.3 and 2.4 show the range of primary antibodies utilised throughout the following investigations. The preparation is then incubated with a 'secondary' antibody that specifically binds to IgGs of the primary antibody host species (Table 2.5). For the fluorescent method, this second antibody is conjugated to a fluorophore that emits fluorescent light when exposed to a particular wavelength of light. Some secondary antibodies are conjugated to the vitamin biotin which will, in turn, bind, to an avidin (egg-white glycoprotein)- fluorophore complex. This fluorescent method was utilised to allow for colocalisation studies. The specific primary and secondary antibodies utilised in the individual inviestigations are given in the following chapters.

Prior to antibody incubation, tissue sections and fixed cell monolayers were washed for three, ten minute intervals in a solution of isotonic phosphate buffered saline, 0.01 M PBS. Tissue sections and cell monolayers were then incubated with primary antibodies on a slow rotating shaker platform for two to three hours at room temperature and then for a further twelve to eighteen hours (overnight) at 4°C. Primary antibodies were diluted in a diluent solution of 0.01 M PBS containing 0.3% Triton X-100 (Sigma). After incubation with the primary antibodies preparations were washed three times over 30 minutes in PBS before incubating for approximately two hours in the, biotinylated or fluorophore-conjugated,

Table 2.3

Immunohistochemical markers – mouse monoclonal primary antibodies

Code	Reactivity	Dilution	Source
SMI32	dephosphorylated NF-M & NF-H	1:1000	Sternberger Monoclonals Inc.
SMI312	phosphorylated NF-M & NF-H*	1:1000	Sternberger Monoclonals Inc.
SMI310	phosphorylated NF-H	1:2000	Sternberger Monoclonals Inc.
RT97	phosphorylated NF-M & NF-H	1:500	Boehringer Mannheim
ß-amyloid	ß-amyloid	1:500	DAKO
ApoE	apolipoprotein E	1:500	Boehringer Mannheim
GFAP	glial fibrillary acidic protein	1:2000	DAKO
Ferritin	human ferritin	1:5000	ICN Biomendicals Inc.
GAP43	growth associated protein 43	1:1000	Boehringer Mannheim
MAP2	microtubule associated protein 2	1:1000	Boehringer Mannheim

*cocktail of mouse monoclonal antibodies

Table 2.4

Immunohistochemical markers – rabbit polyclonal primary antibodies

Code	Reactivity	Dilution	Source
R-NFH	minimally dephosphorylated NF-H	1:500	Serotec
R-NFM	phosphorylation independant NF-M	1:500	Serotec
Tau	4R tau	1:2000	DAKO
CgA	large synaptic vesicles	1:500	DAKO
ß-amyloid	ß-amyloid 1-42(43)	1:500	Zymed
ß-amyloid (pan)	all ß-amyloid peptides	1:500	QCB
ApoE	apolipoprotein E	1:2000	DAKO
Ubiquitin	ubiquitinated filaments	1:100	DAKO
Calretinin	calretinin	1:2000	Swant

Table 2.5

Secondary antibodies

Lot	Reactivity	Raised in	Conjugate	Dilution	Source
F1206	Mouse IgG	Horse	FITC	1:200	Vector
J0311	Rabbit IgG	Goat	Biotin	1:200	Vector*†
H0118	Mouse IgG	Goat	Biotin	1:200	Vector*†
036(101)	Mouse IgG	Goat	HRP	1:2000	DAKO †
115(302)	Rabbit IgG	Goat	HRP	1:2000	DAKO †

FITC - fluorescien isothiocyanate

* visualised with streptavidin Texas Red (Amersham 1:200) (fluorescence)

† visualised with the chromogen, 3, 3' diaminobenzidine (DAB) (Sigma) (peroxidase)

secondary antibodies diluted in the same diluent solution at room temperature on the shaker platform. Any incubations with conjugated fluorophores were performed in the dark to preserve the intensity of labelling. This incubation was again followed by a series of three, ten minute washes in PBS. If a biotinylated second antibody was used, the tissue was further incubated in streptavidin Texas Red for two hours followed by three more PBS washes. Control preparations with the primary antibody omitted were processed in conjunction with all investgations. Tissue preparations were mounted on glass slides using 'Permafluor' mounting medium (Immunotech). Labelled coverslips were similarly prepared by mounting face down on glass slides with Permafluor.

For single labelling chromogen-based invesitgations, a similar protocol was used as that outlined above. Prior to primary antibody incubation, the endogenous peroxidase acitivity was abolished by placing sections in a mix of 3% hydrogen peroxide (Sigma) and absolute methanol (BDH Chemicals) 1:3 for fifteen minutes. The material was then incubated in the primary antibody diluted in the standard diluent solution for approximately twelve to eighteen hours. After washing, the material was incubated for approximately two hours with the appropriate biotinylated mouse-specific or rabbit-specific secondary antibodies (Table 2.5) diluted in the standard diluent solution. This incubation was again followed by a series of three, ten minute washes in PBS. Material was then incubated in an Avidin Biotin Complex / Horse Radish Peroxidase (HRP) amplification solution (DAKO) for one hour at room temperature on a shaker platform. Following washing in PBS labelling was visualised by exposure to a solution of the chromogen 3', 3 diaminobenzidine (DAB) (Sigmafast tablet kit, Sigma). When the correct labelling intensity was reached, the material was washed in a PBS solution to stop the precipitation reaction. Sections were mounted on glass chrome alum-gelatine subbed slides. Mounted sections were allowed to dry onto

subbed slides overnight before being rehydrated in MilliQ® water for fifteen minutes. This was followed by dehydration through increasing concentrations of ethanol (three minutes in 70%, 3 minutes in 95%, three minutes in 100% and a further five minutes in 100% ethanol). The slides were then cleared with two, five minute immersions in xylene before coverslipping using Eukitt (Carl Zeiss) mounting media.

2.3 Immunoblots

Samples of unfixed frozen pons from a non-demented control case and cortex from an AD case were homogenised in cold PBS using a hand held homogeniser (Jencons Scientific). Homogenised tissue was stored in aliquots at -20°C. Prior to separation, aliquots were diluted in Laemmli sample buffer (Bio-Rad Laboratories) 1:4 (wt / vol) with 5% ß-mercaptoethanol (Bio-Rad Laboratories), heat treated for five minutes at 95°C and then cooled on ice for five minutes. Twenty microlitres of this sample was separated on a 7.5% polyacrylamide gel using SDS-PAGE (polyacrylamide gel electrophoresis) (Mini-PROTEAN® II system, Bio-Rad Laboratories). Broad range biotinylated molecular weight standards (Bio-Rad Laboratories) were also run on each gel to allow protein size determination. For protein separation, a voltage of 90V was applied at room temperature until completion. After separation, proteins were transferred to nitrocellulose sheets (Bio-Rad Laboratories) using a Mini Trans-Blot® Electrophoretic transfer Cell (Bio-Rad Laboratories). For transfer, a voltage of 100V was applied for 70 minutes at 4°C. After rinsing in Tris Buffered Saline with Tween (TTBS), membranes were saturated with a blocking solution of 5% skimmed milk in TTBS for one hour. Again after rinsing in TTBS, membranes were cut into strips and each strip incubated overnight with primary antibody diluted in blocking solution. After the primary antibody incubation the strips were washed in TTBS and incubated with the appropriate HRP conjugated mouse-specific or rabbit-

specific secondary antibodies (Tables 2.3 and 2.4) diluted in blocking solution for two hours. Following secondary antibody incubation and a final series of washes in Tris Buffered Saline (TBS), the blots were treated a solution of the chromogen DAB (Sigmafast tablet kit, Sigma). After development the strips were washed briefly in MilliQ® before using an Apple Colour One scanner to digitally record the result.

2.4 Cortical cell culture

Primary dissociated cortical cells were prepared using standard culture procedures (Banker & Goslin, 1991) in a media selective for neuronal cells, Neurobasal™ (Gibco BRL, Life Technologies) (Brewer et al., 1993; Brewer, 1995, 1997). Pregnant Hooded Wistar rats (eighteen days gestation) were killed by carbon dioxide exposure. Embryos were rapidly removed using sterile techniques, and, after removal of skull and meninges, the neocortical hemispheres were dissected, and placed in 10 mM N-2-Hydroxethypiperazine-N'-2-ethanesulphonic acid (HEPES) buffer (BDH Chemicals) with 0.25% trypsin (BDH Chemicals) at 37°C for 20 minutes. After initial enzymatic digestion, dissociation was completed via trituration using pipettes of decreasing caliber. Prior to plating viability of the cell suspension was assessed using trypan-blue (Sigma, Cell Culture) dye exclusion. Cells were then plated at a density of 5.0×10^5 cells/cm^2 on glass coverslips (Fisher Scientific) in an initial plating media, consisting of Neurobasal™ media (Gibco BRL, Life Technologies), 2% B27 supplement (Gibco BRL, Life Technologies), 10% foetal calf serum (FCS) (CSL Ltd) 0.5 mM L-glutamine (Gibco BRL, Life Technologies), 25 μM glutamate (Gibco BRL, Life Technologies) and 3 ml/L gentamicin (David Bull Laboratories, Faulding). Coverslips had previously been acid treated (two hours in 69% nitric acid (BDH Chemicals) prior to extensive washes in MilliQ® water) and preincubated overnight with poly-L-lysine (Sigma) (1 mg/ml in borate buffer, pH 7.4), rinsed and

covered with 2 ml of the initial plating media. Cultures were kept in an incubator (Imbros) at 37°C in a humidified atmosphere of 5% CO_2. After one day *in vitro* (DIV 1), the initial plating media was replaced with a 'subsequent', serum free, growth media containing Neurobasal™, 2% B27 supplement, 0.5 mM L-glutamine and 3 ml/L gentamicin. This culture media was replenished every three days by removing one third of the volume of media and replacing with new 'subsequent' growth media. Before immunohistochemical labelling the cell monolayers were fixed in solution of 0.01 M PBS and 4% paraformaldehyde (BDH Chemicals).

2.5 Image Analysis

Fluorescence-labelled preparations were viewed with a Leitz Dialux 22EB epifluorescence microscope equipped with specific filter blocks for the selective visualisation of fluorescein isothiocyanate (FITC) and Texas Red / tetramethyl rhodamine isothiocyanate (TRITC). The maximum excitation wavelengths, at which the fluorophores are visualised, are 440 nm and 660 nm respectively. The difference in these wavelengths enables the visualisation of both anti-mouse primary antibodies (FITC-conjugated) and anti-rabbit antibodies (Texas-Red conjugated) within the same speciman. By using different combinations of primary antibodies, and their respective secondary antibodies, the colocalisation of markers within various structures were examined. The third filter set, UV, of the Leitz Dialux microscope was utilised for the visualisation of thioflavine S labelled material. Images from this microscope were digitally captured using a CCD camera (Ikegami ICD-4CE, Tsushinki Co) attached to a Power PC Macintosh computer running the NIH Image Analysis program (version 1.61). Adobe Photoshop (version 4.0 and 5.5) was utilised to prepare figures from collected images. These figures were printed on an Epson Stylus Colour 800 printer. Alternatively, photos of the material immunolabelled with the indirect fluorescence method

were taken with a Wild Leitz camera attached to the Leitz Dialux microscope. Similarly, chromogen labelled material was also viewed on an Olympus microscope (BX50) fitted with a camera. Kodak TMAX black and white film was used in both cameras. Black and white film was developed using Kodak developer and fixer. Negatives were printed on Ilford multi-grade glossy photographic paper.

2.6 Confocal Microscopy

Confocal microscopy was performed using an Optiscan F900e krypton/argon scanning laser system attached to an Olympus microscope (BX60) and an Hewlett Packard Pentium II computer. The Optimate 5.2 image analysis program was utilised to execute detailed measurements and analysis of the captured image sets. Figures were prepared from collected images using Adobe Photoshop 5.5 and printed using an Epson Stylus colour 800 printer.

2.7 Electron Microscopy

Cell monolayers to be examined using electron microscopy were fixed in solution of 0.01 M PBS and 2.5% gluteraldehyde (Probing & Structure) for 30 minutes. After fixation monolayers were washed twice in PBS for five minutes. Cells were then fixed in a solution of 1% osmium tetroxide (ProSciTech) for 30 minutes, and washed twice in MilliQ® water for five minutes each. The coverslips were then stained and treated with a solution of 4% uranyl acetate (BDH Chemicals) for 30 minutes followed by five minute periods of dehydration in 30%, 50%, 70%, 95% and two changes of 100% alcohol. After two successive washes in propylene oxide (BDH Chemicals), each for five minutes, the cells were infiltrated with a mix of 50% propylene oxide/50% Procure 812 resin (ProSciTech) and then left for eighteen hours. This solution was then replaced with 100% Epon resin, left

for four hours and then replaced with a fresh solution of 100% epon before embedding. After embedding (specific details given in appropriate chapters) cells were sectioned using a Leica Reichert Ultracut S microtome. Semi-thin sections (0.5 μm) were intially collected, stained with toludene blue (Reactifs RAL) and examined. Areas of interest were confirmed and ultra-thin sections (70 nm) cut and mounted on Formvar (Probing & Structure) coated single-slot copper grids (Bio-Rad Laboratories). Additional staining with 5% uranyl acetate for 30 minutes in the dark was performed and then staining with Reynolds lead citrate (Ajax Chemicals) for ten minutes in an anhydrous atmosphere, completed the processing procedure. Material was then examined on a Philips EM410 electron microscope. Photos were taken on electron microscopy plate film (Kodak 4489). Black and white film was developed using Kodak developer and fixer. Negatives were printed on Ilford multi-grade glossy photographic paper.

All solutions specific to the above procedures are given in Appendix A.

THE NEUROCHEMICAL AND MORPHOLOGICAL DIVERSITY OF PLAQUE ASSOCIATED DYSTROPHIC NEURITES IN THE EARLY AND LATE STAGES OF ALZHEIMER'S DISEASE

3.1 Introduction

A subset of ß-amyloid plaques in AD are associated with clusters of abnormal neuronal processes referred to as DNs. The presence of these neuritic plaques has been considered to be a pathological correlate of dementia in AD (Mirra et al., 1991). However, determining the mechanistic link between these two hallmark changes remains a fundamental issue in AD research and, therefore, provided the focus for this initial investigation.

Recent published reports have indicated that not all DNs are comprised of the same neurochemical constituents. For example, while it is generally accepted that the neurofibrillary pathology of AD is comprised of the abnormal form of the tau protein, numerous reports have indicated that DNs may be distinguished by either tau or NF abundant forms (Dickson et al., 1988; Masliah et al., 1993b; Vickers et al., 1994b; Su et al., 1996). Similarly, some synaptic markers, and even APP, are present in DNs that lack either NFs or tau (Yasuhara et al., 1994; Wang & Munoz, 1995; Saunders et al., 1998). Recently, investigation of the brains of individuals who may be in a preclinical stage of the disease, characterised by the presence of cortical ß-amyloid plaques but the absence of neocortical NFTs and pronounced dementia (Morris et al., 1996; Vickers, 1997), have indicated that early DN forms are associated with profound neurofilamentous changes in the absence of tau abnormalities (Vickers et al., 1996). Other studies have also indicated that significant tau pathology is a relatively late event in DN formation (Benzing et al., 1993; Su et al., 1996).

The purpose of this initial study was to investigate cortical DN formation and the localisation of a wide range of implicated proteins, including cytoskeletal and synaptic markers, at both the early and late stages of the AD disease process. Both pathological staging (Braak & Braak, 1991) and clinicopathological (Morris et al., 1996) studies indicate that the early, or preclinical, stage of AD is characterised by minor cognitive impairment and the presence of ß-amyloid plaques, but not tau-immunoreactive neurofibrillary pathology, in neocortical areas. This investigation, therefore, has a particular focus on the specific complement of NF epitopes present in DNs in early and late AD. This data provides new information on the neurochemical diversity of plaque associated DNs and suggests a sequence relating to the precise cellular changes that ultimately result in neuronal degeneration and dementia.

3.2 Experimental procedures

3.2.1 Case details

The samples used in the immunohistochemical investigations included six cases of confirmed AD (66, 72, 76, 83, 84 and 86 years of age) and 8 preclinical AD cases (59, 61, 62, 71, 78, 80 and 86 years of age) (Tables 2.1 and 2.2 for source and fixation details).

3.2.2 Immunoblots

To confirm the reactivity of the NF antibodies and to investigate previously purported cross reactivity between tau and phosphorylation-dependent NF antibodies (Ksiezak-Reding et al., 1987; Mirra et al., 1991), Western blots were prepared and labelled with the individual antibodies used in this investigation. Standard Western blot protocol was utilised as outline in Chapter 2.3 using the following primary antibodies; SMI312 (control- 1:2000, AD - 1:1000), SMI32 (control - 1:2000, AD - 1:200), RT97 (control and AD - 1:2), R-NFM (control - 1:2000, AD - 1:500) and R-NFH (control - 1:2000 and AD 1:1000). To further characterise the phosphorylation state of the two rabbit polyclonal antibodies, R-NFH and R-NFM, and to confirm the commercially specified phosphorylation states of the mouse NF antibodies, prior to primary antibody incubation the nitrocellulose blots were pretreated with alkaline phosphatase (12.5 μg/ml) (Sigma) in TTBS overnight at 37°C. Control blots (TTBS only) were processed concurrently.

3.2.3 Immunohistochemistry

Basic immunohistochemistry protocol was utilised for all investigation as outlined in Chapter 2, any changes or additions to this protocol are described below. The distribution and degree of colocalisation of cytoskeletal proteins (NF, tau) was determined using double labelling immunohistochemistry with a selection of the primary antibodies indicated in Tables 2.3 and 2.4. Rabbit antibodies to NF-H, NF-M, and 4Rtau (four MT binding domains) were combined alternatively with mouse antibodies to modified (phosphorylated (SMI312 and RT97) and dephosphorylated (SMI32)) NFs in all cases. The relationship between

cytoskeletal protein labelling and ß-amyloid, as well as the synaptic marker, chromogranin A (CgA), was also investigated in all cases using double labelling immunofluorescence. Sections in which ß-amyloid was to be visualised were pre-treated in 90% formic acid prior to incubation in either primary antibody. For all fluorescence labelling, mouse monoclonal antibodies were visualised with a horse anti-mouse secondary antibody conjugated to FITC whereas the rabbit polyclonals were visualised with a goat anti-rabbit antibody conjugated to biotin followed by streptavidin Texas Red (Table 2.5).

For quantitation of the coexistence of cytoskeletal epitopes in DNs, one hundred plaques were considered for each of the antibody combinations. However, in some preclinical AD cases, due to the presence of limited plaque pathology, the maximum number of clustered DNs present was considered (50-100) for determining the extent of colocalisation.

3.3 Results

3.3.1 Immunoblots

Western blot analysis of the reactivity of the NF antibodies supported both the commercial claims and the immunohistochemical observations that were made throughout the investigation. Both normal brain (without a neurological disorder) and AD brain were used as the protein source (Figure 3.1). Labelling of bands by both SMI312 and RT97, at approximately 200 kDa and 160 kDa, decreased after pretreatment with alkaline phosphatase, thereby suggesting that these antibodies are directed to phosphorylated NF-H and NF-M epitopes. Results were similar for samples of AD cortex tested. SMI32 labelled dephosphorylated NF-M and NF-H as previously outlined (Lee et al., 1988a; Vickers et al., 1994b). The R-NFM antibody was specific in its labelling of NF-M at approximately 160 kDa. This labelling was unchanged in the alkaline phosphatase pretreated blots. The R-NFH antibody labelled a number of bands at approximately 200 kDa. Labelling decreased slightly in the alkaline phosphatase pretreated blot suggesting that some epitopes recognised by R-NFH were phosphorylation specific.

3.3.2 Preclinical Alzheimer's disease

All of the NF antibody markers revealed clusters of abnormal neurites in the 'preclinical' cases. Double labelling also demonstrated that all of the NF immunoreactive (with mouse antibodies) clusters of abnormal neurites were present within ß-amyloid plaques, but that not all plaques in these cases were associated with DNs (Figure 3.2). These DNs had either a bulb- or ring-like morphology. R-NFM and R-NFH labelled abnormal neurites showed high degrees of colocalisation with all three mouse NF antibodies, SMI32, SMI312 and RT97 (Table 3.1, Figure 3.3). This pattern of labelling was consistent throughout all preclinical cases.

Figure 3.1

Western blots of control brain (pons) and AD brain (cortex) homogenates confirming the reactivity of the neurofilament markers. Lanes 1-3 show reactivity of SMI312 with normal brain (lane 1), normal brain after alkaline phosphatase treatment (lane 2) and Alzheimer's disease brain (lane 3). SMI312 labelled a band at approximately 200 kDa corresponding to NF-H. This labelling was not present in the alkaline phosphatase treated blot. Similar results were obtained using RT97 (lanes 4-6). Two bands were labelled by RT97 in the normal (lane 4) and AD (lane 6) homogenates at approximately 160 kDa and 200 kDa. Again, this labelling diminished after alkaline phosphatase pretreatment (lane 5). SMI32 labelled a single band in the normal AD sample at approximately 200 kDa (lane 7), however, after alkaline phosphatase treatment two bands were labelled at approximately 200 and 160 kDa (lane 8). Lane 9 shows the labelling of a single band at approximately 160 kDa by the R-NFM antibody, this labelling pattern did not change with alkaline phosphatase pretreatment (lane 10). The R-NFH antibody labelled a series of bands at approximately 200 kDa in the normal brain homogenate (lane 11). This decreased slightly after dephosphorylation of the protein by alkaline phosphatase (lane 12).

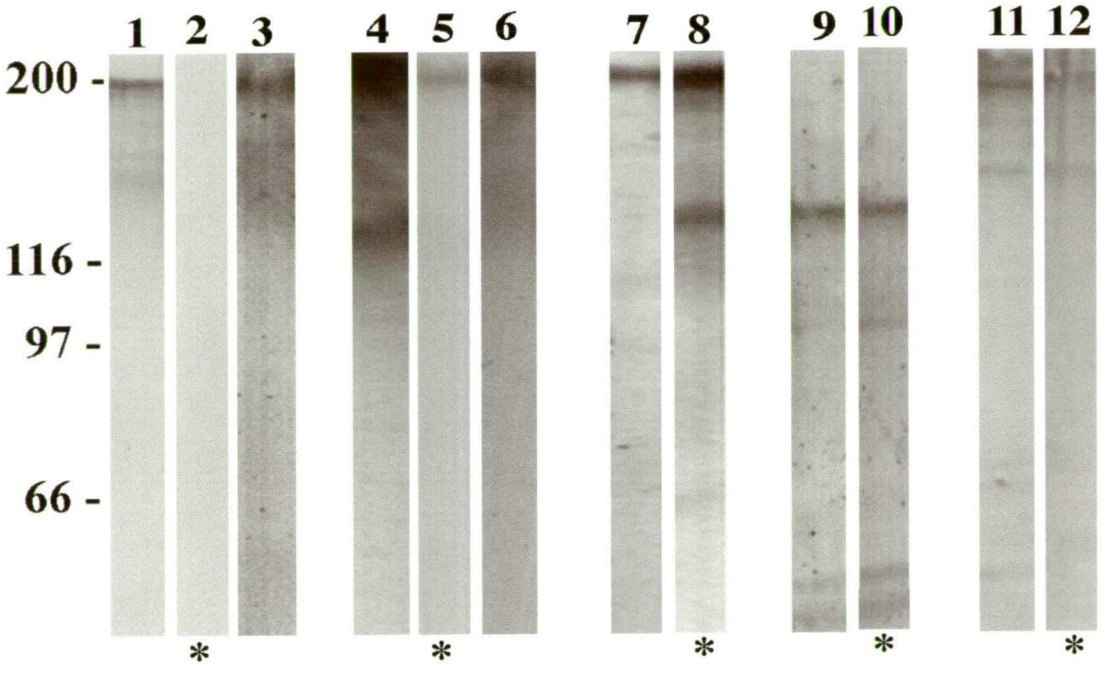
1 2 3 4 5 6 7 8 9 10 11 12
200 -
116 -
97 -
66 -
*
*
*
*
*
* Alkaline phosphatase pretreated

Figure 3.2

Double labelling for ß-amyloid (A,C) and NFs (B,D) in a 70 year-old preclinical AD case. Arrows indicate ring-like structures labelled with either SMI32 (B) or SMI312 (D), localised with the plaques. Similarly, arrowheads show bulb-like DNs within the clusters of abnormal neurites also labelled by each of the NF antibodies.

Scale Bar = 20 μm (A,B,C and D)

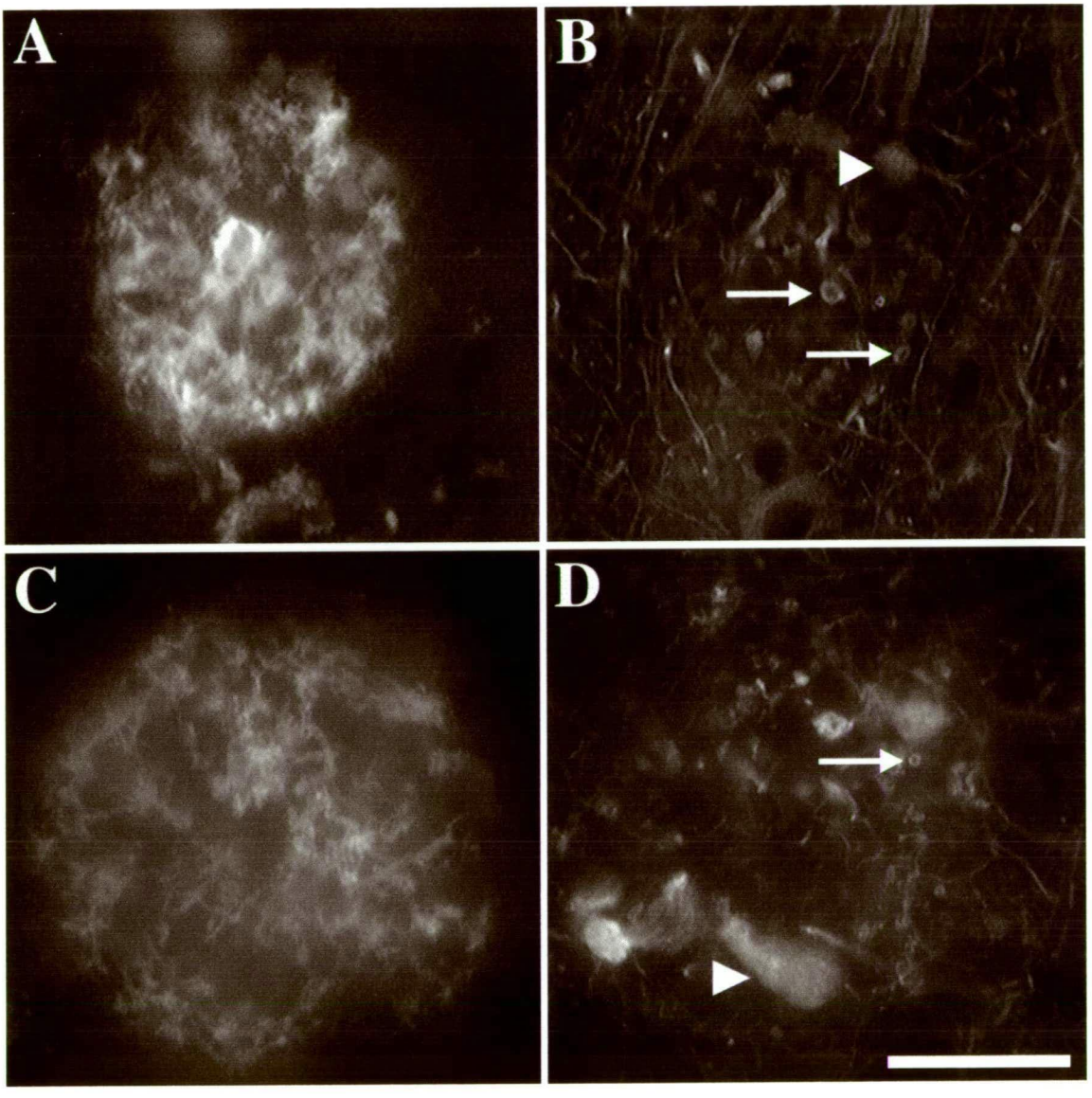
A
B
C
D

Figure 3.3

Double labelling for NFs (A,B,C) and a marker for synaptic change (D) in the superior frontal gyrus of preclinical AD cases. A and B show double labelling with SMI312 (A) and R-NFH(B) in layer II of a 70 year-old preclinical AD case. The two markers for NFs showed complete colocalisation with regards to labelling of the abnormal neurites within the cluster. Labelling with RT97(C) and CgA(D) in the same case, show a cluster of abnormal neurites in which some individual neurites are colocalised for both markers (arrow).

Scale Bars = 20 μm (A and B) and 10 μm (C and D)

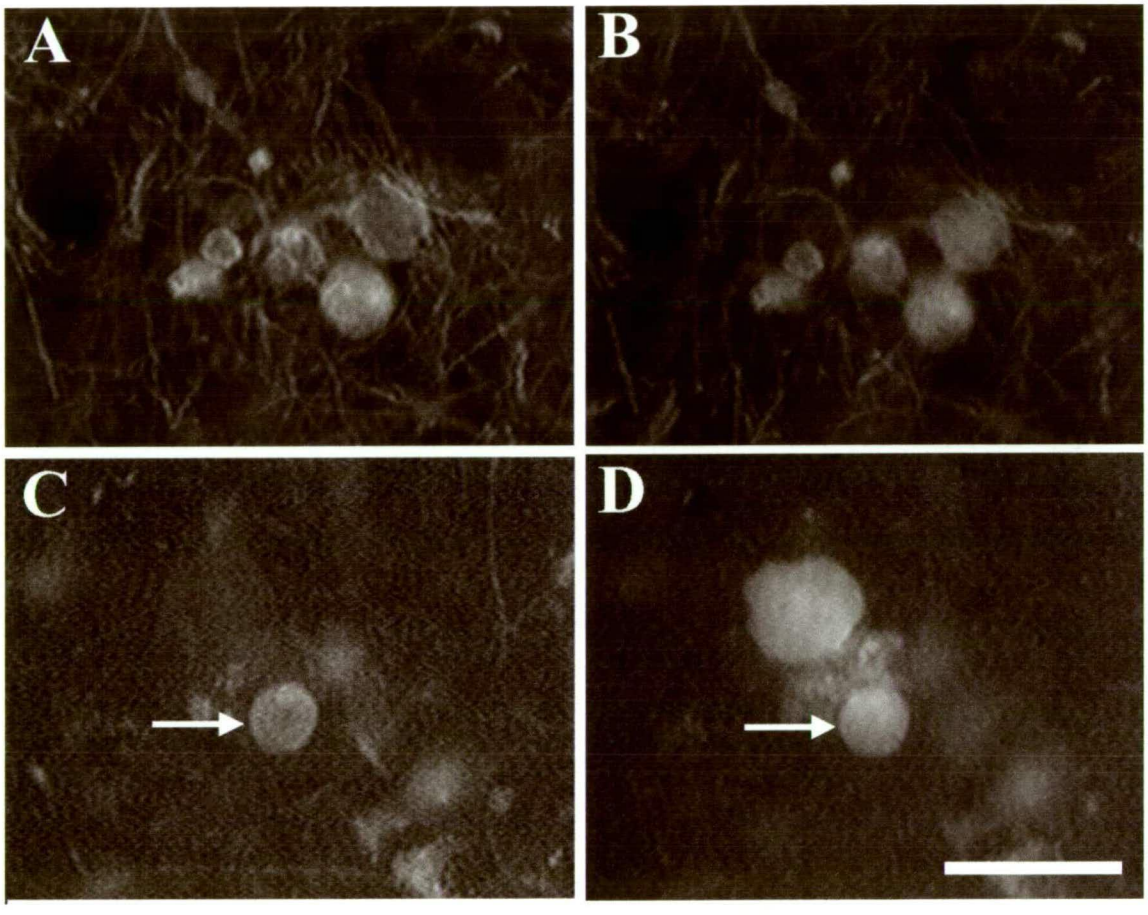
A
B
C
D

Table 3.1

Colocalisation between cytoskeletal markers in plaque associated dystrophic neurites

Labelling	Preclinical AD (n = 4)	Late AD (n = 6)
	(mean % colocalisation ± SE)	
R-NFH with SMI32	72.67 ± 16.50	76.40 ± 20.82
SMI32 with R-NFH	83.67 ± 6.66	98.80 ± 1.30
R-NFH with SMI312	98.75 ± 1.89	96.83 ± 5.38
SMI312 with R-NFH	95.25 ± 4.27	94.17 ± 7.49
R-NFH with RT97	84.00 ± 10.68	90.80 ± 6.83
RT97 with R-NFH	95.50 ± 1.29	24.20 ± 5.50
R-NFM with SMI32	82.67 ± 1.53	83.00 ± 4.64
SMI32 with R-NFM	95.33 ± 4.16	97.60± 5.37
R-NFM with SMI312	95.25 ± 4.11	97.00 ± 5.06
SMI312 with R-NFM	97.75 ± 1.26	96.17 ± 5.85
R-NFM with RT97	68.75 ± 3.86	83.17 ± 12.62
RT97 with R-NFM	99.25 ± 7.93	17.50 ± 8.31
PHF-tau with SMI32	-	5.00 ± 2.00
SMI32 with PHF-tau	-	0.5 ± 1.00
PHF-tau with SMI312	-	15.20 ± 1.30
SMI312 with PHF-tau	-	17.00 ± 6.78
PHF-tau with RT97	-	71.40 ± 6.47
RT97 with PHF-tau	-	84.00 ± 5.74

In contrast, double labelling verified that no neuritic plaques, identified by labelling with mouse antibodies to NFs, contained neurites labelled with the rabbit antibody to tau. Furthermore, there were no singular or clustered neurites labelled with the tau antibody in any part of these sections.

CgA labelling was found to be granular and punctate but plaque-like in general morphology. In addition, larger bulbar neurites were often present within these plaque-like structures. The CgA labelled structures were particularly concentrated in layers II, III, V and VI. Double labelling demonstrated that the larger, bulbar CgA labelled structures co-existed with the clustered NF labelled neurites. However, NF and CgA immunoreactivity were localised generally to different structures (Figure 3.3). Occasionally, CgA labelling formed a 'cap' around NF immunoreactive neurites.

3.3.3 Alzheimer's disease

NF immunolabelling of DNs in AD cases was predominantly bulb-like, with very few ring-like structures observed (Figures 3.4-3.6). Conversely, most AD cases demonstrated ring-like NF labelled structures throughout the neuropil, independent of the localisation of ß-amyloid.

The clustered abnormal neurites showed a high degree of colocalisation between the rabbit (R-NFM and R-NFH) and mouse (SMI32 and SMI312) NF antibodies, independent of the phosphorylation state of the epitope at which the antibody was directed (76-98% colocalised) (Table 3.1, Figure 3.4). There was, however, a distinct discrepancy between the colocalisation patterns of RT97 and the rabbit NF antibodies (Table 3.1). In these cases although the majority of R-NFM and R-NFH labelled clustered DNs were also labelled for RT97 (83% and 90% colocalised, respectively) a much smaller proportion of RT97 labelled DNs were colocalised with the two rabbit antibodies (17% and 24% respectively). RT97 immunopositive clusters of DNs that had no R-NFM or R-NFH labelled structures within them were also present (Figure 3.4). Those DNs colocalised for both RT97 and one of the rabbit antibodies

Figure 3.4

Double labelling for RT97 (A) and R-NFM (B) in layer II of the superior frontal gyrus of a 71 year-old AD cases shows a cluster of DNs immunoreactive for RT97 but not for R-NFM. Labelling in the same case with SMI32 (C) and R-NFM (D) shows complete colocalisation of the two NF antibodies within a large cluster of abnormal neurites. The arrow head indicates autofluorescent lipofuscin pigment visualised with microscope filters for FITC and Texas Red.

Scale Bar = 20 μm (A,B,C and D)

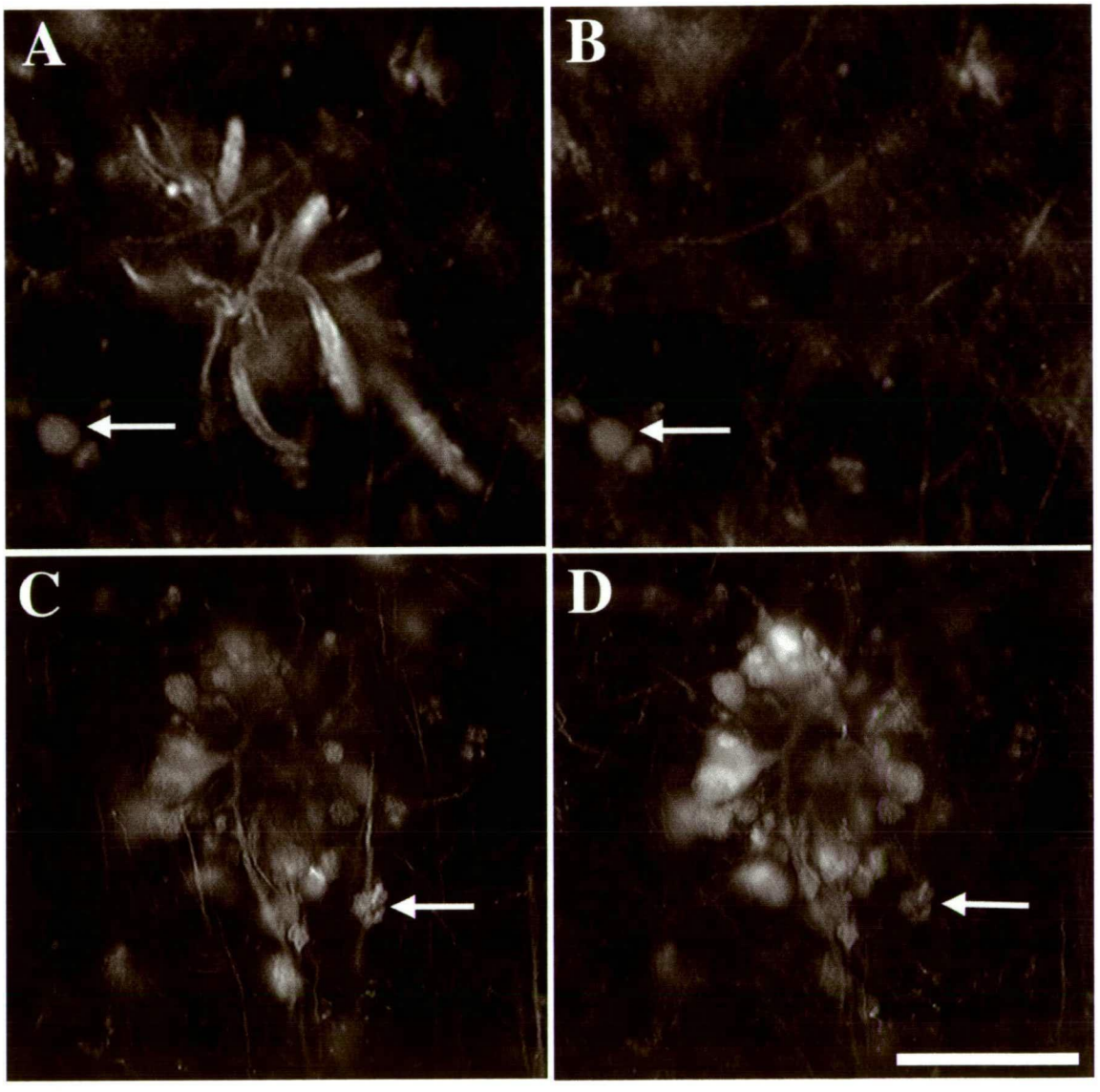
A
B
C
D

were globular or spherical in morphology whereas the RT97 labelled neurites that were not colocalised with the other NF markers were angular and elongated. A low degree of RT97 labelling was present in NFTs throughout the cortical layers.

Tau immunoreactivity was also present in DNs with an angular and elongated morphology. In AD cases, tau immunoreactive DNs were in considerably more abundance than NF labelled DNs. In addition, for most NF and tau double labelling combinations, immunolabelling for these cytoskeletal markers was localised to different DNs (Table 3.1). However, RT97 did show a high degree of colocalisation with tau (71%). For all other antibody combinations, colocalisation to individual DNs took the form of a bulb-like NF labelled structures with a tau immunoreactive central, or core, region (Figure 3.5).

The density of CgA immunopositive structures was considerably greater in AD cases than in preclinical cases, however, the general laminar distribution remained constant with the majority of labelling occurring in layers II, III, V and VI. Most bulb-like CgA immunoreactive structures were not immunoreactive for NFs. However, the larger globular CgA labelled structures were consistently colocalised with larger bulb-like NF immunopositive DNs (Figure 3.6). CgA labelling did not colocalise with the angular and elongated DNs immunoreactive for RT97.

Figure 3.5

Double labelling of abnormal neurites in a 72 year-old AD case at two different focal planes throughout a cluster of DNs. A) shows a cluster of predominantly SMI312 immunoreactive DNs (green). A small core of tau labelling (red) can be seen within one of the neurites, as indicated by the arrows. B) shows that deeper within the cluster the same tau core is more prominent (arrow) and an additional NF immunoreactive neurite can also be seen to have an extensive tau immunoreactive central element (open arrow).

Scale Bar = 40 μm (A and B).

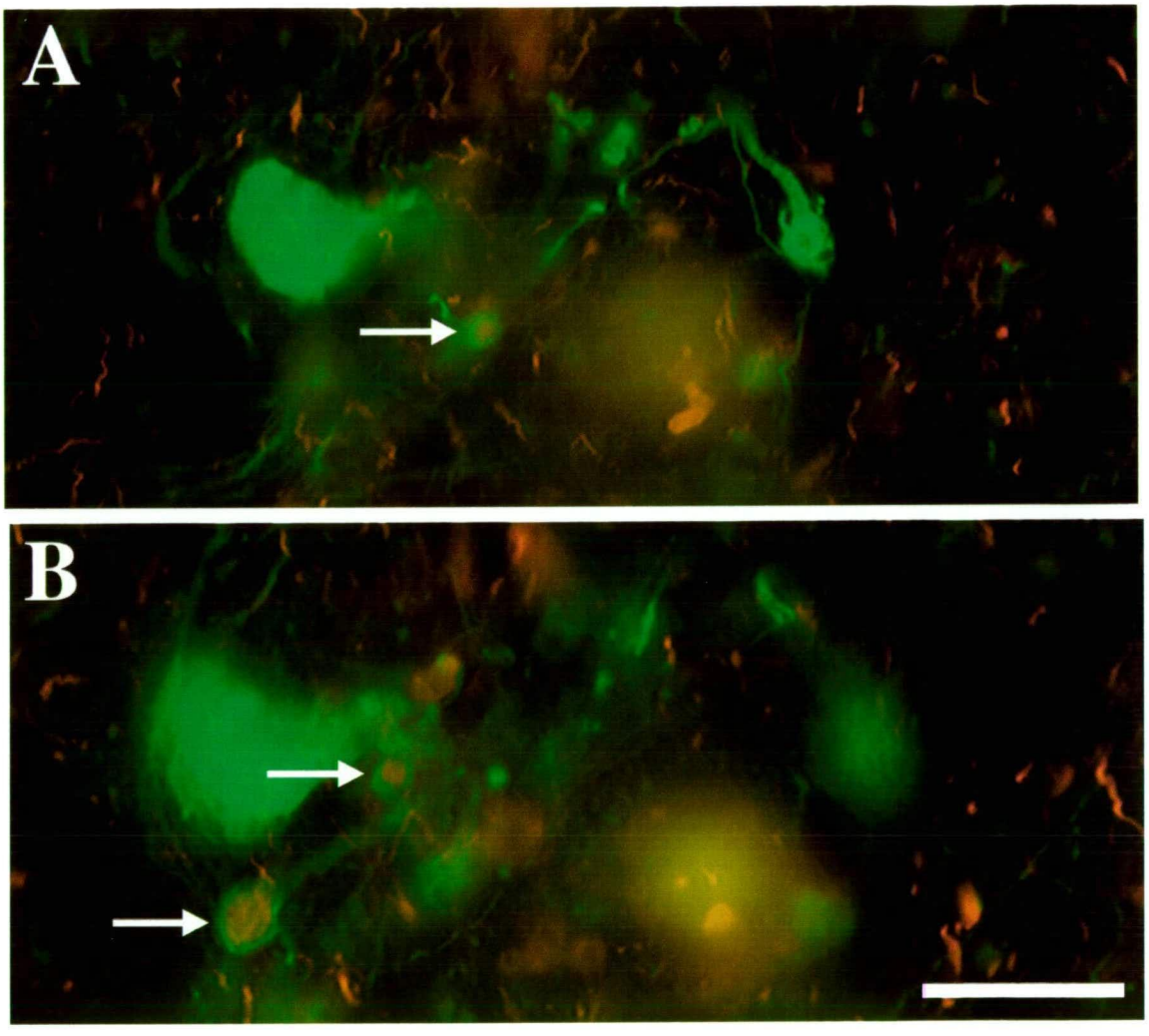
A
B

Figure 3.6

Relationship between NF (RT97) immunoreactive DNs (A) and labelling for the synaptic marker CgA (B) in layer III of the neocortex of a 73 year old AD case. Some neurites show colocalisation for both markers (arrow), whereas other distinct RT97 immunopositive neurites are unlabelled for CgA (arrowhead).

Scale Bar = 20 μm (A and B)

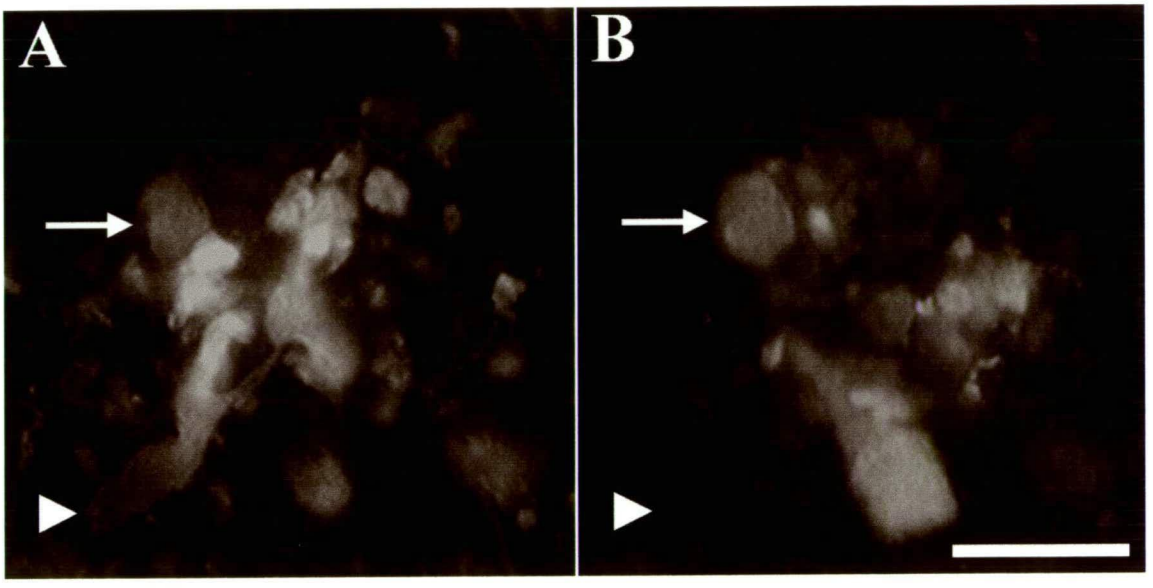
A
B

3.4 Discussion

A common phenomena associated with both preclinical and end-stage AD cases was the association between ß-amyloid plaques and clusters of DNs. All clusters of abnormal neurites were found to be localised with ß-amyloid deposits, however, not all deposits were associated with DNs. Detailed analysis of this relationship revealed a significant morphological and neurochemical diversity with respect to the clustered DNs (Table 3.2). In preclinical AD cases, DNs were characterised by the presence of either NF or CgA labelling, with these markers only occasionally colocalised to the same neurite. Interestingly, NFs were found within both bulb- and ring-like structures, whereas CgA labelled neurites were bulbar. AD cases were characterised by the appearance of angular and elongated DNs that were labelled with the antibody to tau. In these cases, NF labelling was found in bulb-like structures, but not in rings, within plaques, and a further subgroup of DNs showed mostly exclusive CgA labelling. In addition, some NF immunolabelled bulb-like structures had a tau immunoreactive core. Of note, NF labelled rings were present throughout the cortical grey matter in AD cases.

Table 3.2

Neurochemical diversity of dystrophic neurites

DN Type	Dystrophic Neurite Neurochemistry	Dystrophic Neurite Morphology	Preclin. AD	AD
1	NF only	bulb- and ring-like	✓	✓
2	APP colocalised with CgA	globular / bulb-like	✓	✓
3	NF colocalised with CgA	globular / bulb-like	✓	✓
4	NF with PHF-tau or thioflavine core	globular / bulb-like	-	✓
5	Tau and/or thioflavine-S	elongated / angular	-	✓

Summarised from current chapter and Dickson et al., 1988; Masliah et al., 1993b; Saunders et al., 1998; Su et al., 1996; Vickers et al., 1994b; Vickers et al., 1996; Wang & Munoz, 1995.

These diverse morphological and neurochemical changes associated with the neuritic reaction to plaques may indicate important features of DN development. This process is likely to take many years, from the initial preclinical phase of an accumulating insoluble ß-amyloid burden to the clinical stage characterised by the maturation of neurofibrillary pathology and eventual neuronal degeneration. These DNs showed a high degree of colocalisation of both phosphorylated and dephosphorylated NF epitopes. The presence of this mixture of epitopes is unusual as dephosphorylated epitopes are normally principally localised to the somatodendritic domain (Sternberger & Sternberger, 1983). These results show that phosphorylated and dephosphorylated NF epitopes can coexist in DNs, an observation that suggests a specific alteration in the processing of NFs.

The presence of CgA labelled neurites within both AD and preclinical AD cases may represent a form of reactive sprouting and synaptogenesis. This sprouting reaction may require the absence of normal NF proteins (Tetzlaff & Bisby, 1989), explaining why CgA labelling forms a cap of reactivity over some NF labelled DNs, and why most CgA labelled DNs were not immunoreactive with NF antibodies.

The data presented in this chapter indicates that the abnormalities in tau processing that contribute, for example, to the development of highly insoluble PHFs, may occur later in the disease process. These results extend previous findings (Masliah et al, 1993b; Vickers et al., 1994b; Yasuhara et al., 1994) of the localisation of NF and tau immunolabelling to different subpopulations of DNs. However, the presence of NF labelled DNs with a core region of tau immunoreactivity strongly suggests that these abnormal neurites may mature through initially NF abundant forms to morphologically different DNs containing insoluble PHFs. A similar progression of molecular events have been proposed for NFT development (Vickers et al., 1992b). This sequence of cytoskeletal alterations may be due to the close interrelationship of cytoskeletal proteins in nerve cells, including NFs with MTs (Letterier et al., 1982). Thus, the

abnormal processing or disruption of one cytoskeletal element may be expected to lead to changes in other cytoskeletal proteins.

The absence of NF immunopositive rings in plaques in AD may be indicative of an earlier complete disintegration of severed distal axonal terminal segments. However, the presence of NF immunopositive rings throughout the grey matter in AD may result from the gradual anterograde degeneration of the whole axonal tree of affected neurons. Finally, RT97 was notable for its labelling of angular and elongated DNs in the AD cases. These DNs were also labelled for tau, indicating that the NF antibody may also be cross-reacting with specific PHF-tau epitopes, as previously suggested (Ksiezak-Reding et al., 1987, Nukina et al., 1987).

Whereas the stages of NFT formation and development have been widely investigated and acknowledged, similar detail regarding DN formation has not been established. The first experimental chapter of this thesis indicates that there are three subsets of DNs in AD, including predominantly NF, tau or synaptic forms. Investigation of the precise interrelationship between these DN subtypes using multiple labelling immunohistochemistry suggests that DNs may mature from NF-containing forms to the abnormal neurites containing profoundly altered cytoskeletal proteins such as tau. The synaptic markers may reveal a further subset of axons undergoing reactive synaptogenesis. These results confirm a role for NF in the development of the DNs associated with ß-amyloid plaques, further to this studies utilising preclinical AD cases suggest that an accumulation of NFs may represent one of the earliest pathological phenomena associated with the disease.

Recent data has indicated that the same morphological and neurochemical heterogeneity, noted in the current investigation of plaque associated DNs, is present within axons undergoing a response to physical damage (King et al., 1997, 2000).* Acute axonal injury in a rodent experimental model of brain trauma resulted in the formation of neurofilamentous bulb- and ring-like accumulations (Figure 3.7). Detailed immunohistochemical analysis revealed the

* In this experimental model, a fine gauge needle is placed into the neocortex of anaesthetised adult rats (King et al., 1997).

Figure 3.7

NF immunolabelling of abnormal neuritic structures following physical damage in the rodent neocortex. Occasional bulb- (eg large arrow) and ring-like structures (eg arrowhead) labelled with R-NFH (A) are not labelled by SMI312 (B). The fine arrows in (B) indicate bulb- and ring- like strucutres labelled with SMI312 and also colocalised with R-NFH labelling (A). Ultrastructural analysis of the rat cortex post-injury revealed axons containing a number of multilamellar bodies and other degenerative structures, with a central core of NFs (C) (asterisk). Other investigators have described identical structures within DNs in AD (D) (Dickson, 1997).

Scale Bar = 100 μm (A and B)

Magnification = 15800x (C and D)

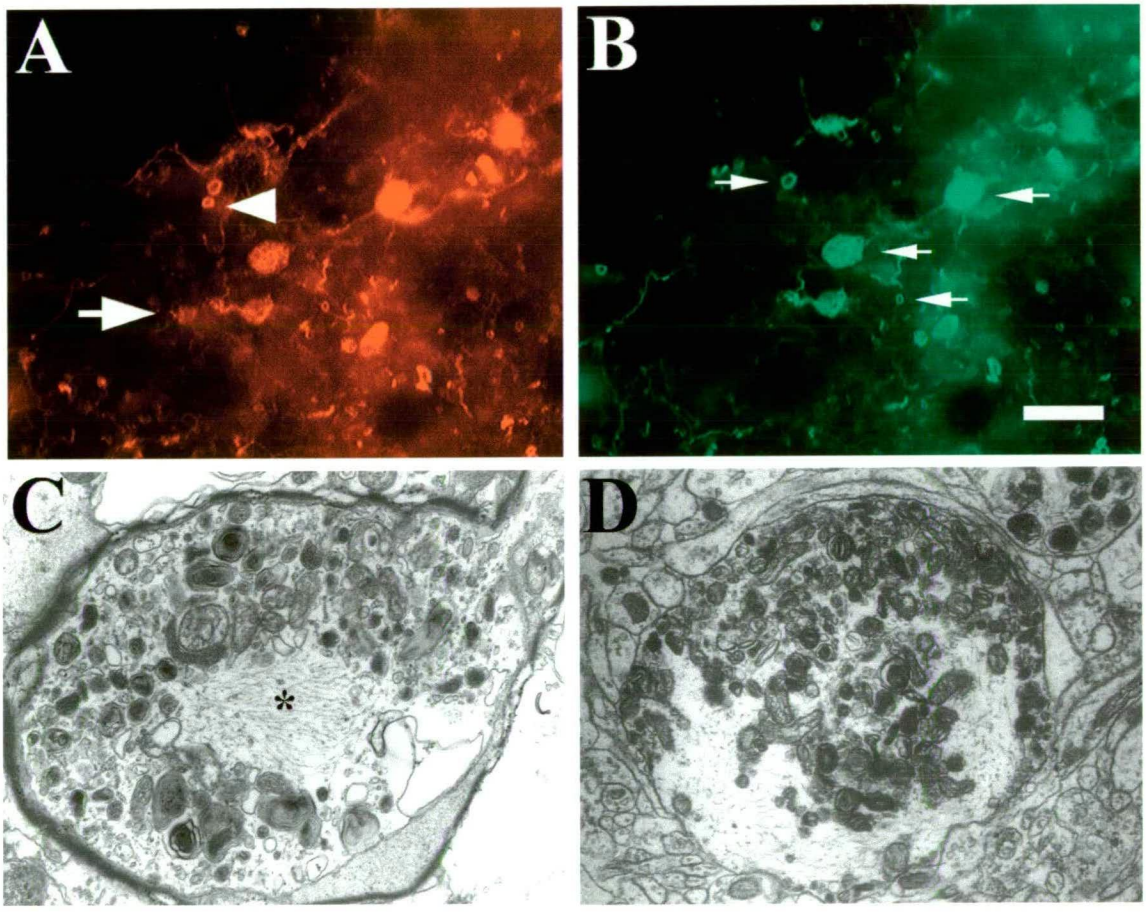
A
B
C
D

same expression pattern of NF epitopes as that found in the preclinical and end-stage AD cases (Table 3.1 compared to Table 3.3) (King et al., 2000). Furthermore, ultrastructural analysis of the axons reacting to damage revealed changes such as abnormal mitochondria, multilamellated bodies and dense core vesicles that were identical to those observed in AD DNs (Terry et al., 1964; Masliah et al., 1993a; Dickson, 1997). Based on these similarities it has been proposed that ß-amyloid plaque deposition in AD may cause sufficient physical disruption to the surrounding neuropil to trigger the stereotypical reaction of nerve cells that follows physical injury, leading to abnormal axonal sprouting and associated cytoskeletal changes (King et al., 1997, 2000; Vickers, 1997).

Table 3.3

Colocalisation between NF epitopes in abnormal neuritc structures following physical damage to the rodent neocortex

Labelling	% Colocalisation
R-NFH with SMI32	62.65
SMI32 with R-NFH	99.41
R-NFH with SMI312	92.05
SMI312 with R-NFH	97.93
R-NFH with RT97	82.70
RT97 with R-NFH	99.20
R-NFM with SMI32	71.20
SMI32 with R-NFM	86.25
R-NFM with SMI312	90.65
SMI312 with R-NFM	82.00
R-NFM with RT97	75.50
RT97 with R-NFM	91.95

King et al., 2000

DETAILED ANALYSIS OF ß-AMYLOID PLAQUE ASSOCIATED DYSTROPHIC NEURITES IN ALZHEIMER'S DISEASE USING CONFOCAL MICROSCOPY

4.1 Introduction

Standard immunohistochemical methods and fluorescence microscopy were previously utilised to effectively analyse the exact complement of epitopes expressed within the clusters of abnormal neurites associated ß-amyloid plaques in AD. However, due to the limitations of the standard microscope, similarly detailed analyses of plaque and DN morphology and how these two pathological hallmarks of AD interact spatially could not be obtained. Therefore, in the present study confocal microscopy was utilised. This method of analysis allowed the optical sectioning of fluorescence-labelled tissue, even from relatively thick sections, thereby allowing the visualisation of complete plaques rather than isolated sections. Through the digital processing of this information it was possible to elaborate a three dimensional view of labelled elements and to examine in detail the abnormal changes in axons associated with ß-amyloid plaque formation and the effect of plaque development on surrounding processes.

The heterogeneity of plaque morphology has been noted by a number of early investigators in the field of AD research (Wisniewski & Terry, 1973; Ulrich, 1985). This lead to the development of various different typing schemes that have been consistently modified and updated with the advent of more sensitive staining and immunolabelling methods. The form of microscopy utilised in individual investigations has also been recognised as an important contributor to the accurate description of plaque morphology.

Historically, the confocal microscope has been used to study a number of neurobiological phenomena. For example it has been used in conjunction with intracellular or membrane bound fluorescent dyes, to follow the growth and long-term changes of nerve terminals, and also with voltage and Ca^{2+} -sensitive indicator dyes to observe patterns of electrical activity (Reviewed by Fine et al., 1988). More recently it has been utilised in the field of AD research to investigate aspects of the pathological changes that occur. Masliah and collegues concluded, from their investigation of the alterations that occur in synapses and axons, that many of the tau abnormal neurites commonly localised with ß-amyloid plaques were continuous with synaptophysin-positive distended terminals (Masliah et al., 1993a). Others have used confocal microscopy to investigate various aspects of senile plaque morphology in end-stage AD cases (Schmidt et al., 1995; Cruz et al., 1997) and also the relationship between senile plaques and astrocytes (Kato et al., 1998). In the current investigation confocal microscopy was utilised to accurately quantitate the various plaque morphological types in both preclinical and end-stage AD cases and furthermore investigate their association with clusters of DNs.

4.2 Experimental procedures

4.2.1 Case details

The samples used in the current confocal microscopy investigations included five cases of confirmed AD (74, 74, 83, 88 and 92 years of age) and five preclinical AD cases (78, 81, 84, 90 and 91 years of age) (Table 2.1 for source and fixation details).

4.2.2 Staining

To investigate the morphology of ß-amyloid plaques, 100 µm sections of SFG from the preclinical and end-stage AD cases (Table 2.1) were stained with thioflavine S (Sigma) for three minutes at room temperature, protected from the light. After staining, sections were differentiated in two, ten minute rinses of 50% ethanol and 50% 0.01 M PBS before final washes in 0.01 M PBS.

4.2.3 Immunohistochemistry

The basic double-labelling immunohistochemistry protocol was utilised as outlined in Chapter 2, any changes or additions to this protocol are described below. The relationship between NF immunoreactive DNs and ß-amyloid was investigated in all cases. Sections in which ß-amyloid was to be visualised were pre-treated in 90% formic acid prior to incubation in either primary antibody. A rabbit-antibody which recognises all carboxy-terminal variants of ß-amyloid (Aß1-40 and Aß1-42(43)), pan ß-amyloid, was combined alternatively with mouse monoclonal antibodies to modified (phosphorylated (SMI312) and dephosphorylated (SMI32)) NFs in both preclinical and end-stage AD cases. The colocalisation patterns of cytoskeletal proteins (NF, tau) within individual abnormal neurites was also investigated using double labelling immunohistochemistry by combining the rabbit antibodies to 4Rtau (four MT binding domains) with the SMI312 mouse

monoclonal NF antibody. To determine the effect of ß-amyloid plaque development on surrounding processes, preclinical and end-stage AD material was double labelled with the pan ß-amyloid antibody and the mouse monoclonal antibody to MAP2 (see Tables 2.3 and 2.4 for primary antibody details). For all fluorescence labelling, mouse monoclonal antibodies were visualised with a horse anti-mouse secondary antibody conjugated to FITC whereas the rabbit polyclonals were visualised with a goat anti-rabbit antibody conjugated to biotin followed by streptavidin Texas Red avidin D (Table 2.5).

4.2.3 Confocal Microscopy

Laser confocal scanning microscopy, using an Optiscan F900e krypton/argon system attached to an Olympus microscope, was utilised to investigate the morphology of various plaque types and the localisation patterns of DNs within the plaque substructure. Fluorescein and Texas Red labelled preparations were recorded simultaneously in separate channels. Representative plaques were optically sectioned at intervals of 1-2 μm for distances of approximately 20-30 μm through a plaque. This information was then utilised to create three-dimensional images of the varying plaque types present throughout the cases. Plaques were categorised as either 'diffuse', 'dense-cored' or 'fibrillar'. Similar sectioning methods were utilised for material double labelled with the antibodies to ß-amyloid, however, distances of only 5-10 μm were sectioned due to antibody penetration limitations. Detailed analysis of the plaque substructure was performed using the Optimate 5.2 program. Measurements of plaque size and core size were obtained. The prevalence of each plaque type was determined by examining in detail one hundred plaques, throughout all cortical layers, in all cases. Further to this, the proportion of each plaque type that was neuritic, ie associated with either NF labelled (preclinical AD cases) or tau labelled (end stage AD cases) abnormal neurites, was also determined. Diffuse amyloid was noted to be

highly variable in its size and deposition patterns. Therefore, for the purpose of these investigations, only spherical deposits with a minimum diameter of approximately 40 μm were considered.

Confocal microscopy was further utilised to perform an analysis of the plaque associated DNs in the AD cases. The 40 μm sections double labelled with the rabbit antibody to tau and the mouse antibody to phosphorylated (SMI312) NFs were used for these analyses. Clusters of DNs were optically sectioned at 0.5-1 μm intervals. 'Optimate' was again utilised for size measurements. The proportion of NF immunoreactive DNs that had a tau immunoreactive core was quantified by sectioning through one hundred non continuous DNs labelled by either SMI312 or SMI32 per AD case. These counts were made throughout the layers, and included all morphological types of DNs.

4.3 Results

4.3.1 Preclinical Alzheimer's disease

Staining with thioflavine S and labelling with antibodies to ß-amyloid revealed a number of morphologically distinct plaques. Serial sectioning throughout these plaques uncovered key features specific to each plaque type. A subset of plaques were notable for their dense-core of ß-amyloid surrounded by indistinct wispy labelling (Figure 4.1). These plaques were approximately 40-60 μm in diameter. Other plaques were coreless and were comprised of large numbers of distinct fibrils (Figure 4.2). These fibrillar plaques tended to have distinct pores and irregularities within their structure and were of a similar size to the dense-cored plaques ie 50-70 μm. Of note, the ß-amyloid labelling in the outer regions of both of these plaque types was confluent. Three dimensional visualisation of these structures suggested that these plaques were spherical. Sequential optical sectioning revealed distinct similarities between the fibrillar and dense-cored plaques at levels on and immediately below the surface. Diffuse deposits that were more variable in size (10-180 μm), irregular in shape, and without distinct edges were also present (Figure 4.3). Specific plaques type were not localised to particular layers, however, layer I was notable for its lack of any form of ß-amyloid labelling. Variation between cases was low with regards to patterns of ß-amyloid labelling. Quantitation of the three plaque types revealed that the majority of ß-amyloid deposits were diffuse (average of 54%). Dense-cored and fibrillar plaques accounted for the remaining 24% and 22% of plaques, respectively.

Of the diffuse plaques counted per case, an average of 12% were associated with NF immunopositive DNs. However, 47% of fibrillar plaques and 82% of dense-cored plaques were neuritic. There was no correlation between laminar location and the association with DNs. The NF immunoreactive DNs exhibited a variety of morphological types including

Figure 4.1

Nine sequential confocal images sectioned through a dense core plaque stained with thioflavine-S in a preclinical AD case (83 yrs). The images were captured at intervals of approximately 3.6 μm. The total depth of the sectioned plaque was 28.56 μm. Images show a distinct central core of ß-amyloid surrounded by a void or clearing and then an outer rim of ß-amyloid.

Scale Bar = 20 μm

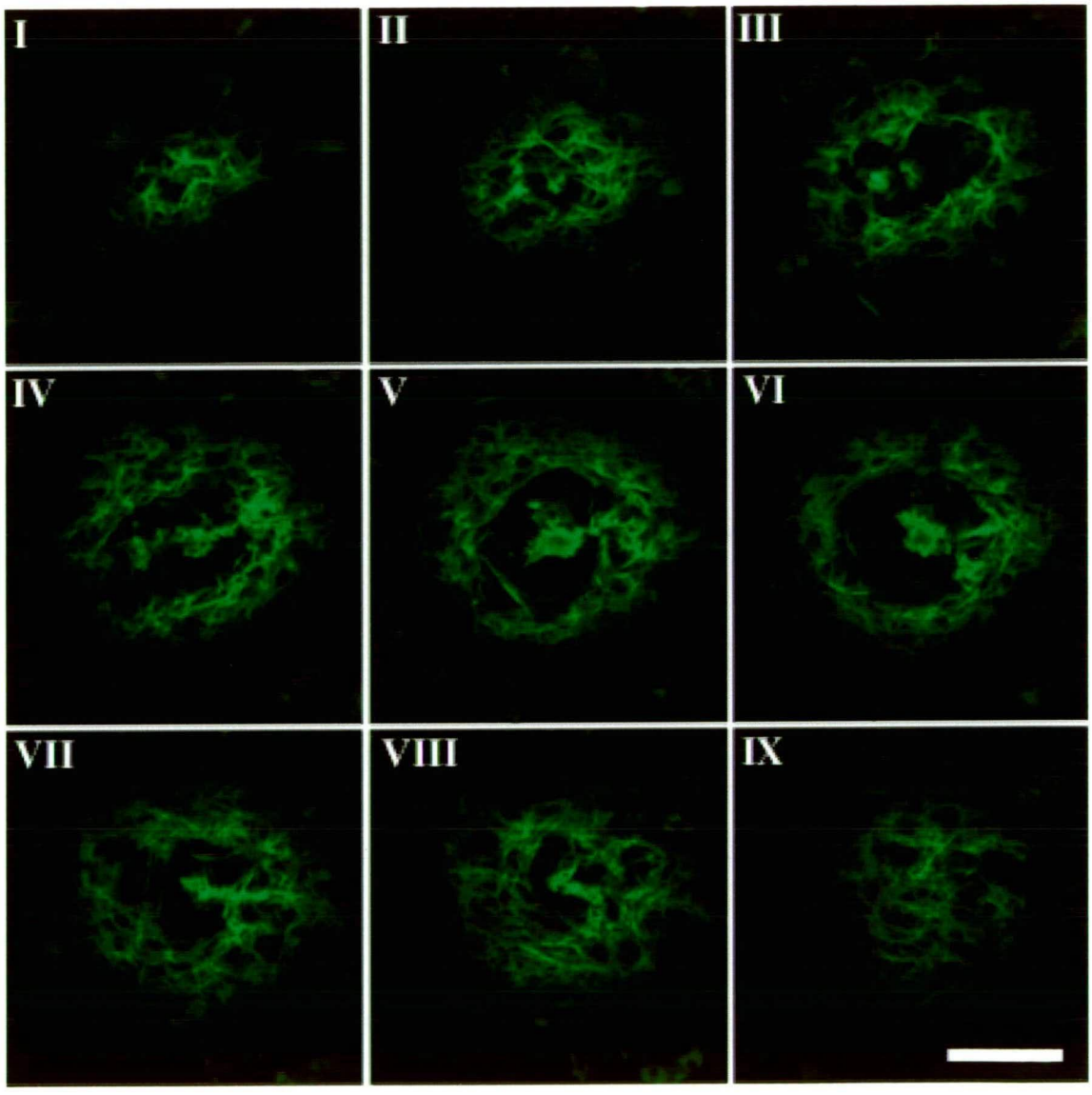
I
II
III
IV
V
VI
VII
VIII
IX

Figure 4.2

Nine sequential confocal images sectioned through a dense core plaque stained with thioflavine-S in a preclinical AD case (81 yrs). The images were captured at intervals of approximately 4.4 μm. The total depth of the sectioned plaque was 34.68 μm. The fibrillar plaques showed dense ß-amyloid accumulations throughout the plaque structure. In the central regions these accumulations often appeared as spoke-like accumulations, emanating from a denser central accumulation. Distinct pores within the plaque were obvious in deeper sections.

Scale Bar = 20 μm

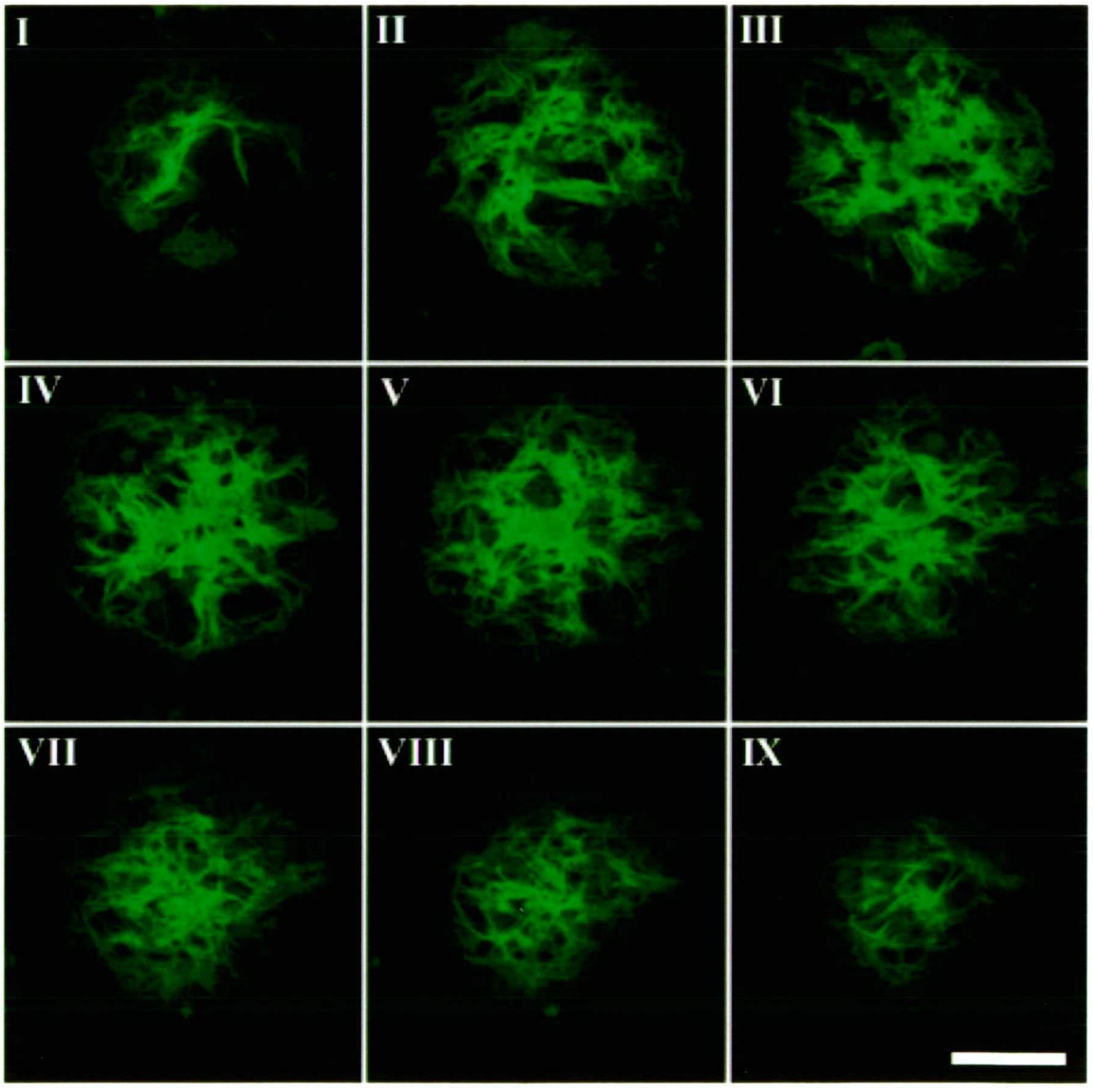
I
II
III
IV
V
VI
VII
VIII
IX

Figure 4.3

Six sequential confocal images sectioned through a diffuse plaque labelled with an antibody to ß-amyloid in an end-stage AD case (74 yrs). The images were captured at intervals of approximately 0.8 μm. The total depth of the plaque that was sectioned was 5 μm. These deposits were generally larger in diameter, however, considerably smaller in depth. Only small changes in the plaque structure were noted in the different optical sections.

Scale Bar = 50 μm

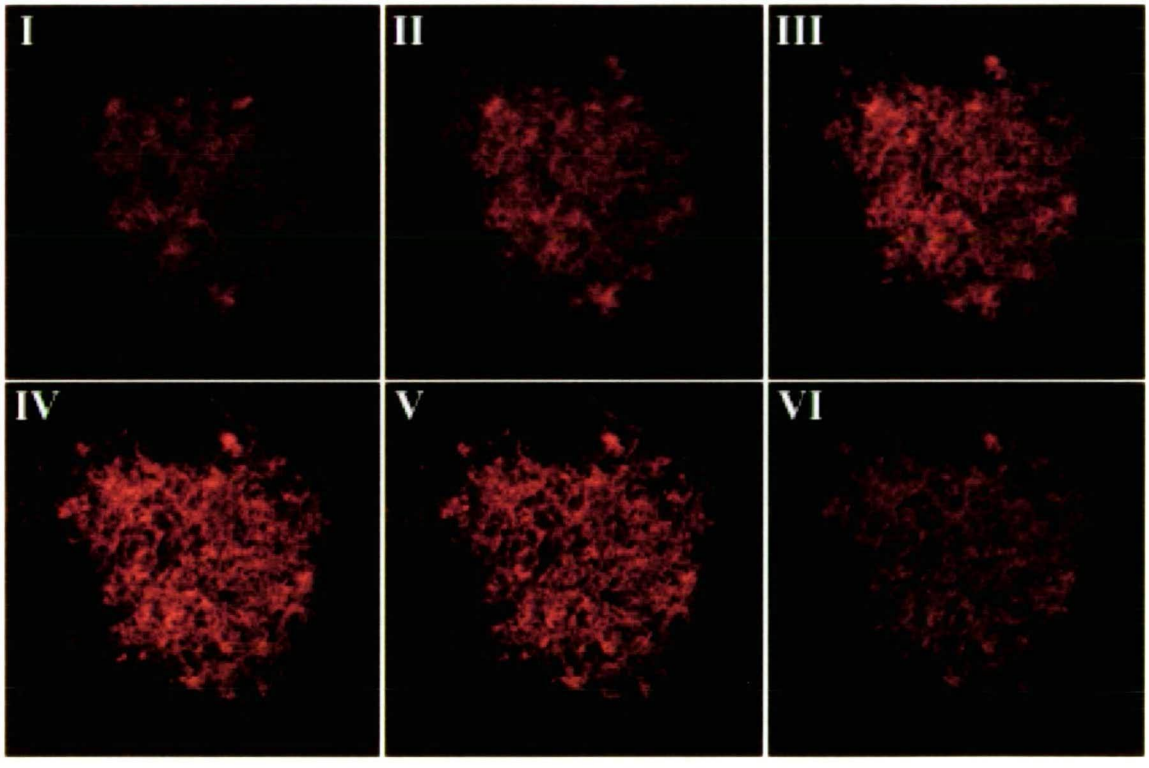
I
II
III
IV
V
VI

bulb and ring-like structures. These structures were labelled by both SMI32 and SMI312 but not labelled by the antibody to tau. Optical sectioning through neuritic plaques indicated that the larger bulb-like neurites were generally located within larger pores or holes in the amyloid substructure (Figure 4.4). In the dense-cored plaques these pores mostly occupied the area directly adjacent to the ß-amyloid core, whereas in diffuse and fibrillar plaques they were non-uniformly dispersed throughout the plaque. The larger bulb-like DNs were often continuous with fine processes of normal diameter. Many of these processes appeared to be passing through holes in the plaque and then immediately terminated with a large swelling or NF accumulation (Figure 4.5). The ring-like structures also appeared to be co-located to cavities within the ß-amyloid plaque. However, these cavities were smaller in dimension to those occupied by the larger bulbs.

4.3.2 Alzheimer's disease

The same categories of ß-amyloid deposits were present in the end-stage AD cases as those noted in the preclinical material ie diffuse, fibrillar and dense-cored. ß-amyloid labelling was, however, more intense and spread throughout the layers. Large numbers of diffuse ß-amyloid immunopositive deposits were present throughout layer I with many dense-cored plaques present within layer V. The prevalence of the three plaque types was notably different in the AD cases as compared to the preclinical AD cases. In these cases an average of 49% of spherical ß-amyloid deposits were fibrillar, 20% dense-cored and 31% diffuse.

Double labelling with the antibodies to ß-amyloid and MAP2 revealed a distinct morphological change within the dendrites in close association with both fibrillar and dense-cored ß-amyloid plaques. However, no changes in dendritic morphology or the

Figure 4.4

Double labelling with antibodies to ß-amyloid (red) and phosphorylated NFs (green) showing the relationship between plaque morphology and the location of the abnormal neurites in preclinical AD cases. For each example (A (81 yrs) and B (91 yrs)) three optical sections throughout the fibrillar plaques (i, ii and iii) and a cumulative multiple brightness image (iv) are shown. Arrows indicate neurofilamentous bulb-like structures.

Scale Bar = 20 μm (A and B)

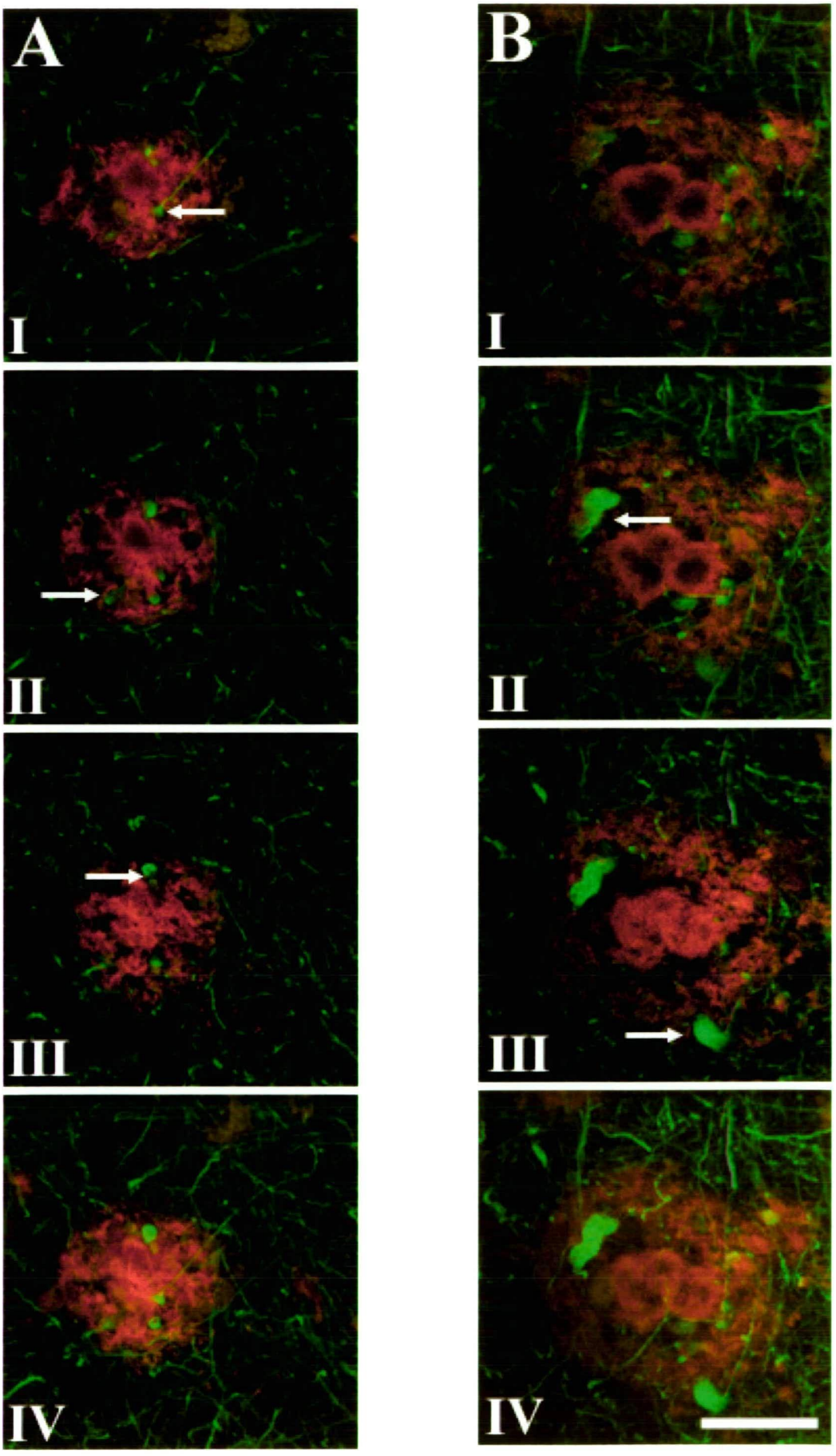
A
I
II
III
IV
B
I
II
III
IV

Figure 4.5

Double labelling with antibodies to ß-amyloid (red) and phosphorylated NFs (green) showing further examples of the relationship between plaque morphology and the location of the abnormal neurites in preclinical AD cases. For each example (A and B (81 yrs)) three optical sections throughout the dense cored plaques (i, ii and iii) and a cumulative multiple brightness image (iv) are shown. Arrowheads indicate neurofilamentous ring-like structures and arrows, bulb-like structures.

Scale Bar = 20 μm (A and B)

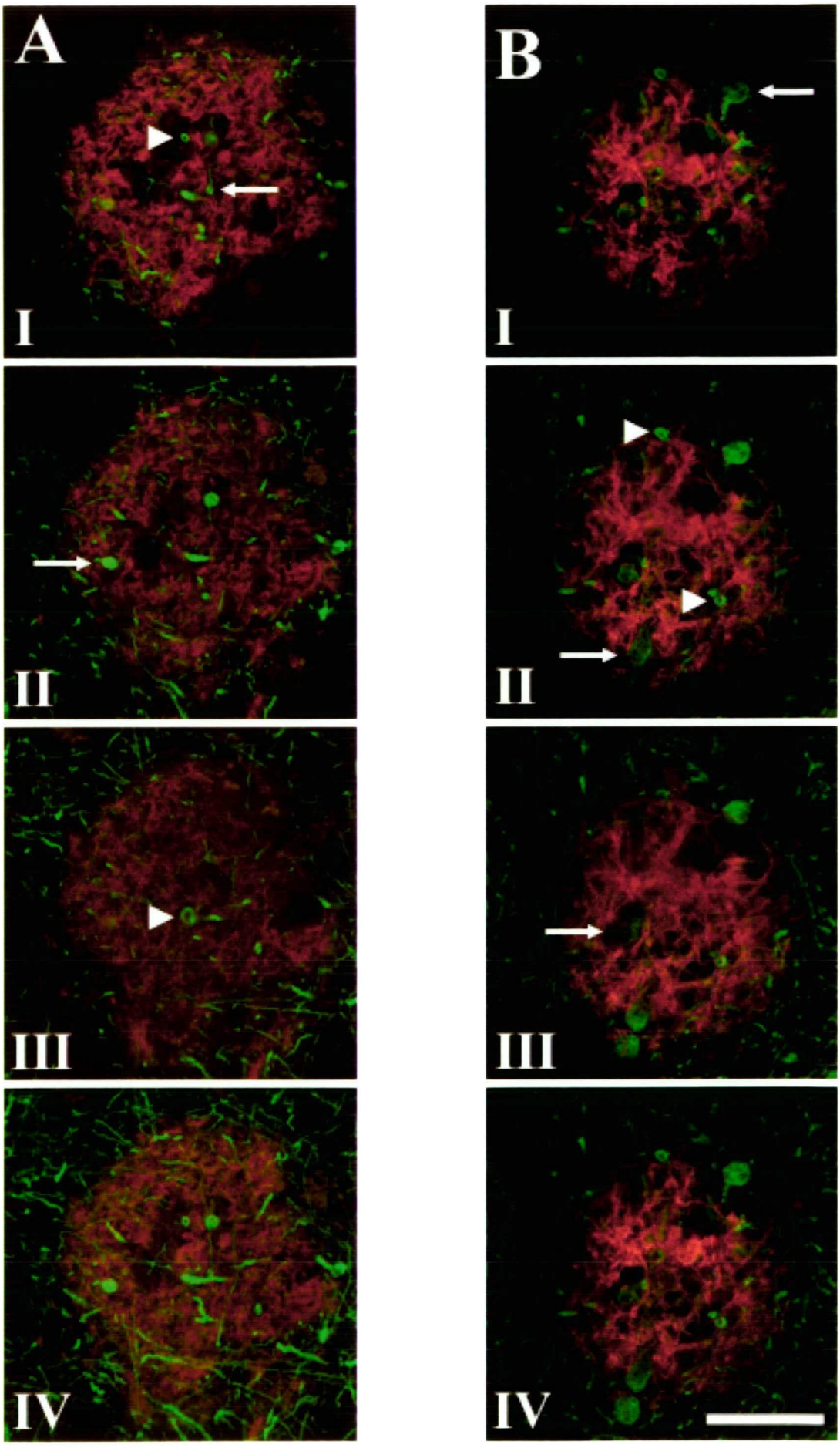
A
I
II
III
IV
B
I
II
III
IV

course of their growth was noted in processes associated with diffuse deposits (Figure 4.6). This pattern of labelling was consistent throughout both case types.

Labelling of thioflavine-S stained material with an antibody to tau revealed that 82% of dense-cored plaques, 47% of fibrillar plaques and 12% of diffuse deposits were neuritic. The predominant morphological DN types were bulb-like structures of varying sizes (3-8 μm) and also elongated, fusiform structures (10-20 μm). Both forms exhibited immunoreactivity to anti-tau and anti-NF antibodies. The pattern of distribution of the bulb-like DNs closely resembled that encountered for similar DNs in the preclinical cases. Generally, the bulb-like structures were located within the pores of the plaque (Figure 4.7). The more tortured and elongated DNs, had a somewhat different distribution within the ß-amyloid plaques. Rather than occupying pores they emerged from small pores and did not appear to cause changes to surrounding ß-amyloid. Consequently, they were located in all areas of plaques including within the central region (Figure 4.7).

Analysis of the NF immunopositive DNs with the confocal microscope and optical sectioning through the structures confirmed the presence of a tau immunoreactive core within a subset of these pathological structures. Initially this pattern of labelling was thought to be restricted to the bulb-like DNs (Figure 4.8), however, confocal microscopy also revealed tau immunoreactive cores within the longer more cylindrical DNs (Figure 4.9). In these structures only the very outer rim showed anti-NF labelling. Confocal investigation of non-connected NF immunopositive DNs revealed that an average of 30% had a tau core. Many of these cores were only visible after optically sectioning through the DN clusters.

Figure 4.6

MAP2 labelled dendrites (green) showed distinct curving around dense cored plaques (A), whereas limited change was noted in similarly labelled processes associated with diffuse ß-amyloid deposits (B). For each example (A and B) three optical sections throughout the plaque (i, ii and iii) and a cumulative multiple brightness image (iv) are shown. Arrows indicate curved dendrites. Both sets of images were taken from an end-stage AD case, 73 years of age.

Scale Bar = 15 μm (A and B)

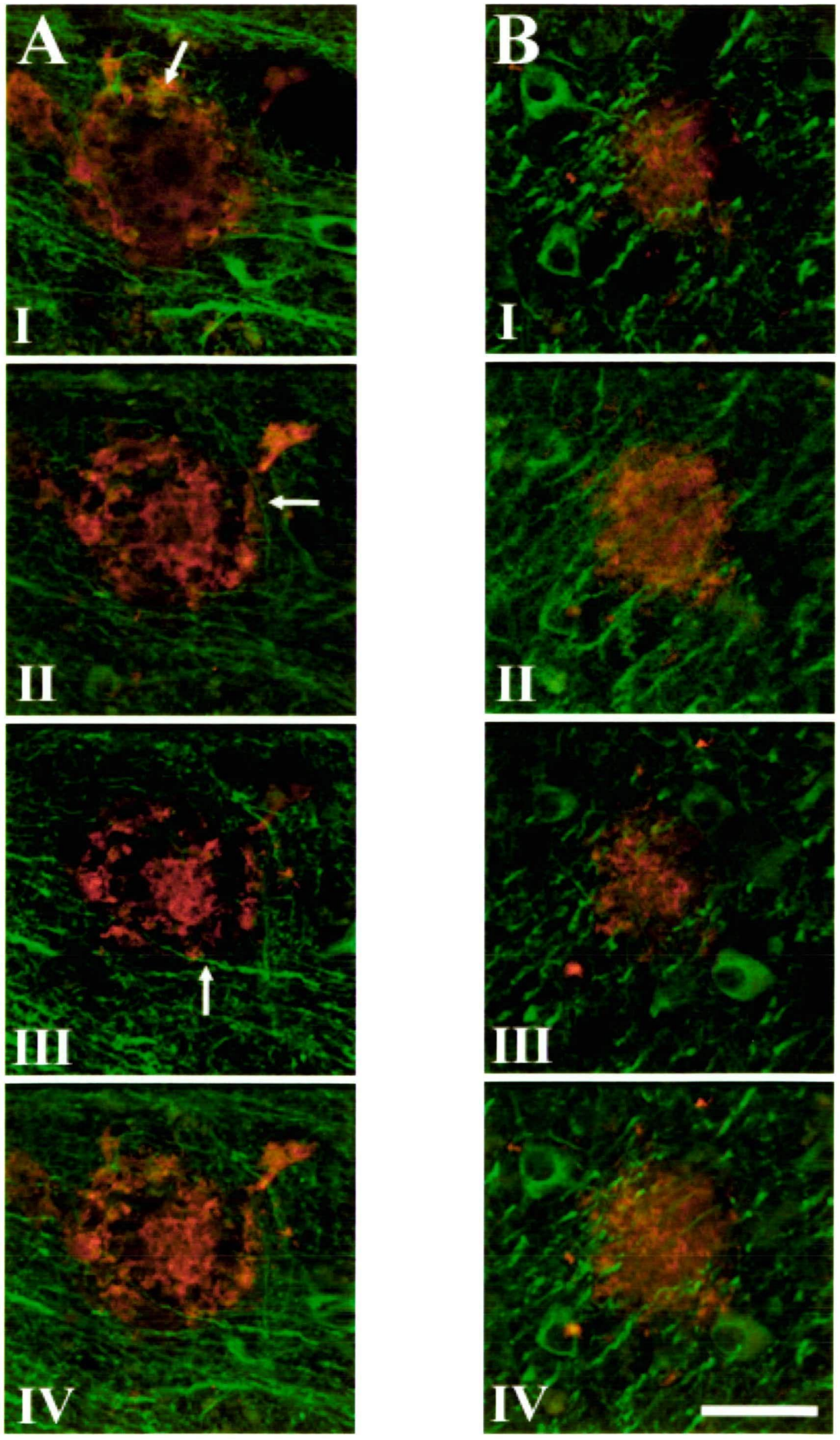
A
I
II
III
IV
B
I
II
III
IV

Figure 4.7

Double labelling with antibodies to ß-amyloid (red) and tau (green) showing the relationship between plaque morphology and the location of the abnormal neurites in end stage AD cases. For each example (A (84 yrs) and B (92 yrs)) three optical sections throughout the plaque (i, ii and iii) and a cumulative multiple brightness image (iv) are shown. A) shows a diffuse plaque, associated with clusters of DNs. Arrowheads indicate long distended DNs exhibiting classical tau morphology, whereas arrows indicate neurofilamentous bulb-like accumulations of similar morphology to those noted in preclinical AD cases.

Scale Bar = 15 μm (A and B)

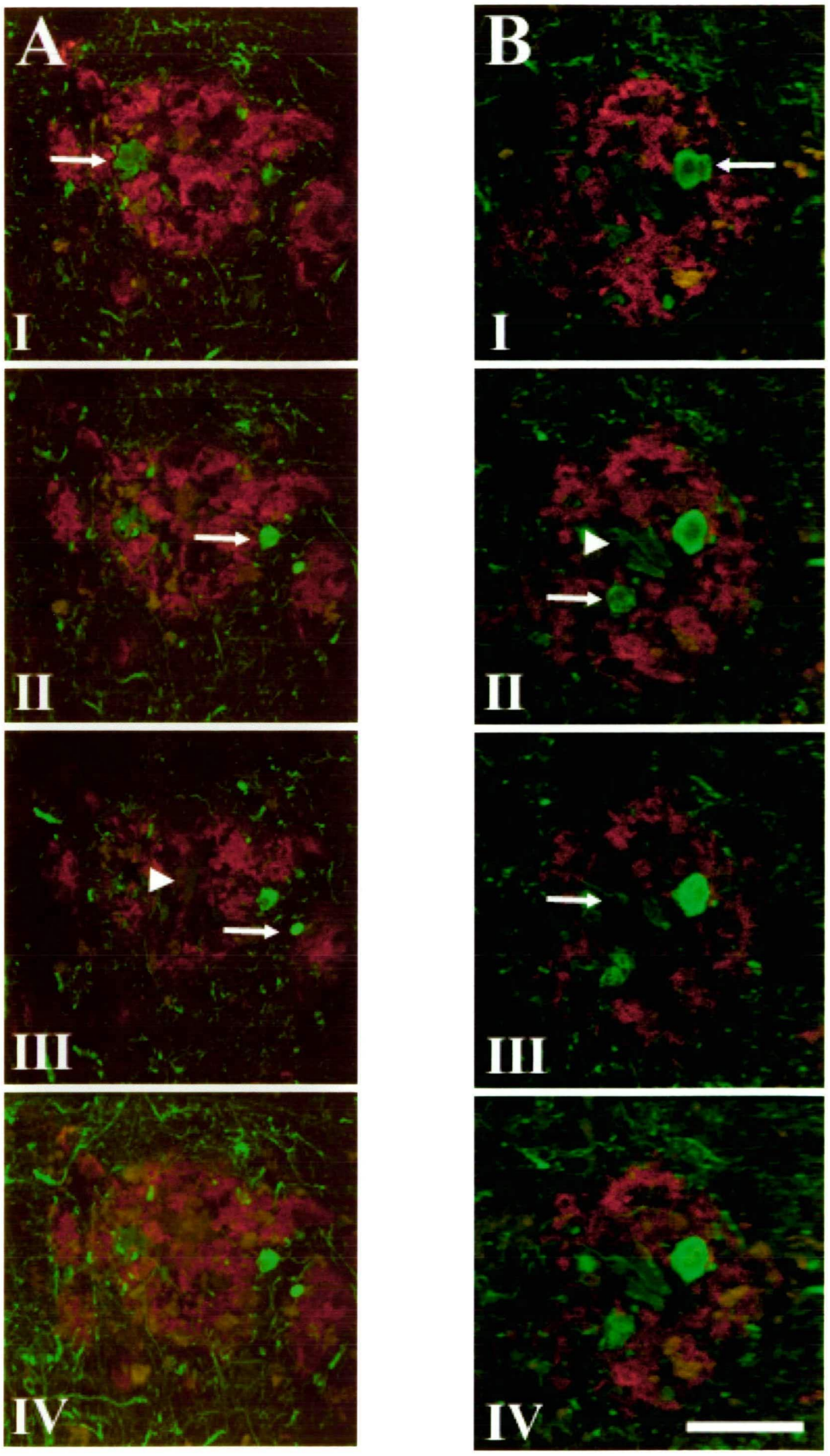
A
I
II
III
IV
B
I
II
III
IV

Figure 4.8

Double labelling of bulb-like NF (green) immunopositive DNs with tau cores (red) in AD cases (A(72 yrs), B(84 yrs), C(84 yrs) and D(74 yrs).

Scale Bars = 15 μm (A, B and C) and 20 μm (D)

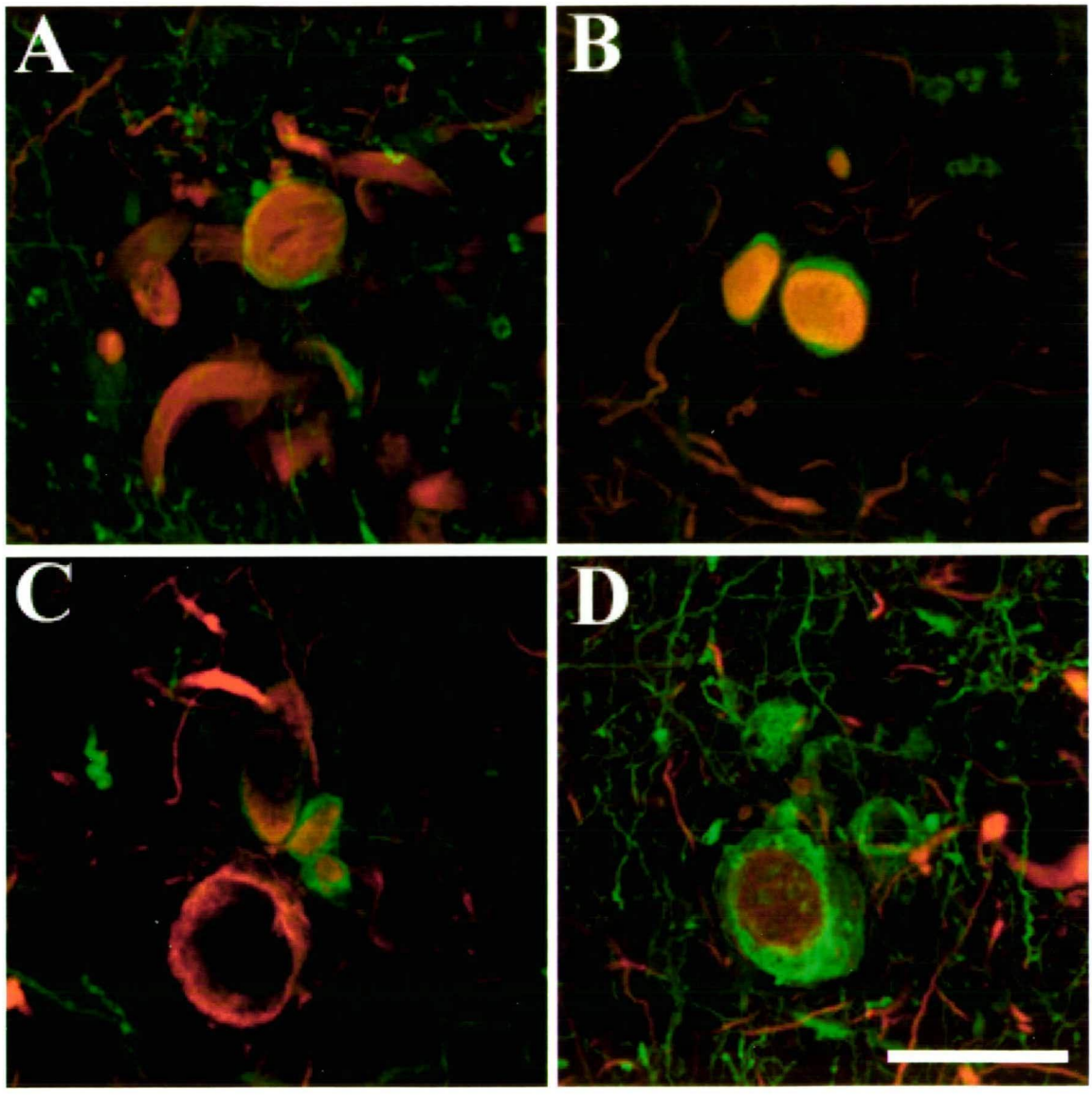
A
B
C
D

Figure 4.9

Double labelling of elongated fusiform NF (green) immunopositive DNs with tau cores in AD cases (red) (A(84 yrs), B(74 yrs), (72 yrs) and D(84 yrs).

Scale Bars = 15 μm (A), 15 μm (B), 20 μm (C) and 15 μm (D)

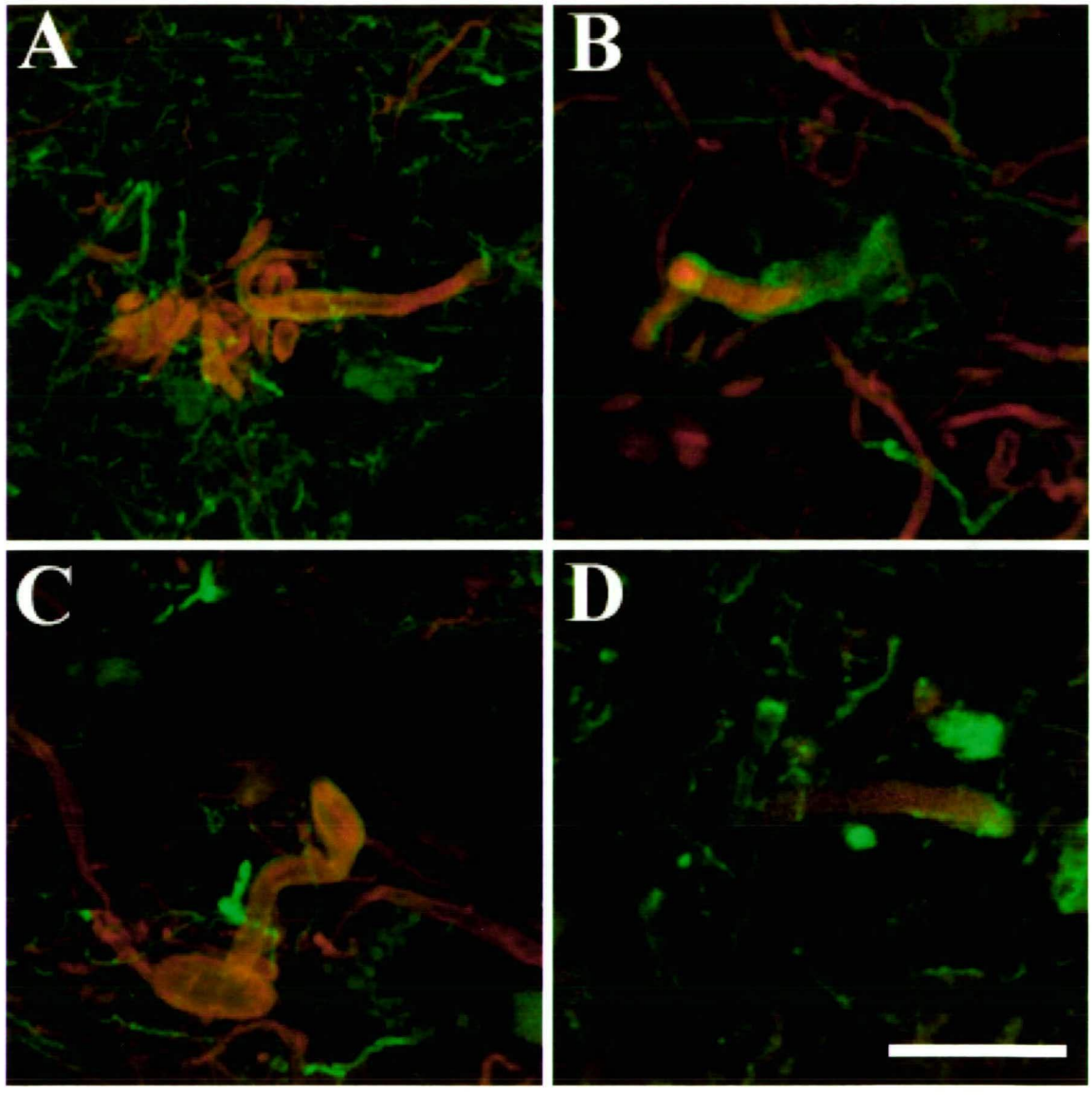
A
B
C
D

4.4 Discussion

The current investigation confirms previous reports that ß-amyloid plaques are not uniform structures (Ikeda et al., 1989; Wisniewski et al., 1989; Dickson, 1997). Both the preclinical and end-stage AD cases exhibited considerable diversity with regards to the morphological types of ß-amyloid deposits that were present. Although, historically, plaques have been grouped into varying numbers of different morphological types this study found that all plaques investigated could adequately be assigned to one of three distinct types either dense-cored, fibrillar or diffuse. Confocal microscopy was utilised to section through amyloid deposits to accurately categorise plaque type and to investigate the composition of individual plaques. Importantly, this procedure revealed a potential for incorrect plaque classification if only one focal plane was considered, as is often the case with routine microscopy. This was particularly important when discriminating between fibrillar and dense-cored plaques.

The presence of ß-amyloid plaques of varying morphology has been noted by a number of investigators (Wisniewski & Terry, 1973; Ulrich, 1985; Masliah et al., 1993a; Schmidt et al., 1995; Dickson, 1997; Armstrong, 1998). Two main hypothesis have been developed to account for the observation. Firstly, that one type of plaque is converted into another, ie that the different plaque types represent stages in the life history of a single type of plaque (Ikeda et al., 1990). The second hypothesis is that each plaque type evolves independently of the others and, therefore, unique factors are involved in their formation (Armstrong, 1998). In this investigation the prevalence of diffuse, fibrillar and dense-core plaques was variable between case types but did not correlate with disease progression as all plaque types were evident within both preclinical and end-stage AD. These data suggest that the life history theory of plaque development is unlikely to be strictly correct. Further to this,

the presence of dense-core plaques in preclinical AD cases suggests that these lesions are not confined to cases in the very end stages of the disease (Rozemuller et al., 1989; Ikeda et al., 1990).

A common phenomena in AD is the association between plaques and clusters of DNs. As noted in the preceding chapter, all clusters of abnormal neurites were found to be localised with ß-amyloid deposits, however, not all deposits were associated with DNs. Analysis revealed that this association was not governed by the morphological characteristics of the plaque as all plaque types were associated with DN clusters, albeit at varying rates. In addition, the rare but notable association of diffuse amyloid deposits with clusters of DNs, in both the preclinical and end stage AD cases, further argues against the likelihood of diffuse amyloid representing an early, transient and inert stage of plaque development (Yamaguchi et al., 1988). This less structured type of deposit is able to cause damage to surrounding nerve cell processes resulting in the development of clusters of NF and tau immunopositive DNs similar to those associated with the more defined and compact dense-cored and fibrillar plaques. However, it should be noted that in accordance with other investigators, dense-cored and fibrillar plaques had a more pronounced effect on surrounding dendrites as compared to diffuse plaques (Knowles et al., 1999). These results suggests that the physical presence of certain plaque types is able to influence surrounding processes, however, a further non-morphological trait differentiates damaging and non-damaging deposits.

A notable morphological and neurochemical diversity has previously been reported in the abnormal neurites associated with ß-amyloid deposits (Dickson et al., 1988; Vickers et al., 1994b; Yasuhara et al., 1994; Wang & Munoz, 1995; Su et al., 1996; Saunders et al., 1998).

Confocal microscopy provided a means to investigate this diversity more fully and to consider the interrelationship between DNs and ß-amyloid plaques in a manner not possible with a conventional microscope. Preclinical cases were again characterised by the presence of NF immunopositive bulb and ring-like DNs that were not labelled with antibodies to tau, and end stage cases, by NF and tau immunoreactive bulb-like neurites and swollen fusiform processes. The NF accumlations in the preclinical cases may represent one of the earliest pathological changes that occurs in AD (Vickers et al., 1996). In both preclinical and end stage AD cases the bulb-like DNs occupied large pores within the plaque substructure. Cruz and collegues also reported the occupation of such pores by cellular elements in AD cases (Cruz et al., 1997). Similar pores were present in non-neuritic plaques. Therefore, it is unlikely that the physical presence of the abnormal neurite results in the formation of the pore. The structures appear to form in the area of least resistance. The more elongated NF immunoreactive DNs are morphologically identical to those structures labelled by antibodies to tau in end stage AD cases. These structures appeared as torturous processes that seemed to taper at the end most closely associated with the ß-amyloid deposit. This taper may represent a point of focal constriction exerted by the plaque which may initiate the accumulation of NFs within these processes. Other investigators have similarly described a swelling and disruption of normal morphology in axons (Benes et al., 1991) and dendrites (Knowles et al., 1999) observed passing through plaques. Optical sectioning revealed that the DNs observed in the current investigation were mostly non-continuous as opposed to single branched processes, which has previously been proposed (Masliah et al., 1993a).

Double labelling with antibodies to phosphorylated NFs (SMI312) and tau again revealed the presence of NF immunoreactive bulb-like structures with a tau core which may

correspond to a transitional stage of DN development. Optical sectioning allowed for accurate quantitation of this class of abnormal neurite. Approximately 30% of NF immunoreactive DNs in end-stage AD cases were found to have a tau immunoreactive central region. Further to this, whereas previous reports describe this pattern of labelling in bulb-like DNs it is now clear that this distinct pattern of labelling is also present in a proportion of classical elongated tau immuoreactive DNs. These results further implicate NFs in the development of not only the earliest abnormal neurites associated with plaque development but also the accumulation of tau within these process.

In this investigation, through the use of confocal imaging techniques, it was concluded that ß-amyloid plaques are morphologically diverse. All plaque types are present in both the early and late stages of AD and are associated with large clusters of abnormal neurites. The subtype of DN found within these clusters is not related to plaque morphology, however, the location within the ß-amyloid deposit did correlate with particular features of the plaque structure. Furthermore, the density of the plaque was found to influence the distribution of surrounding dendritic processes. Results suggest that a further plaque attribute is responsible for the differential association between some ß-amyloid deposits and DN clusters. The lack of correlation between the density of DNs and their proximity to plaques suggests that this attribute is unlikely to be associated with ß-amyloid toxicity.

RELATIONSHIP BETWEEN APOLIPOPROTEIN E AND THE AMYLOID DEPOSITS AND DYSTROPHIC NEURITES OF ALZHEIMER'S DISEASE

5.1 Introduction

ApoE has been identified as performing a number of roles in cell biology, including the transport of cholesterol and other lipids throughout the body (Mahley et al, 1988). It has also been implicated in the reactive response of neurons following damage (Poirier, 1994). Inheritance of the ε4 allelic version of the ApoE gene is a risk factor for the development of AD (Corder et al., 1993; Saunders et al., 1993). It is notable that head injury and ApoE genotype may act synergestically to increase risk for AD (Mayeux et al., 1995) and that poor clinical outcome from head trauma is also associated with inheritance of ε4 alleles (Jordan et al., 1997; Teasdale et al., 1997; Friedman et al., 1999). The mechanisms underlying the role of ApoE in responses to injury and also AD are yet to be clarified.

Immunohistochemical studies have shown that ApoE is localised to the pathological hallmarks of AD, such as plaques (Wisniewski & Frangione, 1992; Han et al., 1994; Kida et al., 1994; Gearing et al., 1995; Uchihara et al., 1995; Sheng et al., 1996) and possibly also NFTs (Han et al., 1994; Benzing & Mufson, 1995). Single labelling immunoperoxidase studies have described a degree of discordance in the distribution of ApoE and ß-amyloid labelling between and within specific brain structures (Han et al., 1994; Kida et al., 1994; Gearing et al., 1995; Uchihara, et al., 1995; Sheng et al., 1996).

In this investigation the relationship between ApoE immunolabelling and ß-amyloid deposition, neuritic plaques and NFTs was examined using immunofluorescent double labelling techniques. Multiple labelling fluorescent methods provided an opportunity to directly examine specific hypotheses on the relevance of ApoE localisation to the development of the pathological hallmarks of AD. Thus, ß-amyloid plaques of varying morphology throughout the cortical layers were investigated for their degree of colocalisation with ApoE immunoreactivity. In addition the localisation of ApoE labelling with respect to neurofibrillary pathology was examined. Finally, aged non-demented cases that contain cortical ß-amyloid plaques, and may represent preclinical AD (Morris et al., 1996), were utilised to investigated the localisation of ApoE labelling in the early stages of AD. Determination of the role of the ApoE protein in AD is crucial for elucidating the sequence of pathological events that ultimately result in dementia.

5.2 Experimental procedures

5.2.1 Case details

In these experiments investigating the relationships between ApoE, ß-amyloid plaques and neurofibrillary pathology six cases of confirmed AD (65, 66, 71, 72, 73, and 74 years of age) and four preclinical AD cases (61, 62, 70 and 71 years of age) (Tables 2.1 and 2.2 for source and fixation details) were utilised.

5.2.2 Immunohistochemistry

Both single labelling (chromogen precipitation) and double labelling (fluorescence) methods were used to visualise ApoE and ß-amyloid immunoreactivity. Basic immunohistochemistry protocol was utilised as previously outlined in Chapter 2, any changes or additions to this protocol are described below.

Sections of the superior frontal gyrus in which ß-amyloid was to be visualised were pre-treated with 90% formic acid and then extensively washed in PBS prior to primary antibody incubations. Antibodies utilised for this study are described in Tables 2.3 and 2.4. For single-labelled, immunoperoxidase preparations, mouse monoclonal antibodies to ß-amyloid and ApoE were used. For double labelling preparations, the mouse monoclonal antibody to ApoE was combined either with the rabbit polyclonal antibody to ApoE or one of the two rabbit antibodies to ß-amyloid. For further investigation of ApoE and its relationship with DNs in AD cases, the mouse monoclonal ApoE antibody was combined alternatively with rabbit polyclonal antibodies to ubiquitin and tau. The degree of colocalisation was determined by counting the proportion of ApoE positive plaques colocalised with DNs present in either layers II and III or V and VI. One hundred plaques were counted, from these supra- and infra-granular areas, of each case. For the purpose of quantitation neuritic plaques were classified as either sparse, (1-5

DNs per plaque in the plane of focus), or clustered, (>5 DNs). Double labelling was also conducted between the mouse antibody to ß-amyloid and the rabbit antibodies to tau and ubiquitin.

The rabbit polyclonal antibody to ApoE was used in double labelling investigations in conjunction with the mouse monoclonal SMI310, as the latter antibody labels the early to middle stages of NFT formation (Vickers et al., 1992b). The proportion of immunopositive tangles that were ApoE and/or SMI310 immunopositive, in layers V and VI, was determined. Similarly the ApoE antibody was used in conjunction with the mouse monoclonal antibody SMI32 to investigate the association of ApoE with the early stages of DN formation in plaque-containing non-demented cases (Vickers et al., 1996).

In all double labelling immunofluorescence investigations, antibodies were visualised with a horse anti-mouse IgG conjugated to FITC and a goat anti-rabbit IgG conjugated to biotin, followed by streptavidin Texas Red (Table 2.5).

5.3 Results

5.3.1 Single labelling for ApoE and ß-amyloid

The distribution of immunoperoxidase labelling for ApoE in the SFG of the AD cases was similar across all individuals and closely resembled previous reports (Wisniewski & Frangione, 1992; Rebeck et al., 1993; Han et al., 1994; Kida et al., 1994; Benzing & Mufson, 1995; Gearing et al., 1995; Uchihara et al., 1995; Sheng et al., 1996). Of note, the intensity of immunolabelling for ApoE was highest in formic acid pretreated sections. ApoE-labelled structures in the prefrontal cortex of AD cases included plaques, small cells with astrocyte-like morphology and arterioles (Figure 5.1). Similar patterns of ApoE labelling were present in the entorhinal, occipitotemporal and inferior temporal cortices of AD cases (Figure 5.1). In addition, the anti-ApoE antibodies labelled NFTs in layer II of the entorhinal cortex, most of which were likely to be extracellular (Vickers et al., 1992b). In preclinical AD individuals, ApoE immunoreactivity was found in plaque-like structures only in the cases showing ß-amyloid immunoreactive deposits. In all preclinical AD cases, ApoE immunoreactivity was also present in arterioles principally localised to the underlying white matter and glial cells. The immunohistochemical profile obtained was consistent throughout AD cases and throughout preclinical AD cases regardless of post mortem interval and variations in fixation protocol.

5.3.2 Double labelling for ApoE and ß-amyloid

Double labelling with the mouse and rabbit antibodies to ApoE verified that both of these antibodies were labelling the same structures in tissue sections. Double labelling immunofluorescence was utilised to directly examine the relationship between ApoE and ß-amyloid immunoreactivity in frontal cortex sections (Figure 5.2). Many of the spherical and diffuse plaque-like structures immunoreactive for ß-amyloid in layer I and

Figure 5.1

Single labelling for ApoE in the SFG (A), and entorhinal cortex (B), of an AD case (layers indicated on the left). In the SFG, ApoE labelled plaques are particularly predominant in layers II, III and V (eg arrows). In the entorhinal cortex ApoE labels plaques (eg arrow) and also extracellular tangles in layer II (arrowhead).

Scale bar = 100 μm (A and B)

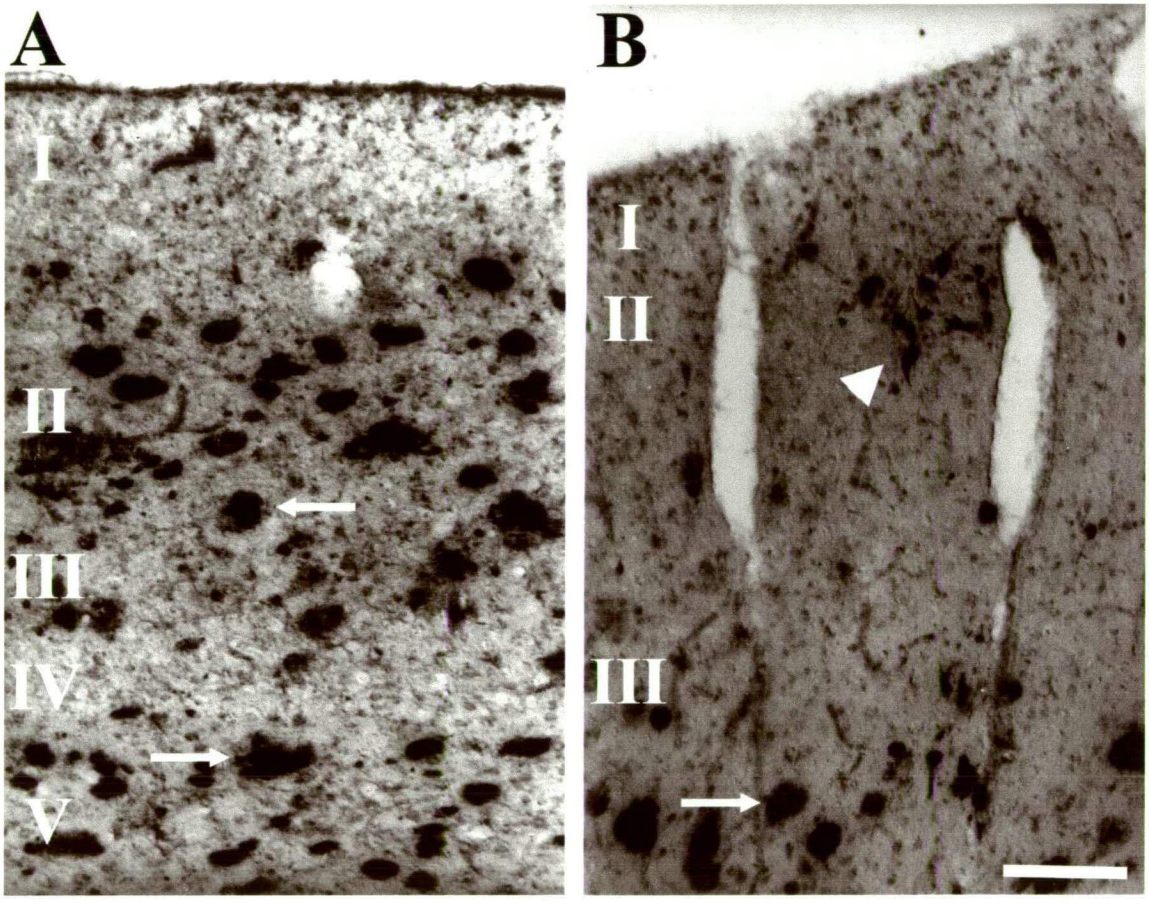
A
I
II
III
IV
V
B
I
II
III

Figure 5.2

Double labelling for ß-amyloid (A) and ApoE (B) in the superior frontal gyrus of a 66 year old AD case (layers indicated on left). The ß-amyloid plaques localised to layer I are not immunoreactive for ApoE. In other supragranular layers there is a high degree of colocalisation of these markers to individual plaques.

Scale bar =100 μm (A and B)

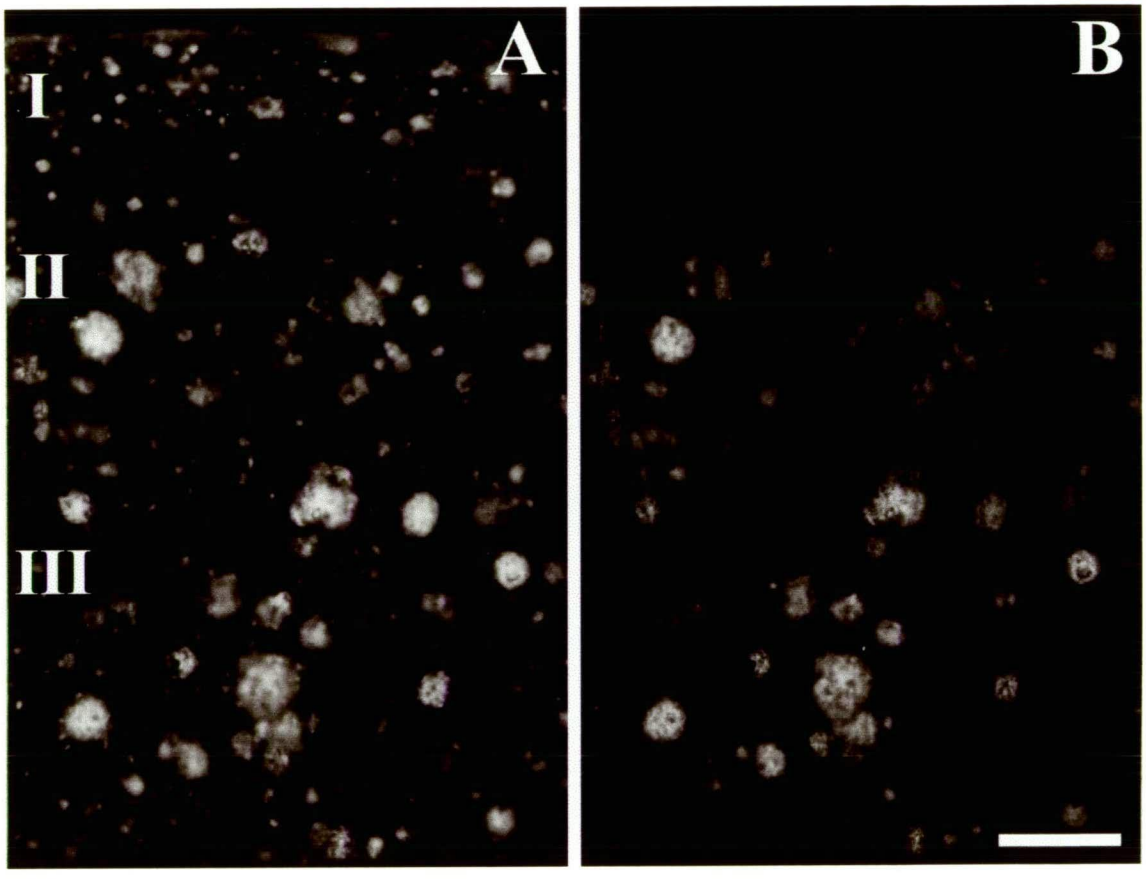
A
B
I
II
III

the outer region of layer II were consistently unlabelled for ApoE (Figure 5.2). The same observations were made in all AD cases. In other cortical layers, there was a high degree of colocalisation of ApoE and ß-amyloid to plaques. For all dense-core plaques, the core structure was consistently labelled for both ApoE and ß-amyloid, but the outer portions were often immunoreactive only for ß-amyloid (Figure 5.3). Many other plaque-like structures were incompletely labelled for ApoE relative to ß-amyloid (Figure 5.3), with only the innermost regions of the plaque showing ApoE immunoreactivity. Most of the plaques displaying extensive ApoE immunoreactivity were spherical and localised to layer III and the deeper portions of layers II and V. There were no plaque-like structures labelled for ApoE that were not also immunoreactive for ß-amyloid. Some plaques contained small spherical structures (2-5 μm) which were labelled for ApoE but not ß-amyloid (Figure 5.3).

Where ApoE and ß-amyloid were colocalised, immunoreactivity for both was present in the same fibrillar material. Arterioles showing strong ApoE immunoreactivity in these cases were either faintly immunolabelled or non-immunoreactive for ß-amyloid. ApoE-labelled blood vessels and astrocytes did not show a specific association with plaques.

In all preclinical AD cases containing ß-amyloid plaques, most, but not all, spherical and diffuse ß-amyloid deposits were also variably labelled for ApoE (Figure 5.3). Conversely, there were no ApoE immunoreactive plaques that were not also immunoreactive for ß-amyloid. As described above for clinical AD cases, small spherical ApoE immunopositive structures were occasionally observed in association with the ApoE plaques in preclinical AD cases and these were not immunopositive for ß-amyloid (Figure 5.3).

Figure 5.3

Double labelling for ß-amyloid (A,C,E) and ApoE (B,D,F) in the SFG. A and B show a dense-core plaque in layer II of a 66 year old AD case. The core is well labelled by both markers, but the remaining plaque is more extensively immunoreactive for ß-amyloid relative to ApoE. In layer V of a 72 year old AD case (C,D), not all ß-amyloid plaques (C) are ApoE immunoreactive (D) (arrows), and some ß-amyloid deposits are incompletely labelled for ApoE (arrowhead). In layer II of a 61 year old, preclinical AD case, a ß-amyloid deposit (E) is incompletely labelled for ApoE (F). The arrow in F indicates a spherical structure associated with the plaque that is labelled for ApoE but not for ß-amyloid.

Scale bar = 25 μm (A,B,E and F) and 50 μm (C and D)

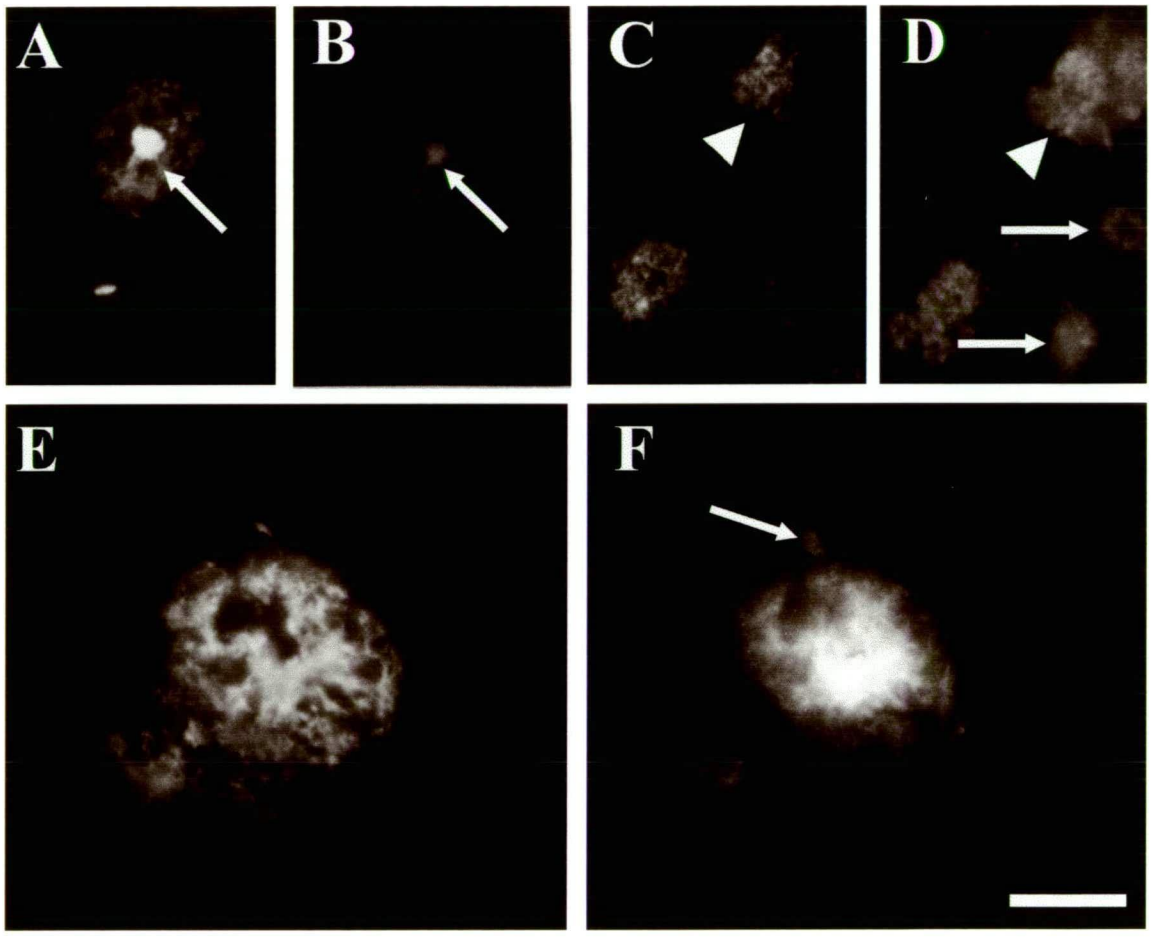
A
B
C
D
E
F

5.3.3 Association between ApoE and dystrophic neurites

All ApoE labelled plaques in the AD cases could be classified as neuritic, based on the presence of tau/ubiquitin immunoreactive DNs in double labelling preparations (Figure 5.4). Conversely, not all ß-amyloid labelled plaques were associated with DNs, with plaques in layer I notably lacking a neuritic component. The number of DNs present within ApoE labelled plaques was, however, variable. Therefore, for the purpose of quantitation, neuritic plaques were classified as either sparse (1-5 DNs) or clustered (>5 DNs). Quantitation of double labelled preparations demonstrated a greater proportion of ApoE immunopositive plaques associated with ubiquitin-labelled, clustered DNs in layers II and III (68±7% (S.D.)) relative to cortical layers V and VI (32±5%). Parallel investigations of double labelling using ß-amyloid with tau gave similar results ie. 59±2% of ß-amyloid immunopositive plaques in layers II and III contained clusters of DNs (highly neuritic) compared to 34±8% in layers V and VI.

Plaque-associated DNs in preclinical AD cases containing ß-amyloid deposits are labelled with NF antibodies but not with markers for tau or ubiquitin (Su et al., 1996; Vickers et al., 1996), and clusters of these abnormal neurites are preferentially located to cortical layers II and III (Vickers et al., 1996). In this investigation, double labelling in such cases demonstrated that all clusters of NF immunoreactive DNs were present within ApoE labelled plaque-like structures, but not all ApoE immunoreactive plaques were associated with abnormal neurites (Figure 5.4).

Notably, the ApoE-labelled spherical structures associated with plaques were not labelled with DN markers in either the clinical or preclinical AD cases.

Figure 5.4

Double labelling for ApoE (A,C,E) and markers for neurofibrillary pathology (B,D,F) in the SFG. A and B show double labelling with ApoE and tau in layer II of a 72 year old AD case. One plaque is associated with a cluster of DNs (arrow) whereas a nearby plaque (arrowhead) is less neuritic. Double labelling with ApoE (C) and SMI32 (D) in layer II of 62 year old preclinical AD case shows an association between ApoE positive plaques and clusters of SMI32 immunopositive DNs. Similarly, double labelling for ApoE (E) and SMI310 (F) in an 86 year old with end stage AD shows a NFT that is immunopositive for both markers (arrowhead) in association with other NFTs that are ApoE immunopositive only (eg arrows).

Scale bar = 50 μm (A,B,C,D,E and F)

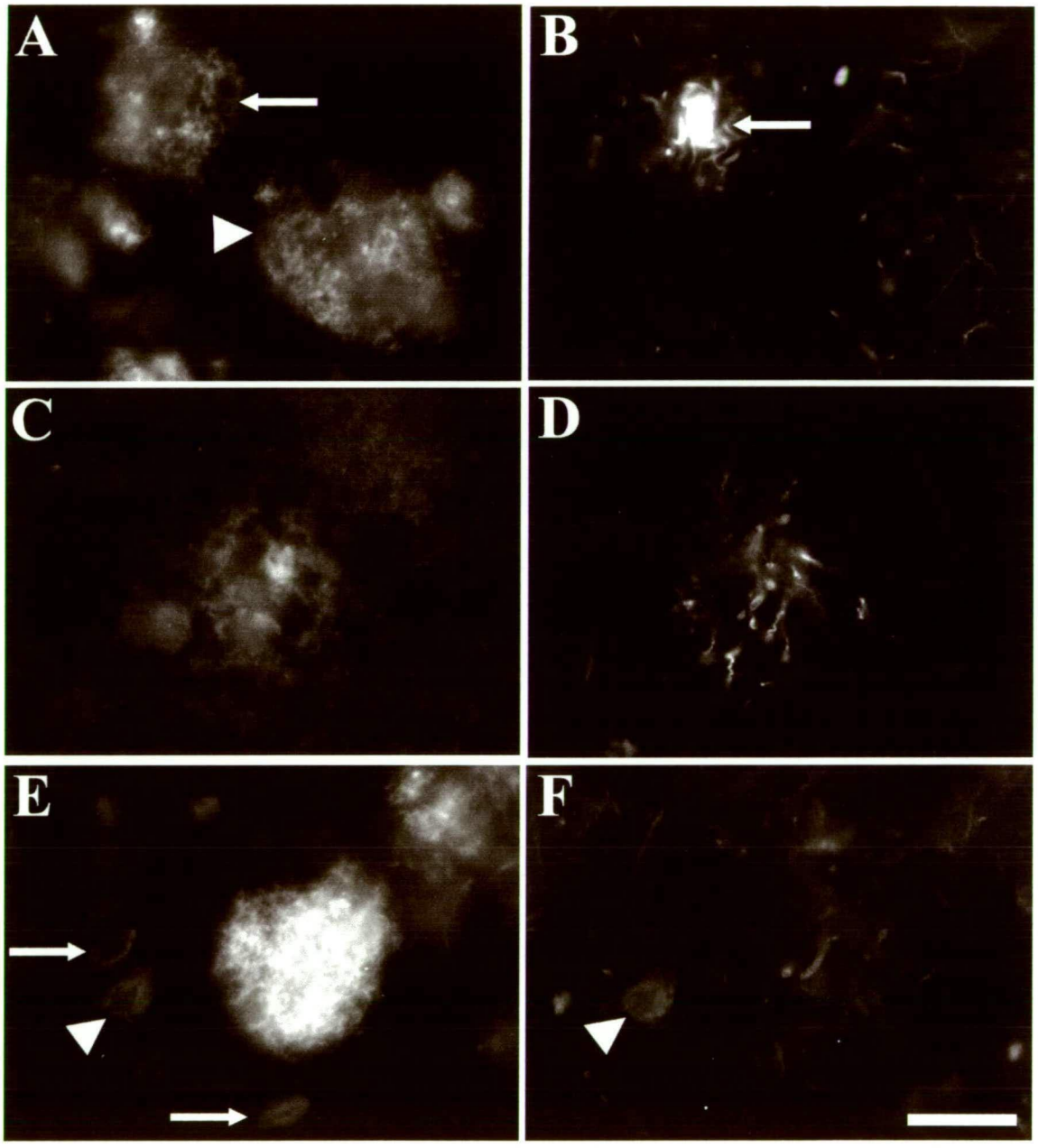
A
B
C
D
E
F

5.3.4 ApoE and neurofibrillary tangles in Alzheimer's disease

Earlier studies have demonstrated that the series of AD cases utilised in this investigation could be subdivided into high and low NFT density categories (Sampson et al., 1997). In this respect, the most severely affected AD case (NFT density more than twice that of any other AD case) contained both cell bodies and NFTs that were labelled for ApoE (Figure 5.4). In contrast, no NFTs were ApoE immunoreactive in the SFG of the other five AD samples. In formic acid treated sections from AD cases, the NF antibody, SMI310, is a marker for the early to middle stages of NFT formation (Vickers et al., 1994b, 1996). Therefore, this antibody was utilised in double labelling investigations to determine the proportion of ApoE labelled NFTs that were intracellular (SMI310 immunopositive) and the proportion that were extracellular (SMI310 immunonegative) in the high NFT density AD case described above. Quantitation showed that only 10% of ApoE positive NFTs in layer V were also labelled with SMI310 (Figure 5.4). Conversely, 68% of the SMI310-labelled NFTs were not labelled for ApoE. This indicates that most ApoE labelled NFTs in the prefrontal cortex of this case are likely to be extracellular end-stage forms.

5.4 Discussion

Double labelling immunohistochemistry was utilised in this chapter to directly examine the localisation of ApoE in relation to the pathological hallmarks of AD. Although the specific ApoE genotype is not known for the cases investigated in this study, highly consistent patterns of ApoE localisation, particularly relative to ß-amyloid deposition, were observed. Similarly, the same general pattern of ApoE immunolabelling has been reported in AD cases across ApoE genotypes (Price et al., 1991; Han et al., 1994; Gearing et al., 1995; Sheng et al., 1996). The results obtained confirm that ApoE immunoreactivity is principally localised to plaques, and also show that this protein is present within a specific subset of the plaques labelled for ß-amyloid. In this respect, ß-amyloid plaques located in cortical layer I were consistently unlabelled for ApoE. Furthermore, even where ApoE and ß-amyloid were present in the same plaque, ApoE immunoreactivity within the plaque was usually incomplete relative to ß-amyloid. Dense-core plaques typically had only the most central elements labelled for ApoE. These data indicate that the involvement of ApoE in plaque formation is likely to be secondary to that of ß-amyloid (ie all plaques contain ß-amyloid but not necessarily ApoE), and that the presence of ApoE in some plaques reflects a very specific feature of the disease.

ApoE has been shown to bind to ß-amyloid both *in vitro* (Strittmatter et al., 1993a, 1993b; LaDu et al., 1994) and *in vivo* (Namba et al., 1991; Wisniewski et al., 1992; Russo et al., 1998). It is also colocalised with fibrillar ß-amyloid in APP^{V717F} transgenic mice (Bales et al., 1999) and has been shown to have a pro-fibrillogenic activity *in vitro* (Gallo et al., 1994; Ma et al., 1994). Therefore, it has been suggested that ApoE may operate as a chaperone-like factor in ß-amyloid plaque formation, by promoting the assembly of insoluble ß-amyloid (Wisniewski & Frangione, 1992; Ma et al., 1994).

Thus, the localisation of ApoE to a specific subset of plaques may serve to augment ß-amyloid fibril formation in these deposits. The presence of ApoE in plaques, in cases that may correspond to preclinical AD, indicates that this protein may be involved in the early stages of formation of certain plaques. This may serve to further enhance the insolubility of certain plaques prior to dementia.

Double labelling verified that the ApoE-positive plaques corresponded to the 'neuritic' forms of ß-amyloid plaques (see also chromogen based double labelling results - Uchihara et al., 1995; Sheng et al., 1996), although the degree to which they were associated with abnormal neurites varied with the laminar location of the plaque. Results detailed in the previous two chapters provide evidence that the development of a subset of plaques causes physical damage to surrounding axons which leads to reactive cytoskeletal changes, eventually resulting in neurofibrillary pathology (Vickers et al., 1996; King et al., 1997; Vickers, 1997). Interestingly, neuritic plaques are more commonly found in the supragranular layers in both preclinical (Vickers et al., 1996) and clinical (Masliah et al., 1993a) AD cases, which may reflect the susceptibility of neuronal connections whose axons terminate in these layers (Vickers et al., 1996). This suggests that ApoE, by contributing to the fibrillogenesis of certain plaques, may enhance their ability to cause damage to axons. This hypothesis is strongly supported by recent data obtained from studies utilising the APP^{V717F} transgenic mouse line (Bales et al., 1997; 1999; Holtzman et al., 2000). These mice were manipulated to express mouse, human or no ApoE. A severe plaque associated neuritc dystrophy was noted in the transgenic mice expressing mouse or human ApoE. Further to this expression of ApoE4 resulted in substantially more fibrillar deposits as compared to ApoE3 (Holtzman et al., 2000). Collectively these results indicate a critical role for ApoE in neuritic plaque formation.

Alternatively, ApoE may have a functional role in the remodelling and sprouting of damaged neuritic processes (Su et al., 1996; Stone et al., 1998; Horsburgh et al., 1999; Teter et al., 1999a, 1999b) , indicating that the localisation of ApoE to certain plaques may be secondary to their role in the neuronal changes that lead to DN formation (Su et al., 1996). However, ApoE labelling was also present in plaques in the infragranular layers that had a relatively low neuritic component, and many plaques containing ApoE labelling in the preclinical cases were not associated with DNs. Coupled with the observation of the consistent presence of ApoE in specific domains of certain plaques in AD, this suggests that ApoE may have a more direct role in ß-amyloid plaque formation rather than the neuronal reaction to injury. The former possibility is strengthened by observations of the association of other apolipoproteins with ß-amyloid formation in AD (Wisniewski & Frangione, 1992), as well as the possible role of ApoE in promoting other amyloidegenic diseases (Wisniewski & Frangione, 1992; Kindy et al., 1995; Chargé et al., 1996).

It is important to note that ApoE also labelled spherical structures within some plaques and these were not immunoreactive with antibodies to ß-amyloid or the markers for DNs. It is possible that these may correspond to microglial cells (Uchihara et al., 1995). It has been suggested that ApoE may be present in DNs within plaques (Han et al., 1994), although double labelling in the current study indicates that antibodies to ApoE do not label either the early or late stages of DN formation. In addition, it has been reported that ApoE immunoreactivity is present in NFTs (Han et al., 1994; Benzing & Mufson, 1995). In the current report, only the case with the highest NFT density showed ApoE labelling of NFTs in the prefrontal cortex, and double labelling demonstrated that the great majority of these were end-stage, extracellular forms of this pathological

hallmark. In addition, ApoE labelling was also present in the extracellular NFTs located in the outer layers of the entorhinal cortex of the AD cases. This data confirms a previous report stating that ApoE may be binding principally to the extracellular forms of NFTs (Benzing & Mufson, 1995). These cumulative data suggest that ApoE is unlikely to have a direct role in the generation of the cytoskeletal pathology that comprises DNs or NFTs.

Therefore, in this investigation it was concluded that ApoE binds, in an incomplete fashion, to a specific subset of plaques in AD and that this may assist fibrillogenesis in these plaques and possibly enhance their ability to cause physical damage to surrounding axons. Allelic variations of ApoE may contribute differentially towards the relative insolubility of plaques, thus explaining the greater number of neuritic plaques associated with inheritance of particular ApoE genotypes (Rebeck et al., 1993; Schmechel et al 1993; Corder et al., 1994; Olichney et al., 1996).

THE SEQUENCE OF CELLULAR CHANGES FOLLOWING LOCALISED AXOTOMY TO CORTICAL NEURONS IN GLIA-FREE CULTURE MIMIC THE DEVELOPMENT OF DYSTROPHIC NEURITES IN ALZHEIMER'S DISEASE

6.1 Introduction

It has been proposed that many of the cytoskeletal changes following a direct form of cortical neuron damage (King et al., 1997, 2000; Adlard, In Press; Chapter 3) are similar to the reactive changes described in both human and experimental brain injury studies (Maxwell et al, 1997). Of particular interest are the similarities between the neuronal response to injury and the specific early forms of abnormal neurites associated with ß-amyloid plaque formation in AD (see Chapter 3) (Vickers et al., 1996; King et al., 1997). This similarity has led to the novel hypothesis that plaque formation in AD causes deformation of the neuropil, compression of axons and the triggering of the neuronal response to injury followed by abnormal axonal sprouting.

Both the neuronal changes associated with ß-amyloid plaque formation and following various forms of brain injury have been purported to be influenced by the actions of non-neuronal cells such as oligodendroglia, astrocytes and microglia (Vickers et al., 2000), but the precise role of these cell types in directing the neuronal response is unclear. For example, some research groups emphasise the deleterious effect of glia on post-injury regeneration in central neurons, either, for example, by the inhibitory action of myelin-associated proteins (Bregman et al., 1995), glial-associated growth-inhibitory factors (e.g. metallothionein III (Uchida et al., 1991) or extracellular matrix proteins (Fawcett, 1997; Fitch & Silver, 1997), whereas recent studies also note that specific glia cell types produce growth factors which may encourage neurite growth (Batchelor et al., 1999). The formulation of a specialised neuron specific media, Neurobasal™, optimised for the survival and differentiation of embryonic neurons in

the absence of glial cell types, has recently permitted the growth of pure neuronal cultures *in vitro* (Brewer et al., 1993). This provides a unique opportunity to study an isolated neuronal response to injury without the confounding results introduced by the presence of non-neuronal cells.

In this study, an *in vitro* model of axonal damage, utilising the Neurobasal™ culture media (Brewer et al., 1993), was developed to study the intrinsically derived reaction of central neurons to injury. Investigations had a focus on the time course of cytoskeletal changes following injury as well as the temporal association of reactive and regenerative cellular alterations. Alterations in neuronal cytoskeletal proteins appear to be a crucial event in the initial reactive changes following physical damage to nerve cells. In this respect, preliminary evidence indicates a loss of normal microtubular structures (Meller et al., 1987; Maxwell et al., 1997) and a specific misalignment, accumulation and dephosphorylation of NFs (Meller et al., 1993a, 1994; Pettus & Povlishock, 1996; King et al., 1997). Many of these changes are thought to be preparative for an attempt at adaptive sprouting or regeneration (Ditella et al., 1994). Therefore, in the current study, markers for NFs and the growth-associated protein, GAP43, were utilised. In particular, the primary goal of these studies was to determine whether an *in vitro* model of axonal injury would replicate the neuritic changes associated with *in vivo* cortical neuron axotomy as well as the early stages of neuronal pathology in AD.

6.2 Experimental procedures

6.2.1 *In vitro* neuronal injury model

Neuronal cultures were prepared according to the protocol outlined in Chapter 2. One day before performing injury investigations, coverslips were transferred to individual sterile petri dishes and allowed to reacclimatise to incubator conditions. On DIV 14 and 21, injuries were performed by transecting individual axonal bundles under microscope guidance (Leitz Fluovert, inverted microscope), using a size fifteen sterile scalpel blade. Cuts were made at a distance of between approximately 50-150 μm from the cell body clusters (Figure 6.1). Two axon bundle transections per coverslip were made. Non-injured control monolayers were processed concurrently. Digital images were captured before and after injury to aid relocation of the cut site using a CCD camera (Ikegami ICD-4CE, Tsushinki Co) attached to a Power PC Macintosh computer using NIH Image software (version 1.61). After injury, cells were returned to the incubator for varying time periods before fixation with 4% paraformaldehyde for immunohistochemistry.

6.2.2 Immunohistochemistry

The damaged axons were investigated at pre-established time intervals of 1, 6, 12, 24 and 72 hours post injury (PI) using immunohistochemistry. The distribution and degree of colocalization of the growth associated protein, GAP43, and the high molecular weight subunit of the NF triplet, NF-H, was determined using double labelling immunohistochemistry. A rabbit polyclonal antibody to NF-H (R-NFH) (Serotec, 1:1000) was combined with a mouse antibody to GAP43 (Boeringher Mannheim, 1:1000) for experimental and control cultures. To investigate the prevalence of non-neuronal cells, mouse monoclonal antibodies to glial fibrillary acidic protein (GFAP) (DAKO, 1:2000) and ferritin (ICN Biomedicals Incorporated, 1:5000) were utilised. Further double labelling was performed with a rabbit polyclonal antibody to the calcium binding protein calretinin (Swant®, 1:2000) and a mouse monoclonal antibody to non-phosphorylated NFs, SMI32 (Sternberger Monoclonals Incorporated,

Figure 6.1

Neuronal cultures at DIV 21, before (A) and after (B) localised physical injury. Arrow indicates point of transection.

Scale Bar = 125 μm

A
B

1:2000), to investigate the relationship between cortical non-pyramidal and pyramidal neurons in culture.

The mouse monoclonal antibodies were visualised with a horse anti-mouse secondary antibody conjugated to FITC whereas the rabbit polyclonal was visualised with a goat anti-rabbit antibody conjugated to biotin followed by streptavidin Texas Red. Fluorescence-labelled coverslips were mounted using Permafluor (Immunotech) and viewed with a Leica fluorescence microscope. Images were again digitally captured using a CCD camera (Ikegami ICD-4CE, Tsushinki Co) attached to a Power PC Macintosh computer. Laser confocal scanning microscopy, using an Optiscan F900e krypton/argon system attached to an Olympus BX50 microscope, was utilised to investigate the localisation patterns of GAP43 and NF-H within damaged axons.

6.2.3 Electron microscopy

Coverslips were prepared according to routine electron microscopy techniques as outlined in Chapter 2.7. After the coverslips had been infiltrated with resin they were embedded and polymerised. In this respect, beam capsules were filled with resin and then the individual coverslips were inverted and placed on top. They were then placed in an oven at 60°C for 48 hours to polymerise the resin. After polymerisation and cooling, the beam capsule can be removed, leaving the coverslip attached to the resin stud. The glass coverslip was removed (leaving the intact cells within the resin) by alternatively dipping the stud, with coverslip attached, into boiling water for two minutes and then into liquid nitrogen for two minutes. The differential rates of expansion and contraction of the resin and glass causes the coverslip to shatter and to detach from the resin (Withers & Banker, 1998). The embedded cells were examined with a disecting microscope and areas of interest marked. The stud was trimmed back to this area for sectioning. The protocol outlined above enables sections parallel to the substrate to be cut, thereby allowing visualisation of large areas of culture in a single section. After embedding standard sectioning and staining protocols were utilised (Chapter 2.7).

6.3 Results

6.3.1 Neuronal development *in vitro*

Cortical cultures have been shown to develop through a series of well-defined steps (Dotti & Banker, 1987; De Lima et al., 1997). The utilization of the Neurobasal™ media did not appear to alter the early growth patterns in neurons. Briefly, soon after seeding, the cells partly reaggregated and attached to the coverslip. The adhered neurons appeared as rounded, dissociated single cells with either no processes or fine poorly defined single processes (Figure 6.2A). On the third day *in vitro* (DIV 3), multiple process formation began. Processes were clearly differentiated, morphologically, with both long axons and branching dendrites present (Figure 6.2B). At these early time points there was considerable cell death as indicated by the large amount of non-adhered debris and loosely attached cells. A large proportion of these dying cells were likely to correspond to the non-neuronal population whose survival is selected against by the Neurobasal™ media (Brewer et al., 1993; Brewer et al., 1995, 1997). On DIV 5, most cells were adhered as large clusters of cell bodies. Many of these cell clusters had small caliber processes, with interconnecting bundles of processes between them (Figure 6.2C). The leading tips of most processes had distinct triangular growth cone-like morphology, and showed concentrated labelling with the antibody to GAP43. The complexity of these process networks continued to increase with time until DIV 21, with the axonal bundles between clustered cells becoming thicker (Figure 6.2D). From this time point onwards, no further axonal projections or dendritic branching was evident. There were no growth cones on the ends of projections and GAP43 labelling was uniform throughout. On DIV 21 occasional R-NFH labelled, ring-like structures were observed. These structures were variable both in size and thickness. The larger (≈ 3 μm) R-NFH immunopositive rings were often continuous with fine axons and more irregular in shape as compared to the smaller rings (≈ 1.5 μm). These ring-like structures were intermittently present throughout the axonal fasciculations of the mature cultures (DIV 21 onwards). Neither form of ring-like structure showed labelling with antibodies to GAP43.

Figure 6.2

Neuronal development *in vitro* at DIV 1 (A), 3 (B), 5 (C) and 21 (D). The cultures developed from single neurons (A) to small cell clusters with distinct axons and dendrites (B). As the culture matured more extensive cell body clusters joined by fine axons developed (C). Finally by DIV 21, a complex array of cell clusters with an extensive network of interconnecting axonal bundles were present (D).

Scale Bar = 25 μm (A and B), 50 μm (C) and 125 μm (D)

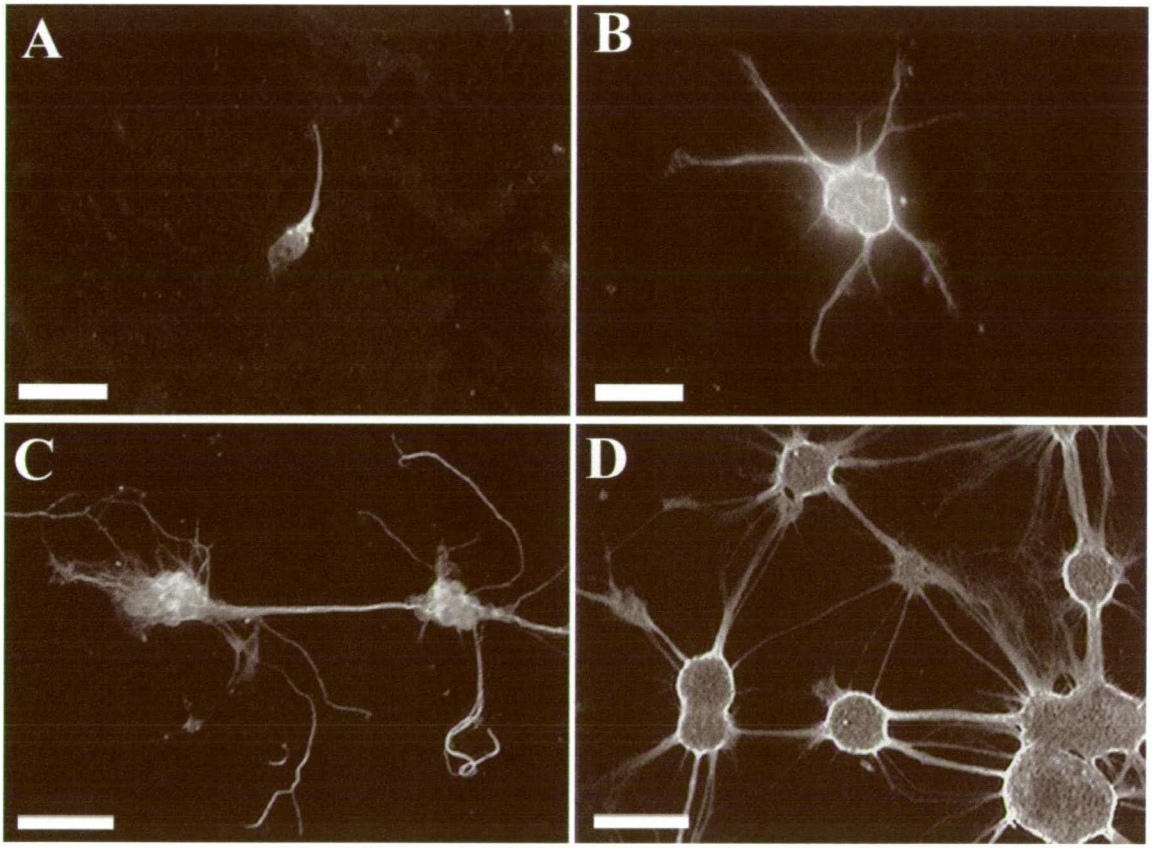
A
B
C
D

The antibodies SMI32 and anti-calretinin are routinely used to selectively label pyramidal cell bodies and non-pyramidal interneurons, respectively (Sampson et al., 1997). In a similar fashion to the mature neocortex, double labelling for these two markers demonstrated that no nerve cells were labelled for both NFs and calretinin. SMI32 and anti-MAP2 labelling was present in most nerve cells, particularly those contained in clusters (Figure 6.3A). Calretinin immunopositive interneurons were present occasionally within the clusters, however, most neurons of this type were growing either singularly or in smaller groups of 1-5 cells (Figure 6.3B). Calretinin immunopositive neurons accounted for less than 5% of the total cell population. Similarly, immunolabelling of cell monolayers with antibodies to GFAP and ferritin confirmed that non-neuronal glial cells were not present. A minority of fibres within the axonal bundles were found to be labelled with the antibody to MAP2 suggesting that they may correspond to dendrites (Figure 6.3C). Considerably more of these fibres were immunopositive with antibodies to NFs, a specific marker for axons (Figure 6.3D).

6.3.2 Ultrastructure of neuronal cultures

To further characterise the neuronal cultures the ultrastructure of the mature cell monolayers (DIV 21) was investigated using transmission electron microscopy (Figure 6.4). The large interconnecting process bundles, emanated from within the cell body cluster (Figure 6.4A). Close examination of the bundles, revealed the presence of both MTs and NFs within the nerve cell processes (Figures 6.4B, 6.4C, 6.4D). Oligodendrocytes were not present, and axons were notably non-myelinated.

6.3.3 Neuronal response to localised trauma

At DIV 7, the neuronal cultures demonstrated continued development, as evidenced by the GAP43 labelling of growth cones at axonal tips. Furthermore, prominent axonal connections between nerve cell clusters were not present, therefore, they were not used for the transection investigations. While transected fibres were apparent, no other specific morphological changes were observed following NF-H or GAP43 immunolabelling at any of the time points PI, in the

Figure 6.3

MAP2 labelling (A) of the predominant cell type found throughout the cell clusters. Calretinin immunopositive interneurons were also present, however, with considerably lower frequency compared to NF labelled cells (B). Occasional fibres within the connecting fibre bundles were labelled for MAP2 (C), however, the majority of fibres were NF-H immunopositive (D). Arrow heads indicate a fibre immunopositive for MAP2 but not labelled by antibodies to NF-H.

Scale Bar = 30 μm (A), 20 μm (B) and 30 μm (C and D)

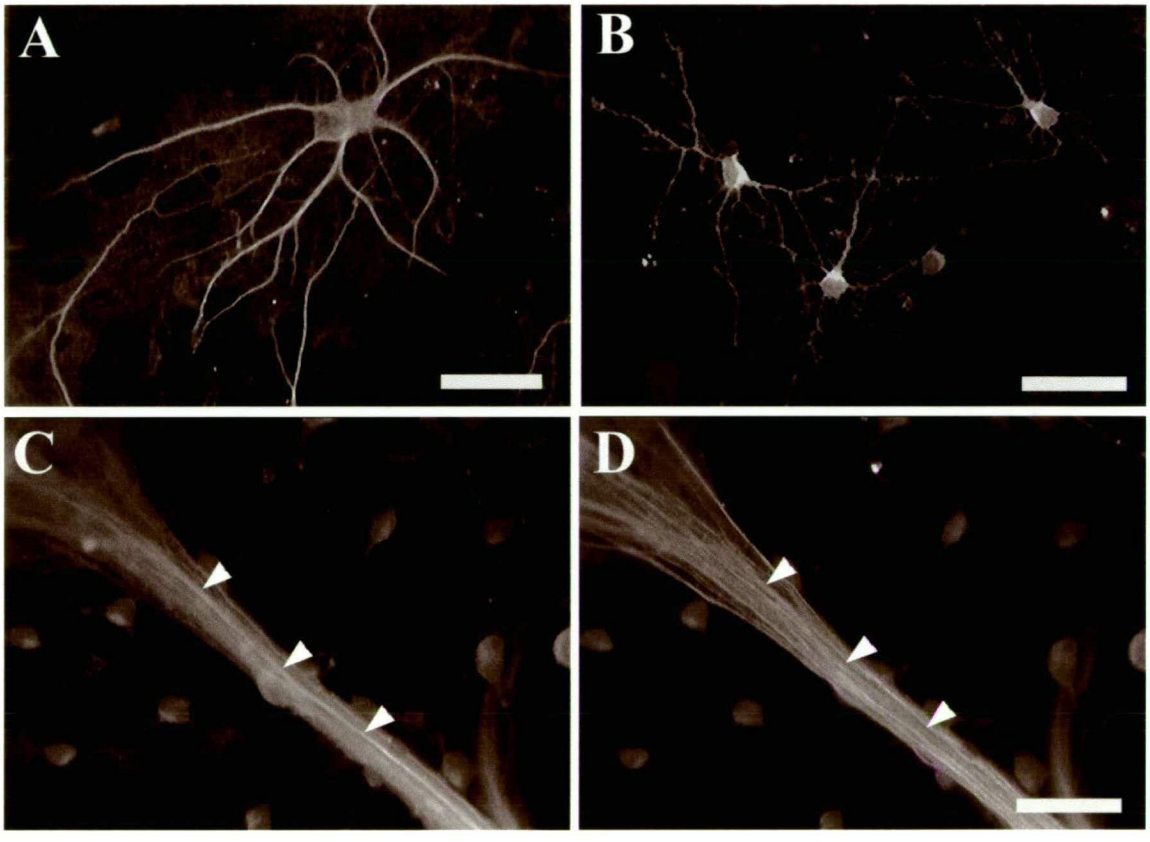
A
B
C
D

Figure 6.4

Ultrastructure of normal growth in pure neuronal cultures at DIV 21. Large interconnecting process bundles, emanated from within the cell body cluster. Neuronal cells (n) flanked both sides of the process bundle (p), prior to the interconnecting processes leaving the cluster (A). Both MTs (arrows) (B and C) and NFs (arrowhead) (D) were evident within the nerve cell processes.

Magnification = 10400x (A), 16900x (B and C) and 31000x (D)

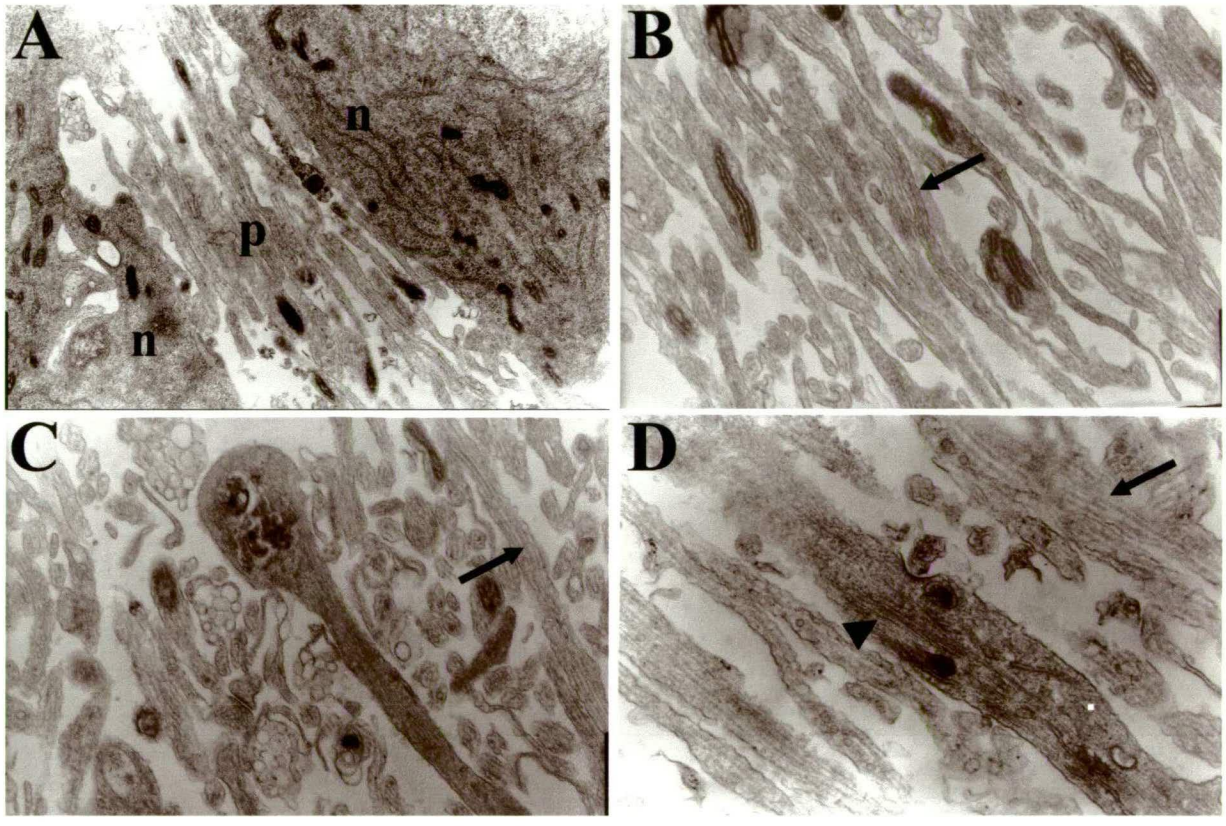
A
n
p
n
B
C
D

DIV 14 cultures (Figure 6.5A). Similarly, no NF (Figure 6.5B) or GAP43 (Figure 6.5C) immunolabelled axons emanated from the cut axonal stump at three days after injury.

Very few changes within axons were present at one hour post transection in cultured neurons injured after DIV 21 (Figure 6.6A and 6.6B). Some NF-H labelled axonal thickening had occurred but no GAP43 immunopositive alterations were present. However, in these mature cultures at six and twelve hours after injury, distinct changes were evident that were not present in the immature cultures at the same time points. There were extensive accumulations of ten to twenty NF-H immunopositive ring-like structures within the cut stumps. These rings were variable in size with an average diameter of approximately 2 μm. Their shape was generally irregular and many were continuous with the labelled fine processes. No GAP43 labelling was present throughout, or associated with, the ring-like structures (Figure 6.6C). Similar changes were present on both sides of the transected axonal bundle.

At 24 hours PI, NF-H immunopositive ring-like structures were present within the axonal stump, however, their frequency had decreased to approximately one to five per transected axonal bundle. Bulb-like accumulations of NF-H immunoreactivity were now also present within the transected axon bundles (Figure 6.6D and 6.6E). Some bulbs had fine processes or sprout-like protuberances associated with them. These bulb- and ring- like structures were not labelled for GAP43. However, there was an increase in punctate GAP43 labelling throughout the damaged area, particularly localised to the cut stump region (Figure 6.6F).

At three days PI in the DIV 21 cultures another series of changes were present. There were no distinctly labelled NF-H immunopositive ring- or bulb- like structures. A number of fine processes, a single axon in thickness, extended from the cut face of the axonal bundle. These processes were GAP43 and NF-H immunopositive, with GAP43 labelled growth cones at their tip (Figure 6.7A). High magnification investigation of the growth cones revealed strong GAP43 labelling and a lack of NF labelling within the growth cone extremities (Figure 6.7B).

Figure 6.5

Cultures injured at DIV 14 showed no NF-H labelled ring- or bulb-like reactive changes at twelve hours PI (A). Similarly no NF-H (B) or GAP43 (C) immunopositive axons or fibres were present beyond the cut face of the axonal bundles three days after injury in the DIV 14 cultures.

Scale Bar = 20 μm (A) and 20 μm (B and C)

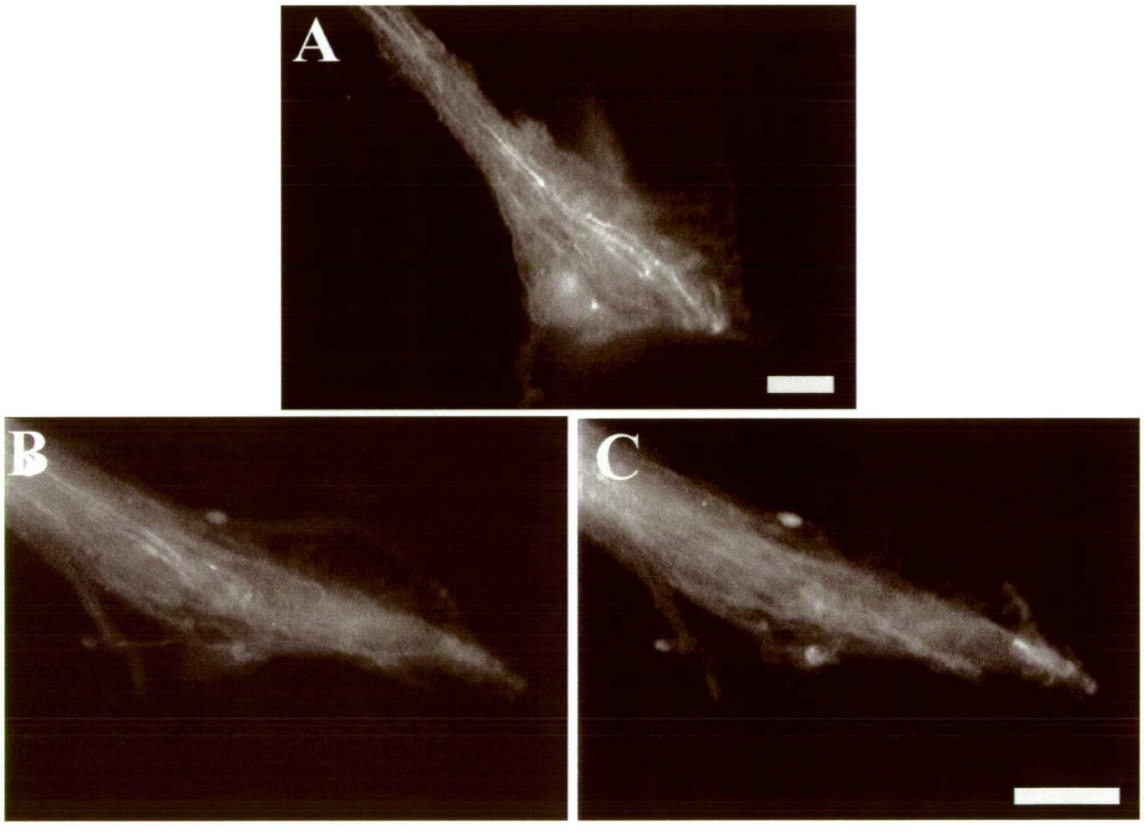
A
B
C

Figure 6.6

Confocal scanning laser microscope image showing no NF-H (A) or GAP43 (B) immunopositive reactive structures within transected axons (DIV 21) at one hour PI. Arrow indicates slight axonal thickening. Distinct changes were evident at twelve hours after injury in mature (DIV 21) cultures (C). Confocal image shows labeling for GAP43 (green) was increased within transected axons. NF-H labeling (red) showed extensive accumulations of NFs which appeared as ring-like structures, as indicated by the arrows. At 24 hours PI occasional NF-H immunopositive rings were still present (arrows), in addition to distinct NF labelled bulb-like structures (arrow heads) (D and E). Confocal image showing no direct colocalization of NF-H (red) immunopositive rings and GAP43 (green) at this time point (F).

Scale Bar = 10μm (A, B and F), 15 μm (C) and 20 μm (D and E)

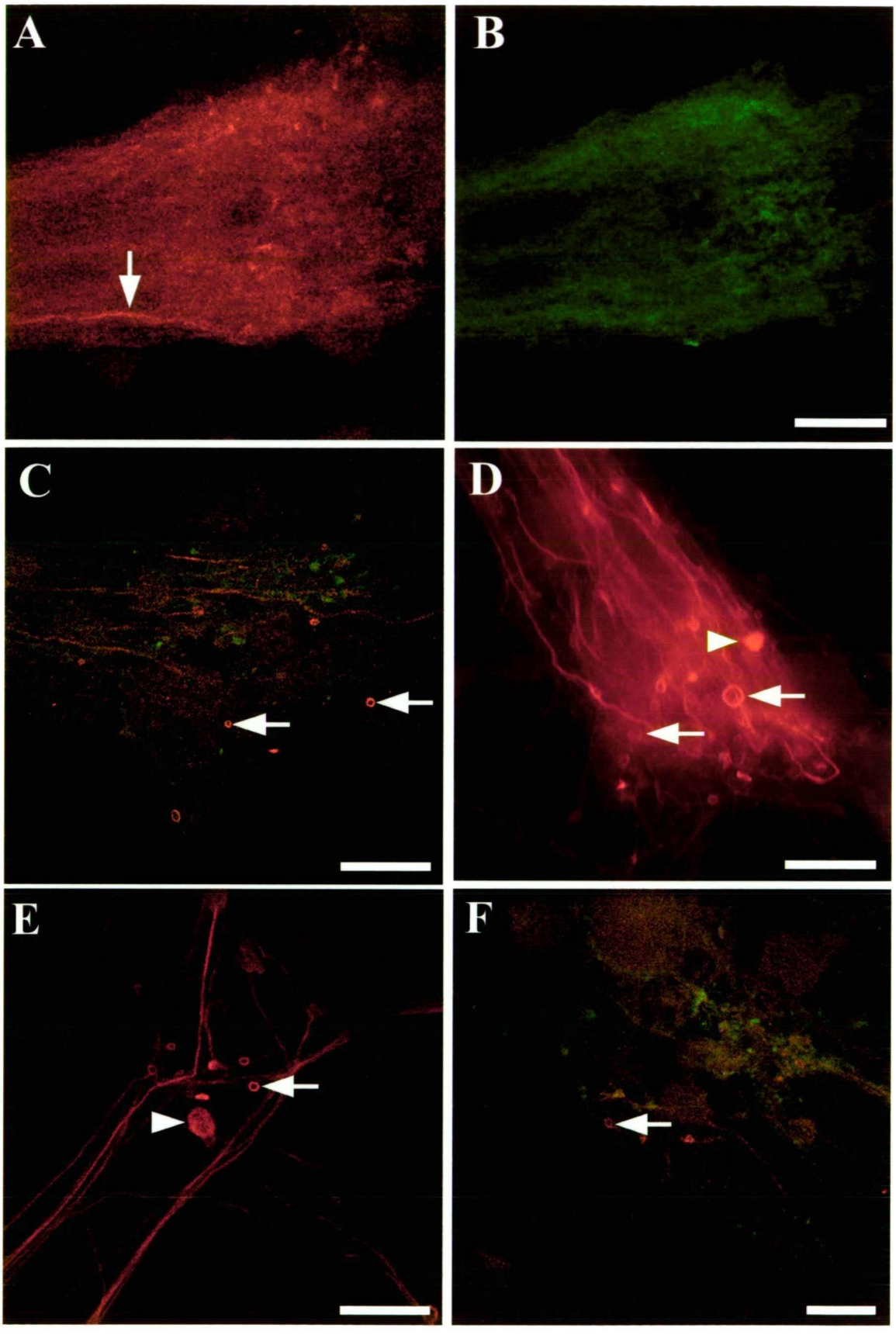
A
B
C
D
E
F

Figure 6.7

At three days PI in the DIV 21 cultures a number of fine processes, a single axon in thickness, emanated from the cut face of the axonal bundle. These processes were GAP43 (A) and NF-H immunopositive with GAP43 labelled growth cones at their tip (arrows). NFH labelling was present throughout the axon (red), as indicated by the arrow head, but was absent from the GAP43 labelled (green) growth cones (arrows) (B).

Scale Bar = 25 μm (A) and 5 μm (B)

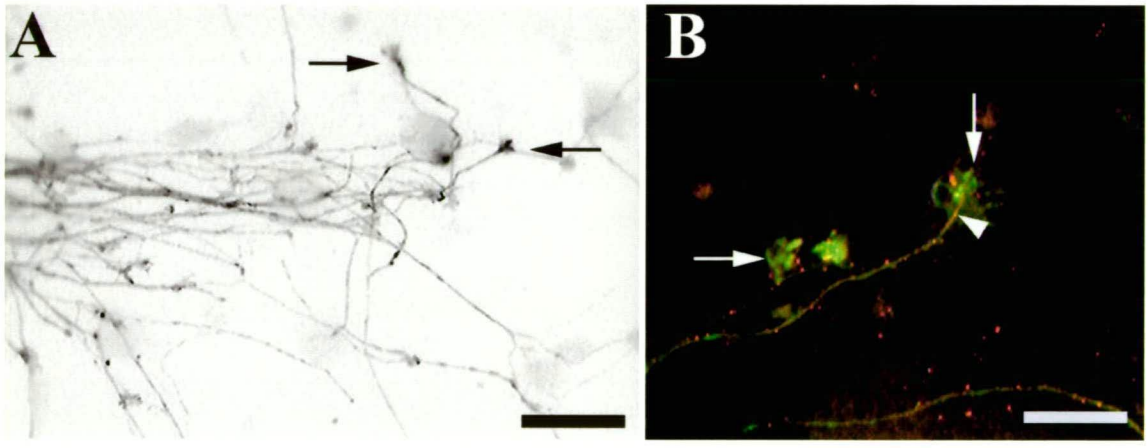
A
B

The results obtained at all time points were the same for both of the two transections per coverslip and were consistent throughout the five series of separate culture experiments.

6.4 Discussion

The process of cellular differentiation of cerebral cortical neurons *in vitro* resembled the development of these cells in the intact tissue (Dotti & Banker, 1987). Although confined to a two dimensional substrate, the axons and dendrites that develop in neuronal cultures differ from one another in form, in molecular composition and in synaptic polarity, just as their counterparts *in situ* do (Bartlett & Banker, 1984; Dotti et al., 1988). The cultured cortical neurons in the current study could be differentiated into subtypes based on their neurochemical identity, which were similar to subgroups of pyramidal and non-pyramidal cells *in vivo* (Sampson et al., 1997), supporting the proposal that organised cell migration is not a prerequisite for the differentiation of single cortical neurons (De Lima et al., 1997).

In cortical and hippocampal cultures the presence of process connections between large cell body clusters is routinely reported. These networks have alternatively been termed neurite bundles (Sole, 1980), process networks (Murphy & Horrocks, 1993a, 1993b), multifiber bundles (Mire et al., 1970; Bird, 1978) and fasciculations (DeLima et al., 1997). Similar patterns of growth were noted in this investigation where the neuronal selective media Neurobasal™ was utilised. The extensive formation of neuritic bundles between cell clusters enabled ease of transection under microscopic guidance.

Two general approaches to axon transection *in vitro* have been previously utilised in 'mixed' neuron/glial cultures. These models primarily differ with regards to whether the initial insult is delivered non specifically, to all cells within a culture monolayer (Tecoma et al., 1989; Muhkin et al., 1997), or to a limited number of cells (Levi & Meyer, 1945; Shaw & Bray, 1977; Gross et al., 1983; Yawo & Kuno, 1983; Lucas et al., 1985). Whereas the responses of dendrites to transection in mixed dissociated hippocampal cultures have been extensively investigated (Dotti & Banker, 1987; Emery et al., 1987; Banker & Goslin, 1991), similar investigations have not been performed on neocortical axons *per se* in a purely neuronal environment. However, a recent investigation involving the stretching of single axons in a neuron-like cell

line (N-Tera2) demonstrates that primary neuritic damage is associated with misprocessing of cytoskeletal elements such as NFs (Smith et al., 1999), as suggested by numerous *in vivo* studies (Maxwell et al., 1997). In the current study the fate of damaged axons was revealed by specific markers including antibodies to GAP43 and phosphorylated NFs.

The axonal changes that occur following injury with the current model were shown to follow a 'stereotypy' in their response. The initial reactive changes in axons involving NFs demonstrate specific morphological features, including bulb- and ring-like structures (Guillery, 1965; Meller et al., 1993a, 1994; Vickers et al., 1996; King et al., 1997, 2000). Examination of the time course of appearance of these structures showed that the presence of NF-containing rings, the classic distal reaction of traumatised axons (Guillery, 1965; Vickers, 1997) clearly preceded the development of NF immunopositive bulb-like structures. Ultrastructural analysis of morphologically identical structures in an *in vivo* model of cortical physical damage showed that the ring-like structures correspond to accumulations of filaments surrounding a core of 1-2 mitochondria, whereas bulbs consisted of swollen myelinated and some non-myelinated processes (King et al., 2000). Additionally, both forms of neuritic pathology demonstrated a loss of microtubules *in vivo*. The mid-axonal location of the ring-like structures suggests that it is unlikely that they correspond to axonal terminals as previously proposed (Guillery, 1965; Roots, 1983) and may instead be indicative of more generalised axonal cytoskeletal alterations. It may be that the ring-like structures in the *in vitro* and *in vivo* experimental models represent 'collapsed' axons where the loss of microtubules and compaction of NFs results in general cytoskeletal disarrangement and the accumulation of organelles. Bulb-like structures may therefore represent expanded axonal segments. Similar neurofilamentous changes have been noted in other models of physical damage and also in the very early stages of AD (Chapter 3; Guillery, 1965; Meller et al., 1993a, 1994; Vickers et al., 1996; King et al., 1997; King et al., 2000).

NF alterations in injured neurons appear to play an important role in the subsequent attempt by neurons to sprout, as indicated by poor regeneration in NF deficient mice (Zhu et al., 1997) and quail (Jiang et al., 1996) following peripheral nerve injury. Further to this, it has been demonstrated *in vivo* that diffusely injured axons can mount a sustained regenerative attempt that is associated with a reorganisation of their cytoskeleton and accompanied by an up regulation of GAP43 (Christman et al., 1997). In the current *in vitro* investigation, following the initial NF changes, at twelve hours PI, the stereotypical reaction to injury also involved an accumulation of GAP43 and subsequent sprouting. In addition, there was distinct GAP43 labelling of axonal sprouts and growth cones emanating from the cut axonal stump at three days PI. Interestingly, the GAP43 and NF reactive changes that occur post-transection appear to be confined to different cellular compartments, as indicated by the lack of colocalisation. This suggests that GAP43, and not NFs, is associated with the distal response of the injured axon. It cannot be determined definitively whether the regenerating axons emerge from previously damaged neurites or from uninjured neurons in the cell clusters – this may be achieved by following the reaction of single cultured nerve cells in future studies. However, it is notable that three weeks of growth and differentiation by these neurons is required for this sprouting response whereas neurons at 14 DIV show markedly reduced ability to regenerate post-injury, although many of the neurons in clusters would be still in the process of elaborating their axonal process. This would indicate that the sprouting response may be more closely associated with the differentiation state of the injured neurons, rather than emanating from undamaged cell bodies.

Ultrastructural studies have supported the proposition that sprouting processes emerge from reactive axons (Yaghmai & Povlishock, 1992) and the proximal axonal stump (McHale et al., 1995) following injury to the CNS. Furthermore, labelling for GAP43, has been localised to sprouting axons several days after both traumatic brain injury (Christman et al., 1997) and following axonal transection in hippocampal slices *in vitro* (McKinney et al., 1997). In the

latter study it was proposed that such injury-related sprouting may ultimately give rise to epileptiform activity within the brain (McKinney et al., 1997).

Finally, the neurofilamentous changes identified in the current model were rarely observed PI in DIV 14 cultures but were numerous in DIV 21 injured axons, indicating that cultured neurons have to reach a certain level of maturity before responding in the above outlined stereotypical fashion. Similar age dependent reactive changes have been reported by Murphy and Horrocks (1993b) in their investigations of the effects of ischaemia and glutamate toxicity on neurons in mixed culture. They concluded that neurons in culture for between two to three weeks (DIV14-21) mature and this maturation increases the susceptibility to ischaemic injury. Cells in culture for less than two weeks were unaffected by the same level of ischaemia. These data clearly indicate that neuronal responses to both mechanical and physiological insults is governed by the maturity of the cell.

The current study has demonstrated that the neuronal alterations following axotomy *in vitro* resemble the changes observed *in vivo* in adult animals (Guillery, 1965; Meller et al., 1993a, 1994; King et al., 1997, 2000). In addition, as the culturing conditions do not support glial cells, it suggests that the stereotypical changes that occur represent an internal neuronal response and do not require external factors possibly derived from non-neuronal cells. This *in vitro* model is also relevant to AD as it replicates the early cytoskeletal pathology of this condition in the form of bulb- and ring-like structures showing an accumulation of NFs (Chapter 3; Vickers et al., 1996; King et al., 1997). In a similar fashion to the subtypes of plaque-associated DNs in AD (Chapter 3), neurites responding to injury in the current study could be distinguished by their content of either NF or sprouting-related markers.

The current *in vitro* model may also be used to investigate therapeutic agents that may inhibit deleterious aspects of the neuronal response to injury. For example, we have recently utilised an *in vivo* model of brain injury to examine whether cytoskeletal stabilising drugs may inhibit

the neuronal reaction to injury (Adlard, In Press), a strategy that may be helpful in preventing post-trauma cytoskeletal disruption and/or aberrant sprouting, and perhaps the evolution of neuronal pathology in Alzheimer's disease. The ability to replicate key injury-related neuronal changes in culture will enable the more rapid screening of potentially clinically relevant neuroactive agents.

GENERAL DISCUSSION

7.1 Discussion

While there have been major advances in unravelling important features of the pathology, epidemiology and genetics of AD in recent years, progress in determining a therapeutic strategy to prevent, attenuate or effectively treat AD has been hampered by the lack of understanding of the cellular mechanism leading to neuronal degenerations and dementia. The central aim of this thesis is to contribute towards a greater understanding of this mechanism, particularly with regards to the role of NFs in the development of neurofibrillary pathology.

The introductory chapter in this thesis presented a review of the literature on both the neuronal cytoskeleton and the pathological hallmarks of AD, with a particular emphasis on the relationship between the two. It was noted that most investigators of cytoskeletal alterations in AD focus on the MT associated protein, tau, that is present in neurofibrillary pathology as PHFs (Wischik et al., 1988). However, more recent investigations found that abnormal tau is absent from the DNs that are present within presymptomatic or preclinical AD cases. Instead the predominant cytoskeletal alteration in these cases is the abnormal accumulation of NFs. Furthermore, evidence suggesting selective vulnerability to NFT development of NF immunopositive neurons (Vickers et al., 1992b, Hof et al., 1990) further implicated NFs as playing an important role in the pathogenesis of AD. A widely reported phenomena in this area is the association between clusters of DNs and ß–amyloid deposits (Hof & Morrison, 1994). There is considerable controversy within the literature regarding

which of these hallmark structures is the initiating pathological lesion. Several hypotheses have been proposed to explain this association, however, all are yet to be proven unequivocally. This background information prompted an initial investigation of the relationship between ß-amyloid deposits and abnormal or dystrophic neurites.

Some investigators propose that not all clusters of DNs are associated with ß–amyloid plaques, therefore, suggesting the possibility that neuritic abnormalities may precede ß-amyloid deposition (Martin et al., 1994). In this investigation, experiments utilising double labelling immunohistochemistry confirmed that all clusters of DNs in both preclinical and end-stage AD cases were associated with ß-amyloid plaques, however, not all amyloid deposits were neuritic. These results support the hypothesis that the initiating pathological lesion in AD is the ß-amyloid plaque and that neurofibrillary pathology is a secondary change (Selkoe, 1994). This association was not dependent on the morphology of the plaque with all plaque types, including diffuse deposits, associated with clusters of DNs. Further to this, all plaque types were present in both preclinical and end-stage AD, including dense-cored plaques. This result further supports the premise that the morphologically variable plaque types, that are widely reported by investigators, are likely to represent independently evolved structures (Armstrong, 1998) and challenges the assumption that they are indicative of the stages of the life history of a single plaque (Ikeda et al., 1990).

The lack of correlation between the morphology of ß-amyloid plaques and their tendency to cause damage to surrounding nerve cell processes implied that a further factor differentiates damaging from non-damaging plaques. The protein ApoE has been suspected as having a role in AD primarily due to the identification of the ε4 allele as a genetic risk factor for the

disease (Corder et al., 1993), however, this role has not been fully elucidated. Several reports have emphasised the association of ApoE with either ß-amyloid plaque formation (Wisniewski & Frangione, 1992; Kida et al., 1994; Gearing et al., 1995; Sheng et al., 1996) or the development of neurofibrillary pathology (Benzing & Mufson, 1995; Han et al., 1994). In this thesis, the association between ApoE and the pathological hallmarks of AD in preclinical and end-stage AD cases was determined, with the view of investigating the hypothesis that the protein ApoE contributes to the formation of AD pathology.

Utilisation of multiple label immunohistochemical methods enabled the direct examination of the localisation of ApoE immunoreactivity relative to ß-amyloid plaques, DNs and NFTs. In AD cases, ß-amyloid plaques showing high ApoE immunoreactivity were localised to layers II, III and V of the neocortex. In layer I, ß-amyloid plaques were unlabelled for ApoE, and plaques in other layers were typically incompletely labelled for ApoE relative to ß-amyloid. Dense-core plaques labelled for ß-amyloid often had only the central portions labelled for ApoE. Unlike ß-amyloid labelled plaques, all ApoE immunoreactive plaques were associated with DNs. In preclinical AD cases, most plaques were double labelled for ß-amyloid and ApoE. ApoE did not label DNs or the early stages of NFT formation, indicating that ApoE may not be directly involved in neurofibrillary pathology. The specific presence of ApoE in plaques associated with DNs in demented cases suggests that ApoE may contribute toward a higher degree of ß-amyloid fibrillogenesis, enhancing the ability of certain plaques to cause damage to surrounding axons. Alternatively, as ApoE has been demonstrated to have a role in the remodelling and sprouting of axons and synaptic terminals following neural damage (Poirier, 1994), it may be acting to mobilise and redistribute cholesterol following plaque-induced damage,

promoting the reformation of membranous structures and subsequent sprouting/regeneration.

DNs are complex structures exhibiting immunoreactivity to a wide range of proteins including various components of the cytoskeleton. There has been some controversy over the origin of DNs, although the balance of evidence suggest that they represent altered, probably abnormally sprouting axons (Masliah et al., 1993b; Praprotnik et al., 1996; Vickers et al., 1996). One of the specific aims of this thesis was to investigate the diversity of plaque-associated DNs in both the early and late stages of AD. In the studies addressing this aim, a particular emphasis was placed on clarifying the role of NFs in the development of this pathological hallmark.

Preclinical AD was characterised by the presence of abnormal neurites containing either NF or CgA immunoreactivity in the absence of tau labelling. NF immunoreactive DNs in preclinical AD could be further subclassified into bulb- and ring-like structures. These abnormal neurites contained both phosphorylated and dephosphorylated NF epitopes. Therefore, an abnormal accumulation of variably phosphorylated NFs represent the earliest cytoskeletal alteration associated with DN formation and, therefore, one of the earliest pathological phenomena associated with the disease. Identification of the earliest form of neuronal pathology of AD holds the key to understanding the relationship between ß-amyloid plaque formation and neuronal degeneration. The elucidation of this early preclinical stage of the disease provides another potential target for the development of effective therapeutic strategies aimed at preventing or slowing the development of classical PHF-tau pathology and nerve cell death.

DNs in AD could be subdivided into predominantly NF, tau or CgA immunolabelled forms. The NF immunopositive DNs expressed the same complement of phosphorylation- and dephosphorylation-dependent epitopes as observed in preclinical cases. These DNs could again be subclassified based on their morphology, into bulb-like structures and also swollen, torturous neurites. NF immunopositive ring-like structures were not present in these cases, and supported the premise that this form of DN was transient and characteristic of the very early stages of neuritc pathology development in AD. Immunohistochemical labelling of the end-stage AD material demonstrated that the majority of NF immunoreactive DNs were bulb-like, whereas most of the more swollen and elongated processes were tau immunopositive. Close examination of the end-stage AD material double labelled for both NFs and tau revealed a distinct third class of abnormal neurite, NF immunoreactive bulb-like neurites with a core region labelled for tau. It was proposed that this class of abnormal neurites may represent an important transitional stage in DN development that is currently rarely recognised by many investigators. Using the confocal microscope to optically section through NF immunoreactive DNs, it was possible to quantitate the proportion of neurites that show this association between the two cytoskeletal proteins. Data showed that this labelling pattern was considerably more prevalent than initial examination using standard fluorescent microscopy suggested. Whereas the stages of NFT formation and development have been widely investigated, similar detail regarding DN formation has not been established. The results of this thesis indicate that DNs may 'mature' through NF-abundant forms to the neurites containing the profoundly altered filaments labelled for tau and confirm a role for NF in the development of the DNs associated with ß-amyloid plaques.

Thus the initial AD neuronal pathology is characterised by an accumulation of NFs. While the studies on preclinical AD have supported the proposal that cellular changes involving NFs may be important in the staging of neurofibrillary pathology, it was the morphological forms of the early DNs that provided a crucial clue as to how ß–amyloid plaques cause neuronal pathology. Recently, our laboratory determined that the NF immunopositive bulb- and ring-like DNs associated with plaques in preclinical AD were morphologically identical to changes that occur within damaged axons in a rodent experimental model of localised brain trauma (King et al., 1997). This initial observations lead to the preliminary hypothesis that physically damaged rat cortical axons may serve as a model for the early neuronal pathology of AD.

In the current investigations, the neurochemical heterogeneity of the DNs present in preclinical and end-stage AD was assessed. The distribution and degree of colocalisation of various components of the NF triplet in various phosphorylation states, was determined using multiple double labelling immunohistochemistry. A distinct expression pattern of NF epitopes was present in both the preclinical and end-stage AD cases. Interestingly, similarly detailed immunohistochemical analysis in the rodent *in vivo* experimental model revealed the same expression pattern of NF epitopes (King et al., 2000). Therefore, the rigorous investigation of the exact complement of NF epitopes localised to preclinical AD DNs provided further support for the preliminary hypothesis that the axonal changes that occur in response to physical damage model the earliest neurofibrillary pathological changes that occur in axons in response to ß-amyloid plaque formation. Thus, the gradual emergence of plaques from the late middle age onwards may cause physical damage to surrounding axons, resulting in a sprouting response by the affected neuron. Ultimately, the chronic persistent stimulation of this sprouting response results in abnormal neuronal filamentous

pathology throughout the nerve cells, eventually leading to degeneration of specific cortical connections and dementia (Vickers et al., 1996; King et al., 1997; Vickers, 1997; King et al., 2000).

Nerve cells respond to structural injury with a complex set of morphological, neurochemical and gene expression changes, most of which are directed towards an attempt by the neuron to adapt to such trauma by sprouting and regeneration. Consideration of the literature uncovers many parallels between the neuronal response to physical trauma and the changes that occur with DN and NFT formation in AD.

NFs are normally excluded from the synaptic terminals in most axons, but ring-like accumulations of NFs occur in this neuronal domain following axonal damage (Gray & Hamlyn, 1962; Guillery, 1965). Neurofilamentous hypertrophy also occurs in the proximal and distal stumps of transected central and peripheral axons, with distal segments of damaged axons gradually undergoing Wallarian degeneration (Ramon y Cajal, 1928; Lanners & Grafstein, 1980; Meller, 1987; Hall et al, 1989; Tetzlaff & Bisby, 1989; McHale et al., 1995). The morphology of the proximal and distal segments of the physically damaged axons resemble the bulb- and ring-like DNs of preclinical AD (King et al., 1997, 2000). Similarly, an accumulation of perikaryal NFs is also reported in the cell body reaction to physical injury (Torvick, 1976; Schlaepfer, 1987; Silveira et al., 1994) and in AD (Vickers et al., 1992b, 1994b; Nakamura et al., 1997).

Phosphorylation-dependent NF epitopes, normally localised to the axonal domain (Sternberger & Sternberger, 1993), appear in the cell bodies of acutely damaged neurons. Similarly, phosphorylated NF epitopes have been localised to cortical nerve cell bodies in

AD (Masliah et al., 1993b). The reverse modification occurs in axons. After physical trauma dephosphorylated NF epitopes, normally localised to the perikaryal domain (Sternberger & Sternberger, 1983), transiently occur in damaged axons as well as in distal axonal segments following Wallarian degeneration (Meller et al., 1993b, 1994; King et al., 1997). Dephosphorylated NFs were likewise localised to the DNs of both preclinical and end-stage AD in the current investigations.

Many central neurons, when damaged exhibit some form of sprouting (Wigley & Berry, 1988; Hopkins & Bunge, 1991; Deller & Frotscher, 1997; McKinney et al., 1997). This attempt at regeneration may, however, lead to inappropriate new connections that can cause elevated epileptiform activity (McKinney et al., 1997). Interestingly, in this investigation, and other recent studies, subgroups of DNs localised to plaques that generally lack cytoskeletal epitopes but contain synaptic markers indicative of adaptive sprouting have been identified (Chapter 3; Saunders et al., 1998; Su et al., 1998). The AD related changes in tau may also follow the neuronal reaction to physical damage. For example, increased expression of the developmental form of the tau protein occurs following physical injury in adult animals (Chambers & Muma, 1997), and this isoform of tau is an intrinsic component of neurofibrillary pathology (Jakes et al., 1991). Furthermore, tau proteins are enriched in regenerating axons (Yin et al., 1995) and the abnormally phosphorylated sites on tau in AD recapitulate tau modification during axonal growth (Pope et al., 1993).

Finally, further evidence linking physical injury and AD, is the identification of head trauma as a risk factor. Both single episodes and repeated head injury, as in the case of boxers (dementia pugilistica) have been identified as increasing the risk of AD (Heyman et al., 1984; Mortimer et al., 1985; Graves et al., 1990; Mortimer et al., 1991; Katzman &

Kawas, 1994). Furthermore, the NFTs characteristic of AD are very similar to those that occur following repetitive head injury, as experienced by boxers (Lampert & Hardman, 1984; Roberts et al., 1990; Tokuda et al., 1991; Geddes et al., 1996, 1999) or by individuals demonstrating self-abuse behaviour (Hof et al., 1991b).

The final aim of this thesis was to develop an *in vitro* model that mimics the effects of ß-amyloid plaques on surrounding neuronal processes and, therefore, complements the existing *in vivo* model. The advantages of *in vitro* models of neuronal responses to injury include the ability to control and manipulate the extracellular environment, elimination of often confounding effects introduced by the circulatory system such as hypoxia and ischemia and the possibility of low cost screening of potential therapeutic agents. The current investigation had a focus on the time course of cytoskeletal changes following physical injury to axons as well as the temporal association of reactive and regenerative cellular alterations. Therefore, isolated pure neuronal cultures with markers for NFs and the growth-associated protein, GAP43, were utilised.

The neuronal response to axotomy was closely linked with nerve cell maturity. In summary, after transection, mature cortical neurons underwent a series of stereotypical changes that are independent of the presence of other confounding cells (astroglia, microglia, oligodendrocytes etc) and factors, such as cytokines, chemokines, interleukins and growth factors that may be released by these cell types. These reactive changes, which occurred independent of the presence or effects of glial cell populations, involved the development of NF-labelled ring- and bulb-like structures, followed by GAP43 accumulation and ultimately culminated in a sprouting response. These reactive cellular changes faithfully modelled the

consequences of *in vivo* axotomy as well as the earliest stages of DN formation in response to ß-amyloid plaque formation in AD.

Collectively the results obtained from the investigations outlined in this thesis, in the light of work by other investigators, dispute a number of the popular theories developed to explain the mechanism underlying AD. Furthermore, these results support a newly evolving hypothesis that links two of the pathological hallmark changes of AD, the ß-amyloid plaque and the DN.

7.2 Final conclusions

With the changing demographics of society world wide, disorders that affect the elderly are increasingly prevalent (Price et al., 1998). Because of this prevalence and the magnitude of the morbidity associated with AD it is imperative that a greater understanding of the pathogenic mechanisms involved in AD is obtained. This will ultimately lead to the development of more effective treatments that either prevent or ameliorate this disease. In conclusion, in this study, the following contributions to a greater understanding of the cellular mechanism underlying AD were made. Figure 7.2 shows a diagramatic representation of these findings.

- ***NFs have a role in the development of neurofibrillary pathology in AD.***

The results of this thesis challenge one of the common assumptions made in AD research, that is that the changes associated with tau are the primary cytoskeletal alteration in AD and, furthermore, NFs play no significant role in the development of neurofibrillary pathology. Accumulations of NFs as distinct bulb and ring-like structures were identified as the earliest form of axonal pathology in preclinical AD, preceding classical PHF-tau pathology. The following transitional stage in DN development, the formation of a tau core within the NF immunopositive bulb-like structures, was also identified and further characterised.

- ***ß-amyloid plaques may cause physical damage to surrounding axons.***

A pervading belief among supporters of the amyloid cascade hypothesis is that ß–amyloid is toxic to nerve cells. Based on the similarities between preclinical AD DNs and the abnormal neurites that develop following physical trauma to axons it has recently been proposed that ß-amyloid plaque deposition in AD may cause physical damage to

surrounding processes (King et al., 1997, 2000; Vickers, 1997) as opposed to toxic damage. Alternatively, axons may have a limited repertoire of responses to any insult, such that a toxic factor within the plaque cannot not be totally excluded as the initiator of neurofibrillary pathology.

- ***ApoE may contribute to the ability of plaques to damage surrounding processes.***

The protein ApoE colocalised selectively with those ß-amyloid plaques associated with clusters of DNs. These results imply that ApoE may play a role in determining the ability of plaques to injure processes, perhaps through increased fibrillogenesis.

- ***An in vitro model of axonal injury replicates preclinical AD neuronal pathology.***

At present there is no model that effectively replicates all aspects of the complicated AD paradigm. In this investigation a model of the very earliest neurofibrillary changes that occur in AD was developed. The advantages of this model include its relative inexpensiveness, as compared to the funds required for the development of transgenic models, and more importantly as this system models the earliest preclinical changes that occur in AD it provides a new tool for assessing the effectiveness of potential therapeutic agents which are aimed at stabilising the cytoskelton before the development of NFT, nerve cell degeneration and dementia.

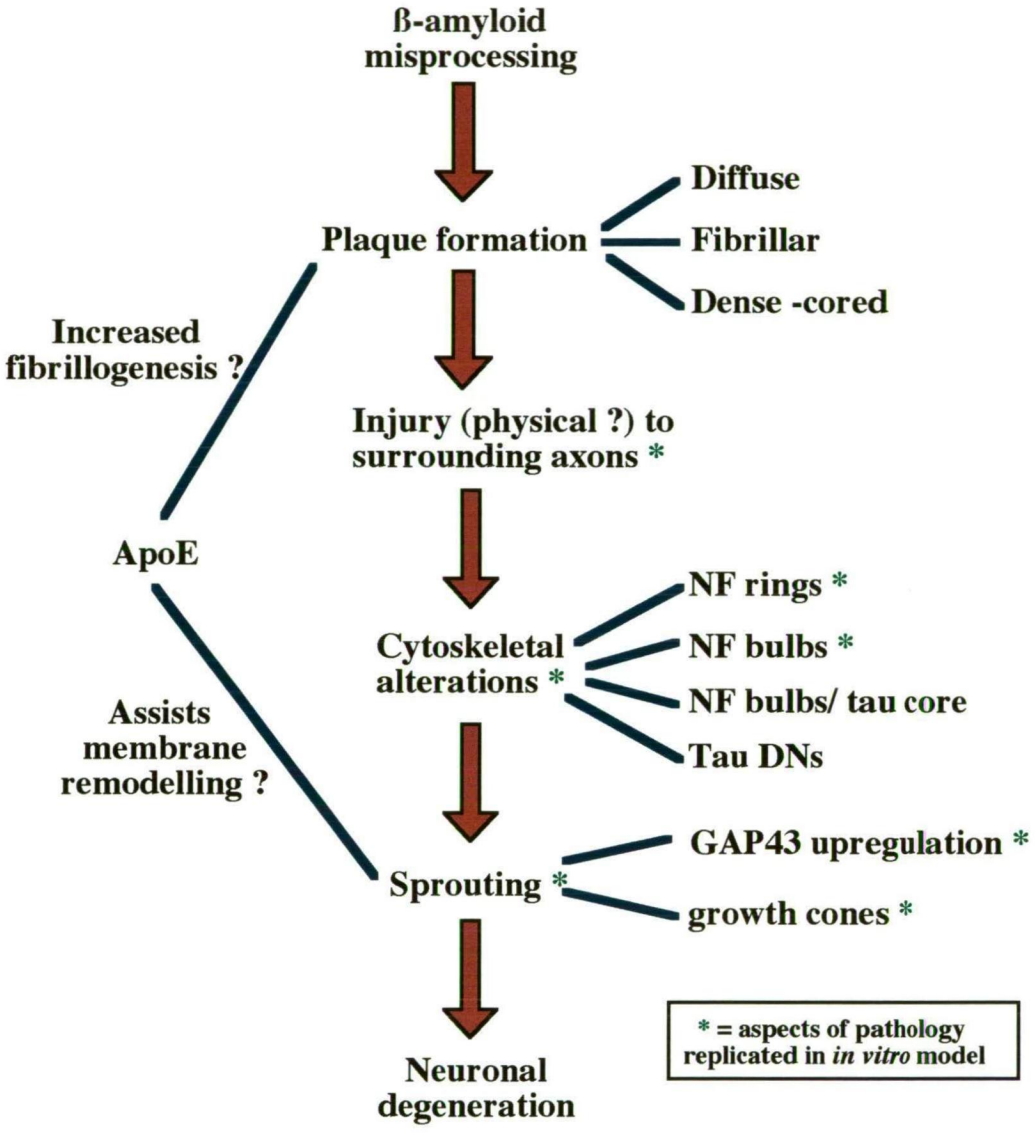

Figure 7.2

The cellular mechanism underlying AD

REFERENCES

Adlard, P.A., King, C.E. & Vickers, C.E. The effects of taxol on the central nervous system response to physical injury. *Acta Neuropathol.* (In Press).

Angelides, K.J., Smith, K.E. & Takeda, M. (1989) Assembly and exchange of intermediate filament proteins of neurons; neurofilaments are dynamic structures. *J. Cell Biol.* **108,** 1495-506.

Arai, H., Lee, V.M.-Y., Otvos, L. Jr., Greenberg, B.D., Lowery, D.E., Sharma, S.K., Schmidt, M.L. & Trojanowski, J.Q. (1990) Defined neurofilament, tau, and beta-amyloid precursor protein epitopes distinguish Alzheimer from non-Alzheimer senile plaques. *Proc. Natl. Acad. Sci. U.S.A.* **87,** 2249-2253.

Arai, H., Higuchi, S., Matsushita, S., Yuzuriha, T., Trojanowski, J.Q. & Lee, V.M.-Y. (1994) Expression of ß-amyloid precursor protein in the developing human spinal cord. *Brain Res.* **642,** 132-136.

Arias, C., Arrieta, I. & Tapia, R. (1995) Beta-amyloid peptide fragment 25-35 potentiates the calcium-dependent release of excitatory amino acids from depoalized hippocampal slices. *J. Neurosci. Res.* **41,** 561-566.

Armstrong, R.A. (1998) ß-Amyloid plaques: Stages in life history or independent origin? *Dement. Geriatr. Cogn. Disord.* **9,** 227-238.

Arnold, S.E., Hyman, B.T., Flory, J., Damasio, A.R. & Van, H.G. (1991) The topographical and neuroanatomical distribution of neurofibrillary tangles and neuritic plaques in the cerebral cortex of patients with Alzheimer's disease. *Cereb. Cortex* **1,** 103-116.

Arriagada, P.V., Growdon, J.H., Hedly-Whyte, T. & Hyman, B.T. (1992a) Neurofibrillary tangles not senile plaques parallel duration and severity of Alzheimer's disease. *Neurology* **42,** 631-639.

Arriagada, P.V., Marzloff, K. & Hyman, B.T. (1992b) Distribution of Alzheimer-type pathologic changes in nondemented elderly individuals matches the pattern in Alzheimer's disease. *Neurology* **42,** 1681-1688.

Baas, P.W., Deitch, J.S., Black, M.M. & Banker, G.A. (1988) Polarity orientation of microtubules in hippocampal neurons: uniformity in the axon and nonuniformity in the dendrite. *Proc. Natl. Acad. Sci. U.S.A.* **85,** 8335-8339.

Bales, K.R., Verina, T., Dodel, R.C., Du, Y., Alstiel, L., Bender, M., Hyspol, P., Johnstone, E.M., Little, S.P., Cummins, D.J., Piccardo, P., Ghetti, B. & Paul, S.M. (1997) Lack of apolipoprotein E dramatically reduces amyloid beta-peptide deposition. *Nat. Genet.* **17,** 263-264.

Bales, K.R., Verina, T., Cummins, D.J., Du, Y., Fishman, C.E., DeLong, C.A., Piccardo, P., Petegnief, V., Ghetti, B. & Paul, S.M. (1999) Apolipoprotein E is essential for amyloid deposition in the APP(V717F) transgenic mouse model of Alzheimer's disease. *Proc. Natl. Acad. Sci. U.S.A.* **96,** 15233-15238.

Bancher, C., Brunner, C., Lassman, H., Budka, H., Jellinger, K., Wiche, B., Seitelberger, F., Grundke-Iqbal, I., Iqbal, K. & Wisniewski, H.M. (1989) Accumulation of abnormally phosphorylated τ precedes the formation of neurofibrillary tangles in Alzheimer's disease. *Brain Res.* **477,** 90-99.

Bancher, C., Grundke-Iqbal, I., Iqbal, K., Fried, V.A., Smith, H.T. & Wisniewski, H.M. (1991) Abnormal phosphorylation of tau precedes ubiquitination in neurofibrillary pathology of Alzheimer disease. *Brain Res.* **539,** 11-18.

Banker, G. & Goslin, K. (1991) Culturing nerve cells. Cambridge: MIT Press

Barger, S.W. & Harmon, A.D. (1997) Microglial activation by Alzheimer amyloid precursor protein and modulation by apolipoprotein E. *Nature* **388,** 878-881.

Bartlett, W.P. & Banker, G.A. (1984) An electron microscopic study of the development of axons and dendrites by hippocampal neurons in culture. II. Synaptic relationships. *J. Neurosci.* **4,** 1954-1965.

Batchelor, P.E., Liberatore, G.T., Wong, J.Y., Porritt, M.J., Freichs, F., Donnan, G.A. & Howell, D.W. (1999) Activated macrophages and microglia induce dopaminergic sprouting in the injured striatum and express brain-derived neurotrophic factor and glial cell line-derived neurotrophic factor. *J. Neurosci.* **19,** 1708-1716.

Behl, C., Davis, J.B., Lesley, R. & Schubert, D. (1994) Hydrogen peroxide mediates amyloid beta protein toxicity. *Cell* **77,** 817-827.

Benes, F.M., Farol, P.A., Majocha, R.E., Marotta, C.A. & Bird, E.D. (1991) Evidence for axonal loss in regions occupied by senile plaques in Alzheimer cortex. *Neuroscience* **42,** 651-600.

Benzing, W.C., Ikonomovic, M.D., Brady, D.R., Mufson, E.J. & Armstrong, D.M. (1993) Evidence that transmitter containing dystrophic neurites precede paired helical filament and Alz-50 formation within senile plaques in the amygdala of nondemented elderly and patients with Alheimer's disease. *J. Comp. Neurol.* **334,** 176-191.

Benzing, W.C. & Mufson, E.J. (1995) Apolipoprotein E immunoreactivity within neurofibrillary tangles: Relationship to tau and PHF in Alzheimer's disease. *Exp. Neurol.* **132,** 162-171.

Berg, L. (1988) Clinical Dementia Rating (CDR) *Psychopharmacol. Bull.* **25,** 637-639.

Berg, L., McKeel, D.W. Jr., Miller, J.P., Storandt, M., Rubin, E.H., Morris, J.C., Baty, J., Coats, M., Norton, J., Goate, A.M., Price, J.L., Gearing, M., Mirra, S.S. & Saunders, A.M. (1998) Clinicopathologic studies in cognitively healthy aging and Alzheimer's disease: relation of histologic markers to dementia severity, age, sex, and apolipoprotein E genotype. *Arch. Neurol.* **55,** 326-335.

Bernhardt, R. & Matus, A. (1984) Light and electron microscope studies of the distribution of microtubule-associated prottein 2 in rat brain; a difference between dendritic and axonal cytoskeleton. *J. Comp. Neurol.* **226,** 203-221.

Bierer, L.M., Hof, P.R., Purohit, D.P., Carlin, L., Schmeidler, J., Davis, K.L. & Perl, D.P. (1995) Neocortical neurofibrillary tangles correlate with dementia severity in Alzheimer's disease. *Arch. Neurol.* **52,** 81-88.

Binder, L.I., Frankfurter, A. & Rebhun, L.I. (1985) The distribution of tau in the mamalian central nervous system. *J. Cell Biol.* **101,** 1371-1378.

Bird, M.M. (1978) Microsurgical transection of small nerve fibre bundles *in vitro*. Effects on axons, growth cones and glial cells. *Cell Tissue Res.* **190,** 525-38.

Black, M.M. & Lasek, R.J. (1980) Slow components of axonal transport; two cytoskeletal networks. *J. Cell Biol.* **86,** 616-623.

Blacker, D., Haines, J.L., Rodes, L., Terwedow, H., Go, R.C.P., Harrell, L.E., Perry, R.T., Basset, S.S., Chase, G., Meyers, D., Albert, M.S. & Tanzi, R. (1997) ApoE-4 and age at onset of Alzheimer's disease: The NIMH Genetics Initiative. *Neurology* **48,** 139-147.

Blikstad, I., Sundkvist, I. & Eriksson, S. (1980) Isolation and characterization of profilactin and profilin from thymus and brain. *Eur. J. Biochem.* **105,** 425-433.

Bloom, G.S., Wagner, M.C., Pfister, K.K. & Brady, S.T. (1988) Native structure and physical properties of bovine brain kinesin and identification of the ATP-binding subunit polypeptide. *Biochemistry* **27,** 3409-3416.

Bondareff, W., Harrington, C.R., Wischik, C.M., Hauser, D.L. & Roth, M. (1995) Absence of abnormal hyperphosphorylation of tau in intracellular tangles in Alzheimer's Disease, *J. Neuropathol. Exp. Neurol.* **54,** 5, 657-663.

Borchelt, D.R., Thinakaran, G., Eckman, C.B., Lee, M.K., Davenport, F., Ratovitsky, T., Prada, C.M., Kim, G., Seekins, S., Yager, D., Slunt, H.H., Wang, R., Seeger, M., Levey, A.I., Gandy, S.E., Copeland; N.G., Jenkins, N.A., Price, D.L., Younkin, S.G. & Sisodia, S.S. (1996) Familial Alzheimer's disease-linked presenilin 1 variants elevate Aß1-42/1-40 ratio *in vitro* and *in vivo*. *Neuron* **17,** 1005-1013.

Borchelt, D.R., Ratovitski, T., van Lare J., Lee, M.K., Gonzales, V., Jenkins, N.A., Copeland, N.G., Price, D.L. & Sisodia, S.S. (1997) Accelerated amyloid deposition in the brains of transgenic mice coexpressing mutant presenilin 1 and amyloid precursor proteins. *Neuron* **19,** 939-945.

Braak, H., Braak, E., Grundke-Iqbal, I. & Iqbal, K. (1986) Occurrence of neuropil threads in the senile human brain and in Alzheiemr's disease. A third location of paired helical filaments outside of neurofibrillary tangles and neuritic plaques. *Neurosci. Lett.* **65,** 351-355.

Braak, H. & Braak, E. (1988) Neuropil threads occur in dendrites of tangle-bearing nerve cells. *Neuropathol. Appl. Neurobiol.* **14,** 39-44.

Braak, H. & Braak, E. (1991) Neuropathological staging of Alzheimer-related changes. *Acta Neuropathol.* **82,** 239-259.

Braak, H., Braak, E. & Strothjohann, M. (1994) Abnormally phosphorylated tau protein related to the formation of neurofibrillary tangles and neuropil threads in the cerebral cortex of sheep and goat. *Neurosci. Lett.* **171,** 1-4.

Brady, S.T., Lasek, R.J. & Allen, R.D. (1982) Fast axonal transport in extruded axoplasm from squid giant axon. *Science* **218,** 1129-1131.

Brady, S.T. (2000) Neurofilaments run sprints not marathons. *Nat. Cell Biol.* **2,** 43-45.

Bramblett, G.T., Goedert, M., Jakes, R., Merrick, S.E,, Trojanowski, J.Q. & Lee, V.M.-Y. (1993) Abnormal tau phosphorylation at Ser396 in Alzheimer's disease recapitulates development and contributes to reduced microtubule binding. *Neuron* **10,** 1089-1099.

Brandt, R., Lee, G., Teplow, D.B., Shalloway, D. & Abdel-Ghany, M. (1994) Differential effect of phosphorylation and substrate modulation on tau's ability to promote microtubule growth and nucleation. *J. Biol. Chem.* **269,**11776-11782.

Brandt, R. (1998) Cytoskeletal mechanisms of axon outgrowth and pathfinding. *Cell Tiss. Res.* **292,** 181-189.

Breen, K.C., Bruce, M. & Anderton, B.H. (1991) Beta-amyloid precursor protein mediates neuronal cell-cell and cell-surface adhesion. *J. Neurosci. Res.* **28,** 90-100.

Bregman, D.S., Kunkel–Bagden, E., Schnell, L., Dai., H.N., Gao, D. & Schwab, M.E. (1995) Recovery from spinal cord injury mediated by antibodies to neurite growth inhibitors. *Nature* **378,** 498-501.

Brewer, G.J., Torricelli, J.R., Evege, E.K. & Price. P.J. (1993) Optimized survival of hippocampal neurons in B27-supplemented Neurobasal™, a new serum-free medium combination. *J. Neurosci. Res.* **35,** 567-576.

Brewer, G.J. (1995) Serum-free B27 neurobasal medium supports differentiated growth of neurons from the striatum, substantia nigra, septum, cerebral cortex and dentate gyrus. *J. Neurosci. Res.* **42,** 674-683.

Brewer G.J. (1997) Isolation and culture of adult rat hippocampal neurons. *J. Neurosci. Methods* **71,** 143-155.

Brion, J-P., Couk, A-M., Bruce, M., Anderton, B. & Flament-Durand, J. (1991) Synaptophysin and chromagranin A immunoreactivities in senile plaques of Alzheimer's disease. *Brain Res.* **539,** 143-150.

Busciglio, J., Hartmann, H., Lorenzo, A., Wong, C., Baumann, K., Sommer, B., Staufenbiel, M. & Yankner, B.A. (1997) Neuronal localization of Presenilin-1 and association with amyloid plaques and neurofibrillary tangles in Alzheimer's disease. *J. Neurosci.* **17,** 5101-5107.

Butner, K.A. & Kirschner, M.W. (1991) Tau protein binds to microtubules through a flexible array of distributed weak sites. *J. Cell Biol.* **115,** 717-730.

Caceres, A. & Kosik, K.S. (1990) Inhibition of neurite polarity by tau antisense oligonucleotides in primary cerebellar neurons. *Nature* **343,** 461-463.

Cai, X.D., Golde, T.E. & Younkin, S.G. (1993) Release of excess amyloid beta protein from a mutant amyloid beta protein precursor. *Science* **259,** 514-516.

Campbell, M.J. & Morrison, J.H. (1989) Monoclonal antibody to neurofilament protein (SMI-32) labels a subpopulation of pyramidal neurons in the human and monkey neocortex. *J. Comp. Neurol.* **282,** 191-205.

Campbell, M.J., Hof, P.R. & Morrison, J.H. (1991) A subpopulation of primate corticocortical neurons is distinguished by somatodendritic distribution of neurofilament protein. *Brain Res.* **539,** 133-136.

Carden, M., Trojanowski, J., Schlaepfer, W. & Lee, V.M.-Y. (1987) Two-stage expression of neurofilaments during rat neurogenesis with early establishment of adult phosphorylation patterns. *J. Neurosci.* **7,** 3489-3504.

Carpenter, M.K., Crutcher, K.A. & Kater, S.B. (1993) Analysis of the effects of Alzheimer's plaques on living neurons. *Neurobiol. Aging* **14,** 207-215.

Chambers, C.B. & Muma, N.A. (1997) Tau mRNA isoforms following sciatic nerve axotomy with and without regeneration. *Mol. Brain Res.* **48,** 115-124.

Chargé, S.P.B., Esiri, M.M., Bethune, C.A., Hansen, B.C. & Clark, A. (1996) Apolipoprotein E is associated with islet amyloid and other amyloidoses: Implications for Alzheimer's disease. *J. Pathol.* 1996; **179,** 443-447.

Chartier-Harlin, M.C., Crawford, F., Houlden, H., Warren, A., Hughes, D., Fidani, L., Goate, A., Rossor, M., Roques, P., Hardy, J. & Mullan, M. (1991) Early-onset Alzheimer's disease caused by mutations at codon 717 of the beta-amyloid precursor protein gene. *Nature* **353,** 844-846.

Christman, C.W., Salvant, J.B., Walker, S.A. & Povlishock, J.T. (1997) Characterization of a prolonged regenerative attempt by diffusey injured axons following traumatic injury in adult cat: a light and electron microscopic immunocytochemical study. *Acta Neuropathol.* **94,** 329-337.

Citron, M., Oltersdorf, T., Haass, C., McConlogue, L., Hung, AY., Seubert, R., Vigo-Pelfrey, C., Lieberburg, I. & Selkoe, D.J. (1992) Mutation of the ß-amyloid precursor protein in familial Alzheimer's disease increases ß-protein production. *Nature* **360,** 672-674.

Citron, M., Vigo-Pelfrey, C., Teplow, D.B., Miller, C., Schenk, D., Johnston, J., Winblad, B., Venizelos, N., Lannfelt, L. & Selkoe, D.J. (1994) Excessive production of amyloid beta-protein by peripheral cells of symptomatic and presymptomatic patients carrying the Swedish familial Alzheimer disease mutation. *Proc. Natl. Acad. Sci. U.S.A.* **91,** 11993-11997.

Citron, M., Westaway, D., Xia, W., Carlson, G., Diehl, T., Levesque, G., Johnson-Wood, K., Lee, M., Seubert, P., Davis, A., Kholodenko, D., Motter, R., Sherrington, R,, Perry, B., Yao, H., Strome, R., Lieberburg, I. Rommens, J., Kim, S., Schenk, D., Fraser, P., St. George-Hyslop, P. & Selkoe, D.J. (1997) Mutation presenilins of Alzheimer's disease increases production of 42-residue amyloid ß-protein in both transfected cells and transgenic mice. *Nat. Med.* **3,** 67-72.

Citron, M., Eckman, C.B., Diehl, T.S., Corcoran, C., Ostaszewski, B.L., Xia, W.M., Levesque, G., Hyslop, P.S., Younkin, S.G. & Selkoe, D.J. (1998) Additive effects of PS1 and APP mutations on secretion of the 42-residue amyloid beta-protein. *Neurobiol. Dis.* **5,** 107-116.

Cohlberg, J.A., Hajarian, H., Tran, T., Alipourjeddi, P. & Noveen, A. (1995) NF protein heterotetramers as assembly intermediates. *J. Biol. Chem.* **270,** 9334-9339.

Cole, G.M., Masliah, E., Shelton, E.R., Chan, H.W., Terry, R.D. & Saitoh, T. (1991) Accumulation of amyloid precursor fragment in Alzheimer plaques. *Neurobiol. Aging* **12,** 85-91.

Cook, D.G., Forman, M.S., Sung, J.C., Leight, S., Kolson, D.L., Iwatsubo, T., Lee, V.M.-Y. & Doms, R.W. (1997) Alzheimer's Aß(1-42) is generated in the endoplasmic reticulum/intermediate compartment of NT2N cells. *Nat. Med.* **3,** 1021-1023.

Corder, E.H., Saunders, A.M., Strittmatter, W.J., Schmechel, D.E., Gaskell, P.C., Small, G.W., Roses, A.D., Haines, J.L. & Pericak-Vance, M.A. (1993) Gene dose of apolipoprotein E type 4 allele and the risk of Alzheimer's disease in late onset families. *Science* **261,** 921-923.

Corder, E.H., Saunders, A.M., Risch, N.J., Strittmatter, W.J., Schmechel, D.E., Gaskell, P.C., Rimmler, J.B., Locke, P.A., Conneally, P.M., Schmader, K.E., Small, G.W., Roses, A.D., Haines, J.L. & Pericak-Vance, M.A. (1994) Protective effect of apopolipoprotein E type 2 allele for late-onset Alzheimer's disease. *Nat. Genet.* **7,** 180-184.

Cork, L.C., Sternberger, N.H., Sternberger, L.A., Casanova, M.F., Struble, R.G. & Price, D.L. (1986) Phosphorylated neurofilament antigens in neurofibrillary tangles in Alzheimer's disease. *J. .Neuropathol. Exp. Neurol.* **45,** 56-64.

Cras, P., Kawai, M., Siedlak, S., Mulvihill, P., Gambetti, P., Lowery, D., Gonzalez-DeWhitt, P., Greenberg, B. & Perry, G. (1990) Neuronal and microglial involvement in ß-amyloid protein deposition in Alzheimer's disease. *Am. J. Pathol.* **137,** 241- 246.

Cras, P., Kawai, M., Lowrey, D., Gozalez-deWhitt, P., Greenberg, B. & Perry, G. (1991) Senile plaques neurites in Alzheimer's disease accumulate amyloid precursor protein. *Proc. Natl. Acad. Sci. U.S.A.* **88,** 7552-7556.

Cruts, M., van Duijn, C.M., Backhovens, H., van den Broek, M., Wehnert, A., Serneels, S., Sherrington, R., Hutton, M., Hardy, J., St. George-Hyslop, P.H., Hoffman, A. & Van Broeckhoven, C. (1998) Estimation of the genetic contribution of presenilin-1 and -2 mutations in a population-based study of presenile Alzheimer disease. *Hum. Mol. Genet.* **7,** 143-151.

Cruz, L., Urbanc, B., Buldyrev, S.V., Christie, R., Gomez-Isla, T., Havlin, S., McNamara, M., Stanley, H.E. & Hyman, B.T. (1997) Aggregation and dissaggregation of senile plaques in Alzheimer's disease. *Proc. Natl. Acad. Sci. U.S.A.* **94,** 7612-7616.

Cummings, B.J., Su, J.H., Geddes, J.W., Van Nostrand, W., Wagner, S., Cunningham, D. & Cotman, C.W. (1992) Aggreagation of the amyloid precursor protein (APP) within degenerating neurons and dystrophic neurites in Alzheimer's disease. *Neuroscience* **48,** 763-777.

Cummings, B.J., Su, J.H., Cotman, C.W., White, R. & Russel, M.J. (1993) Beta-amyloid accumulation in aged canine brain: a model of early plaque formation in Alzheimer's disease. *Neurobiol. Aging* **14,** 547-560.

Cummings, B.J., Head, E., Ruehl, W., Milgram, N.W. & Cotman, C.W. (1996a) The canine as an animal model of human aging and dementia. *Neurobiol. Aging* **17,** 259-268.

Cummings, B.J., Pike, C.J., Shankle, R. & Cotman, C.W. (1996b) Beta-amyloid deposition and other measures of neuropathology predict cognitive status in Alzheimer's disease. *Neurobiol. Aging* **17,** 921-933.

Cummings, B.J., Satou, T., Head, E., Milgram, N.W., Cole, G.M., Savage, M.J., Podlisny, M.B., Selkoe, D.J., Siman, R., Greenberg, B.D. & Cotman, C.W. (1996c) Diffuse plaques contain C-terminal Aß42 and not Aß40: Evidence from cats and dogs. *Neurobiol. Aging* **17,** 653-659.

Dahl, D., Bignami, A., Bich, N.T. & Chi, N.H. (1980) Immunohistochemical characterization of neurofibrillary tangles induced by mitotic spindle inhibitors. *Acta Neuropathol.* **51,** 165-168.

Dahl, D., Selkoe, D.J., Pero, R.T. & Bignami, A. (1982) Immunostaining of neurofibrillary tangles in Alzheimer's senile dementia with a neurofilament antiserum. *J. Neurosci.* **2,** 113-119.

Dautigny, A., Pham-Dinh, D., Roussel, C., Felix, J.M., Nussbaum, J.L., & Jolles, P. (1988) The large neurofilament subunit (NF-H) of the rat: cDNA cloning and in situ detection. *Biochem. Biophys. Res. Commun.* **154,** 1099-1106.

Davies, S.W. & Roberts, P.J. (1988) Model of Huntington's disease. *Science* **241,** 474-475.

Dawson, G.R., Seabrook, G.R., Zheng, H., Smith, D.W., Graham, S., O'Dowd, G., Bowery, B.J., Boyc,e S., Trumbauer, M.E., Chen, H.Y., Van der Ploeg, L.H. & Sirinathsinghji, D.J.

(1999) Age-related cognitive deficits, impaired long-term potentiation and reduction in synaptic marker density in mice lacking the beta-amyloid precursor protein. *Neuroscience* **90,** 1-13.

De Jonghe, C., Cruts, M., Rogaeva, E.A., Tysoe, C., Singleton, A., Vanderstichele, H., Meschino, W., Dermaut, B., Vanderhoeven, I., Backhovens, H., Vanmechelen, E., Morris, C.M., Hardy, J., Rubinsztein, D.C., St. George-Hyslop, P.H. & Van Broeckhoven, C. (1999) Aberrant splicing in the presenilin-1 intron mutation causes presenile Alzheimer's disease by increased Abeta42 secretion. *Hum. Mol. Genet.* **8,** 1529-1540.

De Strooper, B., Saftig, P., Craessaerts, K., Vanderstichele, H., Guhde, G., Annaert, W., Von Figura, K. & Van Leuven, F. (1998) Defficiency of presenilin-1 inhibits the normal cleavage of amyloid precursor protein. *Nature* **391,** 387-390.

De Strooper, B., Annaert, W., Cupers, P., Saftig, P., Craessaerts, K., Mumm, J.S., Schroeter, E.H., Schrijvers, V., Wolfe, M.S., Ray, W.J., Goate, A. & Kopan, R. (1999) A presenilin-1-dependent gamma-secretase-like protease mediates release of Notch intracellular domain. *Nature* **398**, 518-522.

Deller, T. & Frotscher, M. (1997) Lesion-induced plasticity of central neurons: sprouting of single fibres in the rat hippocampus after unilateral entorhinal cortex lesion. *Prog. Neurobiol.* **53,** 687-727.

De Lima, A.D., Merten, M.D.P. & Voigt, T. (1997) Neuritic differentiation and synaptogenesis in serum-free neuronal cultures of the rat cerebral cortex. *J. Comp. Neurol.* **382,** 230-246.

Dickson, D.W., Farlo, J., Davies, P., Crystal, H., Fuld, P. & Yen, S.H. (1988) Alzheimer's disease: A double-labelling immunohistochmeical study of senile plaques. *Am. J. Pathol.* **132,** 86-101.

Dickson, D.W., Wertkin, A., Kress, Y., Ksiezak-Reding, H. & Yen, S.H. (1990) Ubiquitin-immunoreactive structures in normal brains. Distribution and developmental aspects. *Lab. Invest.* **63,** 87-99.

Dickson, D.W., Crystal, H.A., Bevona, C., Honer, W., Vincent, I. & Davies, P. (1995) Correlations of synaptic markers with cognitive status in prospectively studied elderly humans. *Neurobiol. Aging* **16,** 285-298.

Dickson, D.W. (1997) The pathogenesis of senile plaques. *J. Neuropathol. Exp. Neurol.* **56,** 321-339.

Dinsmore, J.H. & Soloman, F. (1991) Inhibition of MAP2 expression affects both morphological and cell division phenotypes of neuronal differnentiation. *Cell* **64,** 817-826.

Ditella, M., Feiguin, F., Morfini, G. & Caceres, A. (1994) Microfilament-associated growth component depends upon tau for its intracellular localization. *Cell Motil. Cytoskel.* **29,** 117-130.

Dong, D.L., Xu, Z.S., Chevier, M.R., Cotter, R.J., Cleveland, D.W. & Hart, G.W. (1993) Glycosylation of mammalian neurofilaments. Localization of multiple O-linked N-acetylglucosamine moieties on neurofilament polypeptides L and M. *J. Biol. Chem.* **268,** 16679-16687.

Dosemeci, A. & Pant, H.C. (1992) Association of cAMP-dependent protein kinase with neurofilaments. *Biochem. J.* **282,** 477-481.

Dotti, C.G. & Banker, G.A. (1987) Experimentally induced alteration in the polarity of developing neurons. *Nature* **330,** 224-226.

Dotti, C.G., Sullivan, C.A. & Banker, G.A. (1988) The establishment of polarity by hippocampal neurons in culture. *J. Neurosci.* **8,** 1454-1468.

Dräger, U.C. & Hofbauer, A. (1984) Antibodies to heavy neurofilament subunit detect a subpopulation of damaged ganglion cells in retina. *Nature* **309**, 624-626.

Drewes, G., Trinczek, B., Illenberger, S., Biernat, J., Schmitt-Ulms, G., Meyer, H.E., Mandelkow, E.M. & Mandelkow, E. (1995) Microtubule-associated protein/microtubule affinity-regulating kinase (p110mark). A novel protein kinase that regulates tau-microtubule interactions and dynamic instability by phosphorylation at the Alzheimer-specific site serine 262. *J. Biol. Chem.* **270,** 7679-7688.

Duff, K., Eckman, C., Zehr, C., Yu, X., Prada, C.M., Perez-tur, J., Hutton, M., Buee, L., Harigaya, Y., Yager, D., Morgan, D., Gordon, M.N., Holcomb, L., Refolo, L., Zenk, B., Hardy, J. & Younkin, S. (1996) Increased amyloid-ß 1-42(43) in the brains of mice expressing mutant presenilin 1. *Nature* **383,** 710-713.

Duff, K. (1997) Alzheimer transgenics models come of age. *Trends. Neurosci.* **20,** 279-280.

Duong, T., Ponnier, E.C. & Scheibel, A.B. (1989) Immunodetection of the amyloid P component in Alzheimer's disease. *Acta Neuropathol.* **78,** 429-437.

Emery, D.G., Lucas, J.H. & Gross, G.W. (1987) The sequence of ultrastructural changes in cultured neurons after dendrite transection. *Exp. Brain Res.* **67,** 41-51.

Escurat, M., Djabali, K., Gumpel, M., Gros, F. & Portier, M.M. (1990) Differential expression of two neuronal intermediate-filament proteins, peripherin and the low-molecular mass neurofilament protein (NF-L), during the development of the rat. *J. Neurosci.* **10,** 769-784.

Evans, K.C., Berger, E.P., Cho, C.G., Weisgraber, K.H. & Lansbury, P.T. (1995) Apolipoprotein E is a kinetic but not a thermodynamic inhibitor or amyloid formation: implications for the pathogenesis and treatment of Alzheimer's disease. *Proc. Natl. Acad. Sci. U.S.A.* **92,** 763-767.

Fawcett, J.W. (1997) Astrocytic and neuronal factors affecting axon regeneration in the damaged central nervous system. *Cell Tissue Res.* **290,** 371-377.

Ferralli, J., Doll, T. & Matus, A. (1994) Sequence analysis of MAP2 function in living cells. *J. Cell Sci.* **107,** 3115-3125.

Ferrer, I., Soriano, E., Tunon, T., Fonseca, M. & Guionnet, N. (1991) Parvalbumin immunoreactive neurons in normal human temporal neocortex and in patients with Alzheimer's disease. *J. Neurol. Sci.* **106,** 135-141.

Fine, A., Amos, W.B., Durbin, R.M. & McNaughton, P.A. (1988) Confocal microscopy: applications in neurobiology. *Trends Neurosci.* **11,** 346-351.

Fitch, M.T. & Silver, J. (1997) Activated macrophages and the blood-brain barrier: Inflammation after CNS injury leads to increases in putative inhibitory molecules. *Exp. Neurol.* **148,** 587-603.

Fonseca, M. & Soriano, E. (1995) Calretinin-immunoreactive neurons in the normal human temporal cortex and in Alzheimer's disease. *Brain Res.* **691,** 83-91.

Forscher. P., Lin, C.H. & Thompson, C. (1992) Novel form of growth cone motility involving site-directed actin filament assembly. *Nature* **357,** 515-518.

Friedman, G., Froom, P., Sazbon, L., Grinblatt, I., Shochina, M., Tsenter, J., Babaey, S., Yehuda, B. & Groswasser, Z. (1999) Apolipoprotein E epsilon 4 genotype predicts a poor outcome in survivors of traumatic brain injury. *Neurology* **52,** 244-248.

Fuchs, E. & Cleveland, D.W. (1998) A structural scaffolding of intermediate filaments in health and disease *Science* **279,** 514-519.

Fukumoto, H., Asami-Okada, A., Suzuki, N., Shimada, H., Ihara, Y. & Iwatsubo T. (1996) Amyloid ß protein deposition in normal aging has the same characterisitics as that in Alzheimer's disease. Predominance of Aß42(43) and association of Aß40 with cored plaques. *Am. J. Pathol.* **148,** 259-265.

Fulton, A.B. (1984) *The cytoskeleton.* Chapman and Hall. New York.

Gallo, G., Wisniewski, T., Choi-Miura, N.H., Ghiso, J. & Frangione, B. (1994) Potential role of apolipoprotein E in fibrillogenesis. *Am. J. Pathol.* **145,** 526-530.

Games, D., Adams, D., Alessandrini, R., Barbour, R., Berthelette, P., Blackwell, C., Carr, T., Clemens, J., Donaldson, T., Gillespie, F., Guido, T., Hagopian, S., Johnsonwood, K., Khan, K., Lee, M., Leibowitz, P., Lieberburg, I., Little, S., Masliah, E., Mcconlogue, L., Montoyazavala, M., Mucke, L., Paganini, L., Penniman, E., Power, M., Schenk, D., Seubert, P., Snyder, B., Soriano, F., tan, H., Vitale, J., Wadsworth, S., Wolozin, B. & Zhao, J. (1995) Alzheimer-type neuropathology in transgenic mice overexpressing V717F ß-amyloid precursor protein. *Nature* **373,** 523-527.

Gearing, M., Schneider, J.A., Robbins, R.S., Hollister, R.D., Mori, H., Games, D., Hyman, B.T. & Mirra, S.S. (1995) Regional variation in the distribution of apolipoprotein E and Aß in Alzheimer's disease. *J. Neuropathol. Exp. Neurol.* **54,** 833-841.

Geddes, G.G., Anderson, K.J. & Cotman, C.W. (1986) Senile plaques as aberrant sprout stimulating structures. *Exp. Neurol.* **94,** 767-776.

Geddes, J.F., Vowles, G.H., Robinson, S.F.D. & Sutcliffes, J.C. (1996) Neurofibrillay tangles, but not Alzheimer-type pathology, in a young boxer. *Neuropathol. Appl. Neurobiol.* **22,** 12-16.

Geddes, J.F., Vowles, G.H., Nicoll, J.A.R. & Révész, T. (1999) Neuronal cytoskeletal changes are an early consequence of repetative head injury. *Acta Neuropathol.* **98,** 171-178.

Geisler, N. & Weber, K. (1981) Self-assembly in vitro of the 68,000 molecular weight component of the mammalian neurofilament triplet proteins into intermediate sized filaments. *J. Mol. Biol.* **152,** 565-571.

Gervais, F.G., Xu, D., Robertson, G.S., Vaillancourt, J.P., Zhu, Y., Huang, J., LeBlanc, A., Smith, D., Rigby, M., Shearman, M.S., Clarke, E.E., Zheng, H., Van Der Ploeg, L.H., Ruffolo, S.C., Thornberry, N.A., Xanthoudakis, S., Zamboni, R.J., Roy, S. & Nicholson, D.W. (1999) Involvement of caspases in proteolytic cleavage of Alzheimer's amyloid-beta precursor protein and amyloidogenic A beta peptide formation. *Cell* **97,** 395-406.

Geula, C., Chuang-Kuo, W., Saroff, D., Lorenzo, A., Yuan, M. & Yankner, B.A. (1998) Aging renders the brain vulnerable to amyloid ß-protein neurotoxicity. *Nat. Med.* **4,** 827-8331.

Ghiso, J., Tagliavini, F., Timmers, W.F. & Frangione, B. (1989) Alzheiemr's disease amyloid precursor protein is present in senile plaques and cerebrospinal fluid; Immunohistochemical and biochemical considerations. *Biochem. Biophys. Res. Commun.* **163,** 430-437.

Giannakopoulos, P., Silhol, S., Jallageas, V., Mallet, J., Bons, N., Bouras, C. & Delaere, P. (1997) Quantitative analysis of tau protein-immunoreactive accumulations and ß amyloid protein deposits in the cerebral cortex of the mouse lemur, *Microcebus murinus. Acta Neuropathol.* **94,** 131-139.

Glenner, G.G. & Wong, C.W. (1984) Alzheimer's disease: initial report of the purification and characterization of a novel cerebrovascular amyloid protein. *Biochem. Biophys. Res. Commun.* **120**, 885-890.

Goate A, Chartier-Harlin MC, Mullan M, Brown J, Crawford F, Fidani L, Giuffra L, Haynes A, Irving N, James L, Mant, R., Newton, P., Rooke, K., Roques, P., Talbot, C., Pericak-Vance, M., Roses, A., Williamson, R., Rossor, M., Owen, M. & Hardy, J. (1991) Segregation of a missense mutation in the amyloid precursor protein gene with familial Alzheimer's disease. *Nature* **349,** 704-706.

Goedert, M., Spillantini, M.G., Potier, M.C., Ulrich, J. & Crowther, R.A. (1989) Cloning and sequencing of the cDNA encoding an isoform of microtubule associated protein tau containing four tandem repeats; differential expression of tau protein mRNSs inhuman brain. *EMBO J.* **8,** 393-399.

Goedert, M., Jakes, R., Crowther, R.A., Six, J., Lubke, U., Vandermeeren, M., Cras, P., Trojanowski, J.Q. & Lee, V.M.-Y. (1993) The abnomal phosphorylation of Tau-protein at Ser-2020 in Alzheimer's disesae recapitulates phosphorylation during development. *Proc. Natl. Acad. Sci. U.S.A.* **90,** 5066-5070.

Goldstein, M.E., Sternberger, N.H. & Sternberger, L.A. (1987) Phosphorylation protects neurofilaments from proteolysis. *J. Neuroimmunol.* **14,** 149-160.

Gowing, E., Roher, A.E., Woods, A.S., Cotter, R.J., Chaney, M., Little, S.P. & Ball, M.J. (1994) Chemical characterization of the Aß17-42 peptide, a component of diffuse amyloid deposits of Alzheimer's disease. *J. Biol. Chem.* **269,** 10987-10990.

Graves, A., White, E., Koepsell, T.D., Reifler, B.V., van Belle, G., Larson, E.B. & Raskind, M. (1990) The association between head trauma and Alzheimer's Disease. *Am. J. Epidemiol.* **131,** 491-501.

Gray, E.G. & Hamlyn, L.H. (1962) Electron microscopy of experimental degeneration in the avian optic tectum. *J. Anat.* **96,** 309-316.

Gregori, L., Fuchs, C., Figueiredo-Pereira, M.E., Van Nostrand, W.E. & Goldgaber, D. (1995) Amyloid beta-protein inhibits ubiquitin-dependent protein degradation in vitro. *J. Biol. Chem.* **270,** 19702-19708.

Gross, G.W., Lucas, J.H. & Higgins, M.L. (1983) Laser microbeam surgery: ultrastructural changes associated with neurite transection in culture. *J. Neurosci.* **3,** 1979-1993.

Grundke-Iqbal, I., Iqbal, K., Quinlan, M., Tung, Y.C., Zaidi, M.S. & Wisniewski, H.M. (1986a) Microtubule-associated protein tau. A component of Alzheimer paired helical filaments. *J. Biol. Chem.* **261,** 6084-6089.

Grundke-Iqbal, I., Iqbal, K., Tung, Y.C., Quinlan, M., Wisniewski, H.M. & Binder, L.I. (1986b) Abnormal phosphorylation of the microtubule associated protein tau (τ) in Alzheimer cytoskeletal pathology. *Proc. Natl. Acad. Sci. U.S.A.* **83,** 4913-4917.

Guillery, R.W. (1965) Some electron microscopical observations of degenerative changes in central nervous synapses. In *Degeneration Patterns in the Nervous System, Progress in Brain Research*, Vol 14. (M. Singer and J.P. Shadé, Eds.), pp.57-73. Elsevier, Amsterdam.

Gunning, P., Hardeman, E., Jeffrey, P. & Weinberger, R. (1998) Creating intracellular structural domains: spatial segregation of actin and tropomyosin isoforms in neurons. *Bioessays* **20,** 892-900.

Haass, C., Schlossmacher, M.G., Hung, A.Y., Vigo-Pelfrey, C., Mellon, A., Ostaszewski, B.L., Lieberburg, I., Koo, E.H., Schenk, D., Teplow, D.B. & Selkoe, D.J. (1992) Amyloid beta-peptide is produced by cultured cells during normal metabolism. *Nature* **359,** 322-325.

Haass, C., Hung, A.Y., Schlossmacher, M.G., Teplow, D.B. & Selkoe, D.J. (1993a) Beta-amyloid peptide and a 3-kDa fragment are derived by distinct cellular mechanisms. *J. Biol. Chem.* **268,** 3021-3024.

Haass, C. & Selkoe, D.J. (1993b) Cellular processing of ß-amyloid precursor and the genesis of amyloid ß-peptide. *Cell* **75,** 1039-1042.

Haass, C., Hung, A.Y., Selkoe, D.J. & Teplow, D.B. (1994) Mutations associated with a locus for familial Alzheimer's disease result in alternative processing of amyloid beta-protein precursor. *J. Biol. Chem.* **269,** 17741-17747.

Hall, G.F., Poulos, A. & Cohen, M.J. (1989) Sprouts emerging from the dendrites of axotomized lamprey central neurons have axon-like ultrastructure. *J. Neurosci.* **9,** 588-599.

Han, S., Hulette, C., Saunders, A.M., Einstein, G., Pericak-Vance, M., Strittmatter, W.J., Roses, A.D. & Schmechel, D.E. (1994) Apolipoprotein E is present in hippocampal neurons without neurofibrillary tangles in Alzheimer's disease and in age-matched controls. *Exp. Neurol.* **128,** 13-26.

Harada, A., Oguchi, K., Okabe, S., Kuno, J., Terada, S., Ohshima, T., Sato-Yoshitake, R., Takei, Y., Noda, T. & Hirokawa, N. (1994) Altered microtubule organization in small calibre axons of mice lacking tau protein. *Nature* **369,** 488-491.

Hardy, J. (1997) Amyloid, the presenillins and Alzheimer's disease. *Trends Neurosci.* **20,**154-159.

Hardy, J. & Israël, A. (1999) In search of gamma-secretase. *Nature* **398,** 466-467.

Hartmann, T., Bieger, S.C., Brül, B., Tienari, P.J., Ida, N., Allsop, D., Roberts, G.W., Masters, C.L., Dotti, C.G., Unsicker, K. & Beyreuther, K. (1997) Distinct sites of intracellular production for Alzheimer's disease Aß40/42 amyloid peptides. *Nat. Med.* **3,** 1016-1020.

Haugh, M.C., Probst, A., Ulrich, J., Kahn, J. & Anderton, B.H. (1986) Alzheimer neurofibrillary tangles contain phosphorylated and hidden neurofilament epitopes. *J. Neurol. Neurosurg. Psychiatry* **49,** 1213-1220.

He, Q., Dent, E.W. & Merli, K.F. (1997) Modulation of actin filament behaviour by GAP-43 (Neuromodulin) is dependent on the phosphorylation status of serine 41, the protein kinase C site. *J. Neurosci.* **17,** 3515-3524.

Heilbroner, P.L. & Kemper, T.L. (1990) The cytoarchitectonic distribution of senile plaques in three aged monkeys. *Acta.Neuropathol.* **81,** 60-65.

Hendriks, L., van Duijn, C.M., Cras, P., Cruts, M., Van Hu,l W., van Harskamp, F., Warren, A., McInnis, M.G., Antonaraki,s S.E., Martin, J.J., Hofman, A. & Van Broeckhoven, C. (1992) Presenile dementia and cerebral haemorrhage linked to a mutation at codon 692 of the beta-amyloid precursor protein gene. *Nat. Genet.* **1,** 218-221.

Heyman, A., Wilkinson, W.E., Stafford, J.A., Helms, M.J., Sigmon, A.H. & Weinberg, T. (1984) Alzheimer's disease: a study of epidemiological aspects. *Ann. Neurol.***15,** 335-341.

Higgins, L.S., Holtzman, D.M., Rabin, J., Mobley, W.C. & Cordell, B. (1994) Transgenic mouse brain histopathology resembles early Alzheimer's disease. *Ann. Neurol.* **35,** 598-607.

Higgins, L.S., Rodems, J.M., Catalano, R., Quon, D. & Cordell, B. (1995) Early Alzheimer disease-like histopathology increases in frequency with age in mice transgenic for ß-APP751. *Proc. Natl. Acad. Sci. U.S.A.* **92,** 4402-4406.

Himmler, A. (1989) Structure of the bovine tau gene: Alternatively spliced transcripts generate a protein family. *Mol. Cell Biol.* **9,** 1389-1396.

Hirokawa, N. (1982) Cross linker system between neurofilaments, microtubules and membranous organelles in frog axons revealed by quick-freeze, deep etching method. *J. Cell Biol.* **94,** 129-142.

Hirokawa, N., Glicksman, M.A. & Willard, M.D. (1984) Organization of mammalian neurofilament polypeptides within the neuronal cytoskeleton. *J. Cell Biol.* **98,** 1523-1536.

Hirokawa, N., Hisanaga, S. & Shiomura, Y. (1988) MAP2 is a component of cross bridges between microtubules and neurofilaments in the neuronal cytoskeleton: quick-freeze, deep-etch immunoelectron and reconstitution studies. *J. Neurosci.* **8,** 2769-2779.

Hirokawa, N., Sobue, K., Kanda, K., Harada, A. & Yorifuji, H. (1989) The cytoskeletal architecture of the presynaptic terminal and molecular structre of synapsin I. *J. Cell Biol.* **108,** 121-126.

Hirokawa, N. (1991) Molecular architecture and dynamics of the neuronal cytoskeleton. In: *The Neuronal Cytoskeleton,* pp. 5-74. Ed. R.D. Burgoyne. Wiley-Liss & Sons, Inc.: New York.

Hirokawa, N. & Takeda, S. (1998) Gene targeting studies begin to reveal the function of neurofilament proteins. *J. Cell Biol.* **143** 1-4.

Hisanaga, S. & Hirokawa, N. (1988) Structure of the peripheral domains of neurofilaments revealed by low angle rotary shadowing. *J. Mol. Biol.* **202,** 297-305.

Hisanaga, S. & Hirokawa, N. (1989) The effects of dephosphorylation on the structure of the projections of neurofilament. *J. Neurosci.* **9,** 959-966.

Hisanaga, S. & Hirokawa, N. (1990a) Dephosphorylation-induced interactions of neurofilaments with microtubules. *J. Biol. Chem.* **265,** 1852-1858.

Hisanaga, S. & Hirokawa, N. (1990b) Molecular architecture of the neurofilament II. Reassembly process of neurofilament L protein *in vitro J. Mol. Biol.* **211,** 871-882.

Hisanaga, S., Kusubata, M., Okumura, E. & Kishimoto, T. (1991) Phosphorylation of neurofilament H subunit at the tail domain by CDC2 kinase dissociates the association to microtubules. *J. Biol. Chem.* **266,** 21798-21803.

Hisanaga, S., Matsuoka, Y., Nishizawa, K., Saito, T., Inagaki, M. & Hirokawa, N. (1994) Phosphorylation of native and reassembled neurofilaments composed of NF-L, NF-M, NF-H by the catalytic subunit of cAMP-dependent protein kinase. *Mol. Biol. Cell* **5,** 161-172.

Hiscock, J.J., Mackenzie, L. & Willoughby, J.O. (1998) Laminar distribution of Fos/calcium-binding protein and Fos/neurofilament protein-labeled neurons in rat motor and sensory cortex after picrotoxin-induced seizures. *Exp. Neurol.* **149,** 373-383.

Hof, P.R., Cox, C. & Morrison, J.H. (1990) Quantitative analysis of a vulnerable subset of pyramidal neurons in Alzheimer's disease: I Superior frontal and inferior temporal cortex. *J. Comp. Neurol.* **301,** 44-54.

Hof, P.R. & Morrison, J.H. (1990) Quantitative analysis of a vulnerable subset of pyramidal neurons in Alzheimer's disease: II. Primary and secondary visual cortex. *J. Comp. Neurol.* **301,** 55-64.

Hof, P.R., Cox, K., Young, W.G., Celio, M.R., Rogers, J. & Morrison, J.H. (1991a) Parvalbumin-immunoreactive neurons in the neocortex are resistant to degeneration in Alzheimer's disease. *J. Neuropathol. Exp. Neurol.* **50,** 451-462.

Hof, P.R., Knabe, R., Bovier, P. & Bouras, C. (1991b) Neuropathological observations in a case of autism presenting with self-injury behaviour. *Acta Neuropathol.* **82,** 321-326.

Hof, P.R. & Morrison, J.H. (1991) Neocortical neuronal subpopulations labeled by a monoclonal antibody to calbindin exhibit differential vulnerability in Alzheimer's disease. *Exp. Neurol.* **111,** 293-301.

Hof, P.R., Nimchinsky, E.T., Celio, M.R., Bouras, C. & Morrison, J.H. (1993) Calretinin-immunoreactive neocortical interneurons are unaffected in Alzheimer's disease. *Neurosci. Lett.* **152,** 145-149.

Hof, P.R. & Morrison, J.H. (1994) The cellular basis of cortical disconnection in Alzheimer disease and related dementing conditions. In: *Alzheimer Disease*, pp. 197-229. Eds. R.D. Terry, R. Katzman, K.L. Bick: Raven.

Hof, P.R., Nimchinsky, E.A. & Morrison, J.H. (1995) Neurochemical phenotype of corticocortical connections in the macaque monkey: quantitative analysis of a subset of neurofilament protein-immunoreactive projection neurons in frontal, parietal, temporal, and cingulate cortices. *J. Comp. Neurol.* **362**, 109-133.

Hoffman, P.N. & Lasek, R.J. (1975) The slow component of axonal transport. Identification of major structural polypeptides of the axon and their generality maong mammalian neurons. *J. Cell Biol.* **66,** 351-366.

Hoffman, P.N., Lasek, R.J., Griffin, J.W. & Price, D.L. (1983) Slowing of the axonal transport of neurofilament proteins during development. *J. Neurosci.* **3,** 1694-1700.

Hoffman, P.N., Cleveland, D.W., Griffin, J.W., Landes, P.W., Cowan, N.J. & Price, D.L. (1987) Neurofilament gene expression: A major determinant of axonal calibre. *Proc. Natl. Acad. Sci. U.S.A.* **84,** 3472-3476.

Hogan, M.V., Pawlowska, Z., Yang, H.A., Kornecki, E. & Ehrlich, Y.H. (1995) Surface phosphorylation by ecto-protein kinase C in brain neurons: a target for Alzheimer's beta-amyloid peptides. *J. Neurochem.* **65,** 2022-2030.

Holcomb, L., Gordon, M.N., McGowan, E., Yu, X., Benkovic, S., Jantzen, P., Wright, K., Saad, I., Mueller, R., Morgan, D., Sanders, S., Zehr, C., O'Campo, K., Hardy, J., Prada, C.-M., Eckman, C., Younkin, S., Hsiao, K. & Duff, K. (1998) Accelerated Alzheimer-type phenotype in transgenic mice carrying both mutant amyloid precursor protein and presenilin 1 transgenes. *Nat. Med.* **4,** 97-100.

Holtzman, D.M., Bales, K.R., Tenkova, T., Fagan, A.M., Parsdanian, M., Sartorius, L.J., Mackey, B., Olney, J., McKeel, D., Wozniak, D. & Paul, S.M. (2000) Apolipoprotein E isoform – dependent amyloid deposition and neuritic degeneration in a mouse model of Alzheimer's disease. *Proc. Natl. Acad. Sci. U.S.A.* **97,** 2892-2897.

Hopkins, J.M. & Bunge, R.P. (1991) Regeneration of axons from adult human retina *in vitro*. *Exp. Neurol.* **112,** 243-251.

Horsburgh, K., Kelly, S., McCulloch, J., Higgins, G.A., Roses, A.D. & Nicoll, J.A. (1999) Increased neuronal damage in apolipoprotein E – deficient mice following global ischaemia. *Neuroreport* **10,** 837-841.

Hsiao, K., Chapman, P., Nilsen, S., Eckman, C., Harigaya, Y., Younkin, S., Yang, F. & Cole, G. (1996) Correlative memory deficits, Aß elevation and amyloid plaques in transgenic mice. *Science* **274,** 99-102.

Ikeda, S.I., Allsop, D. & Glenner, G.G. (1989) Morphology and distribution of plaque and related deposits in the brains of Alzheimer's disease and control cases. An immunohistochemical study using amyloid ß-protein antibody. *Lab. Invest.* **60,** 113-122.

Ikeda, S.I., Yanagisawa, M.B., Allsop, D. & Glenner, G.G. (1990) Early senile plaques in Alzheimer's disease demonstrated by histochemistry, immunocytochemistry and electron microscopy. *Hum. Pathol.* **21,** 1221-1226.

Ishii, T., Kametani, F., Haga, S. & Sato, M. (1989) The immunohistochemical demonstration of subsequences of the precursor of the amyloid A4 protein in senile plaques in Alzheimer's Disease. *Neuropathol. Appl. Neurobiol.* **15,** 135-147.

Iwatsubo, T., Okada, A., Suzuki, N., Mizusawa, H., Nukina, N. & Ihara, Y. (1994) Visualization of Aß42(43) and Aß40 in senile plaques with end-specific Aß monoclonals; Evidence that an initially deposited species is Aß42(43). *Neuron* **13,** 45-53.

Iwatsubo, T., Mann, D.M.A., Okada, A., Suzuki, N. & Ihara, Y. (1995) Amyloid ß protein (Aß) deposition: Aß42(43) precedes Aß40 in Down syndrome. *Ann. Neurol.* **37,** 294-299.

Jacobs, D., Sano, M., Karder, K., Bell, K., Bylsma, F., Lefleche, G., Albert, M., Brandt, J. & Stern, Y. (1994) Age at onset of Alzheimer's disease: Relation to pattern of cognitive dysfunction and rate of decline. *Neurology* **44,** 1215-1220.

Jakes, R., Novak, M., Davison, M. & Wischik, C.M. (1991) Identification of 3- and 4-repeat tau isoforms within the PHF in Alzheimer's disease. *EMBO J.* **10,** 2725-2729.

Jarret, J.T., Berger, E.P. & Lansbury, P.T. Jr. (1993) The carboxy terminus of the ß-amyloid protein is critical for the seeding of amyloid formation: implications for the pathogeneis of Alzheiemr's disease. *Biochemistry* **32,** 4693-4697.

Jiang. X.M., Zhao, J.X., Ohnishi, A., Itakura, C., Mitutani, M., Yamamoto, T., Murai, Y. & Ikeda, M. (1996) Regeneration of myelinated fiber after crush injury is retarded in sciatic nerves of mutant Japanese quails deficient in neurofilaments. *Acta Neuropathol.* **92,** 467-472.

Joachim, C., Games, D., Morris, J., Ward, P., Frenkel, D. & Selkoe, D. (1991) Antibodies to non-beta regions of the beta-amyloid precursor protein detect a subset of senile plaques. *Am. J. Pathol.* **138,** 373-384.

Johnson, G.V. (1992) Differential phosphorylation of tau by cyclic AMP dependent protein kinase and CA2+/calmodulin-dependent protein kinase II: metabolic and functional consequences. *J. Neurochem.* **59,** 2056-2062.

Jordan, B.D., Relkin, N.R., Ravdin, L.D., Jacobs, A.R., Bennett, A. & Gandy, S. (1997) Apolipoprotein E epsilon4 associated with chronic traumatic brain injury in boxing. *J. Am. Med. Assoc.* **278,** 136-140.

Julian, J.-P. (1999) Neurofilament functions in health and disease. *Curr. Opin. Neurobiol.* **9,** 554-560.

Kamboh, M.I., Sanghera, D.K., Ferrell, R.E. & DeKosky, S.T. (1995) APOE*4-associated Alzheimer's disease risk is modified by alpha 1-antichymotrypsin polymorphism. *Nat. Genet.* **10,** 486-488.

Kammesheidt, A., Boyce, F.M., Spanoyannis, A.F., Cummings, B.J., Ortegon, M., Cotman, C., Vaught, J.L. & Neve, R.L. (1992) Deposition of ß/A4 immunoreactivity and neuronal pathology in transgenic mice expressing the carboxy-terminal fragment of the Alzheimer amyloid precursor protein. *Proc. Natl. Acad. Sci. U.S.A.* **89,** 10857-10861.

Kanayama, G., Takeda, M., Morihara, T., Miyamae, Y., Shinozaki, K., Nishikawa, T., Niigawa, H. & Nishimura, T. (1997) Temporal and regional profiles of cytoskeletal protein accumulation in the rat brain following traumatic brain injury. *Psychiatry Clin. Neurosci.* **51,** 157-165.

Kang, J., Lemaire, H.G., Unterbeck, A., Salbaum, J.M., Masters, C.L., Grzeschik, K.H., Multhaup, G., Beyreuther, K. & Muller-Hill, B. (1987) The precursor of Alzheimer's disease amyloid A4 protein resembles a cell surface receptor. *Nature* **325,** 733-736.

Kar, S., Seto, D., Gaundreau, P. & Quirion, R. (1996) Beta-amyloid-related peptides inhibit potassium-evoked acetylcholine release from rat hippocampal slices. *J. Neurosci.* **16,** 1034-1040.

Kato, S., Gondo, T., Hoshii, Y., Takahashi, M., Yamada, M. & Ishihara, T. (1998) Confocal observation of senile plaques in Alzheimer's disease: Senile plaque morphology and relationship between senile plaques and astrocytes. *Pathol. Int.* **48,** 332-340.

Katzman, R. & Kawas, C.H. (1994) The epidemiology of dementia and Alzheimer's disease. In: *Alzheimer disease*, pp. 105-122. Eds. R.D. Terry, R. Katzman and K.L. Bick. Raven Press: New York.

Kawamata, T., Tooyama, I., Yamda, T., Walker, D.G. & McGeer, P.L. (1993) Lactotransferrin immunocytochemistry in Alzheimer and normal human brain. *Am. J. Pathol.* **142,** 1574-1585.

Kida, E., Golabek, A.A., Wisniewski, T. & Wisniewski, K.E. (1994) Regional differences in apolipoprotein E immunoreactivity in diffuse plaques in Alzheimer's disease brain. *Neurosci. Lett.* **167,** 73-76.

Kidd, M. (1964) Alzheimer's disease – an electron microscopical study. *Brain* **87,** 307-320.

Kindy, M.S., King, A.R., Perry, G., Debeer, M.C. & Debeer, F.C. (1995) Association of apolipoprotein E with murine amyloid A protein amyloid. *Lab. Invest.* **73,** 469-475.

King, C.E., Jacobs, I., Dickson, T.C. & Vickers, J.C. (1997) Physical damage to rat cortical axons mimics early Alzheimer's neuronal pathology. *Neuroreport* **8,**1663-1665.

King, C.E., Dickson, T.C., Jacobs, I., McCormack, G.H., Riederer, B.M. and Vickers, J.C. (2000) Acute CNS axonal injury models a subtype of dystrophic neurite in Alzheimer's disease. *Alz. Reports* **3,** 31-40.

Klosen, P., Anderton, B.H., Brion, J.P. & van den Bosch de Aguilar, P. (1990) Perikaryal neurofilament phosphorylation in axotomized and 6-OH-dopamine-lesioned CNS neurons. *Brain Res.* **526,** 259-269.

Knowles, R.B., Wyart, C., Buldyrev, S.V., Cruz, L., Urbanc, B., Hasselmo, M.E., Stanley, H.E. & Hyman, B.T. (1999) Plaque-induced neurite abnormalities: Implications for disruption of neural networks in Alzheimer's disease. *Proc. Natl. Acad. Sci. U.S.A.* **96,** 5274-5279.

Kobayashi, N. & Mundel, P. (1998) A role of microtubules during the formation of cell processes in neuronal and non-neuronal cells. *Cell Tissue Res.* **291,** 163-174.

Koliastos, V.E., Applegate, M.D., Kitt, C.A., Walker, L.C., Delong, M.R. & Price, D.L. (1989) Aberrant phosphorylation of neurofilaments accompanies transmitter-related changes in rat septal neurons following transection of the fimbria-fornix. *Brain Res.* **482,** 205-218.

Koo, E.H., Squazzo, S.L., Selkoe, D.J. & Koo, C.H. (1996) Trafficking of cell surface amyloid ß-protein precursor. 1. Secretion, endocytosis and recycling as detected by labelled monoclonal antibody. *J. Cell Sci.* **109,** 991-998.

Kosik, K.S., Duffy, L.K., Dowling, M.M., Abraham, C., McCluskey, A. & Selkoe, D.J. (1984) Microtubule associated protein 2: Monoclonal antibodies demonstrate the selective incorporation of certain epitopes into Alzheimer neurofibrillary tangles. *Proc. Natl. Acad. Sci. U.S.A.* **81,** 7941-7945.

Kovacs, D.M., Fausett, H.J., Page, K.J., Kim, T.W., Moir, R.D., Merriam, D.E., Hollister, R.D., Hallmark, O.G., Mancini, R., Felsenstein, K.M., Hyman, B.T., Tanzi, R.E. & Wasco, W. (1996) Alzheimer-associated presenilins 1 and 2: neuronal expression in brain and localization to intracellular membranes in mammalian cells. *Nat. Med.* **2,** 224-229.

Kowall, N.W., McKee, A.C., Yankner, B.A. & Beal, M.F. (1992) *In vivo* neurotoxicity of beta-amyloid [ß(1-40)] and the ß(25-35) fragment. *Neurobiol. Aging* **13,** 537-542.

Ksiezak-Reding, H., Dickson, D.W., Davies, P. & Yen, S.H. (1987) Recognition of tau epitopes by anti-neuroflament antibodies that bind to Alzheimer neurofibrillary tangles. *Proc. Natl. Acad. Sci. U.S.A.* **84,** 3410-3414.

Ksiezak-Reding, H., Binder, L.I. & Yen, S.H. (1990) Alzheimer disease proteins (A68) share epitopes with tau but show distinct biochemical properties. *J. Neurosci. Res.* **25,** 420-430.

Kwok, J. (1998) Molecular insights into Alzheimer's. *Today's Life Science* **10,** 24-28.

LaDu, M.J., Falduto, M.T., Manelli, A.M., Reardon, C.A., Getz, G.S. & Frail, D.E. (1994) Isoform-specific binding of apolipoprotein E to beta-amyloid. *J. Biol. Chem.* **269,** 23404-23406.

Lampert, P.W. & Hardman, J.M. (1984) Morphological changes in brains of boxers. *J.A.M.A.* **251,** 2676-2679.

Lanners, H.N. & Grafstein, B. (1980) Effect of a conditioning lesion on regeneration of goldfish optic axons; ultrastructural evidence of enhanced outgrowth and pinocytosis. *Brain Res.* **196,** 547-553.

Lasek, R.J., Phillips, L., Katz, M.J. & Autilio-Gambetti, L. (1985) Function and evolution of neurofilament proteins. *Ann. N.Y. Acad. Sci.* **455,** 462-478.

Laskek, R.J., Paggi, P. & Katz, M.J. (1992) Slow axonal transport mechanisms move neurofilaments relentlessly in mouse optic axons. *J. Cell Biol.* **117,** 607-616.

Lee, G., Cowan, N. & Kirschner, M. (1988) The primary structure and heterogeneity of tau protein from mouse brain. *Science* **239,** 285-288.

Lee, G. & Rook, S.L. (1992) Expression of tau protein in non-neuronal cells: microtubule binding and stabilization. *J. Cell Sci.* **102,** 227-237.

Lee, M.K., Xu, Z., Wong, P.C. & Cleveland, D.W. (1993) Neurofilaments are obligate heteropolymers in vivo. *J. Cell Biol.* **122,** 1337-1350.

Lee, V.M.-Y., Carden, M.J., Schlaepfer, W.W. & Trojanowski, J.Q. (1987) Monoclonal antibodies distinguish several differentially phosphorylated states of the two largest rat neurofilament subunits (NF-H and NF-M) and demonstrate their existence in the normal nervous system of adult rats. *J. Neurosci.* **7,** 3474-3488.

Lee, V.M.-Y., Otvos, L., Carden, M.J., Hollosi, M., Dietzschold, B. & Lazzarini, R. (1988a) Identification of the major multiphosphorylation site in mammalian neurofilaments. *Proc. Natl. Acad. Sci. U.S.A.* **85,** 1998-2002.

Lee, V.M.-Y., Otvos, L.,Jr., Schmidt, M.L. & Trojanowski, J.Q. (1988b) Alzheimer disease tangles share immunological similarities with multiphosphorylation repeats in the two large neurofilament proteins. *Proc. Natl. Acad. Sci. U.S.A.* **85,** 7384-7388.

Lee, V.M.-Y., Balin, B.J., Otvos, L.,Jr., & Trojanowski, J.Q. (1991) A68: A major subunit of paired helical filaments and derivatized forms of normal tau. *Science* **251,** 675-678.

Lendahl, U., Zimmerman, L.B. & McKay, R.D. (1990) CNS stem cells express a new class of intermediate filament protein. *Cell* **60,** 585-595.

Letterier, J.F., Liem, R.K.H. & Mushynski, M.L. (1982) Interactions between neurofilaments and microtubule-associated proteins: A possible mechanism for intraorganellar bridging. *J. Cell Biol.* **95,** 982-986.

Levy-Lahad, E., Wasco, W., Poorkaj, P., Romano, D.M., Oshima, J., Pettingell, W.H., Yu, C., Jondro, P.D., Schmidt, S.D., Wang, K., Crowley, A.C., Fu, Y-H., Guenette, S.Y., Galas, D., Nemens, E., Wijsman, E.M., Bird, T.D., Schellenberg, G.D. & Tanzi, R.E. (1995) Candidate gene for the chromosome 1 familial Alzheimer's disease locus. *Science* **269,** 973-977.

Levi, G. & Meyer, H. (1945) Reactive, regressive and regenerative processes of neurons, cultivated *in vitro* and injured with a micromanipulator. *J. Exp. Zool.* **99,** 141-181.

Levy, E., Carman, M.D., Fernandez-Madrid, I.J., Power, M.D., Lieberburg, I., van Duinen, S.G., Bots, G.T., Luyendijk, W. & Frangione, B. (1990) Mutation of the Alzheimer's disease amyloid gene in hereditary cerebral hemorrhage, Dutch type. *Science* **248,** 1124-1126.

Levy-Lahad, E., Wijsman, E.M., Nemens, E., Anderson, L., Goddard, K.A., Weber, J.L., Bird, T.D. & Schellenberg, G.D. (1995) A familial Alzheimer's disease locus on chromosome 1. *Science* **269,** 970-973.

Lewis, S.A., Wang, D. & Cowan, N.J. (1988) Microtubule – associated protein MAP2 shares a microtubule binding motif with tau protein. *Science* **242,** 936-939.

Lichtenberg-Kraag, B., Mandelkow, E.M., Biernat, J., Steiner, B., Schroter, C., Gustke, N., Meyer, H.E. & Mandelkow, E. (1992) Phosphorylation-dependent epitopes of neurofilament epitopes of neurofilament antibodies on tau protein and relationship with Alzheimer tau. *Proc. Natl. Acad. Sci. U.S.A.* **89,** 5384-5388.

Liem, R.K.H. & Hutchinson, S.B. (1982) Purification of the individual componenets of the neurofilament triplet: filament assembly from the 70,000 Dalton subunit. *Biochem.* **21,** 3221-3226.

London, J.A., Biegel, D. & Patcher, J.S. (1996) Neurocytopathic effects of beta-amyloid-stimulated monocytes: a potential mechanism for central nervous system damage in Alzheimer disease. *Proc. Natl. Acad. Sci. U.S.A.* **93,** 4117-4152.

Lucas, J.H., Gross, G.H., Emery, D.G. & Gardner, C.R. (1985) Neuronal survival or death after dendrite transection close to the perikaryon: Correlation with electrophysioogic, morphologic, and ultrastructural changes. *Cent. Nerv. Syst. Trauma* **2,** 231-255.

Ma, J., Yee, A., Brewer, H.B., Das, S. & Potter, H. (1994) Amyloid-associated proteins alpha 1-antichymotrypsin and apolipoprotein E promote assembly of Alzheimer beta-protein into filaments. *Nature* **372,** 92-94.

Mahley, R. (1988) Apolipoprotein E: Cholesterol transport with expanding role in cell biology. *Science* 1988; **240,** 622-630.

Mandelkow, E. & Mandelkow, E.M. (1995) Microtubules and microtubule–associated proteins. *Curr. Opin. Cell Biol.* **7,** 72-81.

Mann, D.M. (1989) Cerebral amyloidosis, ageing and Alzheimer's disease; a contribution from studies on Down's syndrome. *Neurobiol. Aging* **10,** 397-399.

Mann, D.M, Iwatsubo, T., Fukumoto, H., Ihara, Y., Odaka, A. & Suzuki, N. (1995) Microglial cells and amyloid beta protein (A beta) deposition; association with A beta 40-containing plaques. *Acta Neuropathol.* **90,** 472-477.

Mann, D.M., Iwatsubo, T., Pickering-Brown, S.M., Owen, F., Saido, T.C. & Perry, R.H. (1997) Preferential deposition of amyloid beta protein (Abeta) in the form Abeta40 in Alzheimer's disease is associated with a gene dosage effect of the apolipoprotein E E4 allele. *Neurosci. Lett.* **17,** 81-84.

Mansour, H., Bignami, A. & Dahl, D. (1989) Neurofilament phosphorylation in neuronal perikarya following axotomy: A study of rat spinal cord with ventral and dorsal root transection. *J. Comp. Neurol.* **238,** 481-485.

Martin, J.E., Mather, K.S., Swash, M., Garofalo, O., Dale, G.E., Leigh, P.N. & Anderton, B.H. (1990) Spinal cord trauma in man: studies of phosphorylated neurofilament and ubiquitin expression. *Brain* **113,** 1553-1562.

Martin, L.J., Pardo, C.A, Cork, L.C. & Price, D.L (1994) Synaptic pathology and glial responses to neuronal injury precede the formation of senile plaques and amyloid deposits in the aging cerebral cortex. *Am. J. Pathol.* **145,** 1358-1381.

Masliah, E., Terry, R.D., DeTeresa, R.M. & Hansen, L.A. (1989) Immunohistochemical quantification of the synapse-related protein synaptophysin in Alzheimer disease. *Neurosci. Lett.* **103,** 234-239.

Masliah, E., Terry, R.D., Mallory, M., Alford, M. & Hansen, L.A. (1990) Diffuse plaques do not accumulate synapse loss in Alzheimer's disease. *Am. J. Pathol.* **137,** 1293-1297.

Masliah, E., Hansen, L., Albright, T., Mallory. M. & Terry, R.D. (1991a) Immunoelectron microscopic study of synaptic pathology on Alzheimer disease. *Acta Neuropathol.* **81,** 428-433.

Masliah, E., Mallory, M., Hansen, L., Alford, M., Albright, T., Deteresa, R., Terry, R., Baudier, J. & Saitoh, T. (1991b) Patterns of aberrant sprouting in Alzheimer's disease. *Neuron* **6,** 729-739.

Masliah, E., Mallory, M., Ge, N. & Saitoh, T. (1992) Amyloid precursor is localised in growing neurites of neonatal rat brain. *Brain Res.* **593,** 323-328.

Masliah, E., Mallory, M., Deernink, T., DeTeresa, R., Lamont, S., Miller, A., Terry, R.D., Carragher, R. & Elisman, M. (1993a) Re-evaluation of the structural organization of neuritic plaques in Alzheimer's disease. *J. Neuropathol. Exp. Neurol.* **52,** 619-632.

Masliah, E., Mallory, M., Hansen, L., Alford, M., DeTeresa, R. & Terry, R.D. (1993b) An antibody against phosphorylated neurofilaments identifies a subset of damaged association axons in Alzheimer's disease. *Am. J. Pathol.* **142,** 871-882.

Masliah, E., Sisk, A., Mallory, M., Mucke, L., Schenk, D. & Games, D. (1996a) Comparison of neurodegenerative pathology in transgenic mice overexpressing V717F beta-amyloid precursor protein and Alzheimer's disease. *J. Neurosci.* **16,** 5795-5811.

Masliah, E., Mallory, M., Veinberg, I., Miller, A. & Samuel, W. (1996b) Alterations in apolipoprotein E expression during aging and neurodegeneration. *Prog. Neurobiol.* **50,** 493-503.

Masters, C.L., Multhaup, G., Simms, G., Pottgiesser, J., Martins, R.N. & Beyreuther, K. (1985) Neuronal origin of a cerebral amyloid: neurofibrillary tangles ofAlzheimer's disease contain the same protein as the amyloid of plaque cores and blood vessels. *EMBO J.* **4,** 2757-2763.

Mattiace, L.A., Kress, Y., Davies, P., Ksiezak-Reding, H., Yen, S-H. & Dickson, D.W. (1991) Ubiquitin-immunoreactive dystrophic neurites in Down's Syndrome brains. *J. Neuropathol. Exp. Neurol.* **50,** 547-559.

Matus, A., Ackermann, M., Pehling, G., Byers, H.R. & Fujiwara, K. (1982) High actin concentrations in brain dendritic spines and postsynaptic densities. *Proc. Natl. Acad. Sci. U.S.A.* **79,** 7590-7594.

Matus, A. (1988) Microtubule-associated proteins: Their potential role in determining neuronal morphology. *Ann. Rev. Neurosci.* **11,** 29-44.

Maxwell, W.L., Povlishock, J.T. & Graham, D.L. (1997) A mechanistic analysis of nondisruptive axonal injury: a review. *J. Neurotrauma* **14,** 419-440.

Mayeux, R., Ottman, R., Maestre, G., Ngai, C., Tang, M.X., Ginsberg, H., Chun, M., Tycko, B. & Shelanski, M. (1995) Synergistic effects of traumatic head injury and apolipoprotein-ε4 in patients with Alzheimer's disease. *Neurology* **45,** 555-557.

McGeer, P.L., Akiyama, H., Kawamata, T., Yamada, T., Walker, D.G. & Ishii, T. (1992) Immunohistochemical localization of beta-amyloid precursor protein sequences in Alzheimer and normal brain tissue by light and electron microscopy. *J. Neurosci. Res.* **31,** 428-442.

McHale, M.K., Hall, G.F. & Cohen, M.J. (1995) Early cytoskeletal changes following injury of giant spinal axons in the lamprey. *J. Comp. Neurol.* **353,** 25-37.

McKinney, R.A., Debanne, D., Gahwiler, B.H. & Thompson, S.M. (1997) Lesion-induced axonal sprouting and hyperexcitability in the hippocampus *in vitro*. *Nat. Med.* **3,** 990-996.

Meda, L., Cassatella, M.A., Szendrei, G.I., Otvos, L., Baron, P., Villalba, M., Ferrari, D. & Rossi, F. (1995) Activation of microglial cells by beta-amyloid protein and interferon-gamma. *Nature* **374,** 647-650.

Mehta, N.D., Refolo, L.M., Eckman, C., Saunders, S., Yager, D., Perez-Tur, J., Younkin, S., Duff, K., Hardy, J. & Hutton, M. (1998) Increased Abeta42(43) from cell lines expressing presenilin 1 mutations. *Ann. Neurol.* **43,** 256-258.

Meller, D., Bellander, B.M., Schmidt-Kastner, R. & Ingvar, M. (1993a) Immunohistochemical studies with antibodies to neurofilament proteins on axonal damage in experimental focal lesions in rat. *J. Neurol. Sci.* **117**,164-74.

Meller, D., Schmidt-Kastner, R. &, Eysel, U.T. (1993b) Immunohistochemical studies on neurofilamentous hypertrophy in degenerating retinal terminals of the olivary pretectal nucleus in the rat. *J. Comp. Neurol.* **331,** 531-539.

Meller, D., Eysel, U.T. & Schmidt-Kastner, R. (1994) Transient immunohistochemical labelling of rat retinal axons during Wallerian degeneration by a monoclonal antibody to neurofilaments. *Brain Res.* **648,** 162-166.

Meller, K. (1987) Early structural changes in the axoplasmic cytoskeleton after axotomy studied by cryofixation. *Cell Tissue Res.* **250,** 663-672.

Mendez, J.S. & Finn, B.W. (1975) Use of 6-hydroxydopamine to create lesions in catecholamine neurons in rats. *J. Neurosurg.* **42,** 166-173.

Miller, C.C.J., Brion, J.P., Calvert, R., Chin, T.K., Eagles, P.A.M., Downes, M.J., Flament-Durant, J., Haugh, M., Kahn, J., Probst, A., Urlich, J. & Anderton, B.H. (1986) Alzheimer's paired helical filaments share epitopes with neurofilament side arms. *EMBO J.* **5,** 269-276.

Mire, J.J., Hendelman, W.J. & Bunge, R.P. (1970) Observations on a transient phase of focal swelling in degenerating unmyelinated nerve fibers. *J. Cell Biol.* **45,** 9-22.

Mirra, S.S., Heyman, A., Mckeel, D., Sumi, S.M., Crain, B.J., Brownlee, L.M., Vogel, F.S., Hughes, J.P., Van Belle, B. & Berg, L. (1991) The consortium to establish a registry for Alzheimer's disease (CERAD). Part II. Standardization of the neuropathological assessment of Alzheimer's disease. *Neurology* **41,** 479-486.

Moechars, D., Dewachter, I., Lorent, K., Reverse, D., Baekelandt, V., Naidu, A., Tesseur, I., Spittaels, K., Haute, C.V., Checler, F., Godaux, E., Cordell, B., &Van Leuven, F. (1999). Early phenotypic changes in transgenic mice that overexpress different mutants of amyloid precursor protein in brain. *J. Biol. Chem.* **274**, 6483-6492.

Montoya, S.E., Aston, C.E., DeKosky, S.T., Kamboh, M.I., Lazo, J.S. & Ferrell, R.E. (1998) Bleomycin hydrolase is associated with risk of sporadic Alzheimer's Disease. *Nat. Genet.* **18,** 211-212.

Morishima-Kawashima, M., Hasegawa, M., Takio, K., Suzuki, M., Yoshida, H., Titani, K. & Ihara, Y. (1995) Proline-directed and non-proline directed phosphorylation of PHF tau. *J. Biol. Chem.* **270,** 823-829.

Morris, J.C., McKeel, D.W.,Jr., Storandt, M., Rubin, E.H., Price, J.L., Grant, E.A., Ball, M.J. & Berg, L. (1991) Very mild Alzheimer's disease: informant-based clinical, psychometric, and pathologic distinction from normal aging. *Neurology* **41,** 469-478.

Morris, J.C., Storandt, M., McKeel, D.W., Rubin, E.H., Price, J.L., Grant, E.A. & Berg, L. (1996) Cerebral amyloid deposition and diffuse plaques in "normal" aging: Evidence from presymptomatic and very mild Alzheimer's disease. *Neurology* **46,** 707-719.

Morrison, J.H., Lewis, D.A., Campbell, M.J., Huntley, G.W., Benson, D.L. & Bouras, C. (1987) A monoclonal antibody to non-phosphorylated neurofilament protein marks the vulnerable cortical neurons in Alzheimer's disease. *Brain Res.* **416,** 331-336.

Mortimer, J.A., French, L.R., Hutton, J.T. & Schuman, L.M. (1985) Head injury as a risk factor for Alzheimer's disease. *Neurology* **35,** 264-267.

Mortimer, J.A., van Duijn, C.M., Chandra, V., Fratiglioni, L., Graves, A.B., Heyman, A., Jorm, A.F., Kokmen, E., Kondo, K., Rocca, W.A., Shalat, S., Soininen, H. & Hofman, A. (1991) Head trauma as a risk factor for Alzheimer's disease: a collaborative re-analysis of case-control studies. EURODEM Risk Factors Research Group. *Int. J. Epidemiol.* **20,** Suppl 2:S28-35.

Moss, T.H. & Lewkowicz, S.J. (1983) The axon reaction in motor and sensory neurones of mice studied by a monoclonal antibody marker of neurofilament protein. *J. Neurol. Sci.* **60,** 267-280.

Mukhin, A.G., Ivanova, S.A., Knoblach, S.M. & Faden, A.I. (1997) New *in vitro* model of traumatic neuronal injury: Evaluaton of secondary injury and glutamate receptor-mediated neurotoxicity. *J. Neurotrauma* **14,** 651-663.

Mullan, M., Crawford, F., Axelman, K., Houlden, H., Lilius, L., Winblad, B. & Lannfelt, L. (1992) A pathogenic mutation for probable Alzheimer's disease in the APP gene at the N-terminus of beta-amyloid. *Nat. Genet.* **1,** 345-347.

Murphy, E.J. & Horrocks, L.A. (1993a) A model for compression trauma: pressure-induced injury in cell cultures. *J. Neurotrauma* **10,** 431-444.

Murphy, E.J. & Horrocks, L.A. (1993b) Mechanisms of hypoxic and ischemic injury – Use of cell culture models. *Mol. Chem. Neuropathol.* **19,** 95-106.

Murrell, J., Farlow, M., Ghetti, B. & Benson, M.D. (1991) A mutation in the amyloid precursor protein associated with hereditary Alzheimer's disease. *Science* **254,** 97-99.

Nakamura, S., Tamaoka, A., Sawamura, N., Shoji, S., Nakayama, H., Ono, F., Sakakibara, I., Yoshikawa, Y., Mori, H., Goto, N., & Doi, K. (1995) Carboxyl end-specific monoclonal antibodeis to amyloid ß protein (Aß) subtypes 9Aß40 and Aß42(43) differentiate Aß in senile and amyloid angiopathy in brains of aged cynomolgus monkeys. *Neurosci. Lett.* **201,** 151-154.

Nakamura, M., Araki, M., Oguro, K. & Masuzawa, T. (1997) Differential distribution of 68 Kd and 200 Kd neurofilament proteins in the gerbil hippocampus and their early distributional changes following transient forebrain ischemia. *Exp. Brain Res.* **89,** 31-39.

Nalbantoglu, J., Tirado-Santiago, G., Lahsaini, A., Poirier, J., Goncalves, O., Verge, G., Momoli, F., Welner, S.A., Massicotte, G., Julien, J.P. & Shapiro, M.L. (1997) Impaired learning and LTP in mice expressing the carboxy terminus of the Alzheimer amyloid precursor protein. *Nature* **387,** 500-505.

Namba, Y., Tomonga, M., Kawasaki, H., Otomo, E. & Ikeda, K. (1991) Apolipoprotein E immunoreactivity in cerebral amyloid deposits and neurofibrillary tangles in Alzheimer's disease and kuru plaque amyloid in Creutzfeldt-Jacob disease. *Brain Res.* **541,** 163-166.

Narindrasorasak, S., Lowrey, D., Altman, R., Gonzalez-DeWhitt, P.A., Greenberg, B.D. & Kisilevsky, R. (1992) Characterisation of high affinity binding between laminin and Alzheimer's disease amyloid precursor proteins. *Lab. Invest.* **7,** 643-652.

Nelson, P.T. & Saper, C.B. (1995) Ultrastructure of neurofibrillary tangles in the cerebral cortex of sheep. *Neurobiol. Aging* **16,** 315-323.

Nelson, W.J & Lazarides, E. (1984) The patterns of expression of two ankyrin isoforms demonstrate distinct steps in the assembly of the membrane skeleton in neuronal morphogenesis. *Cell* **39,** 309-320.

Neve, R.L., Harris, P., Kosik, K.S., Kurnit, D.M. & Donlon. T.A. (1986) Identification of cDNA clones for the human microtubule-associated protein, tau, and chromosomal localization of the genes for tau and microtubule associated protein 2. *Mol. Brain Res.* **1,** 271-280.

Neve, R.L. & Robakis, N.K. (1998) Alzheimer's disease: a re-examination of the amyloid hypothesis *Trends. Neurosci.* **21,** 15-19.

Nixon, R.A. & Lewis, S.E. (1986) Differential turnover of phosphate groups on neurofilament subunits in mammalian neurons *in vivo*. *J. Biol. Chem.* **261,** 16298-16301

Nixon, R.A. & Logvinenko, K.B. (1986) Multiple fates of newly synthesized neurofilament proteins; evidence for a stationary neurofilament network distributed nonuniformly along axons of retinal gangloin neurons. *J. Cell Biol.* **102,** 647-659.

Nixon, R.A., Lewis, S.E. & Marcotta, C.A. (1987) Posttranslational modification of neurofilament proteins by phosphate during axoplamsic transport in retinal ganglion cell neurons. *J. Neurosci.* **7,** 1145-1158.

Nixon, R.A. & Shea, T.B. (1992) Dynamics of neuronal intermediate filaments: a developmental perspective. *Cell Motil. Cytoskel.* **22,** 81-91.

Nixon, R.A., Lewis, S.E., Mercken, M. & Sihag, R.K. (1994a) [32P] orthophosphate and [35S] methionine label separate pools of neurofilaments with markedly different axonal transport kinetics mouse retinal ganglion cells *in vivo*. *Neurochem. Res.* **19,** 1445-53.

Nixon, R.A., Pasevich, P.A., Sihag, R.K. & Thayer, C.Y. (1994b) Phosphorylation on carboxyl terminus domains of neurofilament preoteins in retinal ganglion cell neurons *in vivo*: influences on regional neurofilament accumulation, interneurofilament spacing, and axon caliber. *J. Cell Biol.* **126,** 1031-1046.

Nukina, N., Kosik, K.S. & Selkoe, D.J. (1987) Recognition of Alzheimer paired helical filaments by monoclonal neurofilament antibodies is due to cross reaction with tau protein. *Proc. Natl. Acad. Sci. U.S.A.* **84,** 3415-3419.

Oblinger, M.M., Wong, J. & Parysek, L.M. (1989) Axotmy induced changes in the expression of a type III neuronal intermediate filament gene. *J. Neurosci.* **9,** 3766-3775.

Okabe, S., Miyasaka, H. & Hirokawa, N. (1993) Dynamics of the neuronal intermediate filaments *J. Cell Biol.* **121,** 375-386.

Okonkwo, D.O., Pettus, E.H., Moroi, J. & Povlishock, J.T. (1998) Alteration of the neurofilament sidearm and its relation to neurofilament compaction occurring with traumatic axonal injury. *Brain Res.* **784,** 1-6.

Olichney, J.M., Hansen, L.A., Galasko, D., Saitoh, T., Hofstetter, C.R., Katzman, R. & Thal, L.J. (1996) The apolipoprotein E ε4 allele is associated with increased neuritic plaques and cerebral amyloid angiopathy in Alzheimer's disease and Lewy body variant. *Neurology* **47,** 190-196.

Oyama, F., Sawamura, N., Kobayashi, K., Morishima-Kawashima, M., Kuramochi, T., Ito, M., Tomita, T., Maruyama, K., Saido, T.C., Iwatsubo, T., Capell, A., Walter, J., Grünberg, J., Ueyama, Y., Haass, C. & Ihara, Y. (1998). Mutant presenilin 2 transgenic mouse: effects of an age-dependent increase of amyloid ß-protein 42 in the brain. *J. Neurochem.* **71,** 1313-1322.

Pachter, J.S. & Liem, R.K.H. (1985) α-Internexin, a 66-kD intermediate filament-binding protein from mammalian central nervous tidssues. *J. Cell. Biol.* **101,** 1316-1322.

Pahlsson, P., Shakin-Eshleman, S.H. & Spitalnik, S.L. (1992) N-linked glycosylation of beta-amyloid precursor protein. *Biochem. Biophys. Res. Commun.* **189,** 1667-1673.

Pappolla, M.A., Omar, R.A., Sambarmurti, K., Anderson, J.P & Robakis, N.K. (1992) The genesis of the senile plaque. Further evidence in support of its neuronal origin. *Am. J. Pathol.* **141,** 1151-1159.

Parysek, L.M. Wolosewick, J.J. & Olmstead, J.B. (1984) MAP4: a microtubule associated protein specific for a subset of tissue microtubules. *J. Cell. Biol.* **99,** 2287-2296.

Paschal, B.M., Shpetner, H.S. & Vallee, R.B. (1987) MAP IC is a microtubule activated ATPase which translocates microtubules in viro and has dynein like properties. *J. Cell Biol.* **105,** 1273-1282.

Perry, G., Rizzuto, N., Autilio-Gambetti, L. & Gambetti, P. (1985) Paired helical filaments from Alzheimer disease patients contain cytoskeletal components. *Proc. Natl. Acad. Sci. U.S.A.* **82,** 3916-3920.

Perry, G., Friedman, R., Shaw, G. & Chau, V. (1987) Ubiquitin is detected in neurofibrillary tangles and senile plaque neurites of Alzheiemr disease brains. *Proc. Natl. Acad. Sci. U.S.A.* **84,** 3033-3036.

Perry, G., Lipphardt, S., Mulvihill, P., Kancherla, M., Mijares, M., Gambetti, P., Sharma, S., Maggiora, L., Cornette, J. & Lobl, T. (1988) Amyloid precursor protein in senile plaques of Alzheimer disease. *Lancet* **2,** 746.

Pettus, E. & Povlishock, J. (1996) Characterization of a distinct set of intra-axonal ultrastructural changes associated with traumatically induced alteration in axolemmal permeability. *Brain Res.* **772,** 1-11.

Pike, C.J., Cummings, B.J. & Cotman, C.W. (1992) Beta-Amyloid induces neuritic dystrophy *in vitro*: similarities with Alzheimer pathology. *Neuroreport* **3,** 769-772.

Pike, C.J., Burdick, D., Walencewicz, A.J., Glabe, C.G. & Cotman, C.W. (1993) Neurodegeneration induced by beta-amyloid peptides *in vitro* the role of peptide assembly state. *J. Neurosci.* **13,** 1676-1687.

Podlisny, M.B., Stephenson, D.T., Frosch, M.P., Tolan, D.R., Lieberburg, I., Clemens, J.A. & Selkoe, D.J. (1993) Microinjection of synthetic amyloid-beta protein in monkey cerebraal cortex fails to produce acute neurotoxicity *Am. J. Pathol.* **142,** 17-24.

Poirier, J. (1994) Apolipoprotein E in animal models of CNS injury and in Alzheimer's disease. *Trends in Neurosci.* **17,** 525-530.

Pope, W., Enam, S.A., Bawa, N., Miller, B.E., Ghanbari, H.A. & Klein, W.L. (1993) Phosphorylated tau epitope of Alzheimer's disease is coupled to axon development in the avian central nervous system. *Exp. Neurol.* **120,** 106-113.

Praprotnik, D., Smith, M.A., Richey, P.L., Vinters, H.V. & Perry, G. (1996) Filament heterogeneity within the dystrophic neurites of senile plaques suggests blockage of fast axonal transport in Alzheimer's disease. *Acta Neuropathol.* **91,** 226-235.

Price, D.L., Sisodia, S.S. & Borcheldt, D.R. (1998) Genetic neurodegenerative disease; the human illness and transgenic models. *Science* **282,** 1079-1083.

Price, J.L., Davis, P.B., Morris, J.C. & White, D.L. (1991) The distribution of tangles, plaques and related immunohistochemical markers in healthy aging and Alzheimer's disease. *Neurobiol. Aging* **12,** 295-312.

Price, J.L. & Morris, J.C. (1999) Tangles and plaques in nondemented aging and 'preclinical' Alzheimer's disease. *Ann. Neurol.* **45,** 358-368.

Probst, A., Basler, V., Bron, B. & Ulrich, J. (1983) Neuritic plaques in senile dementia of Alzheimer type: a Golgi analysis in the hippocampal region. *Brain Res.* **268,** 249-254.

Probst, A., Langui, D., Ipsen, S., Robakis, N. & Ulrich, J. (1991) Deposition of ß/A4 protein along neuronal plasma membrane in diffuse senile plaques. *Acta Neuropathol.* **83,** 21-29.

Qian, S., Jiang, P., Guan, X.M., Singh, G., Trumbauer, M.E., Yu, H., Chen, H.Y., Van de Ploeg, L.H. & Zheng, H. (1998) Mutant human presenilin 1 protects presenilin 1 null mouse against embryonic lethality and elevates Aß1-42/43 production. *Neuron* **20,** 611-617.

Quon, D., Wang, R., Catalano, R., Marian Scardina, J., Murakami, K. & Cordell, B. (1991) Formation of ß-amyloid protein deposits in brains of transgenic mice. *Nature* **352,** 239-241.

Ramon y Cajal, S. (1928) Degeneration and regeneration of the nervous system. Oxford University Press, London.

Rebeck, G.W., Reiter, J.S., Strickland, D.K. & Hyman, B.T. (1993) Apolipoprotein E in sporadic Alzheimer's disease: Allelic variation and receptor interactions. *Neuron* **11,** 575-580.

Rebeck, G.W., Perls, T.T., West, H.L., Sodhi, B.A., Lipsitz, L.A. & Hyman, B.T. (1994) Reduced apolipoprotein ε4 allele frequency in the oldest Alzheimer's patients and cognitively normal individuals. *Neurology* **44,** 1513-1516.

Riederer, B.M., Zagon, I.S. & Goodman, S.R. (1986) Brain spectrin (240/235) and brain spectrin(240/235E): two distinct spectrin subtypes with different locations within mammalian neural cells. *J. Cell Biol.* **102,** 2088-2097.

Roberts, G.W., Allsop, D. & Bruton, C. (1990) The occult aftermath of boxing. *J. Neurol. Neurosurg. Psychiatry.* **53,** 373-378.

Rogaev, E.I., Sherrington, R., Rogaev, E.A., Levesque, G., Ikeda, M., Liang, Y., Chi, H., Lin, C., Holman, K., Tsuda, T., Mar, L., Sorbi, S., Nacmias, B., Piacentini, S., Amaducci, L., Chumakov, I., Cohen, D., Lannfelt, L., Fraser, P.E. ,Rommens, J.M. & St. George - Hyslop, P.H. (1995) Familial Alzheimers disease in kindreds with missense mutations in a gene on chromosome 1 related to the Alzheimers disease type 3 gene. *Nature*. **376,** 775-778.

Roher, A.E., Lowenson, J.D., Clarke, S., Woods, A.S., Cotter, R.J., Gowing, E. & Ball, M.J. (1993a) ß-Amyloid (1-42) is a major component of cerebrovascular amyloid deposits; Implications for the pathology of Alzheimer's disease. *Proc. Natl. Acad. Sci. U.S.A.* **90,** 10836-10840.

Roher, A.E., Palmer, K.C., Yurewicz , E.C., Ball, M.J. & Greenberg, B.D. (1993b) Morphological and biochemical analyses of amyloid plaque core proteins purified from Alzheimer disese brain tissue. *J. Neurochem.* **61,** 1916-1926.

Roots, B.I. (1983) Neurofilament accumulation induced in synapses by leupeptin. *Science* **221,** 971-972.

Rosenfeld, J., Dorman, M.E., Griffin, J.W., Sternberger, L.A., Sternberger, N.H. & Price, D.L. (1987) Distribution of neurofilament antigens after axonal injury. *J. Neuropathol. Exp. Neurol.* **46,** 269-282.

Roses, A.D. (1995) On the metabolism of apolipoprotein E and the Alzheimer diseases. *Exp. Neurol.* **132,** 149-156 .

Rozemuller, J.M., Eikelenboom, P., Stam, F.C., Beyreuther, K. & Masters, C. (1989) A4 protein in Alzheimer's disease: Primary and secondary cellular events in extracellular amyloid deposition. *J. Neuropathol. Exp. Neurol.* **48,** 674-691.

Russo, C., Angelini, G., Dapino, D., Piccini, A., Piomobo, G., Schettini, G., Chen, S., Teller, J.K., Zaccheo, D., Gambetti, P. & Tabaton, M. (1998) Opposite roles of apolipoprotein E in normal brains and in Alzheimer's disease. *Proc. Natl. Acad. Sci. U.S.A.* **95,** 15598-15602.

Sampson, V.L., Morrison, J.H. & Vickers, J.C. (1997) The cellular basis for the relative resistance of parvalbumin and calretinin immunoreactive neocortical neurons to the pathology of Alzheimer's disease. *Exp. Neurol.* **145,** 295-302.

Sanberg, P.R., Calderon, S.F., Giordano, M., Tew, J.M. & Norman, A.B. (1989) The quinolinic acid model of Huntington's disease: locomotor abnormalities. *Exp. Neurol.* **105,** 45-53.

Saunders, A.M., Strittmatter, W.J., Schmechel, D., St. George-Hyslop, P.H., Pericak-Vance, M.A., Joo, S.H., Rosi, B.L., Gusella, J.F., Crapper-MacLachlan, D.R., Alberts, M.J., Hulette, C., Crain, B., Goldgaber, D. & Roses, A.D. (1993) Association of apolipoprotein E allele ε4 with late-onset familial and sporadic Alzheimer's disease. *Neurology* **43,** 1467-1472.

Saunders, H.L., Dickson, T.C., & Vickers, J.C. (1998) Immunolocalisation of ß-amyloid precursor protein tp plaque-associated synaptic alterations in the early and late stages of Alzheimer's disease. *Alzheimer's Reports* **1,** 111-119.

Schenk, D., Barbour, R., Dunn, W., Gordon, G., Grajeda, H., Guido, T., Hu, K., Huang, J., Johnson-Wood, K., Khan, K., Kholodenko, D., Lee, M., Liao, Z., Lieberburg, I., Motter, R., Mutter, L., Soriano, F., Shopp, G., Vasquez, N., Vandevert, C., Walker, S., Wogulis, M., Yednock, T., Games, D. & Seubert, P. (1999) Immunization with amyloid-beta attenuates Alzheimer-disease-like pathology in the PDAPP mouse. *Nature* **400,** 173-177.

Scheuner, D., Eckman, C., Jensen, M., Song, X., Citron, M., Suzuki, N., Bird, T.D., Hardy, J., Hutton, M., Kukull, W., Larson, E., Levy-Lahad, E., Viitanen, M., Peskind, E., Poorkaj, P., Schellenberg, G., Tanzi, R., Wasco, W., Lannfelt, L., Selkoe, D. & Younkin, S. (1996) Secreted amyloid beta-protein similar to that in the senile plaques of Alzheimer's disease is increased in vivo by the presenilin 1 and 2 and APP mutations linked to familial Alzheimer's disesae. *Nat. Med.* **2,** 864-870.

Schlaepfer, W.W. (1987) Neurofilaments: structure, metabolism and implications in disease. *J. Neuropathol. Exp. Neurol.* **46,** 117-129.

Schliwa, M. & Potter, M. (1986) Relationship between the organization of actin bundles and vinculin plaques. *Cell Tissue Res.* **246,** 211-218.

Schmechel, D.E., Saunders, A.M., Strittmatter, W.J., Crain, B.J., Hulette, C.M., Joo, S.H., Pericak-Vance, M.A., Goldgaber, D. & Roses, A.D. (1993) Increased amyloid beta-peptide deposition in the cerebral cortex as a consequence of apolipoprotein E genotype in late-onset Alzheimer's disease. *Proc. Natl. Acad. Sci. U.S.A.* **90,** 9649-9653.

Schmidt, M.L., Lee, V.M.-Y. & Trojanowski, J.Q. (1990) Relative abundance of tau and neurofilament epitopes in hippocampal neurofibrillary tangles. *Am. J. Pathol.* **136,** 1069-1075.

Schmidt, M.L., Lee, V.M.-Y. & Trojanowski, J.Q. (1991) Comparative epitope analysis of neuronal cytoskeletal proteins in Alzheimer's disease senile plaque neurites and neuropil threads. *Lab. Invest.* **64,** 352-357.

Schmidt, M.L., DiDario, A.G., Lee, V.M.-Y. & Trojanowsk, J.Q. (1994) An extensive network of PHF tau-rich dystrophic neurites permeates neocortex and nearly all neuritic and diffuse amyloid plaques in Alzheimer disease. *FEBS Lett.* **344,** 69-73.

Schmidt, M.L., Robinson, K.A., Lee, V.M.-Y. & Trojanowski, J.Q. (1995) Chemical and immunological heterogeneity of fibrillar amyloid in plaques of Alzheimer's disease and Down's syndrome brains revealed by confocal microscopy. *Am. J. Pathol.* **147,** 503-515.

Schneider, A., Biernat, J., von Bergen, M. & Mandelkow, E. (1999) Phosphorylation the detaches tau protein from microtubules (Ser262, Ser214) also protects it against aggregation into Alzheimer paired helical filaments. *Biochemistry* **38,** 3549-3558.

Schroer, T.A., Steuer, E.R. & Sheetz, M.P. (1989) Cytoplasmic dynein is a minus end-directed motor for membranous organelles. *Cell* **56,** 937-946.

Schwab, C. & McGeer, P.L. (1998) Tubulin immunopositive structures resembling intracellular neurofibrillary tangles. *Neurobiol. Aging* **19,** 41-45.

Selkoe, D.J., Podlisny, M., Joachim, C. Vickers, E.A., Lee, G., Fritz, L.C. & Oltersdorf, T. (1988) ß-amyloid precurso protein of Alzheimer's disease occurs as 110 to 135 kilodalton membrane-associated proteis in neural and non neural tissues. *Proc. Natl. Acad. Sci. U.S.A.* **85,** 7341-7345.

Selkoe, D.J. (1989) Molecular pathology of amyloidogenic proteins and the role of vascular amyloidosis in AD. *Neurobiol. Aging* **10,** 387-395.

Selkoe, D.J. (1994) Alzheimer's disease: a central role for amyloid. *J. Neuropathol. Exp. Neurol.* **53,** 438-447.

Seubert, P., Vigo-Pelfey, C., Esh, F., Lee, M., Dovey, H., Davis, D., Sinha, S., Schlossmacher, M., Whaley, J., Swindlehurst, C., McCormack, R., Wolfert, R., Selkoe, D., Lieberburg, I. & Schenk, D (1992) Isolation and quantification of soluble Alzheimer's beta-peptide from biological fluids. *Nature* **359,** 325-327.

Sharp, D.J., Yu, W. & Baas, P.W. (1995) Transport of dendritic microtubules establishes their nonuniform polarity orientation. *J. Cell Biol.* **130,** 93-103.

Sharp, D.J., Kuriyama, R. & Baas, P.W. (1996) Expression of a kinesin-related motor protein induces Sf9 cells to form dendrite-like processes with nonuniform microtubule polarity orientation. *J. Neurosci.* **16,** 4370-4375.

Shaw, G. & Bray, D. (1977) Movement and extension of isolated growth cones. *Exp. Cell Res.* **104,** 55-62.

Shaw, G., Winialski, D. & Reier, P. (1988) The effect of axotomy and deafferentation on phosphorylation dependent antigenicity of neurofilaments in rat superior cervical ganglion neurons. *Brain Res.* **460,** 227-234.

Shaw, G. (1991) Neurofilament proteins In: *The Neuronal Cytoskeleton*, pp. 185-214. Eds. R.D. Burgoyne. Wiley-Liss: New York.

Sheng, J.G., Mrak, R.E. & Griffin, W.S.T. (1996) Apolipoprotein E distribution among different plaque types in Alzheimer's disease: implications for its role in plaque progression. *Neuropathol. Appl. Neurobiol.* **22,** 334-341.

Sherrington, R., Rogaev, E.I., Liang, Y., Rogaev, E.A., Levesque, G., Ikeda, M., Chi, H., Lin, C., Li, G., Holman, K., Tsuda, T., Mar, L., Foncin, J.-F., Bruni, A.C., Montesi, M.P., Sorbi, S., Rainero, I., Pinessi, L., Nee, L., Chumakov, I., Pollen, D., Brookes, A., Sanseau, P., Pollinsky, R.J., Wasco, W., Da Silva, H.A.R., Haines, J.L., Pericak-Vance, M.A., Tanzi, R.E., Roses, A.D., Frase, P.E., Rommens, J.M. & St. George-Hyslop, P.H. (1995) Cloning of a gene bearing missence mutations in early-onset familial Alzheimer's disease. *Nature* **375,** 754-760.

Shoji, M., Hirai, S., Yamaguchi, H., Harigaya, Y. & Kawarabayashi, T. (1990) Amyloid ß-protein precursor accumulates in dystrophic neurites of senile plaques in Alzheiemr-type dementia. *Brain Res.* **512,** 164-168.

Sihag, R.K. & Nixon, R.A. (1990) Phosphorylation of the amino-terminal head domain of the middle molecular mass 145-kDa subunit of neurofilaments. Evidence for regulation by second messenger-dependent protein kinases. *J. Biol. Chem.* **265,** 4166-4171.

Sihag, R.K. & Nixon, R.A. (1991) Identification of Ser-55 as a major protein kinase A phosphorylation site on the 70-kDa subunit of neurofilaments. Early turnover during axonal transport. *J. Biol. Chem.* **266,** 18861-18867.

Silveira, L.C., Russelakis-Carneiro, M. & Perry, V. (1994) The ganglion cell response to optic nerve injury in the cat: differential responses revealed by neurofibrillar staining. *J. Neurocytol.* **23,** 75-86.

Siman, R., Card, J.P., Nelson, R.B. & Davis, L.G. (1989) Expression of ß-amyloid precursor protein in reactive astrocytes following neuronal damage. *Neuron* **3,** 275-285.

Smith, D.L., Wolf., J.A., Lusardi, T.A., Lee, V.M.-Y. & Meaney, D.F. (1999) High tolerance and delayed elastic response of cultured axons to dynamic stretch injury. *J. Neurosci.* **19,** 4263-4269.

Sole, G.M. (1980) The effects of microsurgical transection of neurite bundles *in vitro* before and after exposure to colchicine. *J. Anat.* **130,** 777-788.

St. George-Hyslop, P.H. & Westaway, D.A. (1999) Alzheimer's disease. Antibody clears senile plaques. *Nature* **400,** 116-117.

Steinert, P.M. & Roop, D.R. (1988) Molecular and cellular biology of intermediate filaments. *Ann. Rev. Biochem.* **57,** 593-625.

Sternberger, L.A. & Sternberger, N.H. (1983) Monoclonal antibodies distinguish phosphorylated and nonphosphorylated forms of neurofilaments *in situ*. *Proc. Natl. Acad. Sci. U.S.A.* **80,** 6126-6130.

Stone, D.J., Rozovsky, I., Morgan, T.E., Anderson, C.P. & Finch, C.E. (1998) Increased synaptic sprouting in response to estrogen via an apolipoprotein E dependent mechanism: implications for Alzheimer's disease. *J. Neurosci.* **18,** 3180-3185.

Strittmatter, W.J., Saunders, A.M., Schmechel, D., Pericak-Vance, M., Enghild, J., Salvesen, G.S. & Roses, A.D. (1993a) Apolipoprotein E: high-avidity binding to beta-amyloid and

increased frequency of type 4 allele in late-onset familial Alzheimer disease. *Proc. Natl. Acad. Sci. U.S.A.* **90,** 1977-1981.

Strittmatter, W.J., Weisgraber, K.H., Huang, D.Y., Dong, L., Salvesen, G.S., Pericak-Vance, M., Schmechel, D., Saunders, A.M., Goldgaber, D. & Roses, A.D. (1993b) Binding of human apolipoprotein E to synthetic amyloid ß peptide: Isoform-specific effects and implications for late-onset Alzheimer's disease. *Proc. Natl. Acad. Sci. U.S.A.* **90,** 8098-8102.

Sturchler-Pierrat, C., Abramowski, D., Duke, M., Wiederhold, K.H., Mistl, C., Rothacher, S., Ledermann, B., Burki, K., Frey, P., Paganetti, P.A., Waridel, C., Calhoun, M.E., Jucker, M., Probst, A., Staufenbiel, M. & Sommer, B. (1997) Two amyloid precursor protein transgenic mouse models with Alzheimer's disease-like pathology. *Proc. Natl. Acad. Sci. U.S.A.* **94,** 13287-13292.

Su, J.H., Cummings, B.J. & Cotman, C.W. (1996) Plaque biogenesis in brain aging and Alzheimer's disease. I. Progressive changes in phosphorylation states of paired helical filaments and neurofilaments. *Brain Res.* **739,** 79-87.

Su, J.H., Cummings, B.J. & Cotman, C.W. (1998) Plaque biogenesis in brain aging and Alzheimer's disease. II. Progressive transformation and developmental sequence of dystrophic neurites. *Acta Neuropathol.* **96,** 463-471.

Suzuki, A. (1997) Amyloid beta-protein induces necrotic cell death mediated by ICE cascade in PC12 cells. *Exp. Cell Res.* **234,** 507-511.

Suzuki, N., Cheung, T.T., Cai, X.D., Odaka, A., Otvos, L., Eckman, C., Golde, T.E. & Younkin, S.G. (1994) An increased percentage of long amyloid ß protein secreted by familial amyloid ß protein precursor (βAPP_{717}) mutants. *Science* **264,** 1336-1340.

Takeda, S., Okabe, S., Funakoshi, T. & Hirokawa, N. (1994) Differential dynamics of neurofilament H protein and neurofilament L protein in neurons. *J. Cell Biol.* **127,** 173-185.

Tamaoka, A., Odaka, A., Ishibashi, Y., Usami, M., Sahara, N., Suzuki, N., Nukina, N., Mizusawa, H., Shoji, S., Kanazawa, I.. & Mori, H. (1994) APP717 missense mutation affects the ratio of amyloid beta protein species (A beta 1-42/43 and a beta 1-40) in familial Alzheimer's disease brain. *J. Biol. Chem.* **269,** 32721-32724.

Tanzi, R., Kovacs, D.M., Kim, T.W., Moir, R.D., Guenette, S.Y. & Wasco, W. (1997) The presenillin genes and their role in early onset AD. *Alzheimer's Dis. Rev.* **1,** 90-98.

Tapscott, S.J., Bennet, G.S. & Holtzer, H. (1981) Neuronal precursor cells in the chick neural tube express neurofilament proteins. *Nature* **292,** 836-838.

Teasdale, G.M., Nicoll, J.A., Murray, G. & Fiddes, M. (1997) Association of apolipoprotein E polymorphism with outcome after head injury. *Lancet* **350,** 1069-1071.

Tecoma, E.S., Monyer, H., Goldberg, M.P. & Choi, D.W. (1989) Traumatic neuronal injury *in vitro* is attenuated by NMDA antagonists. *Neuron* **2,** 1541-1545.

Tekirian, T.L., Cole, G.M., Russel, M.J., Wekstein, D.R., Patel, E., Snowdon, D.R., Markesbery, W.R. & Geddes, J.W. (1996) Carboxy terminal of ß-amyloid deposits in aged human, canine and polar bear brains. *Neurobiol. Aging.* **17,** 249-257.

Terry, R.D., Gonatas, N.K. & Weiss, M. (1964) Ultrastructural studies in presenile dementia. *Am. J. Pathol.* **44,** 269-297.

Terry, R.D., Masliah, E., Salmon, D.P., Butters, N., Deteresa, R., Hill, R.. Hansen, L.A. & Katzman, R. (1991) Physical basis of cognitive alterations in Alzhiemer's disese; synapse loss is the major corrlate of cognitive impairment. *Ann. Neurol.* **30,** 572-580.

Terry, R.D., Masliah, E. & Hansen, L.A. (1994) Structural basis of the cognitive alterations in Alzheimer disease. In: *Alzheimer disease*, pp. 179-196. Eds. R.D. Terry, R. Katzman & K.L. Bick. Raven Press: New York.

Terry, R.D. (1996) The pathogenesis of Alzheimer disease: An alternative to the amyloid hypothesis *J. Neuropathol. Exp. Neurol.* **55,** 1023-1025.

Teter, B., Harris-White, M.E., Frautschy, S.A. & Cole, G.M. (1999a) Role of apolipoprotein E and estrogen in mossy fiber sprouting in hippocampal slice cultures. *Neuroscience* **91,** 1009-1016.

Teter, B., Xu, P.T., Gilbert, J.R., Roses, A.D., Galasko, D. & Cole, G.M. (1999b) Human apolipoprotein E isoform-specific differences in neuronal sprouting in organotypic hippocampal culture. *J. Neurochem.* **73,** 2613-2616.

Tetzlaff, W., Bisby, M.A. & Kreutzberg, G. (1988) Changes in cytoskeletal protein synthesis in the rat facial nucleus following axotomy. *J. Neurosci.* **8,** 3181-3189.

Tetzlaff, W., & Bisby, M.A. (1989) Neurofilament elongation into regenerating facial nerve axons. *Neuroscience* **29:** 659-666.

Thal, D.R., Arendt, T., Waldmann, G., Hozer, M., Zedlick, D., Rüb, U. & Schober, R. (1998) Progression of neurofibrillary changes and PHF-τ in end-stage Alzheimer's disease is different from plaque and cortical microglial pathology. *Neurobiol. Aging* **19,** 517-525.

Tokuda, T., Ikeda, S., Yanagisawa, N., Ihara, Y. & Glenner, G.G. (1991) Re-examination of ex-boxers' brains using immunohistochemistry with antibodies to amyloid ß-protein and tau protein. *Acta Neuropathol.* **82,** 280-285.

Tomita, S., Kirino, Y. & Suzuki, T. (1998) Cleavage of Alzheimer's amyloid precursor protein (APP) by secretases occurs after O-glycosylation of APP in the protein secretory pathway. Identification of intracellular compartments in which APP cleavage occurs without using toxic agents that interfere with protein metabolism. *J. Biol. Chem.* **273,** 6277-6284.

Torack, R.M., Roth, K.A. & Miller, J.W. (1996) Neuronal argyrophilia and phosphorylated neurofilament accumulation secondary to deafferentation. *J. Neuropathol. Exp. Neurol.* **55,** 466-470.

Torvik, A. (1976) Central chromatolysis and the axon reaction: a reappraisal. *Neuropathol. Appl. Neurobiol.* **2,** 423-432.

Traub, P., Vorgias, C.E. & Nelson, W. (1985) Interaction *in vitro* of the neurofilament triplet proteins from porcine spinal cord with natural RNA and DNA. *Mol. Biol. Rep.* **10,** 129-136.

Uchida, Y., Takio, K., Titani, K., Ihara, Y. & Tomonaga, M. (1991) The growth inhibitory factor that is deficient in the Alzheimer's disease brain is a 68 amino acid metallothionein-like protein. *Neuron* **7,** 337-47.

Uchihara, T., Duyckaerts, C., He, Y., Kabayashi, K., Seilhean, D., Amouyel, P. & Hauw, J.J. (1995) ApoE immunoreactivity and microglial cells in Alzheimer's disease brain. *Neurosci. Lett.* **195,** 5-8.

Ulrich, J. (1985) Alzheimer changes in nondemented patients younger than sixty-five: Possible early stages of Alzheimer's disease and senile dementia of Alzheimer type. *Ann. Neurol.* **17,** 273-277.

Verano, A., Chandran, R., Faraldi, F., Bennet, D. & Reyes, M.G. (1990) Volume density of senile plaques in Alzheimer's disease. *J. Neuropathol. Exp. Neurol.* **49,** 307. Abstract

Vickers, J.C. & Costa, M. (1992a) The neurofilament triplet is present in distinct subpopulations of neurons in the central nervous system of the guinea pig. *Neuroscience* **49,** 273-278.

Vickers, J.C., Delacourte, A. & Morrison, J.H. (1992b) Progressive transformation of the cytoskeleton associated with normal aging and Alzheimer's disease. *Brain Res.* **594,** 273-278.

Vickers, J.C., Morrison, J.H., Friedrich, Jr. V.L., Elder, G.A., Perl, D.P., Katz, R.N. & Lazzarini, R.A. (1994a) Age-associated and cell type-specific neurofibrillary pathology in transgenic mice expressing the human mid-sized neurofilament subunit. *J. Neurosci.* **14,** 5603-5612.

Vickers, J.C., Riederer, B.M., Marugg, R.A., Buee-Scherrer, V., Buee, L., Delacourte, A. & Morison, J.H. (1994b) Alterations in neurofilament protein immunoreactivity in human hippocampal neurons related to normal aging and Alzheimer's disease. *Neuroscience.* **62,** 1-13.

Vickers, J.C., Chin, D., Edwards, A-M., Sampson, V., Harper, C. & Morrison, J. (1996) Dystrophic neurite formation associates with age-related ß amyloid deposition in the neocortex: clues to the genesis of neurofibrillary pathology. *Exp. Neurol.* **141,**1-11.

Vickers, J.C. (1997) A cellular mechanism for the neuronal changes underlying Alzheimer's disease. *Neuroscience* **38,** 629-639.

Vickers, J.C., Dickson, T.C., Adlard, P.A., Saunders, H.L., King, C.E. & McCormack, G. (2000) The cause of neuronal degeneration in Alzheimer's disease. *Prog. Neurobiol.* **60,** 139-165.

Walker, L.C., Masters, C., Beyreuther, K. & Price, D.L. (1990) Amyloid in the brains of aged squirrel monkeys. *Acta Neuropathol.* **80,** 381-387.

Wang, D. & Munoz, D.G. (1995) Qualitative and quantitative differences in senile plaque dystrophic neurites of Alzheimer's disease and normal aged brain. *J. Neuropathol. Exp. Neurol.* **54,** 584-586.

Wang, J-Z., Grundke-Iqbal, I. & Iqbal, K. (1996) Glycosylation of microtubule associated protein tau: An abnormal posttranslational modification in Alzheimer's disease. *Nat. Med.* **2,** 871-875.

Wang, L., Ho, C., Sun, D., Liem, R.K.H. & Brown, A. (2000) Rapid movement of axonal neurofilaments interrupted by prolonged pauses. *Nat. Cell Biol.* **2,** 137-141.

Weingarten, M.D., Lockwood, A.H., Hwo, S.Y. & Kirschner, M.W. (1975) A protein factor essential for microtubule assembly. *Proc. Natl. Acad. Sci. U.S.A.* **72,** 1858-1862.

Wible, B.A., Smith, K.E. & Angelides, K.J. (1989) Resolution and purification of a neurofilament-specific kinase. *Proc. Natl. Acad. Sci. U.S.A.* **86,** 720-724.

Wigley, C.B. & Berry, M. (1988) Regeneration of adult rat retinal ganglion cell processes in monolayer culture: comparisons between cultures of adult and neonatal neurons. *Brain Res.* **470,** 85-98.

Wille, H., Drewes, G., Biernat, J., Mandelkow, E.M. & Mandelkow, E. (1992) Alzheimer-like paired helical filaments and antiparallel dimers formed from microtubule-associated protein tau *in vitro*. *J. Cell Biol.* **118,** 573-584.

Wischik C.M., Novak M., Thogersen H.C., Edwards P.C., Runswick M.J., Jakes R., Walker J.E., Milstein C., Roth, M. & Klug, A. (1988) Isolation of a fragment of tau derived from the core of the paired helical filament of Alzheimer's disease. *Proc. Natl. Acad. Sci. U.S.A.* **85,** 4506-4510.

Wischik, C.M., Edwards, P.C., Lai, R.Y.K., Gertz, H.N.J., Xuereb, J.H., Paykel, E.S., Brayne, C., Huppert, F.A., Mukatova-Ladinska, E.B., Mena, R., Roth, M. & Harrington, C.R. (1995) Quantitative analysis of tau protein in paired helical filament preparations; Implications for the role of tau protein phosphorylation in PHF assembly in Alzheimer's disease. *Neurobiol. Aging* **16,** 409-431.

Wisniewski, H.M., Johnson, A.B., Raine, C.S., Kay, W.J. & Terry R.D. (1970) Senile plaques and cerebral amyloidosis in aged dogs. *Lab. Invest.* **23,** 287-296.

Wisniewski, H.M., Ghetti, B. & Terry, R.D. (1973) Neuritic (senile) plaques and filamentous changes in aged rhesus monkeys. *J. Neuropathol. Exp. Neurol.* **32,** 566-584.

Wisniewski, H.M. & Terry, R.D. (1973) Reeaxamination of the pathogenesis of the senile plaque. Progress in Neuropathology. Vol II Grune and Stratton ?????1973 1-26

Wisniewski, H.M., Narang, H.K. & Terry, R.D. (1976) Neurofibrillary tangles of paired helical filaments. *J Neurol. Sci.* **27,** 173-181.

Wisniewski, H.M., Sturman, J.A. & Shek, J.W. (1982) Chronic model of neurofibrillary changes induced in mature rabbits by metalic aluminium. *Neurobiol. Aging.* **3,** 11-22.

Wisniewski, H.M., Bancher, C., Barcikowska, M., Wen, G.Y. & Currie, J. (1989) Spectrum of mrophological appearance of amyloid deposits in Alzheimer's disease. *Acta Neuropathol.* **78,** 337-347.

Wisniewski, T. & Frangione, B. (1992) Apolipoprotein E: a pathological chaperone protein in patients with cerebral and systemic amyloid. *Neurosci. Lett.* **135,** 235-238.

Wisniewski, T., Golabek, A., Matsubara, E., Ghiso, J. & Frangione, B. (1993) Apolipoprotein E: binding to soluble Alzheimer's beta-amyloid. *Biochem. Biophys. Res. Commun.* **192,** 359-365.

Withers, G.S. & Banker, G. 'Characterizing and studying neuronal cultures' (1998) in Culturing Nerve Cells, 2nd Edition, Edited by Gary Banker and Kimberly Goslin.

Yaghmai, A. & Povlishock, J. (1992) Traumatically induced reactive changes as visualised through the use of monoclonal antibodies targeted to neurofilament subunits. *J. Neuropathol. Exp. Neurol.* **51,** 158-176.

Yamada, E. & Hazama, F. (1993) Different stability of neurofilaments for trypsin treatment after axotomy in the dorsal motor nucleus of the vagal nerve and the hypoglossal nucleus. *Brain Res.* **612,** 210-215.

Yamaguchi, H., Hirai, S., Morimatsu, M, Shoji, M. & Harigaya, Y. (1988) Diffuse type of senile plaques in the brains of Alzheimer-type dementia. *Acta Neuropathol* 77, 113-119.

Yasuhara, O., Kawamata, T., Aimi, Y., McGeer, E.G. & McGeer, P.L. (1994) Two types of dystrophic neurites in senile plaques of Alzheimer disease and elderly non-demented cases. *Neurosci. Lett.* **171,** 73-76.

Yawo, H. & Kuno, M. (1983) How a nerve fiber repairs its cut end. *Science* **222,** 1351-1353.

Yen, S.H., Gaskin, F. & Fu, S.M. (1983) Neurofibrillary tangles in senile dementia of the Alzheimer type share an antigenic determinant with intermediate filaments of the vimentin class. *Am. J. Pathol.* **113,** 373-381.

Yin, H.S., chou, H.C. & Chiu, M.M. (1995) Changes in the microtubule proteins in the developing and transected spinal cords of the bullfrog tadpole: induction of microtubule-associated protein 2c and enhanced levels of Tau and tubulin in regenerating central axons. *Neuroscience* **67,** 763-775.

Zhan, S-S., Kamphorst, W., Van Nostrand, W.E. & Eikelenboom, P. (1995) Distribution of neuronal growth-promotion factors and cytoskeletal proteins in altered neurites in Alzheimer's disesae and non-demented. *Acta Neuropathol.* **89,** 356-362.

Zhang, C., Lambert, M.P., Bunch, C., Barber, K., Wade, W.S., Kraffit, G.A. & Klein, W.L. (1994) Focal adhesion kinase expressed by nerve cell lines shows increased tyrosine phosphorylation in response to Alzheimer's A beta peptide. *J. Biol. Chem.* **269,** 25247-25250.

Zhang, H., Sternberger, N.H., Rubinstein, L.J., Herman, M.M., Binder, L.I. & Sternberger, L.A. (1989) Abnormal processing of multiple proteins in Alzheimer disease. *Proc. Natl. Acad. Sci. U.S.A.* **86,** 8045-8049.

Zhu, Q., Couillard-Depres, S. & Julien, J.P. (1997) Delayed maturation of regenerating myelinated axons in mice lacking neurofilaments. *Exp. Neurol.* **148,** 299-316.

APPENDIX A

0.01M PBS, pH 7.4 (4°C):

100 ml	10X saline stock (90 g NaCl (BDH) per litre MilliQ® water)
40 ml	Na_2HPO_4 (BDH) (28.4 g per litre MilliQ® water)
10 ml	$NaH_2PO_42H_2O$ (BDH) (31.2 g per litre MilliQ® water)
80 ml	MilliQ®

Tissue storage solution (4°C):

0.01 M PBS

0.1% Sodium azide (Sigma)

Tissue storage solution (-20°C):

300 ml	glycerol (BDH)
300 ml	ethylene glycol (BDH)
300 ml	MilliQ®
80 ml	Na_2HPO_4 (BDH) (28.4 g per litre MilliQ® water)
20 ml	$NaH_2PO_42H_2O$ (BDH) (31.2 g per litre MilliQ® water)

4% Paraformaldehyde solution:

40 g	Paraformaldehyde (BDH Laboratory Supplies)
100 ml	$NaH_2PO_42H_2O$ (BDH) (31.2 g per litre MilliQ® water)
400 ml	Na_2HPO_4 (BDH) (28.4 g per litre MilliQ® water)
500 ml	MilliQ®

Solution heated until dissolved

Chrome alum:

2.5 g	Gelatine
0.25 g	Chrom alum
500 ml	MilliQ®

Solution was heated until disolved and then filtered before use.

Borate buffer:

9.54 g	disodium tetraborate
250 ml	MilliQ®

Add to boric acid solution (24.74 g in four litres MilliQ®), until pH reaches 7.4.

1.5M Tris-HCl, pH 8.8:

18.5 g	Tris-base (Sigma)
≈ 100 ml	MilliQ®

pH adjusted to 8.8 with 6M HCl, made up to 100 ml with MilliQ® then filtered

0.5M Tris-HCl, pH 6.8:

6 g	Tris-base (Sigma)
≈ 100 ml	MilliQ®

pH adjusted to 6.8 with 6M HCl, made up to 100 ml with MilliQ® then filtered

10% Sodium dodecyl sulphate (SDS):

10 g	SDS (Bio-Rad Laboratories)
≈ 100 ml	MilliQ®

Stacking gel, 4%:

1.33 ml	acrylamide (Bio-Rad Laboratories)
2.5 ml	0.5M Tris-HCl
100 µl	10% SDS
6.1 ml	MilliQ®

Add 50 µl 10% ammonium persuplhate and 10 µl Tetra-methylethylenediamine (TEMED)

Separating gel, 7.5%:

2.5 ml	acrylamide (Bio-Rad Laboratories)
2.5 ml	1.5M Tris-HCl
100 µl	10% SDS
4.85 ml	MilliQ®

Add 50 µl 10% ammonium persuplhate and 5 µl TEMED

5x Running buffer, pH 8.3:

15 g	Tris-base (Sigma)
72 g	glycine (Bio-Rad Laboratories)
5 g	SDS (Bio-Rad Laboratories)

Make up to one litre with MilliQ®. Dilute 60 ml with 240 ml of MilliQ®, for one run.

Blotting transfer buffer (25nM Tris, 192mM glycine, 20% v/v methanol, pH 8.3):

3.03 g	Tris-base (Sigma)
14.4 g	glycine (Bio-Rad Laboratories)
200 ml	methanol (BDH)

Make up to 1 litre with MilliQ®

Tris buffered saline (TBS) (20 nM Tris-HCl, 500 mM NaCL, pH 7.5):

4.84 g	Tris-base (Sigma
58.48 g	NaCl (BDH)
1.5 L	MilliQ®

pH adjusted to 7.5 with 6M HCl, made up to 2 litre with MilliQ®

Tris buffered saline with tween:

700 ml	TBS
350 µl	Tween 20 (Bio-Rad Laboratories)

Epon resin:

11.66 g	Procure 812 (ProSciTech)
3.30 g	Dodecenyl Succinic Anhydride (ProSciTech)
8.41 g	Nadic Methyl Anhydride (Probing & Structure)

Mix slowly, for 10 minutes with magnetic stirrer. Then add 0.3 g of 2,4,8 – Tri dimethylaminoethyl phenol (Probing & Structure).